Cape Peninsula University of Technology

Rheological and Stability Properties of *Citrullus Lanatus Mucosospermus*, *Lanatus Citroides* and *Moringa Oleifera* Seed Hydrocolloids in Oil-in-Water Emulsion

Olakunbi Olubi

Thesis submitted in fulfilment of the requirements for the degree

Doctor of Food Science and Technology

in the Faculty of Applied Sciences

at the Cape Peninsula University of Technology, Bellville, South Africa

Supervisor: Prof V. A. Jideani
Co-supervisor: Prof Veruscha Fester
Co-supervisor: Dr Anthony Obilana

October 2024

Declaration

I, **Olakunbi Olubi**, declare that this thesis's content represents my original work and that the thesis has not previously been submitted for academic examination toward any qualification. Furthermore, it represents my own opinion and not necessarily those of the Cape Peninsula University of Technology.

Olakunbi Olubi_____ Date_____

Research Outputs

Outputs from this study include the following:

1 **O Olubi**, A Obilana, N Tshilumbu, V Fester, V Jideani (2024) Physicochemical and Functional Properties of Citrullus mucosospermus, *Citroides*, and *Moringa oleifera* Seeds' Hydrocolloids Foods 13 (7), 1131. (Published)

2 **O Olubi**, J Felix-Minnaar, VA Jideani (2024) Nutritional Profiling of Underutilised *Citrullus Lanatus Mucosospermus* Seed Flour Applied Sciences 14 (9), 3709. (Published)

3 **O Olubi**, A Obilana, N Tshilumbu, V Fester, V Jideani Rheological Behaviour of *Citrullus Lanatus Mucosospermus Citroides* and *Moringa Oleifera*, Hydrocolloid (Submitted to food hydrocolloid journal and under peer review). (Submitted)

4 **O Olubi**, A O Obilana, N Tshilumbu, V Fester, V Jideani Rheology Stability of Oil-in-water Emulsion Stabilized by Ci*trullus Lanatus Mucosospermus Citroides* and *Moringa Oleifera*, Hydrocolloid (Article prepared for Food Science and Technology Journal)

5 **O Olubi**, A O Obilana, V.A Jideani Application of Oil Seeds (*Moringa Oleifera*, *Citrullus Lanatus Mucosospermus*, and *Citroides* Melon Seeds) for the Improvement of Nutrition in Food (Critical Review for Food Science and Technology Journal) Submitted

Abstract

When mixed with water, hydrocolloids create gel-like structures and have grown in popularity due to their wide range of applications in food, medicine, and other industries. The extraction of hydrocolloids from natural sources, such as seeds, is an exciting idea because of the potential diversity in composition and function. In a variety of sectors, the use of seeds from *Citrullus lanatus mucosospermus* (egusi, EG), *Citrullus lanatus citroides* (makataan, MA), and *Moringa oleifera* (moringa, MO) as a hydrocolloid is in line with the growing demand for sustainable and natural products worldwide. This study examined hydrocolloids derived from EG, MA, and MO seeds, highlighting their diverse physicochemical and functional properties. Hydrocolloids were extracted from the seeds and analysed for their proximate composition, particle size distribution, and interfacial tension using the hot water extraction method. The raw oilseed flours had varying amounts of protein. Hydrocolloids had a higher protein concentration than raw oilseeds, greatly improving the amino acid profile. Furthermore, the hydrocolloid ash concentration ranged from 4.09% to 6.52% w/w dry weight, accompanied by low-fat levels. Smaller particles in all hydrocolloid samples showed a more narrow and uniform

size distribution, suggesting a better degree of homogeneity in particle size within this range, according to the examination of particle size distribution. This implies a lower chance of size variation for small particles, which may affect their rheological and functional characteristics in different applications. This study also investigated the rheological behaviour of three novel hydrocolloids: egusi seed hydrocolloid (EGH), makataan seed hydrocolloid (MAH), and moringa seed hydrocolloid (MOH) in semi-concentrated (20-50 wt) as well as concentrated (50-75 wt%) slurries, when subjected to a shear steady flow, to reversible minor strain in amplitude as well as frequency sweep modes deformation. The high protein content of these hydrocolloids (48.12%, 34.00%, and 35.00% for MOH, MAH, and EGH, respectively—reduced the interfacial tension. Regardless of the hydrocolloid type and process parameters (pH = 4–9; temperatures =30-75 ^{o}C; mixing time = 1–10 minutes; concentration = 20–50 wt%), semi-concentrated slurries were pseudoplastic materials that behave like viscous liquids with no yield stress; $G^{"} > G^{'}$ in the entire range of strain (0.1–200%). The storage modulus, yield stress, and slurry concentration correlation showed two deflection points/transitional points, 50 wt% and 67 wt%, respectively. The first transition point was present in all three hydrocolloids, whereas the second was only related to EGH and MAH slurries; MOH-based slurries did not display such a point. The first transition point (50 wt%) was associated with the onset of structure formation. The bottle test further confirmed that slurries containing more than 50% by mass hydrocolloids did not flow when inverting the vessels. The second transitional point marked the boundary between the region of the slow or rapid response of the strength or rigidity of the structure of the slurry of EGH and MAH with changes in hydrocolloid concentration. The strength of the structure increased rapidly with the hydrocolloid concentration below this point, whereas a slow increase was observed above the critical point. Conversely, the rigidity of the structure of the slurries displayed an opposite effect. Interestingly, because of its high content of hydrophobic proteins, the dominating mechanism of structure formation within MOH slurries was the entanglement network of polymers (proteins and polysaccharides) whose yield stress originated from the presence of high concentrations of dispersed particulate material within the structure. This gave rise to a weak, predominantly elastic rather than viscous gel with a cohesive energy range of 0.2 – 0.7 kJ. On the other hand, due to their high hydrophilic protein content, the dominant mechanism of structure formation within EGH and MAH slurries could be cross-liking rather than entanglement. This cross-linking generated a predominantly elastic gel with a relatively high cohesive energy of 2-7 kJ.

The effects of extracted hydrocolloid on the stability and rheological behaviours of oil-in-water (O/W) emulsions (MOH, MAH, and EGH) were investigated using plant-based emulsifiers from moringa, makataan, and egusi hydrocolloids. In this work, the mixture design was optimised for each level of limitation between hydrocolloid, oil, and water. Stability testing

was used to experiment with and optimise the mixture. The droplet size distributions, morphology, creaming index, and polydispersity index were all measured on 11 emulsions, and the best emulsion with a stable profile was chosen for further investigation. The rheological characteristics and the microscopic morphology were acquired to understand the mechanism and interaction of droplets in the O/W emulsion. The results indicated that optimal for O/W emulsions was found in samples with 20-30% hydrocolloid, 37-40 % oil and 25-45 % water while using the three hydrocolloids. EGH and MAH, with the lowest hydrocolloid composition, showed the smallest droplet size and highest creaming index values. The study concludes by highlighting the promising potential of hydrocolloids generated from egusi (EG), makataan (MA), and moringa (MO) seeds. These plant-based hydrocolloids displayed different functional features, including increased protein content, considerable rheological behaviour, and excellent stabilisation in oil-water emulsions. Their capacity to produce gel-like structures, lower interfacial tension, and increase structural rigidity is useful in food systems, particularly for thickening, emulsifying, and texture modification. These findings add to the growing interest in using sustainable, natural ingredients to improve food formulation and product durability.

Contents **pages**

Declaration....ii
Abstract....iii
Contents....vi
Acknowledgement....xvii
Dedications....xviii
Glossary....xix

CHAPTER ONE....
MOTIVATION AND DESIGN OF STUDY....
1.1 Introduction....1
1.2 Problem Statement....3
1.3 Broad Objective....3
1.3.1 Specific objectives....3
1.4 Hypothesis....4
1.5 Delineation/Delimitations....5
1.6 Importance of the Study....5
1.7 Expected Outcomes of the Study....5
1.8 Thesis Overview....6
References....9

CHAPTER TWO....
LITERATURE REVIEW....
2.1 Introduction....14
2.1.1 Sources of hydrocolloids....15
2.1.2 Oil seeds as a source of high protein-to-carbohydrate hydrocolloids....17
2.2 Global Significance and Challenges of Oil Seed Production and Processing....19
2.2.1 *Citrullus lanatus* subsp *mucosospermus* (egusi) seed....21
2.2.2 *Citrullus lanatus* subsp *citroides* (makataan) seeds....25
2.2.3 *Moringa oleifera* (moringa) Seeds....26
2.3 Applications of Oil Seeds (*Moringa Oleifera*, *Citrullus Lanatus Mucosospermus*, and *Citroides* Melon Seeds) in Food Products....26
2.3.1 Moringa seed....27
2.3.2 Makataan seed....32
2.3.3 Egusi seed....36

2.4 European Union (EU) Oilseed Hydrocolloid Protein Regulation 37
2.4.1 Nutritional components of seed-based hydrocolloids 38
2.4.2 Functionality of oilseeds as a hydrocolloid 39
2.5 The Stability and Rheological Properties of Emulsion-based Food Products..... 41
2.3.1 Application of hydrocolloids in the food industry 41
2.3.2 Functional uses of hydrocolloids 43
2.4 Emulsions and Uses 44
2.5.1 Rheological properties of an emulsion 44
2.5.2 Thickening property of an emulsion 45
2.5.3 Properties of a diluted food emulsion 46
2.4.4 Rheology of concentrated emulsions 48
2.5 Conclusion 51
References 51

CHAPTER THREE: **PHYSICOCHEMICAL AND FUNCTIONAL PROPERTIES OF *CITRULLUS MUCOSOSPERMUS, CITROIDES,* AND *MORINGA* SEEDS HYDROCOLLOID** .....
Abstract..... 59
3.1 Introduction 59
3.2 Materials and Methods..... 61
3.2.1 Sources of materials and equipment..... 61
3.2.2 Makataan, moringa and egusi seed preparation and defatting..... 62
3.3 Hot Water Hydrocolloid Extraction of Moringa, Makataan and Egusi Hydrocolloids... 63
3.4 Nutritional and Functional Characterisation..... 64
3.4.1 Proximate analysis of moringa, makataan and egusi hydrocolloids 64
3.4.2 Microstructural analysis of moringa, makataan and egusi hydrocolloids using scanning electron microscopy (SEM)..... 65
3.4.3 Colour parameters of moringa, makataan and egusi hydrocolloids 65
3.4.4 Light and polarised light microscopy of moringa, makataan and egusi hydrocolloids structure..... 66
3.4.5 Particle size of moringa, makataan and egusi hydrocolloids 66
3.4.6 Interfacial tension of moringa, makataan and egusi hydrocolloids 66
3.4.7 Visual appearance..... 67
3.5 Amino Acid Composition of Moringa, Makataan and Egusi Hydrocolloids 67
3.6 Sugar Profiling of Moringa, Makataan and Egusi Hydrocolloids 68

3.7 Statistical Analysis 68
3.8 Results and Discussion 68
3.8.1 Hydrocolloid extraction yield from hot water extraction 68
3.9. Proximate Composition of Moringa, Makataan and Egusi Hydrocolloids 70
3.9.1. Sugar composition of egusi, makataan and moringa seed hydrocolloid 73
3.9.2 Amino acids in makataan, moringa and egusi seed hydrocolloids 75
3.10 Physical Properties of Moringa, Egusi and Makataan Seed Hydrocolloid 77
3.10.1 Visual appearance and particle size distribution of egusi, makataan and moringa seed hydrocolloids 77
3.10.2 Microstructure of moringa, makataan and egusi seed hydrocolloids 81
3.10.3 Microscopy light and partially polarised light of egusi, moringa and makataan seed hydrocolloid 83
3.11 Colour of Moringa, Egusi and Makataan Hydrocolloids 84
3.12 Principal Component of Egusi, Makataan and Moringa seed Hydrocolloids 85
3.13 Interfacial Tension of Egusi, Moringa and Makataan Hydrocolloid 86
3.14 Conclusion and Recommendation 89
References 89

CHAPTER FOUR: **RHEOLOGICAL BEHAVIOUR OF *CITRULLUS LANATUS MUCOSOSPERMUS, CITRULLUS CITROIDES AND MORINGA OLEIFERA* SEEDS *HYDROCOLLOID*** .....
Abstract 96
4.1 Introduction 97
4.2 Materials and Methods 99
4.2.1 Sources of materials and equipment 99
4.2.2 Moringa, egusi and makataan hydrocolloid slurry preparation 99
4.3 Rheological Measurements and Bottle Test of Egusi, Makataan and Moringa Slurry 100
4.3.1 Flow properties 101
4.3.2 Amplitude sweep measurements 101
4.3.3 Frequency Sweep Measurements 103
4.3.4 Bottle test 102
4.4 Statistical Analysis 102
4.5 Results and Discussion 102

4.5.1 Rheological properties of moringa, makataan and egusi hydrocolloid in semi-concentrated slurries 102
4.5.2 Shear viscosity at 50 s^{-1} 105
4.5.2 Amplitude sweep to determine structure formation 107
4.6 Rheology of concentrated hydrocolloid slurries of moringa, makataan and egusi 108
4.6.1 Flow properties of concentrated hydrocolloid slurries 108
4.6.2 Viscoelastic properties of concentrated hydrocolloid slurry of moringa, makataan and egusi 112
4.6.3 Elastic behaviour of concentrated hydrocolloids in slurry systems 112
4.7.3 Frequency sweep of concentrated slurry 117
4.7 Conclusion 123
References 124

CHAPTER FIVE: **RHEOLOGY AND STABILITY OF OIL-IN-WATER EMULSION STABILIZED BY *CITRULLUS LANATUS MUCOSOSPERMUS*, *LANATUS CITROIDES* AND *MORINGA OLEIFERA* HYDROCOLLOID** .....
Abstract 130
5.1 Introduction 130
5.2 Source of Materials and Equipment 131
5.2.1 Emulsion preparation and optimisation 131
5.3 Optimal Oil-in-Water Emulsion 132
5.3.1 Functional properties of moringa, egusi and makataan oil-in-water emulsion 133
5.3.2 Creaming Index of moringa, egusi and makataan oil-in-water emulsion 133
5.4 Dynamic Rheological Measurements of Moringa, Egusi and Makataan Oil-in-water Emulsion 133
5.4.1 Stability profile of moringa, egusi and makataan in o/w emulsion 134
5.5 Statistical Analysis 134
5.6 Results and Discussion 134
5.6.1 Emulsification process 134
5.7 Effect of Hydrocolloid Type on the Droplet Size and Kinetics of Refinement 137
5.7.1. Effect of hydrocolloid type on D_{crit} and Θ 139
5.7.2 Effect of dispersed phase concentration on Θ 142
5.8 Emulsion Stability with Time 143
5.8.1 Effect of the hydrocolloid type on the onset of coalescence 146
5.8.2 Effect of dispersed phase concentration on the onset of coalescence for emulsions stabilised by EGH, MAH and MOH 148

5.8.3 Effect of ageing on the kinetics of coalescence 149
5.8.4 Effect of hydrocolloid type on the creaming of the emulsion 154
5.8.5 Rheological characterisation of egusi makataan and moringa o/w emulsion. 159
5.8.6 Flow properties 159
5.9 Conclusion 172
References **173**

CHAPTER SIX: **OVERVIEW OF CHAPTERS, CONCLUSION AND RECOMMENDATION**
6.1 Summary and Conclusions 178
6.2 Future Studies and Recommendations 181

List of Figures

Figures		Pages
1.1	Overview of Chapters	8
2.1	Overview of food hydrocolloid used globally	17
2.2	Regional oil-seed production	20
2.3	Oil-seed production with its product evaluation	20
2.4	(a) Dehulled and (b) Whole Egusi Seed	22
2.5	Defatted egusi flour	23
2.6	Makataan melon seeds embedded in its pulp	25
2.7	Graphical illustration of the content of vitamin A of a loaf of bread made from wheat flour in comparison to those made from a mixture of wheat flour and MOSF with different percentage substitutions	28
2.8	Results obtained from the use of egusi melon seed flour for the fortification of biscuits prepared using wheat and modified using tuber crops.	37
2.9	(A) Egusi gum: (B) Xanthan gum: (C) Guar gum	40
2.10	Changes in rheological behaviour of emulsion with change in volume/concentration fractions	47
3.1	The overview of the process	62
3.2	Seed preparation and extraction of moringa, makataan and egusi hydrocolloids	64
3.3	Hydrocolloid layer formation across the sunflower interface.	67
3.4	Hydrocolloids are from (a) Moringa seed, (b) Egusi seed, and (c) Makataan seed.	69
3.5	Visuals of room temperature water to hydrocolloid (10:10) mi× of Moringa seed (a) 0 sec (b) 24 h; Makataan seed (a) 0 sec (b) 24 h and (a) 0 sec (b) 24 h Egusi seed hydrocolloid.	70
3.6	Histogram of the particle size distribution of the milled hydrocolloids egusi (EGSH), makataan (MASH), and moringa (MOSH).	77
3.7	Histogram of changes in the particle size distribution of hydrocolloids after 10 s (a) Egusi seed hydrocolloid; (b) Moringa seed hydrocolloid; (c) Makataan seed hydrocolloids.	80
3.8	Scanning electron microscopy (SEM) images of freeze-dried Moringa seed hydrocolloid (MOSH), Moringa seed hydrocolloid (MASH) and Egusi seed hydrocolloid (EGSH).	82

3.9	Morphology of extracted hydrocolloid using light and polarise microscopy (a) lights (b) partially polarised.	84
3.10	Principal component scores and loading plots for the nutritional and functional relationship among the hydrocolloids.	86
3.11	Dynamic interfacial tensions of the three hydrocolloids	87
4.1	Overview of Chapter Four	99
4.2	Typical shear rate dependence of the shear stress for EGH, MAH and MOH slurry	103
4.3	Hydrocolloid slurries at (pH=7, Mt=6,S=25%, MT=60) five minutes after inverting the vessels	103
4.4	Typical best fittings of power law (continuous line) model on flow curves of MAH, 30% slurry in water	104
4.5	Shear viscosity of hydrocolloid slurries at 50 S^{-1}	106
4.6	Typical amplitude sweep for MAH hydrocolloid slurries (20, 25, 33.3, 50 wt%)	107
4.7	Typical flow curves obtained for EGH, MAH and MOH hydrocolloids (75 wt%)	109
4.8	Typical best fittings of the Herschel-Bulkley model on the flow curve of MAH hydrocolloid slurry (67%)	109
4.9	Dependence of the yield stress of EGH, MAH and MOH hydrocolloids on the slurry concentration	110
4.10	Image of hydrocolloids dispersion in water at 67% and 75% five minutes after inverting the vessels	111
4.11	Typical amplitude sweep for EGH, MAH, and MOH hydrocolloid slurries (67 wt%).	113
4.12	Dependence of the storage of EGH, MAH and MOH hydrocolloids on the slurry concentration.	115
4.13	Dependence of the cohesive energy of EGH, MAH and MOH hydrocolloids on the slurry concentration.	115
4.14	Typical frequency sweep for egusi, makataan and moringa hydrocolloid slurries (75wt%) showing the storage modulus, loss modulus and damping factor.	117
4.15	Plot for the effect of hydrocolloid concentration on the damping factor	118
4.16	Typical best fittings of the power law model on frequency sweep data of makataan and moringa hydrocolloid slurries.	120
4.17	Complex viscosity of hydrocolloid slurry at 67 % w/w and 75% w/w.	121
4.18	Plot for the superimposition of the shear and complex viscosity.	122

5.1	Typical microscopic images of fresh emulsion (samples prepared using MOH hydrocolloids).	136
5.2	Effect of hydrocolloid type on the average droplet size after 25 mins of emulsification for different processing conditions.	137
5.3	Typical best fitting of the model on the emulsification of oil-in-water in the presence of MAH hydrocolloids	138
5.4	Characteristic refinement time for different processing conditions, emulsions stabilised by EGH, MAH and MOH.	140
5.5	Dimensionless critical diameters (μm) for different processing conditions emulsions stabilised by EGH, MAH and MOH.	141
5.6	Typical droplet size distribution curves associated with different processing conditions at various stages of ageing for the sample prepared using MAH hydrocolloids.	144
5.7	Effect of varying the hydrocolloid type on the start time of coalescence for different emulsion formulation contents.	146
5.8	Effect of hydrocolloid type on the Laplace pressure.	147
5.9	Effect of ageing on the kinetics of coalescence for different emulsion formulation contents for emulsions prepared using EGH.	149
5.10	Effect of ageing on the kinetics of coalescence for different emulsion formulation contents for emulsions prepared using MAH.	150
5.11	Effect of ageing on the kinetics of coalescence for different emulsion formulation contents for emulsions prepared using MOH.	150
5.12	Effect of hydrocolloid type on the creaming index for different emulsion formulation contents (7 days of ageing).	156
5.13	Effect of hydrocolloid type on the creaming index for different emulsion formulation contents (14 days of ageing).	156
5.14	Typical Flow curves of emulsions prepared with MOH and MAH hydrocolloids (runs 5).	160
5.15	Best fittings of Herschel Bulky model on flow curves of MOH stabilised emulsions (Run 5).	160
5.16	Dependence of o/w emulsion yield stress on hydrocolloid type.	162
5.17	Typical amplitude sweep for o/w emulsion stabilise with hydrocolloids (MOH hydrocolloid; run 5).	163
5.18	Dependence of emulsion elasticity on hydrocolloid type (runs 5,8,11).	165
5.19	Typical Frequency sweep for emulsions prepared with EGH, MAH, and MOH showing the storage modulus, and loss modulus (run 5).	167
5.20	Typical Frequency sweep for emulsions prepared with EGH, MAH, and MOH showing the damping factor (run 5).	168

5.21 Typical best fittings of the power law model on frequency sweep data of o/w emulsions prepared with EGH, MAH and MOH. 169

5.22 The typical complex viscosities of emulsions prepared with EGH, MAH and MOH hydrocolloids (run 5). 171

LIST OF TABLES

Tables		Pages
2.1	Amino acid content of some defatted oil seed flour	24
2.2	Some major mineral elements in defatted egusi flour	25
2.3	Application of *Moringa Oleifera* Seed Hydrocolloids in Food	30
2.4	Results obtained from using *citroides* melon seed flour as a substitute for wheat flour in the preparation of biscuits.	34
2.4	Application of *Citroides* Melon Seed Flour in Food	35
3.1	Proximate composition of raw, defatted hydrocolloid of the makataan, moringa and egusi oilseeds	71
3.2	Proximate composition of makataan, egusi and moringa seeds hydrocolloids.	73
3.3	Sugars in egusi, makataan and moringa seed hydrocolloids	74
3.4	Amino acids of makataan, moringa and egusi seed hydrocolloids	76
3.5	Particle size and particle size distribution of moringa, makataan and egusi hydrocolloids.	77
3.6	Change in particle size and size distribution of moringa, makataan and egusi hydrocolloids after 10 s.	79
3.7	Energy Dispersive X-ray of Moringa, Makataan and Egusi seed hydrocolloid.	82
3.8	Colours in Moringa, Makataan and Egusi seed hydrocolloids.	85
3.9	Equilibrium interfacial tensions.	88
4.1	Comparative study for egusi, makataan and moringa slurry at four levels.	100
4.2	Consistency, flow Index and apparent viscosity of a semi-concentrated egusi, moringa and makataan slurry.	105
4.3	Herschel Buckley's representation of moringa, makataan and egusi hydrocolloid slurry according to flow behaviour.	110
4.4	Plateau modulus, critical strain and cohesive energy of concentrated moringa, makataan and egusi hydrocolloid slurry.	114
4.5	Amplitude sweeps of semi-concentrated moringa, makataan and egusi hydrocolloid slurry.	120
5.1	Emulsion optimisation of hydrocolloid, oil and water for 11 Samples.	132
5.2	Values of D_o, D_{crit} and Θ for emulsions prepared using EGH.	138

5.3	Values of D_o, D_{crit} and Θ for emulsions prepared using MAH.	139
5.4	Values of Do, Dcrit and Θ for emulsions prepared using MOH.	139
5.5	Effect of dispersed phase mass fraction on Θ for emulsions stabilised by EGH, MAH and MOH.	142
5.6	Effect of dispersed phase mass fraction on Dcrit and Θ for emulsions stabilised by EGH, MAH and MOH.	148
5.7	Values of the creaming index for emulsions prepared using MAH.	154
5.8	Values of the creaming index for emulsions prepared using MOH.	155
5.9	Values of the creaming index for emulsions prepared using EGH.	155
5.10	Characterisation of optimised emulsions: Droplet Size, Laplace Pressure, Yield Stress, and Regression Coefficient Analysis.	162
5.11	The effect of varying the hydrocolloid type on the plateau modulus and damping factor.	164
5.12	The effect of varying the hydrocolloid type on the plateau damping factor.	170

Language and style used in this thesis are in accordance with the requirements of the *International Journal of Food Science*. This thesis represents a compilation of manuscripts where each chapter is an individual entity, and some repetition between chapters has, therefore, been unavoidable.

Acknowledgement

I am grateful to the following individuals and institutions for their contributions to the completion of this research study.

- Professor Victoria A. Jideani, my Supervisor and Head of Cereals and Legume Biopolymer Research Group at Cape Peninsula University of Technology, for her inspiration and guidance throughout the study.
- My co-supervisors, Prof Veruscha Fester and Dr Anthony O Obilana, thank you for sharing their extensive knowledge and expertise and challenging me to achieve my best.
- Dr. Nsenda Tshilumbu, for his invaluable assistance in data processing and review activities to ensure my data was accurately represented.
- Mr Owen Wilson, Senior Technician in the Department of Food Technology at the Cape Peninsula University of Technology, for assistance with procurement of chemicals and consumables.
- Stellenbosch University for assistance with equipment for scanning electron microscopy, sugars and amino acid profiling.
- The Cape Peninsular University of Technology postgraduate funding.
- Cape Peninsula University of Technology University Research Funding (URF).
- The Departments of Food Science and Technology, Chemical Engineering and Oxidative Stress of the Cape Peninsula University of Technology are responsible for the equipment used in this study.
- The laboratory technicians in the Departments of Food Science and Technology for assistance with laboratory bookings.
- The Cereals and Legumes Biopolymer Research for Food Security research group for moral and technical support. friends and colleagues, Abiodun Ogunleye and Letlotlo Nyenye, Yvonne Maphosa, for assistance and support throughout my PhD journey.

Dedications

This doctoral thesis is dedicated to my Heavenly Father, Lord Jesus Christ, whose blissful grace has guided and sustained me throughout this academic journey. This accomplishment would not have been possible without His divine inspiration and blessings.

Your immense support and wise counsel have been invaluable to my siblings, Kikelomo, Olapeju, Oladimeji, and Bisi Remi. Your unwavering belief in me has been a source of strength and encouragement, and I am deeply grateful for your love and guidance.

To my daughter, Esther Derinmola Olubi, thank you for your patience, support, and understanding. Your presence has been a constant reminder of why I embarked on this challenging yet fulfilling path.

To my beloved husband, Olugbenga Thompson Adeogun, your moral and financial support have been pillars of strength throughout my doctoral studies. Your unwavering faith in my abilities and your constant encouragement have been crucial in helping me achieve this milestone.

To all of you, I express my heartfelt appreciation and gratitude. This achievement is as much yours as it is mine.

Glossary

Abbreviations	Definition/Explanation
a*	Redness
-a*	Greenness
+b*	Yellowness
-b*	Blueness
AQC	Aminoquinolyl-N-hydroxysuccinimidy carbamate
ANOVA	Analysis of variance
AOAC	Association of Official Analytical Chemists
C*	Chroma
DEF	Defatted egusi flour
D_0	Initial Droplet Diameter
Dcrit	Critical Droplet Diameter
Dph	Dispersed Phase Concentration
DF	Degrees of freedom
DSC	Differential scanning calorimetry
EGH	Egusi hydrocolloid
EI	Emulsion Index
Egusi	Emulsion activity index
ESI	Emulsion stability index
H	Total height of emulsion in the tubes
Hc	Height of the Creamed Layer
HLA	Hysteresis loop area
HS	Height of the serum layer
Ht	Total Height of the Emulsion
ICP-OES spectrometry	Inductively coupled plasma-optical emission
IBM SPSS	International Business Machines Corp
K	Consistency index
L*	Lightness
MAH	Makataan hydrocolloid
MAHS	Makataan hydrocolloid slurry

MANOVA	Multivariate analysis of variance
MOHS	Moringa Hydrocolloid slurry
n	Flow behavior index
OBC	Oil binding capacity
R^2	Coefficient of determination / Root mean squared error
SE	Standard error
SEM	Scanning electron microscope
tan δ	Tan Delta
τ (Tau)	Shear stress
Θ	Theta - Contact Angle
η (Eta)	Viscosity
η (Eta Star)	Complex viscosity
$\dot{\gamma}$ (Gamma Dot)	Shear rate
λ (Lambda)	Relaxation time
μ (Mu)	Another symbol for viscosity in fluid dynamics
σ (Sigma)	Normal stress
ϕ (Phi)	Phase angle
WAC	Water holding capacity
WSI	Water solubility index
XRD	X-Ray diffraction
Yc	Calculated value for each data point
h*	Hue

CHAPTER ONE
MOTIVATION AND DESIGN OF STUDY

1.1 Introduction

Rheology is the scientific study of how matter flows and deforms in response to external pressures such as stress or strain, which has important implications for understanding the consistency and texture of foods. Hydrocolloids—hydrophilic polymers that mix with water to generate gel-like structures—are commonly utilised in the food industry to increase viscoelastic qualities (Giménez-Ribes et al., 2024;2). These compounds, which include pectin, guar gum, xanthan gum, and carrageenan, help to thicken, stabilise, gel, and emulsify food matrices, making them vital in both the food and non-food industries (Giménez-Ribes et al., 2024;2). The growing preference for low-cost, sustainable ingredients has highlighted the relevance of plant-based hydrocolloids such as soy lecithin and guar gums, which are frequently preferred over more expensive alternatives (Calton et al., 2023;6 Gao et al., 2024;8).

Traditionally, high-protein hydrocolloids with self-stabilizing capabilities have relied highly on soybean-derived emulsifiers such as lecithin. These emulsifiers are well-known for their capacity to stabilise emulsions, especially in high-protein foods such as plant-based beverages, protein bars, and meat substitutes. Soybean emulsifiers have long been used because of their proven effectiveness, availability, and low cost. As consumer preferences shift towards more diverse and sustainable ingredients, there is increased interest in alternative high-protein hydrocolloids. This trend has prompted researchers to investigate underutilised plant proteins in moringa, peas, and certain legumes. These alternatives not only show potential as self-stabilizing hydrocolloids but also address concerns about soy allergies and the environmental impact of large-scale soybean production (Aschemann-Witzel & Peschel, 2019;3).

Looking ahead, the landscape of high-protein hydrocolloids is projected to broaden beyond soybeans, with an emphasis on discovering other sources with equal or greater emulsification and stabilisation qualities (Okuro et al., 2020;3; Benitez et al., 2020;2). This advancement is critical for developing clean-label and allergen-free food options that appeal to health-conscious and environmentally sensitive-customers (Calton et al., 2023;2). Developing novel plant-based hydrocolloids with self-stabilizing properties is important for diversifying functional components in high-protein food compositions (Lamminen et al., 2019;3). *Moringa oleifera* seeds and certain underutilised melon species, such as the West

African melon (*Citrullus lanatus mucosospermus*, also known as "egusi") and the Southern African melon (*Citrullus lanatus citroides* locally known as "makataan"), are among the sources being investigated (Pegg, 2012:7). The presence of hydroxyl groups in these seed's micronutrient components increases their water-binding capacity, making them excellent candidates for hydrocolloid synthesis. Recent research has shown the successful extraction of hydrocolloids from several natural matrices and their application in food items. Still, moringa seeds' potential as a source of hydrocolloids is mainly untapped (Kitunen et al., 2019:154).

Moringa oleifera, an Indian plant, has attracted interest for its wide range of applications in sectors including environmental research, cosmetics, medicines, and, increasingly, food science (Rosa-Sibakov et al., 2016:305). Due to their high protein content, moringa seeds' coagulant qualities have been especially recognised in water treatment applications. According to previous studies, the proteins and peptides in moringa seeds, which account for around 45% of their makeup, serve as natural cationic polyelectrolytes, resulting in their coagulant properties (Gharibzahedi *et al.*, 2018;2 Jayasinghe & Pahalawattaarachchi, 2016;1; Ursu *et al.*, 2018;3). Similar features have been identified in certain underutilised melon species, including egusi and makataan, which may lead to the development of nutraceutical hydrocolloids to improve the functional aspects of food products (Trujillo, 2016:5).

Egusi, a wild member of the gourd family commonly cultivated in West African countries, stands out for its potential in the food sector. The seeds of the egusi melon are nutrient-dense, comprising roughly 50% edible oil and 30% pure protein, making it a helpful food. Despite their nutritious value, egusi seeds are mainly used as a thickener in local recipes. Its potential as a commercial hydrocolloid is primarily unknown (Aderinola et al., 2020:10). However, egusi hydrocolloids' high water solubility and stability, as well as their gelling capabilities, indicate that they could be a valuable addition to the food sector.

The study of rheology is critical for understanding the properties of these hydrocolloids, notably their behaviour in oil-in-water emulsions (Rosa-Sibakov et al., 2016;5; Zhang et al., 2018;1;). Emulsions are commonly utilised in food items to deliver lipophilic bioactive substances such as vitamins and antioxidants; nevertheless, they are thermodynamically unstable (Pachimalla et al., 2020:13). Stabilising these emulsions requires the use of emulsifiers such as proteins, polysaccharides, and phospholipids. As consumer demand for plant-based and sustainable ingredients rises, studying hydrocolloids derived from underutilised high-protein seeds such as moringa, egusi, and makataan becomes increasingly essential.

1.2 Problem Statement

Despite the numerous nutritional benefits of egusi (*Citrullus lanatus mucosospermus*), makataan (*Citrullus lanatus citroides*), and moringa (*Moringa oleifera*) plant seeds (Lall & Kishore, 2014;4), their utilisation in food applications remains low. Egusi seeds, traditionally when milled into a powder, can be used in dishes like egusi soup, and possess underexplored hydrocolloid properties. These properties could make egusi an excellent source of high-protein and carbohydrate-based hydrocolloids. However, comprehensive studies on the nutritional properties and hydrocolloid potential of makataan, egusi, and moringa flours are lacking.

The hydrocolloid properties of egusi, makataan, and moringa flour must be thoroughly investigated to increase their utilisation in food products and preserve their genetic diversity. Previous research has highlighted the similar nutritional and fatty acid profiles of makataan and egusi seed oils (Nyam et al., 2010;3; Olubi, 2018;4; Highland Essential Oil, 2019;1), suggesting they may possess comparable hydrocolloid properties. These properties could make them viable stabilisers for food and non-food industries, as indicated by Olubi (2018;77).

Currently, makataan flesh is predominantly used for jam production in a local relish known as makataan preserve (Mcgregor, 2012), and there is a lack of data on the functionality and rheological properties of its seed and seed flour, especially in oil-in-water emulsions. Similarly, the high protein content of moringa seeds suggests they could serve as a valuable source of high-protein hydrocolloids, potentially offering nutraceutical benefits that warrant further comparison with the protein content of the two melon species.

Therefore, it is essential to determine the rheological and stability properties of hydrocolloids derived from egusi (*Citrullus lanatus mucosospermus*), makataan (*Citrullus lanatus citroides*), and moringa (*Moringa oleifera*) in oil-in-water emulsions. This exploration will enhance the food application of these species and contribute to understanding their functional properties, potentially leading to new industrial applications and the conservation of their genetic resources.

1.3 Broad Objective

The main aim of this project was to determine the metabolite profile, rheological and stability properties of the hydrocolloids extracted from *Citrullus lanatus mucosospermus*, *lanatus citroides* and *Moringa oleifera* seed in an oil-in-water emulsion.

1.3.1 Specific objectives

The specific objectives of the project were to:

1 Obtain hydrocolloids from defatted egusi, makataan and Moringa seed flours using conventional heat.

2 Compare the nutritional profile of the defatted flours obtained from makataan, egusi melon and moringa seeds.
3 Characterise the functional properties of moringa, egusi and makataan seed hydrocolloid.
4 Evaluate moringa, egusi, and makataan seed hydrocolloid's rheological properties in a water-based slurry.
5 Evaluate the rheological and phase behaviour of egusi, makataan and moringa seed hydrocolloid in an oil-in-water emulsion.

1.4 Hypothesis

The following theories can be developed based on the references currently available on the compositional structure of *Citrullus lanatus mucosospermus* (egusi), *Citrullus lanatus citroides* (makataan), and *Moringa oleifera* (moringa) seeds*:*

1 The high protein content of moringa seeds, hydrocolloids derived from these seeds will have at least 35% protein by weight. However, hydrocolloids derived from egusi and makataan seeds will have even higher protein levels, ranging from 40% to 50%, because of the rich protein composition associated with these melon species.
2 The hydrocolloids made from egusi, makataan, and moringa seeds will create stable oil-in-water emulsions as possible stabilisers. Their high protein content and amphiphilic protein structures are responsible for this stability.
3 The inclusion of proteins and polysaccharides in the compositions of egusi, makataan, and moringa hydrocolloids would result in outstanding rheological qualities, such as viscosity and gelation, which are known to contribute to functional properties in the food system.
4 While variations may result from different seed matrix compositions, the rheological and phase behaviour of hydrocolloids derived from moringa, egusi, and makataan in oil-in-water emulsions will show commonalities because of the similar interactions between their polysaccharide and protein components.
5 The proteins isolated from moringa, egusi, and makataan seeds will exhibit notable differences in their physicochemical and rheological characteristics despite certain functional similarities because of differences in their amino acid profiles, secondary structures, and molecular interactions that are influenced by the compositions of the individual seeds.

1.5 Delineation/Delimitations

1 Defatted egusi (*Citrullus lanatus mucosospermus*) flour from dehulled egusi seed and makataan (*Citrullus lanatus citroides*) flour from dehulled makataan seed were used in this study.

2 Only dehulled *Moringa oleifera* seed was used in this study, not the leaves.

3 Ethanol, not hexane, was used to defat moringa and makataan seed flour, while egusi seed was defatted using a temperature-controlled oil cold-press machine.

1.6 Importance of the Study

The use of hydrocolloids from microorganisms and animal sources has been extensively explored over the years despite the laborious methods of obtaining these hydrocolloids and the high manufacturing cost (Kasprzak et al., 2018). Due to these limitations, research efforts have been geared towards identifying hydrocolloids from sustainable plant sources. Sustainability process that aims to identify and foster innovative technology to produce nutritious food that will help tackle the issues of malnutrition, unemployment and poverty. And solve fundamental food supply problems around the globe. To enable accessibility to nutritional food options by picking from lesser-known and underutilised crops to contribute to the ever-growing hydrocolloid market. Achieving a stable oil-in-water emulsion from moringa, makataan, and egusi hydrocolloid will cater to some of the most promising food & agriculture innovations in our food & non-food industries. This nutritious *Citrullus* species (egusi and makataan is a vital source of income for communities cultivating it and a cheap protein source (Prothro *et al*., 2012). The commercial application of moringa egusi and makataan flour hydrocolloids in the food, beverage and allied industries could mitigate unemployment. A hydrocolloid from a cheap source produced in this study will have a high nutritional composition (Nyam et al., 2010; Highland Essential Oil, 2019; Olubi, 2018). Such hydrocolloids will help South Africa achieve some of its sustainable development goals (SDGs), which include eradicating hunger, food insecurity, and poverty. A functional hydrocolloid will eventually benefit the global world, as this new plant hydrocolloid could be commercially applicable in the food, beverage, pharmaceutical and allied industries.

1.7 Expected Outcomes of the Study

The outcomes of this research will give insight into the application of three novel hydrocolloids in food systems. These will also provide the food industry with a natural, non-toxic, cheaper and readily available natural alternative emulsion stabiliser. The effect of egusi (EGH), moringa (MOH) and makataan (MAH) on the emulsion systems will provide knowledge of the

nature, behaviour and other functions to which these emulsifiers could be exposed. Results of the stabilising and rheological effects will improve understanding of the phenomena by which the emulsions destabilise, thereby allowing this problem to be tackled in advance. Rheological assessments are expected to offer information on the nature of each hydrocolloid and its behaviour when subjected to varying stresses and over time.

This work has published four preliminary research outputs and one main chapter in reputable journals. Firstly, from the first research chapter titled “Physicochemical and Functional Properties of Citrullus mucosospermus, *Citroides*, and *Moringa oleifera* Seeds’ Hydrocolloids, with FOODS Journal. Secondly, from the preliminary studies “Chemical and functional properties of nutrient-dense beverages developed from underutilised Plant Science Today, and “Extraction and Industrial Applications of Macro Molecules” A Review with Current Research in Nutrition and Food Science Journal: Thirdly as part of the subsequent study in the research chapter three is “Nutritional Profiling of Underutilised *Citrullus Lanatus Mucosospermus* Seed Flour” published with Applied Sciences. The submissions have been accepted at different local and international conferences. Lastly, the attainment of a Doctoral degree in Food Science and Technology is also expected from this study.

1.8 Thesis Overview

This thesis comprises five chapters and is structured in article format, with each chapter presented as a stand-alone study (Figure 1.1). Chapter One gives the motivation and design of the study, stating the research problem, broad and specific objectives, hypotheses, delineation of the study, the significance of the research, expected outcomes, results, and contributions.

Chapter two is the literature review. A background on egusi seed hydrocolloid (EGSH), makataan seed hydrocolloid (MASH) and moringa seed hydrocolloid (MOSH) hydrocolloids is given. Sources of hydrocolloids and their potential impact on processing are outlined. Furthermore, the different compositions and extraction methods and the application and uses of composites are discussed. The classification, stability, and destabilisation mechanisms of emulsions are critically examined, emphasising their application in the food industry, beverage emulsions, and hydrocolloid stabilisation of emulsions. The functionality of oilseed as a plant-based hydrocolloid and its phase behaviour, complexing, separation mechanisms, and their effects on different food emulsion systems and prospects are also discussed. The rheology of diluted and concentrated emulsions was also reviewed to determine their behaviour in a double stabilising system. Finally, the importance of rheological knowledge and various models commonly applied in describing rheological data are examined.

Chapter three detailed the physicochemical and functional properties of EGH, MAH and MOH seed hydrocolloids. The macronutrient and micronutrient composition studies were carried out to determine the compositional structure of this hydrocolloid for the formation of a stable emulsifier. Colour (LAB), light and polarised light microscopy, scanning electron microscopy (SEM), particle size determination (mastersizer), and interfacial tension (IT) analysis are conducted and the results are discussed.

Chapter four investigated the rheological properties and bottle test for each hydrocolloid sample in an aqueous medium) observing the flow behaviour, amplitude sweep, frequency sweep) of each hydrocolloid. Chapter five examined the rheology and stability of oil-in-water emulsion stabilised by the three plant-based hydrocolloids. Emulsion stability and rheological properties were evaluated using the mastersizer and rheometer, respectively. The creaming index and ageing of the emulsions were studied and described using several mathematical models. The stability and rheological behaviour of the emulsion stabilised by the ecology of the emulsions were assessed using a rheometer, while stability was evaluated using coalescence and creaming index studies. Chapter six summarises the research and gives the study's general conclusions.

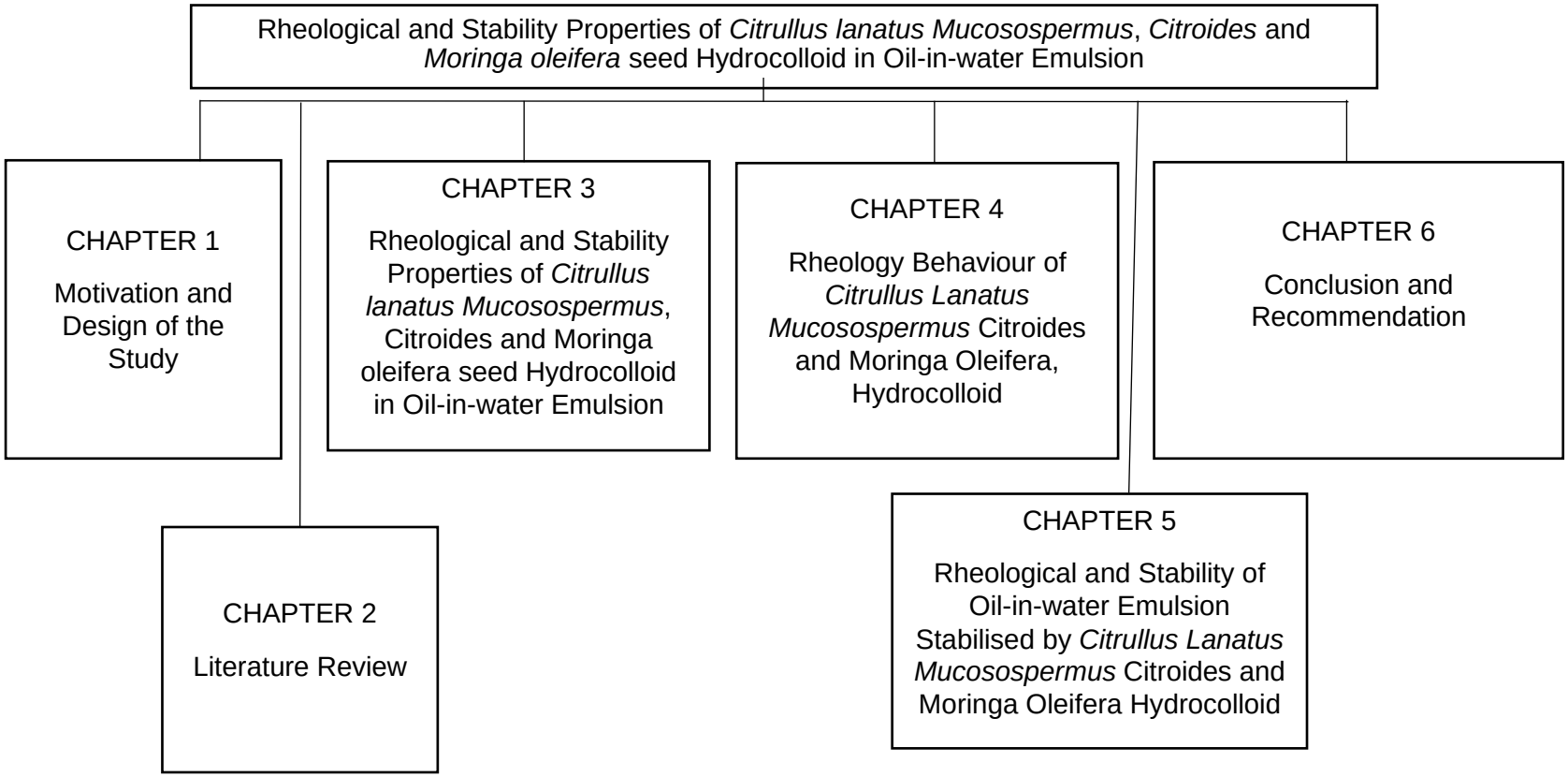

Figure 1.1 Overview of Chapter

References

Abedi, E., Roohi, R., Mohammad, S., Hashemi, B. & Kaveh, S. 2024. Ultrasonics Sonochemistry Investigation of ultrasound-assisted starch acetylation by single- and dual- frequency ultrasound based on rheology modelling, non-isothermal reaction kinetics, and flow / acoustic simulation. *Ultrasonics Sonochemistry*, 102(December 2023): 106737. https://doi.org/10.1016/j.ultsonch.2023.106737.

Aschemann-Witzel, J. & Peschel, A.O. 2019. Consumer perception of plant-based proteins: The value of source transparency for alternative protein ingredients. *Food Hydrocolloids*, 96 (April): 20–28. https://doi.org/10.1016/j.foodhyd.2019.05.006.

A. Addo and A. Bart-Plange. 2009. Kinetics of Water Sorption By Egusi Melon Seeds (Semillas De Melon. *Journal of Agricultural and Biological Science*, 4(6): 5.

A. Bos, M. & van Vliet, T. 2001. Interfacial rheological properties of adsorbed protein layers and surfactants: a review. *Advances in Colloid and Interface Science*, 91(3): 437–471.

Aderinola, T.A., Alashi, A.M., Nwachukwu, I.D., Fagbemi, T.N., Enujiugha, V.N. & Aluko, R.E. 2020. Food Hydrocolloids In vitro digestibility, structural and functional properties of *Moringa oleifera* seed proteins. *Food Hydrocolloids*, 101(August 2019): 105574.

Anwar, M., Rasul, M. & Ashwath, N. 2019. Optimisation of biodiesel production from stone fruit kernel oil Optimization of fruit kernel oil temperature function for a long-term district heat demand forecast the Anwar feasibility of using the. *Energy Procedia*, 160(2018): 268–276. https://doi.org/10.1016/j.egypro.2019.02.146.

Benitez, L.O., Castagnini, J.M., Añón, M.C. & Salgado, P.R. 2020. Development of oil-in-water emulsions based on rice bran oil and soybean meal as the basis of food products can be included in ketogenic diets. *Lwt*, 118(July 2019): 108809. https://doi.org/10.1016/j.lwt.2019.108809.

Calton, A., Lille, M. & Sozer, N. 2023. 3-D printed meat alternatives based on pea and single-cell proteins and hydrocolloids: Effect of paste formulation on process-induced fibre alignment and structural and textural properties. *Food Research International*, 174(P2): 113633. https://doi.org/10.1016/j.foodres.2023.113633.

Cardines, P.H.F., Baptista, A.T.A., Gomes, R.G., Bergamasco, R. & Vieira, A.M.S. 2018. LWT - Food Science and Technology *Moringa oleifera* seed extracts as promising natural thickening agents for the food industry: Study of the thickening action in yoghurt production. *LWT - Food Science and Technology*, 97(April): 39–44.

Efavi, J.K., Kanbogtah, D., Apalangya, V., Nyankson, E., Tiburu, E.K., Dodoo-Arhin, D., Onwona-Agyeman, B. & Yaya, A. 2018. The effect of NaOH catalyst concentration and extraction time on the yield and properties of *Citrullus vulgaris* seed oil as a potential biodiesel feedstock.

South African Journal of Chemical Engineering, 25: 98–102. https://doi.org/10.1016/j.sajce.2018.03.002.

Frazzoli, C., Mazzanti, F., Achu, M.B., Pouokam, G.B. & Fokou, E. 2017. Elements of kitchen toxicology to exploit the value of traditional (African) recipes: The case of Egusi Okra meal in the diet of HIV+/AIDS subjects. *Toxicology Reports*, 4(July): 474–483. https://doi.org/10.1016/j.toxrep.2017.06.008.

Funami, T. 2011. Next target for food hydrocolloid studies: Texture design of foods using hydrocolloid technology. *Food Hydrocolloids*, 25(8): 1904–1914.

Gharibzahedi, S.M.T., Roohinejad, S., George, S., Barba, F.J., Greiner, R., Barbosa-Cánovas, G. V. & Mallikarjunan, K. 2018. Innovative food processing technologies on the transglutaminase functionality in protein-based food products: Trends, opportunities and drawbacks. *Trends in Food Science and Technology*, 75(March): 194–205. https://doi.org/10.1016/j.tifs.2018.03.014.

Giwa, S., Abdullah, L.C. & Adam, N.M. 2010. Investigating 'egusi' (*Citrullus colocynthis* L.) seed oil as potential biodiesel feedstock. *Energies*, 3(4): 607–618.

Gao, K., Rao, J. & Chen, B. 2024. Plant protein solubility: A challenge or insurmountable obstacle. *Advances in Colloid and Interface Science*, 324(December 2023): 103074. https://doi.org/10.1016/j.cis.2023.103074.

Giménez-Ribes, G., Oostendorp, M., van der Goot, A.J., van der Linden, E. & Habibi, M. 2024. Effect of fiber properties and orientation on the shear rheology and Poynting effect in meat and meat analogues. *Food Hydrocolloids*, 149(October 2023): 109509.

Lamminen, M., Halmemies-beauchet-filleau, A., Kokkonen, T. & Jaakkola, S. 2019. Di ff erent microalgae species as a substitutive protein feed for soya bean meal in grass silage based dairy cow diets. *Animal Feed Science and Technology*, 247(October 2018): 112–126. https://doi.org/10.1016/j.anifeedsci.2018.11.005.

Highland Essential Oil. 2019. KALAHARI MELON SEED OIL. , 27(0): 8253.

Ijoyah, M.O., Bwala, R.I. & Iheadindueme, C.A. 2012. Response of cassava, maize and egusi melon in a three-crop intercropping system at Makurdi, Nigeria. *International Journal of Development and Sustainability*, 1(2): 1–10.

Jayasinghe & Pahalawattaarachchi. 2016. Effect of Extraction Methods on the Yield and Physiochemical Properties of Polysaccharides Extracted from Seaweed Available in Sri Lanka. *Poultry, Fisheries & Wildlife Sciences*, 4(1): 1–6. http://www.esciencecentral.org/journals/effect-of-extraction-methods-on-the-yield-and-physiochemical-properties-ofpolysaccharides-extracted-from-seaweed-available-in-sri-2375-446X-1000150.php?aid=75479.

Kasprzak, M.M., Macnaughtan, W., Harding, S., Wilde, P. & Wolf, B. 2018. Food Hydrocolloids

Stabilisation of oil-in-water emulsions with non-chemical modified gelatinised starch. *Food hydrocolloids*, 81: 409–418. https://doi.org/10.1016/j.foodhyd.2018.03.002.

Keisandokht, S., Haddad, N. & Gariepy, Y. 2018. Food Hydrocolloids Screening the microwave-assisted extraction of hydrocolloids from Ocimum basilicum L . seeds as a novel extraction technique compared with conventional heating-stirring extraction. , 74.

Kitunen, V., Korpinen, R., Bhattarai, M., Pitk, L., Lehtonen, M., Mikkonen, K.S., Ilvesniemi, H. & Kilpel, P.O. 2019. Food Hydrocolloids Functionality of spruce galactoglucomannans in oil-in-water emulsions. , 86: 154–161.

Komane, B., Vermaak, I., Kamatou, G., Summers, B. & Viljoen, A. 2017. The topical efficacy and safety of Citrullus lanatus seed oil: A short-term clinical assessment. *South African Journal of Botany*, 112: 466–473. http://dx.doi.org/10.1016/j.sajb.2017.06.028.

Kurozawa, L.E. & Hubinger, M.D. 2017. Hydrophilic food compounds encapsulation by ionic gelation. *Current Opinion in Food Science*, 15: 50–55. http://dx.doi.org/10.1016/j.cofs.2017.06.004.

Kyriacou, M.C., Leskovar, D.I., Colla, G. & Rouphael, Y. 2018. Scientia Horticulturae Watermelon and melon fruit quality : The genotypic and agro-environmental factors implicated. *Scientia Horticulturae*, 234(June 2017): 393–408.

Lall, N. & Kishore, N. 2014. Are plants used for skin care in South Africa fully explored ? *Journal of Ethnopharmacology*, 153(1): 61–84.

Lei, J., Gao, Y., Ma, Y., Zhao, K. & Du, F. 2019. Improving the emulsion stability by regulation of dilational rheology properties. *Colloids and Surfaces A: Physicochemical and Engineering Aspects*, 583(September): 123906. https://doi.org/10.1016/j.colsurfa.2019.123906.

Lupo, B., Maestro, A., Gutiérrez, J.M. & González, C. 2015. Characterisation of alginate beads with encapsulated cocoa extract to prepare functional food: Comparison of two gelation mechanisms. *Food Hydrocolloids*, 49: 25–34.

Mashilo, J., Shimelis, H., Odindo, A.O. & Amelework, B. 2017. Scientia Horticulturae Genetic diversity and differentiation in citron watermelon [Citrullus lanatus var. *citroides*] landraces assessed by simple sequence repeat markers. *Scientia Horticulturae*, 214: 99–106.

Mil, L.E. & Extract, L. 2019. ScienceDirect Improving Stability of Nanoemulsion Containing Centella asiatica, *Materials Today: Proceedings*, 17: 1852–1863.

Mcgregor, C., 2012. Citrullus lanatus germplasm of southern Africa. *Israel Journal of Plant Sciences*, *60*(4), pp.403-413.

Ntui, V.O., Thirukkumaran, G., Azadi, P., Khan, R.S., Nakamura, I. & Mii, M. 2010. *SolocynFusarium wilt and Alternaria leaf spotthis citrullus L.) confers resistance to table integration and expression of wasabi defensin gene in 'Egusi' melon .*

Nyam, K.L., Tan, C.P., Karim, R., Lai, O.M., Long, K. & Man, Y.B.C. 2010. Extraction of tocopherol-

enriched oils from Kalahari melon and roselle seeds by supercritical fluid extraction (SFE-CO2). *Food Chemistry*, 119(3): 1278–1283.

Olubi et al. 2019. Physicochemical and fatty acid profile of egusi oil from supercritical carbon dioxide.

Okuro, P.K., Gomes, A. & Cunha, R.L. 2020. Hybrid oil-in-water emulsions applying wax(lecithin)-based structured oils: Tailoring interface properties. Food Research International, 138(PB): 109798. https://doi.org/10.1016/j.foodres.2020.109798.

Olubi, O. 2018. Functional characteristics of egusi seed (Citrullus lanatus) hydrocolloid and oil in instant egusi soup. *(Master Thesis) Cape peninsula university of technology*, (April). https://www.semanticscholar.org/paper/Functional-characteristics-of-egusi-seed-(Citrullus-Olubi).

Opoku-Boahe, n, YNovick, B.D. & Wubah, D. 2013. Physicochemical characterisation of traditional Ghanaian cooking oils, derived from seeds of Egusi [Citrullus colocynthis] and Werewere [Cucumeropsis manni]. *International Journal of Biological and Chemical Sciences*, 7(1): 387–395.

Pachimalla, P.R., Mishra, S.K. & Chowdhary, R. 2020. Evaluation of hydrophilic gel made from Acemannan and *Moringa oleifera* in enhancing osseointegration of dental implants. A preliminary study in rabbits. *Journal of Oral Biology and Craniofacial Research*, 10(2): 13–19. https://doi.org/10.1016/j.jobcr.2020.01.005.

Pegg, A. 2012. *The application of natural hydrocolloids to foods and beverages*. Woodhead Publishing Limited. http://dx.doi.org/10.1533/9780857095725.1.175.

Rosa-Sibakov, N., Hakala, T.K., Sözer, N., Nordlund, E., Poutanen, K. & Aura, A.M. 2016. Birch pulp xylan works as a food hydrocolloid in acid milk gels and is fermented slowly in vitro. *Carbohydrate Polymers*, 154: 305–312. http://dx.doi.org/10.1016/j.carbpol.2016.06.028.

Trujillo, A.J. 2016. Food Hydrocolloids Enhanced stability of emulsions treated by Ultra-High Pressure Homogenization for delivering conjugated linoleic acid in Caco-2 cells. *Food hydrocolloids*: 1–11.

Tsai, F., Chiang, P., Kitamura, Y., Kokawa, M. & Islam, M.Z. 2017. Food Hydrocolloids Producing liquid-core hydrogel beads by reverse spheri fi cation : Effect of secondary gelation on physical properties and release characteristics. *Food hydrocolloids*, 62: 140–148.

Ursu, A.-V., Djelveh, G., Pierre, G., Delattre, C., Michaud, P., Nasirpour, A. & Saeidy, S. 2018. Emulsion properties of Asafoetida gum: Effect of oil concentration on stability and rheological properties. *Colloids and Surfaces A: Physicochemical and Engineering Aspects*.

Uruakpa, F. 2004. Heat-induced gelation of whole egusi (Colocynthis citrullus L.) seeds. *Food Chemistry*,87(3):349–354. http://linkinghub.elsevier.com/retrieve/pii/S0308814603006319.

Zettel, V. & Hitzmann, B. 2018. Applications of chia (Salvia hispanica L.) in food products. *Trends*

in Food Science and Technology, 80(January): 43–50. https://doi.org/10.1016/j.tifs.2018.07.011.

Zhang, Y., Zhou, F., Zhao, M. & Lin, L. 2018. Food hydrocolloids soy peptide nanoparticles by ultrasound-induced self-assembly of large peptide aggregates and their role on emulsion stability. *Food hydrocolloids*, 74: 62–71. http://dx.doi.org/10.1016/j.foodhyd.2017.07.021.

Zhao, Q., Jiang, L., Lian, Z., Khoshdel, E., Schumm, S., Huang, J. & Zhang, Q. 2019. Journal of Colloid and Interface Science High internal phase water-in-oil emulsions stabilised by food-grade starch. *Journal of Colloid and Interface Science*, 534: 542–548. https://doi.org/10.1016/j.jcis.2018.09.058.

Zhao, S., Tian, G., Zhao, C., Li, Chengxiu, Bao, Y., Dimarco-crook, C., Tang, Z., Li, Chunhong & Julian, D. 2018. The stability of three different citrus oil-in-water emulsions fabricated by spontaneous emulsification. , 269(December 2017): 577–587.

CHAPTER TWO
LITERATURE REVIEW

2.1 Introduction

Hydrocolloids are typically polysaccharides or proteins soluble in cold or hot water (Gravelle & Marangoni, 2021;2). Due to their structural properties and high molecular weight, they serve a critical function in the food business by producing a three-dimensional network, increasing viscosity, and changing food texture. These qualities improve the consistency and texture of food products. Therefore, while selecting an excellent texture-forming substance for innovative food products, evaluate the composition, water and sugar content, metal ions, acidity, and hydrocolloid functions (Gravelle & Marangoni, 2021;3).

Hydrocolloids are derived from various sources, each with its own properties. Guar gum and locust bean gum are examples of seed-based plant hydrocolloids that can stabilise a gel system by raising the viscosity of its continuous phase (Ciurzyńska et al., 2020;3). Soy lecithin is well-known for its ability to emulsify and stabilise foods. Generally, hydrocolloids are recognised as agents for thickening and gelling; however, several biopolymers have been reported to show colossal emulsifying characteristics (Tan et al., 2020;2). Polysaccharides owe their emulsifying properties to their monomer composition, molecular weight, charged surfaces, and the existence of some hydrophobic fractions, like proteins, at the cornerstone of the polysaccharide (Semenova, 2017;15). Amphiphilic polysaccharides are known to enhance emulsions' stability through the steric mechanism of fractions that are hydrophilic, electrostatic repulsion, and oil-water interface adsorption through the hydrophobic fractions (McClements & Gumus, 2016;7). One of the essential properties of these emulsifying agents is their ability to adsorb into the oil-water interface rapidly. They mix with the oil and water phases to reduce the disparity of interactions of their molecules, interfacial tractions and emulsion droplet sizes (Kavitake et al., 2019;449). The presence of high surface charge values (ζ-potential), either positive or negative (greater than +30 mV or lower than −30 mV) in these hydrocolloids, increases the stability of emulsions as well as their flocculation aggregate resistance (Tan et al., 2020;3). The hydrophilic (water-loving) and hydrophobic (water-repelling) amino acids in high-protein hydrocolloids significantly influence their functional properties in food systems. Here's how these amino acid characteristics affect hydrocolloid behaviour. These amino acids have side chains that interact well with water molecules. In hydrocolloids, hydrophilic amino acids help stabilise the water phase of emulsions (Lin et al., 2024;2). They can form hydrogen bonds with water, aiding in the dispersion of oil droplets and maintaining a stable emulsion. Hydrophobic amino acids have side chains that prefer to avoid water, interacting more favourably with oil or fat molecules (Yue et al., 2022;2). In emulsification, hydrophobic amino acids

in hydrocolloids tend to interact with the oil phase, helping to reduce the surface tension between oil and water. This allows for better integration of oil droplets into the aqueous phase, forming a stable emulsion (Gao et al., 2022;6).

Furthermore, hydrocolloids can reduce textural qualities in aqueous or hydrogel form by a mechanism described by the repulsion-adsorption model as a hydrophobic force (Dangi et al., 2019; Pachimalla et al., 2020; Yousefi & Jafari, 2019;). However, they can generate textural flaws; for example, over-stabilization can result in a "jelly-like" springy body in yoghurt, while under-stabilization can result in a "runny" body or severe whey separation

Maintaining food's inherent flavours while retaining their original texture is critical for customer satisfaction. However, advanced properties such as phase interaction, complicated viscosity, lubricity, and water-holding or absorption capacity require development for optimal manufacturing performance. Despite their potential, little research has concentrated on powerful oilseeds with high nutritional qualities as sources of hydrocolloids (Pang et al., 2020;1).

We understand that there have been a lot of comprehensive reviews from the list of literature out there, in which the reviewers have focused on oil-seeds protein functionality of the applications of *moringa oleifera* plant leaves for the fortification of food. Also, another review focused on egusi melon seed prospects for biodiesel production. In contrast, another review focused on mechanising the various methods of processing and melon and their extraction technologies, which was different from the aim of this review. However, for this review, we give a background overview of food hydrocolloids and their functionality, detailing their possible rheological behaviours, their applications and various sources from which they can be obtained, such as oil seeds. The review further discussed oil seeds as a source of protein-to-carbohydrate hydrocolloids, with a prime focus on the underutilised oil seeds such as *Moringa oleifera*, *Citrullus lanatus mucosospermus,* and *Citroides* melon seeds, and their various contents. Lastly, the review critically discussed the multiple applications of these underutilised oil seeds for improving food nutrition.

2.1.1 Sources of hydrocolloids

Hydrocolloids can be found in various sources, including plant, animal, and microbe components, such as xanthan derived from microorganisms. Xanthan gum is a non-gelling substance comprising a ß-1,4-glucose backbone and a trisaccharide chain of two-spaced mannose and glucuronic acid units (Kasprzak et al., 2018;410). This hydrocolloid is typically mixed with gelling agents, such as locust bean hydrocolloid, derived from the carob tree plant seed. This combination is done to obtain hard food gels with high porosity and an attractive appearance for consumers, distinguishing this product from others by creating soft and elastic gel at different concentrations. (Pang et al., 2020;2). The plant source of hydrocolloids has been well-received for its nutraceutical

and functional benefits. The research aims to identify more underutilised hydrocolloid sources with high nutritional profiles. However, exploring high protein and low carbohydrate food additives remains an object of interest.

Locust bean gum, a natural food additive obtained from the carob seed of the carob tree, has been known for its hydrocolloid properties, primarily as a thickener and a stabilising gel. Thermally reversible gels dissolve at temperatures ranging from 55 to 60 degrees Celsius. The interaction of xanthan gum with locust bean gum depends on the combination ratio (optimally 1:1), the ionic environment, and the synergistic impact, which is diminished by high salt concentration and low pH (Tsai et al., 2017;603). Sodium alginate is a polysaccharide, specifically an unbranched manuric and guluronic acid copolymer. It is soluble in cold water, making thermally stable gels without prior heating (Gharibzahedi et al., 2018;192). Gelation at low pH is frequently related to the participation of calcium ions, such as calcium lactate (Yuasa et al., 2019;2). For this reason, alginate is a preferred gelling agent for re-structured food (Ciurzyńska et al., 2020;6), such as freeze-dried products.

Gellan and guar gum are two polymers that are generally considered harmless. Hydrocolloids have been used for their production and application in various industries, including food and pharmaceuticals. For example, guar gum is a potential hydrophilic matrix carrier for oral medication delivery, while it has been utilised as a thickening and gelling agent in the food industries (Yildirim-Mavis et al., 2019;482). Similarly, gellan is an important industrial polymer because of its varied functional qualities and is widely employed in the food, pharmaceutical, plant tissue, and microbiological sectors (Katoch & Roy Choudhury, 2020;2).

Guar gum sugar contains a high concentration of mannose and galactose, which are non-ionic polysaccharides having several −OH groups on their molecules. When guar gum powder is disseminated in water, the molecular chain twists, forming a network structure based on the hydrogen connection between guar gum molecular units (Pang et al., 2020;7). Approximately 70% of fracturing fluids are water-based and derived from guar gum. Guar gum's network structure, which is made up of hydrogen bond interactions, breaks down at higher temperatures. Some researchers have demonstrated that carboxymethylation of the guar gum molecular chain to graft a stiff group can improve temperature resistance (Pang et al., 2020; Yousefi & Jafari, 2019). Guar gum fracturing fluid is suitable for oil fields with temperatures below 120°C. A unique approach must be developed to improve the temperature resistance qualities of guar gum fracturing fluids. via a guar gum gelling system, hydrogen bonding via intermolecular contacts can create a lengthy chain (El-hoshoudy et al., 2020;2). The rheological characterisation of these hydrocolloids reveals their inherent structural complexity. This characterisation assists in the comprehension of their actions. Recently, some researchers have concentrated on generating natural hydrocolloids based on natural polymers or a combination of natural and synthetic polymers, which are biocompatible

and safe for human usage (Grasso et al., 2020;2). These natural sources abound in some choice plant and living organisms, but few oilseeds have been explored for their contribution to these functional food additives pools. However, only a few oilseeds have been thoroughly studied for their contributions to the pool of hydrocolloids. Figure 2.1 depicts the range of dietary hydrocolloids being investigated as of 2024. This analysis demonstrates that high-protein hydrocolloids are still underutilised, with soybeans as the primary focus of research and application.

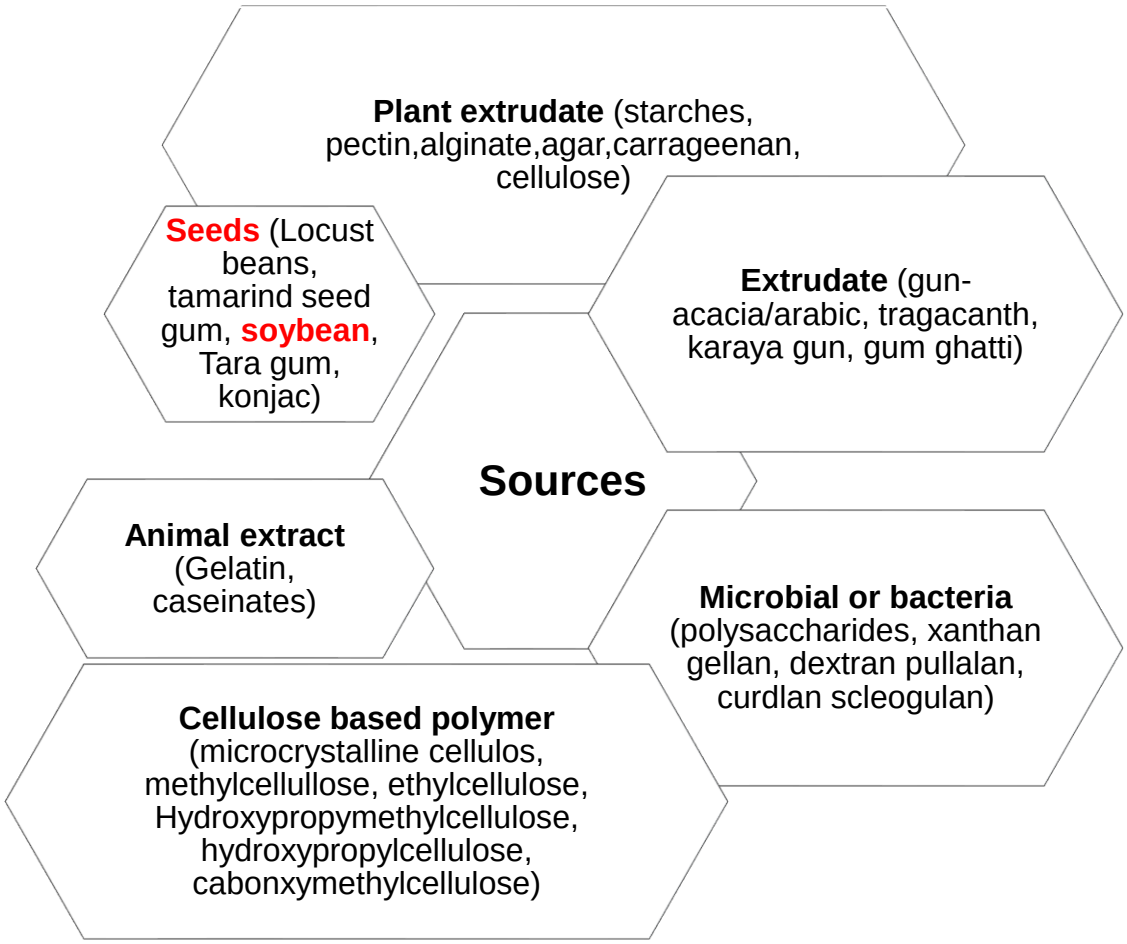

Figure 2.1 Overview of food hydrocolloid used globally

2.1.2 Oil seeds as a source of high protein-to-carbohydrate hydrocolloids

Oilseeds are an essential source of vegetable oils in the food sector. Oils can be derived through mechanical expression or solvent extraction and used in cooking or as food components. According to the United States Department of Agriculture 2021 statistics, palm, soybean, rapeseed,

sunflower seed, palm kernel, peanut, cottonseed, coconut, and olive oil are the world's most widely produced vegetable oils.

For over 150 years, the world has been committed to sustainably feeding a growing global population. As the global population expands from 7 billion to over 9 billion by 2050, consumer values will adjust accordingly (Fernández-Martínez & Velasco, 2012;4; Seifu & Teketay, 2020;3). Climate change is real, and our food processing and agriculture systems must adapt. One of the largest problems for the oilseed processing sector is to sustain the food supply while reducing waste (Seifu & Teketay, 2020;2). Innovation, including technology, digitalisation, and applications, can address global food system challenges such as achieving zero hunger, meeting consumer preferences, creating safer workplaces, promoting transparency, replacing fossil compounds, and improving farming technology.

Innovation is not limited to a particular enterprise, university, or technology platform. This review examines various ways of technical advancement that might aid in the evolution of the oilseeds processing industry. The safety of food oils and proteins is a major concern for the century. Human health must be safeguarded, and the territory's protein and fat sovereignty must be addressed. This autonomy plays a vital role in trade and the economy. The issue is to extract the oil fraction from the oilseeds while maintaining protein quality more effectively.

Many undiscovered or underexplored oilseeds with high oil content or rich bioactive chemicals are viable for consumption or industrial use. Minor or unusual oils include safflower, pumpkin, flaxseed, apricot, and chia seeds (Yashi & Dhiman, 2020;2). With the increasing demand and supply of vegetable oils, oil processing is necessary to completely utilise various oilseeds and enhance oil extraction yield. Oilseed flour proteins are ideal stabilisers. However, they are understudied and replaced with hydrocolloids derived from animals and microbes. Oilseeds can be obtained from many sources of vegetable origin, and their principal modes of defatting are cold pressing, mechanical extraction, or solvent extraction procedures (Geerdts, 2005;4; Nkafamiya et al., 2010;3). After defatting, oil-seed protein could be utilised in place of animal protein in food manufacturing. Oilseeds are mostly high in nutritional composition and can be utilised to generate nutritious meals; nevertheless, certain species remain underutilised.

Soybeans, sunflowers, canola, and sesame are the most well studied oil seeds. Soybean output is expected to increase to about 350 million metric tonnes in Latin America, the Caribbean, and North America by 2025, as it remains the only scientifically investigated high-protein emulsifier (Figure 2.1). Because of the large range of oil-seed sources, research efforts have focused on healthy, underutilised food options to facilitate food production and distribution.

2.2 Global Significance and Challenges of Oil Seed Production and Processing

According to statistical data from the United States Department of Agriculture (2021), among the significant vegetable oils listed, palm, soybean, rapeseed, sunflower seed, palm kernel, peanut, cottonseed, coconut, and olive oil have the most considerable quantity of production globally (Ishaq et al., 2024;2). For over 150 years, the globe has been on an unyielding mission to feed a worldwide population responsibly (Gomes et al., 2020;2). Consumer values are predicted to vary as the global population expands from 7 billion to over 9 billion by 2050, as seen in Figure 2.2 (Grasso et al., 2020). The accuracy of climate change dictates that food processing and agriculture systems evolve. One of the difficulties for the oil-seed processing sector is to sustain the food supply while reducing waste and contributing to greenhouse gas (GHG) reduction (Ayerza(h), 2019;2). Many unknown or underexplored oil seeds have high oil content or rich bioactive chemicals, making them useful for consumption or industrial applications. Minor or unusual oils include safflower, pumpkin, flaxseed, apricot, and chia seeds. With the increasing demand and supply of vegetable oils, oil processing is necessary to utilise various oil seeds and enhance oil extraction yield (Wilberforce et al., 2017;10).

Oil seeds can be obtained from various sources of vegetable origin, and their primary means of defatting include cold pressing, mechanical extraction, or solvent extraction methods (Ebrahimian et al., 2019;150). After defatting, the protein obtained from oil-seed could be used as an alternative to animal protein for food production in the food industries. The most explored oil seeds are soybeans, sunflowers, canola, and sesame. Soybean production is estimated to rise to over 350 million metric tons in Latin America, the Caribbean, and North America by 2025 (Figure 2.2). Due to the wide variety of oil-seed sources, research efforts have been directed toward nutritious, underutilised food options to enable food production and distribution.

Oil-seed production is mainly marketed for the food industry, reaching 598.04 million tons in 2018/2019 (Casoni et al., 2019;2). During the same period, global protein meal production after defatting and oil-seed grew to around 207 million metric tonnes. Soybeans, rapeseed, cottonseed, sunflower seed, and peanuts are among the most plentiful protein meals, accounting for 69%, 12.4%, 6.9%, 5.3%, and 2.8% of global protein meal output, respectively, as shown in Figure 2.3 (Liu et al., 2019;26). Oil-seed meal protein significantly contributes to human daily protein intake, with soybean being the most cultivated oil-seed globally, predominantly by Americans (Zafar et al., 2019;36). Plant oil exports dominate Indonesia and Malaysia by more than 42%, making it one of the agricultural commodities with the highest share of production. This projection is expected to remain stable until 2025 (Figure 2.3). While protein meal production remained low across the region, the production rate is high at 50% in Argentina, indicating the need to explore the meal/flour obtained after oil-seed defatting.

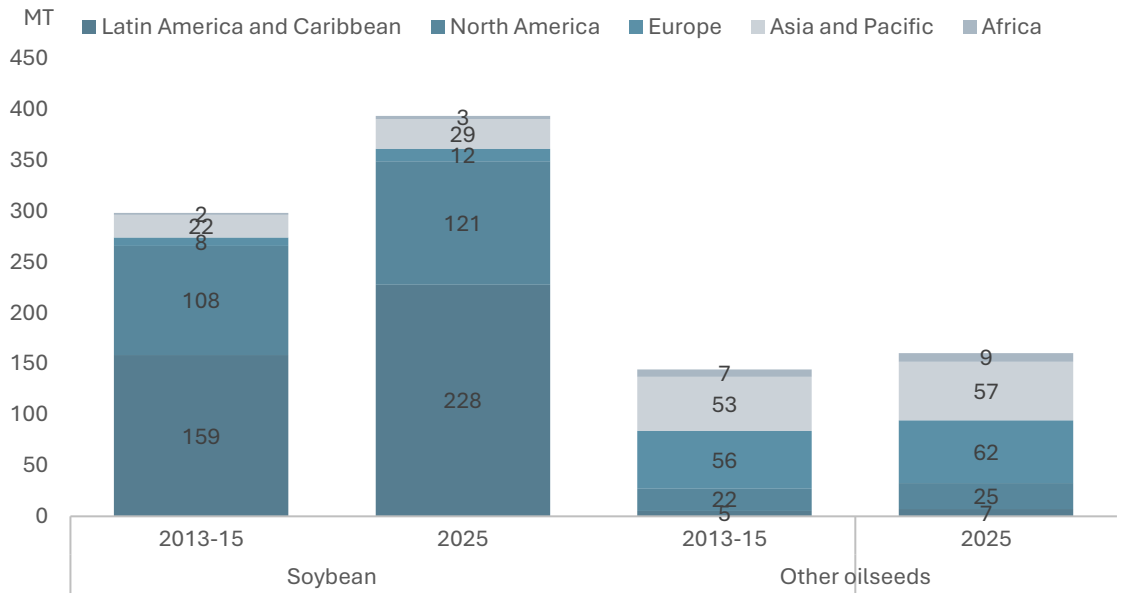

Figure 2.2 Regional oil-seed production (Snapshots, 2016;104)

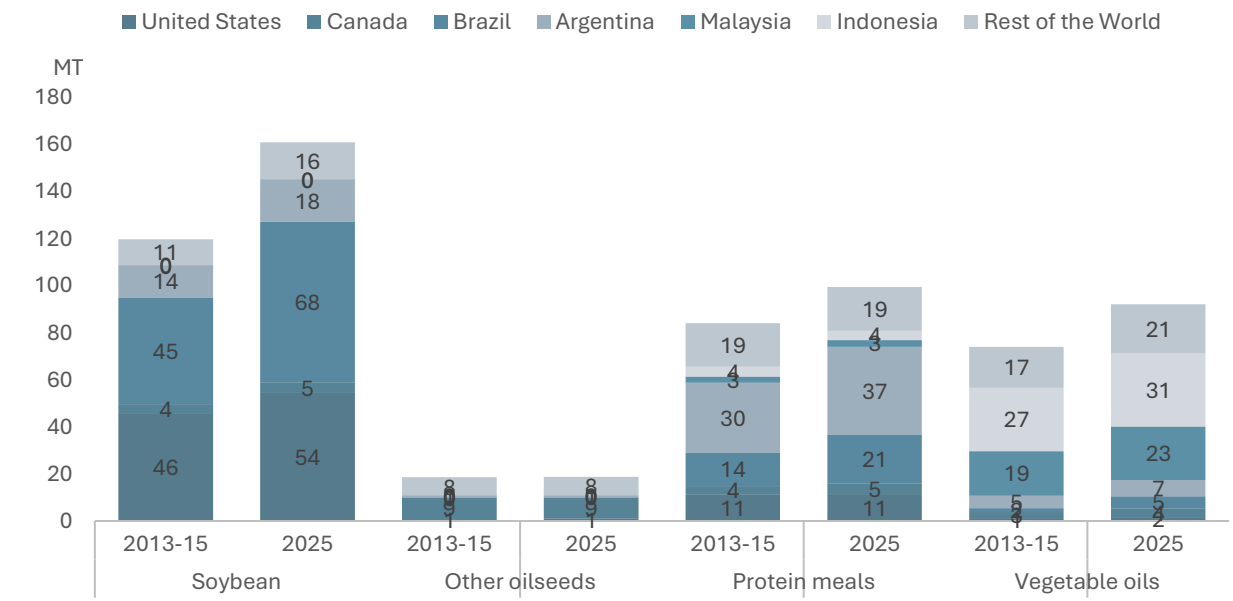

Figure 2.3 Oil-seed production with its product evaluation (Snapshots, 2016;102)

The protein content of defatted meals from dehulled oil seeds is quantified based on their quality, ranging from 35% to 60% (db) (K. Liu et al., 2019;25). The growing demand for highly enriched protein meals has encouraged the increased demand for known oil seeds. However, this growth must create more food options from unknown or underutilised oil seeds. In general, raw oil-seed flour contains anti-nutritional chemicals, such as oligosaccharides, trypsin inhibitors, phytic acid, and tannins, which cause low protein solubility, therefore limiting their culinary applications (Huang et al., 2018;59). In general, raw oil-seed flour contains anti-nutritional chemicals, such as oligosaccharides, trypsin inhibitors, phytic acid, and tannins, which cause low protein solubility, therefore limiting their culinary applications (Rehmani et al., 2019;2).

Processing procedures can boost oil extraction while improving the protein's nutritional and functional qualities. Supercritical fluid extraction, heat treatment, soaking, fermentation, and germination are just a few of the procedures that can be studied (Florowski et al., 2019;130). Germination promotes the release of active components in oil seeds, increases protein content, and removes nondigestible oligosaccharides and antinutritive components. Thus, the seed overcomes limitations such as flavour, odour, and trypsin inhibitors. Soaking is a key step that minimises the amount of oligosaccharides while improving protein functional properties. Soaking seeds in sodium bisulfite solutions or acidic media removes phenolic compounds (A. Addo and A. Bart-Plange, 2009;2). Seed fermentation stimulates protein breakdown into amino acids and peptides, as well as the improvement of certain functional properties. The preparation of nutritious meals with a high protein content is critical in today's culture, prompting the investigation of numerous underutilised sources of protein-based hydrocolloids, such as seeds. These oil seeds include *Moringa Oleifera, Citrullus lanatus mucosospermus*, and *citroides* melon seeds.

2.2.1 *Citrullus lanatus* subsp *mucosospermus* (egusi) seed

Citrullus lanata subsp. mucosospermus is a member of the *Benincaseae* family and the *Cucurbitoideae* subfamily*. Citrullus* is a genus of seven species of desert vines, among which *Citrullus lanatus mucosospermus* is intensively cultivated, primarily for seeds (Nkoana et al., 2022;66). Thunberg first described *Momordica lanata* in 1794, and Matsum and Nakai improved it in 1916, placing it in the *Citrullus* family (Olubi et al., 2021;3). This indigenous plant species, known as egusi melon or bitter melon seed, is largely consumed in Asia, Central and West Africa. Melons are grown as weak stem plants creeping across a surface belonging to *Cucurbitaceae* (Mashilo et al., 2022;29). The cucurbit family contains approximately 95 genera and 750 species, including watermelon and cucumber, both of which have edible and delicious flesh. Citrullus lanatus has four species: *colocynthis, lanatus, rehmii*, and *ecrihosus* (Komane et al., 2017). *Rehmii* and *ecrihosus* are popular in Namibia, but *colocynthis* and lanatus are more common in West and Central Africa. *Citrullus lanatus* subsp *mucosospermus* is classified into two seed kinds in Africa, specifically in

Nigeria, Cameroon, and Central Africa, based on the presence or absence of a black edge. These seed types can be distinguished as various cultivars and are more common in Africa. In some underdeveloped nations, C. lanatus is a vital crop; the seeds of egusi are dehulled to get a white kernel (Figure 2.3), which contains around 50-60% w/w oil, 28-30% w/w protein, 20-10% w/w carbohydrate, 2-3% w/w ash, and 3-4% w/w fibre (Olubi et al., 2024;6).

Melon seed milk was found to contain 3.6% w/w protein, 4.0% w/w fat, and 2.5% w/w carbohydrates, which are comparable to soy milk. As a result, egusi seeds have the potential to enrich both new and classic foods. The cultivation of most cucurbit species, aside from the citrus watermelon, is limited to the local communities that have found the primary food use of such seeds. Its perceived nutritional properties by families of local farmers in the early existence of these seeds in Nigeria date back to the 17th century (Paudel et al., 2019;2). The pulp and seeds of the egusi can be easily separated, with their seed type and coat colour reported to be used to classify them as Bara: large brown seeds with black edges, Serewe: smooth brown seeds without distinctive edges (Frazzoli et al., 2017;476). The Bara class is the most extensively distributed within a geographical area and is attributable to consumers' preferences rather than the physiological adaptation of the crop. In the typically mixed cropping system, farmers in West Africa cultivate egusi melon mixed with other crops like yam, cassava, and maise (Agu et al., 2018;389).

Figure 2.4 **(a)** Dehulled and **(b)** Whole Egusi Seed (Olubi, 2018;10)

Egusi melon is a non-industrial crop that receives less attention from farmers and food industries. In some cases, it serves as an intercrop species planted solely to prevent weeds on a plantation.

The defatted flour of egusi is rich in protein and essential amino acids, making it a functional flour. Using the supercritical extraction method, Olubi et al. (2024) investigated egusi flour's functional and nutritional properties (Olubi et al., 2024). The investigation found the defatted egusi flour to be creamy white, as shown in Figure 2.4, with a high protein content, proving its nutritional value. Defatted egusi flour (60% w/w) has been shown to have a higher protein content than most oil seeds and some chosen animal proteins. Protein is an essential component of all cells in the body. Low protein levels impact nails and hair, as protein is an important component of our bodies. Muscle repair and development take a significant time. Egusi's high-protein flour provides meal alternatives for vegetarians and others who cannot afford high-protein meat and meat products (Mashilo et al., 2017;100).

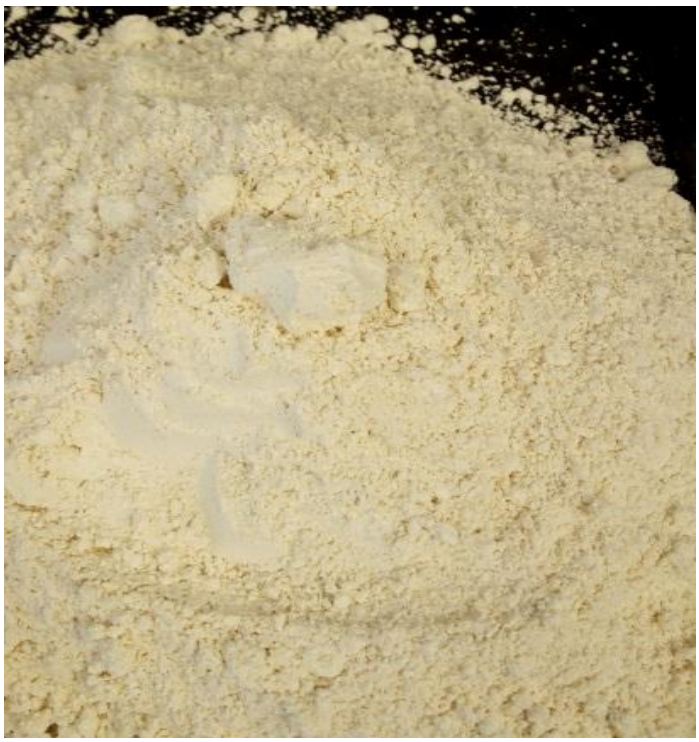

Figure 2.5 Defatted egusi flour (Olubi et al., 2024;6)

Egusi flour's high dietary fibre content makes it an effective ingredient for functional food composition. As a result, it is proposed that consuming defatted egusi flour, which may be converted into pre-cooked, processed food, may provide numerous health benefits, including protection against acute malnutrition and obesity. According to a study in Table 2.1, the amino acid

composition demonstrates that egusi flour contains 14 out of the 22 amino acids in nature. Glutamine is muscles' most common amino acid, accounting for more than 61% of total skeletal muscle. Surprisingly, egusi seeds have more amino acids than moringa and sunflower seeds (Table 2.1). Tables 2.2 and 2.3 demonstrate that defatted egusi flour produced through supercritical extraction included sixteen trace mineral elements and five significant elements.

The major element, phosphorus, was the most abundant in all the defatted egusi flour samples, with values of 1698.9, 1877.8, and 2046.4 mg/100 g, respectively, followed by potassium, magnesium, calcium, and iron. Table 2.2 shows that the phosphorus concentration was comparable to several selected prime oil seeds. These amino acids contribute to oilseeds' high nutritional value, making them a major source of plant-based protein in human diets. The balance of these amino acids also impacts the functional qualities of oilseeds when utilised in food compositions, such as their emulsifying, gelling, and binding capabilities (Al-Mohammad, 2016;4 Olubi et al., 2024,2).

Table 2.1 Amino acids content of some defatted oil-seed flour

Amino acid g/ 100g	Egusi flour	Millet flour	Moringa-seed flour	Soybean flour	Sunflower seed-flour
Histamine	1.50	0.30	8.90	3.00	0.70
Serine	3.00	0.40	5.60	7.40	1.20
Arginine	9.80	1.10	8.50	5.70	2.15
Glycine	3.80	0.07	0.00	11.10	1.50
Aspartic	5.70	0.00	0.00	7.00	2.40
Glutamic	12.90	11.40	6.10	12.00	5.70
Threonine	1.50	3.70	0.80	4.80	0.90
Alanine	3.10	7.30	2.30	5.30	1.10
Proline	2.40	0.00	0.00	0.00	1.10
Lysine	2.60	1.10	4.30	5.40	1.20
Thyrosine	2.00	1.40	0.00	3.20	0.60
Methionine	1.90	0.02	0.67	1.10	0.60
Valine	2.90	0.00	0.00	4.30	1.30
Isoleucine	2.20	2.40	1.40	4.00	1.10
Leucine	4.30	4.70	2.80	8.40	1.70

Source: (Mohammed Nour et al., 2018;4 Olubi et al., 2024;7)

Table 2.2 Some major mineral elements in defatted egusi flour

Mineral (mg/100 g)	Egusi flour	Millet flour	Moringa flour	Soybean flour	Sunflower seed-flour
Ca	201.27	822.40	2100.7	0.30	114.00
K	1413.30	470.00	1349.70	1.90	67.00
Mg	957.80	1.70	449.70	0.30	346.00
Na	9.40	510.00	269.70	0.00	0.00
P	2046.40	283.00	259.70	0.70	689.00
Zn	9.60	30.00	8.10	43.30	5.00
Mn	7.70	6.00	3.00	33.30	1.90
Fe	44.40	91.00	31.00	88.90	6.62

Source: (Yousaf et al., 2021;3 Olubi et al., 2024;7)

2.2.2 *Citrullus lanatus* subsp *citroides* (makataan) seeds

Citroides melon, locally (RSA) known as makataan in a wild form, is subglobose, indehiscent, and up to 200 mm in diameter, with a fruit stalk up to 50 mm long (Nkoana et al., 2022;67). The cultivated fruits range from globose to ellipsoid or oblong, measuring 600 mm long and 300 mm in diameter. The rind of ripe fruit is hairless and silky, complex but not woody. The rind is pale or grey-green in the wild species, generally mottled with irregular longitudinal dark green or grey-green streaks (Masoko et al., 2022;1112). In cultivated form, the rind is often concolourous, yellowish to pale or dark green, mottled with darker green, or marbled with a darker shade (Figure 2.5). *Citrullus lanatus* is not threatened; some authors refer to it as the "least utilised crop." This minimal concern level indicates that the species is neither endangered nor threatened but rather underutilised.

Figure 2.6 Makataan melon seeds embedded in its pulp (Mashilo et al., 2022:30)

In South Africa, it is cultivated during the summer and autumn seasons as it thrives in warm conditions (Mashilo et al., 2022;70). Makataan appears in the Namibia desert as a form of weed. It is drought-resistant, thereby needing minimal input during growth. The fruits are mainly used for fodder and citron peel or pectin production. This plant also occurs as a weed in many countries. Southern Africa has cultivated it with other crops such as sorghum and maise. The tender young leaves and fruits are cooked as green vegetables, while the fruit flesh may be cooked as porridge with a main meal. It is also a valuable stock feed, especially in times of drought. The makataan is a subsistence crop predominantly used to make jam in the Western Cape region of South Africa. The fruit's flesh is cut into squares and made into makataan Konfyt (Jam), an established household recipe for the Afrikaans community (Nkoana et al., 2022;68).

2.2.3 *Moringa oleifera* (moringa) Seeds

Moringa Oleifera (*Moringaceae*) is native to the northwest Indian subcontinent and can be found naturally in dry regions of the Thar Desert, India and Pakistan. It grows worldwide in tropical and subtropical climates. Moringa seeds contain oil of 35–45%, with the concentration of oleic acid also reported to be very high (>73%), rendering moringa an economical seed. The oil composition is exceptional in terms of stability. Oxidation tests showed that *Moringa Oleifera* Lam oil was stable at 100l for up to 80h in relevant industries (Elrys et al., 2019;10). The recognition that moringa oil has a high value in cosmetics increased the interest in seed oil production in new areas. Based on the naturalised moringa trees that grow in different ecosystems of Ecuador, including the arid lands, the moringa can be considered a productive alternative for those dry areas that comprise 20% of the country (Pachimalla et al., 2020;14).

The Moringa plant also grows in tropical areas and has broad biotechnological potential, as reported in water treatment, cosmetics, and food use. Although the *Moringa Oleifera* tree is resistant to most pests, it is susceptible to fungi, ants and mainly termites. The protein in moringa seed and its peptide profile suggest their potential use in functional flour production and a possible hydrocolloid yet to be industrialised (Nonfodji et al., 2020;4).

2.3 Applications of Oil Seeds (*Moringa Oleifera*, *Citrullus Lanatus Mucosospermus*, and *Citroides* Melon Seeds) in Food Products

The oil-seeds seeds of *Moringa Oleifera*, *Citrullus Lanatus Mucosospermus,* and *Citroides* Melon have been explored for their use in improving the quality of food in one way or the other, with various good qualities being reported.

2.3.1 Moringa seed

Because of their rich nutritional and functional qualities, which have been well-studied for their applications in food systems, *Moringa oleifera* seeds are an excellent source of hydrocolloids (Guzmán-Albores et al., 2021;2). The seeds have the potential to be used as a fortifying agent in a variety of food products since they contain substantial levels of protein, fibre, ash, and vital minerals.

Research has indicated that using *Moringa oleifera* seed flour (MOSF) instead of wheat flour can greatly increase the nutritious value of baked goods like bread and cookies as shown in Figure 2.7 (Chinma et al., 2014;2204). Mineral concentrations, including calcium, magnesium, and iron, were also improved. Bolarinwa et al. found similar results: fortifying wheat bread with 5–20% MOSF increased the content of protein, fibre, ash, calcium, potassium, and iron while decreasing the amount of carbohydrates. Interestingly, vitamin A concentration also rose dramatically, correcting deficits common in populations with low nutritional levels (Bolarinwa et al., 2019;197).

Moreover, when moringa seed extract was used in the fortification cookies, it was compared to control cookies (Rabie et al.,.2020;8). The cookies fortified with 2.5–7.5% MOSF had higher levels of protein (6.56–7.69%), ash (1.25–1.47%), and fibre (2.38–2.61%), but their carbohydrate content dropped further, improving the product's nutritional profile. Because MOSF contains proteins and polysaccharides, it is a great seed option for hydrocolloid production, which enhances its ability to bind water and gel and potentially serve as an emulsifier in food systems. Adding MOSF to baked goods also helps low-resource groups that suffer from nutrient deficiencies and provides a sustainable way to enhance food quality. The use of MOSF in other flours, like maize or cassava, should be investigated in future research to increase its applicability in various food systems.

Moringa oleifera seeds' strong nutritional and functional qualities have made them a viable source of hydrocolloids for various food items. Because of their essential proteins, pectins, hemicellulose, and other bioactive ingredients, *Moringa oleifera* seeds can be used as natural thickeners, stabilisers, and emulsifiers in food compositions. Dollah et al. (2014) showed that margarine's nutritional and functional qualities were improved by mixing *Moringa oleifera* seed oil (MOO) with other vegetable oils, such as palm olein, virgin coconut oil, and palm stearin. By altering melting behaviour to create zero-trans tougher oil blends, MOO decreased the amount of unwanted fatty acids (such as lauric and palmitic acid), suggesting that it has the potential to be used as a functional oil modifier. According to Nadeem et al. (2018), adding *Moringa oleifera* seed oil to ice cream recipes instead of 10–30% milk fat raised the amount of oleic acid without impairing the product's composition or sensory qualities.

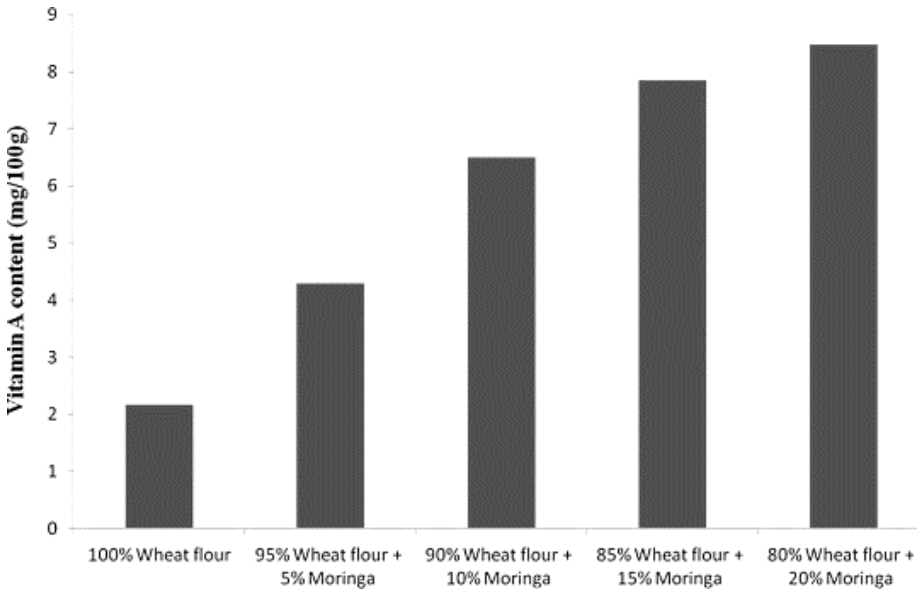

Figure 2.7 Graphical illustration of the vitamin A content of a loaf of bread made from wheat flour compared to those made from a mixture of wheat flour and MOSF with different percentage substitutions (Bolarinwa et al., 2019;198).

As evidence of moringa seed oil's stabilising and antioxidative properties, the substitution dramatically decreased oxidation during storage, with functional ice cream exhibiting a lower peroxide value after three months.

Moringa seed extracts were tested by Cardines et al. (2018) as a yoghurt thickening. The protein content of yoghurts thickened with 0.5%–1.5% moringa seed extract was significantly greater (2.85–3.20 g/100 g) than that of control samples (2.73 g/100 g). The seeds' capacity to thicken was confirmed by microstructural examination, which showed a tight network. This means the seeds can be used as nutritive thickeners to produce yoghurt. Moringa oleifera seeds, which are high in hemicellulose, protein and a source of pectin, perform a variety of uses in food systems as emulsifiers, thickeners, and stabilisers. Their potential to enhance processed foods' nutritional and functional qualities is demonstrated by their use in margarine, ice cream, and yoghurt, establishing moringa seeds as a superior natural source of hydrocolloids. Their use in sustainable food production will grow as more research is done on their various applications and compositional characteristics.

Moringa oleifera's potential as a source of hydrocolloids—protein and carbohydrate combinations that affect their functional qualities, including thickening or emulsifying—is highlighted by its nutritional and culinary uses. Moringa seeds' protein content and

polysaccharides, like hemicellulose and pectin, help them to stabilise emulsions, produce gels, and boost viscosity. The numerous experiments where moringa extracts improved the nutritional makeup of various foods are shown in Table 2.1, highlighting the seeds' dual function as a functional ingredient and a source of nutrients. For example: When bread and biscuits were made with moringa seed flour instead of wheat flour, the texture and stability were improved and the protein, fibre, and mineral content was much boosted. Also, A tight microstructure and increased protein content were produced by the natural thickening action of moringa seed extract.

These illustrations demonstrate the direct correlation between moringa seeds' natural nutritional components—such as proteins and carbohydrates—and their ability to behave as hydrocolloids. *Moringa oleifera* is, hence, a great choice for uses in food systems that call for thickening, stabilising, or emulsifying agents.

Table 2.1 Application of *Moringa Oleifera* Seed Hydrocolloids in Food

Seed Content	Percentage Substitution	Type of Food	Application Type	Summary of Results Obtained	References
Moringa oleifera seed flour	10%; 20% and 30%	Wheat-flour bread	Fortifier	Protein, ash, iron, fibre, magnesium, and Calcium content, as well as the weight of the loaf of bread, increased, while Sodium and Carbohydrate content decreased.	(Chinma et al., 2014)
moringa oleifera seed flour	5%; 10%; 15%; and 20%	Wheat-flour bread	Fortifier	Protein, ash, potassium, iron, fibre, phosphorus, vitamin A and Calcium content of the loaf of bread increased, while Carbohydrate content decreased.	(Bolarinwa et al., 2019)
moringa oleifera seed flour	2.5%; 5.0%; and 7.5%	Wheat cookies	Fortifier	Protein, ash and fibre content increased, while Carbohydrate content decreased.	(Rabie et al., 2020)

Seed Content	Percentage Substitution	Type of Food	Application Type	Summary of Results Obtained	References
moringa oleifera seed oil	30%; 50% and 70%	Margarine	Fortifier	The palmitic, lauric acid, oleic acid and the degree of unsaturation decreased.	(Dollah et al., 2014)
moringa oleifera seed oil	10%; 20% and 30%	Ice-cream	Fortifier, Stabilizer and Preservative	The oleic acid content increased while the Peroxide level decreased.	(Nadeem et al., 2016)
moringa oleifera seed extract	0.5%, 1.0% and 1.5%	Yoghurt	Fortifier and Thickener	A more compact micro-structured yoghurt with increased protein.	(Cardines et al., 2018)

2.3.2 Makataan seed

The seeds of *citroides* melon, which is locally known in South Africa as *makataan*, have been applied to food to improve its nutritional value (Masoko et al., 2022;1112). The use of *citroides* melon seed as a substitution in bakery products has been explored just like that of *moringa oleifera*. In 2015, Wani et al., in a quest to evaluate the possible improvement of the nutritional values of cookies, prepared cookies substituted with *citroides* melon seed proteins with replacement ratios of 2.5%, 5.0%, 7.5% and 10%. Their report observed a significant increase in protein content and a corresponding decrease in the percentage content of carbohydrates in the prepared cookies. The cookies prepared with wheat flour as control showed a percentage protein content of 10.07 ± 0.32%, while the *citroides* melon seed protein substituted cookies had protein content ranging from 11.62 ± 0.19% to 17.48 ± 0.31% based on the degree of substitution and the type of protein applied. The percentage of carbohydrates in the cookies prepared with 100% wheat flour was reported to be 74.72% (Wani et al., 2015;2140).

In comparison, the cookies prepared with the *citroides* melon seed protein had carbohydrate contents ranging from 64.05% to 73.16%, and this was percentage substitution and protein substituted dependent. Notably, the cookies made of 100% wheat flour showed a higher percentage of fibre and ash content compared to the cookies made with the substitution of various percentages of *citroides* melon seed protein, except the fibre content of 7.5% substitution, which showed 1.40 ± 0.05% relative to that of control (100% wheat flour) which was 1.30 ± 0.04% and the ash content of 7.5% substitution of one of the proteins which showed 1.88 ± 0.04% relative to 1.87 ± 0.07% of the control cookies. Hence, the group concluded that using *citroides* melon seed protein as a substitute in the preparation of cookies would significantly improve their nutritional qualities (Wani et al., 2015;2149). Also, another group of researchers led by Kausar et al. (2020) explored the use of *citroides* melon seed flour as an alternative source of protein in the preparation of cookies. The researchers substituted wheat flour with *citroides* melon seed flour with various percentages, which included 10%, 20%, 30%, and 40%. From their report, it can be seen that their results were similar to those obtained by the previous research group, which obtained higher protein content in the cookies prepared with various percentage substitutions using *citroides* melon seed flour (ranging from 9.73 ± 0.15% of 10% substitution to 12.47 ± 0.07 of 40% substitution) compared to the cookies made with 100% wheat flour (8.48 ± 0.16%). The researchers went further to assess the ash and fibre content of the cookies, and a contrasting result was obtained compared to the results obtained by Kausar et al. (2020;208) above. Kausar et al. (2020,202) showed in their report that the ash and fibre contents obtained from the cookies substituted with *citroides* melon seed flour ranging from 1.97 ± 0.02% to 2.36 ± 0.03% (fibre content) and from 1.47 ± 0.01% to 1.85

± 0.03% (ash content) were significantly higher than those of the control cookies with 1.90 ± 0.01% fibre content and 1.40 ± 0.01% ash content, respectively. Like the previous group of researchers led by Wani et al. (2015), this set of researchers also concluded that *citroides* melon seed flour could be applied for cookie preparation to increase the nutritional values such as the ash, fibre, and protein preparation. However, this claim cannot be justified entirely with the results they obtained because, although their results were better than those obtained by Wani et al. (2015), especially in terms of the fibre and ash percentage content, it is necessary to stress that their percentage of substitution were significantly higher than those of Wani et al., (2015). It can, therefore, be argued that there is a possibility of obtaining different sets of results if further optimisation of the substitution process is analysed. Hence, it is encouraged that more critical studies should be carried out to confirm which percentage substitution would give the best outcome (Wani et al., 2015;2153).

Besides cookies, *citroides* melon seed flour has been explored as a substitute for preparing bakery products such as bread and biscuits. In 2022, a study which evaluated the use of *citroides* melon seed flour for the fortification of biscuits was carried out by a group of scientists led by Salem et al. (2022;10). The opinion of the research group was that the substitution of wheat flour using 5%, 10%, 15% and 20% *citroides* melon seed flour in the production of biscuits would yield biscuits with more nutritious values, which was backed by the results obtained from their study (Salem et al. 2022;10). The protein, crude fibre and ash content percentage of the biscuits prepared using *citroides* melon seed flour was found to be significantly higher ($p < 0.05$) than those obtained from the biscuits prepared using wheat flour (Figure 2.6). A contrasting result to the results obtained for protein, crude fibre, and ash was obtained for the total percentage content of carbohydrates present in the biscuits prepared using *citroides* melon seed flour compared to those obtained using wheat flour. It could be observed that there was a decrease in the percentage content of carbohydrates of the biscuits prepared using *citroides* melon seed flour, which ranged from 74.16 ± 0.28% to 78.59 ± 0.62% relative to those obtained from the control biscuits made from 100% wheat flour which showed carbohydrate percentage content of 80.20 ± 0.70% (Salem et al. 2022;16). Given the minor percentage substitutions made by this group of scientists and the significantly different results obtained for the biscuits prepared using *citroides* melon seed flour compared to those prepared using 100% wheat flour, it can be argued that the use of *citroides* melon seed flour can be effective in promoting the nutritive values obtained from biscuits, which is arguably one of the most consumed snacks in the world (Salem et al. 2022;17). Therefore, a rallying call would be that more research should be carried out using different kinds of biscuits and increasing the percentage of substitution to see if the use of *citroides* melon seed flour as a substitute for wheat flour would become an excellent alternative to eating biscuits with high

nutritional value contents. Still, in that same year, another research group investigated the 2.5%, 5.0%, 7.5% and 10% percentage substitutional use of *citroides* melon seed flour for the preparation of bread. Interestingly, the research group reported the percentage protein content of the fortified bread with *citroides* melon seed flour to range from 10.97 ± 0.03% to 12.89 ± 0.00% to be more nutritively valued compared to the control 2.125 ± 0.05% (Bolaji et al., 2022;8).

Table 2.2 Results obtained from using *citroides* melon seed flour as a substitute for wheat flour in baking biscuits. (Salem et al., 2022;15).

Sample	Moisture (%)	Crude Protein (%)	Ether tract (%)	Crude Fiber (%)	Ash (%)	T.C. (Total Carbohydrates) (%)
Control Biscuit	10.06 ± 0.12	7.89 ± 0.30	10.69 ± 0.11	0.40 ± 0.06	1.22 ± 0.07	80.20 ± 0.70
Biscuit + 5% WMSP	9.82 ± 0.10	8.24 ± 0.32	11.62 ± 0.20	1.55 ± 0.08	1.55 ± 0.09	78.59 ± 0.62
Biscuit + 10% WMSP	9.16 ± 0.13	8.45 ± 0.37	12.50 ± 0.19	2.77 ± 0.35	1.82 ± 0.03	77.23 ± 0.44
Biscuit + 15% WMSP	8.99 ± 0.14	8.72 ± 0.11	13.41 ± 0.14	3.08 ± 0.05	2.21 ± 0.06	75.68 ± 0.25
Biscuit + 20% WMSP	8.61 ± 0.19	9.11 ± 0.12	14.25 ± 0.17	4.47 ± 0.06	2.48 ± 0.08	74.16 ± 0.28
Biscuit + 5% GMSP	9.90 ± 0.11	8.17 ± 0.13	11.58 ± 0.33	1.52 ± 0.09	1.44 ± 0.10	78.81 ± 0.26
Biscuit + 10% GMSP	9.33 ± 0.16	8.33 ± 0.33	12.45 ± 0.15	2.72 ± 0.01	1.73 ± 0.05	77.49 ± 0.54
Biscuit + 15% GMSP	9.15 ± 0.14	8.59 ± 0.18	13.36 ± 0.27	3.05 ± 0.09	1.98 ± 0.02	76.07 ± 0.14
Biscuit + 20% GMSP	8.97 ± 0.12	8.97 ± 0.21	14.11 ± 0.01	4.30 ± 0.02	2.33 ± 0.09	74.59 0.64

WMSP: Watermelon seed powder; **GMSP**: Gurma melon seed powder;**T.C.**: Total carbohydrates
values with the same superscripts in columns indicate no significant difference ($p < 0.05$).

Contrastingly, the total ash content per cent and carbohydrate content of the *citroides* melon seed flour was reported to have decreased relative to the control. This was shown from their results of ash content for *citroides* melon seed flour, which ranged from 1.69 ± 0.00% to 3.60 ± 0.01% as against 3.82 ± 0.06% of the control, and the carbohydrate percentage content results ranging from 65.31 ± 0.02% to 70.77 ± 0.02% compared to 72.83 ± 0.05% of the control (Bolaji et al., 2022;13). Even though the results of the carbohydrates obtained are lower than those obtained from the control, they are seen to be a positive decrease, unlike the ash content, which is considered a negative out-turn.

Table 2.3 Application of *Citroides* Melon Seed Flour in Food

Percentage Substitution	Type of Food	Application Type	Results Obtained	References
2.5%; 5.0%; 7.5% and 10%	Cookies	Fortification	A non-significant increase in nutritive values was recorded.	(Wani et al., 2015)
10%; 20%; 30%; and 40%	Cookies	Fortification	A significant increase in nutritive values was recorded.	(Kausar et al., 2020)
5%; 10%; 15% and 20%	Biscuits	Fortification	A significant increase in nutritive values was recorded.	(Salem et al., 2022)
2.5%; 5.0%; 7.5% and 10%	Bread	Fortification	A significant increase in nutritive values was recorded.	(Bolaji et al., 2022)

From the above applications of *citroides* melon seed flour, although they all used substitution of a similar percentage range except for Kausar et al. (2020), which used up to 40% substitution, it can be gathered that there was a consistent increase in the protein content percentage of all the various types of food evaluated, as well as a consistent decrease in the rate of carbohydrates. However, contents like ash fibre have seen their percentages fluctuate from increase (Kausar et al., 2020;212; Salem et al., 2022;15) to decrease (Bolaji et al., 2022;8), depending on the study, as well as a study showing both increase and decrease in the fibre content percentage, depending on the rate of substitution. This, therefore, calls for more studies to be carried out to authenticate these contrasting results for consistency's sake and to enable their applicability in the industry for producing these foods.

2.3.3 Egusi seed

The seed of *Citrullus lanatus* subsp *mucosospermus*, popularly known as egusi melon seed in the western part of Africa, has also been investigated for its use in the fortification of food (Paudel et al., 2019;3). In 2021, a group of scientists explored the physiochemical properties of some prepared biscuits, which were modified using the flour of selected tuber crops such as cassava, sweet potato, Irish potato, and yam and fortified using the egusi melon seed. According to their results, the nutritive contents of the various biscuits, such as the protein content, fibre content, and ash content, varied in their percentage content but were, however, higher in content compared to the control biscuits, which were prepared from wheat flour (Gervase & Oyiza, 2021;197). Also, they further observed a decrease in the percentage content of the carbohydrates in the fortified biscuits compared to those of the control, as shown in Figure 2.7 below. Thus, the research group concluded that they could produce a nutritionally enhanced biscuit with the help of egusi melon used for their fortification. This result, however, agrees with the other results obtained using other oil seeds, as discussed above in subsection 2.3.2. Hence, it could be safe to conclude that these oil seeds could be used to improve the nutritive values of biscuits and other kinds of food. However, it is vital to be aware of the need for more studies to be carried out using these oil seeds as they still need to be explored (Gervase & Oyiza, 2021;198). With the benefits and application of oil seeds being emphasised, the European Union (EU) mandates that oilseed products, particularly those marketed as protein-rich or used as protein sources, must accurately label their protein content. This regulation protects consumers by ensuring they receive the nutritional value advertised on the product and protects public health. More so, they will encourage sustainable farming as the rules help prevent the dilution or adulteration of oilseed products with non-protein fillers. This ensures that the products meet specific quality standards and maintain nutritional integrity.

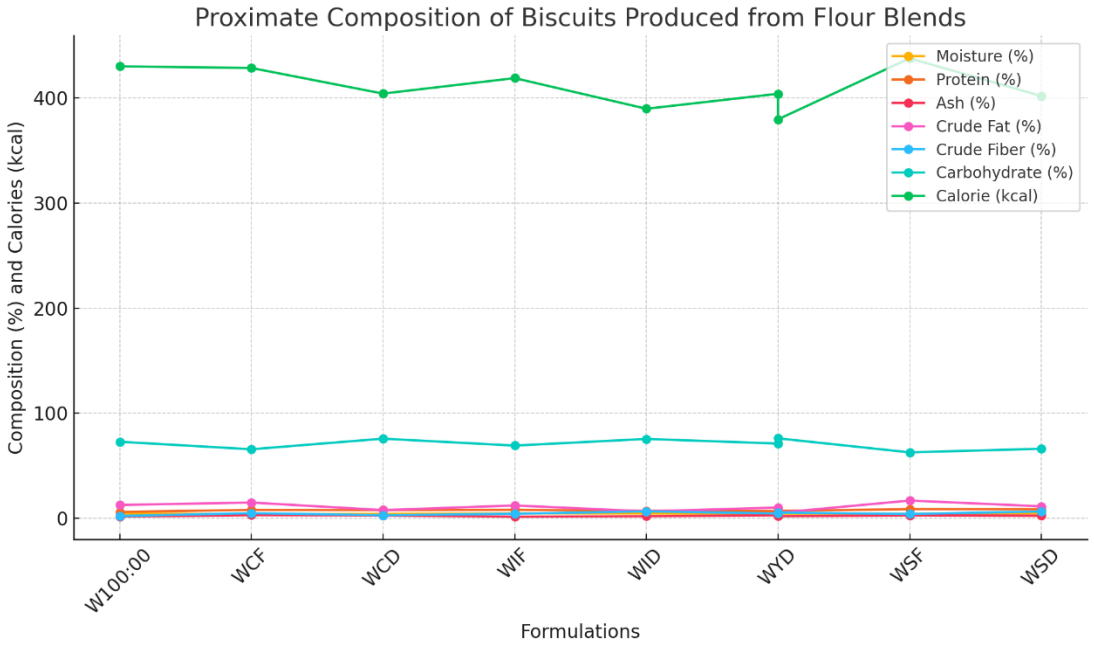

WCF - Wheat (65%), Cassava (25%), Full-fat melon seed meal (10%); WCD - Wheat (65%), Cassava (25%), Defatted melon seed meal (10%); WIF - Wheat (65%), Irish potato (25%), Full-fat melon seed meal (10%); WID - Wheat (65%), Irish potato (25%), Defatted melon seed meal (10%); WYD - Wheat (65%), Yam (25%), Defatted melon seed meal (10%); WSD - Wheat (65%), Sweet potato (25%), Defatted melon seed meal (10%); WSF - Wheat (65%), Sweet potato (25%), Full-fat melon seed meal (10%)

Figure 2.8 Results Obtained from the use of egusi melon seed flour for the fortification of biscuits prepared using wheat and modified using tuber crops

2.4 European Union (EU) Oilseed Hydrocolloid Protein Regulation

The EU has stringent regulations for using food components, including hydrocolloids. These regulations ensure food products are safe for consumption and meet specified quality standards (Viebke et al., 2014;2; Pant et al., 2021;2). The EU has implemented maximum protein concentration limits to ensure that hydrocolloid proteins derived from oilseeds are used effectively without jeopardising food safety. The EU requires hydrocolloid proteins to meet particular safety standards, such as being free of heavy metals, pesticides, and microbiological toxins. This is especially critical for oilseed-derived hydrocolloids, as processing processes (such as solvent

extraction) might introduce pollutants. The EU sets maximum protein content limits for hydrocolloid components to prevent high protein levels from compromising food functionality or posing health hazards (Pirsa & Hafezi, 2023;2). These limitations vary depending on the type of hydrocolloid and its intended use in food formulations. Products containing hydrocolloid proteins must be appropriately marked, specifying the hydrocolloid source (e.g., soy, sunflower) and the protein concentration. This transparency guarantees that consumers are aware of the contents of their food and can make decisions based on dietary requirements or preferences. Hydrocolloid proteins must adhere to the EU's Food Additive Directives, which govern all food additives, including stabilisers and emulsifiers. These directives specify permitted levels and conditions for using hydrocolloids.

2.4.1 Nutritional components of seed-based hydrocolloids

Seed-based hydrocolloids, derived from various seeds such as flaxseed, chia, psyllium, and guar, are gaining popularity in the food industry due to their functional properties and nutritional benefits. These natural polymers can form gels, thicken liquids, and stabilise emulsions, making them valuable ingredients in food formulations. Beyond their functional roles, seed-based hydrocolloids contribute significant nutritional value to food products (Li & Nie, 2016;3).

Dietary fibre is an essential nutritional component of seed-derived hydrocolloids. Many seed-based hydrocolloids, including those derived from flaxseed, psyllium, and guar, include soluble fibre. This fibre dissolves in water, generating a gel-like substance to help lower cholesterol and regulate blood sugar. (Hedayati et al., 2022;2). The increased fibre content also aids digestion by increasing stool size and encouraging intestinal regularity. Flaxseed and psyllium hydrocolloid is an emerging hydrocolloid that is still being investigated, but soybean remains the only confirmed industrialised hydrocolloid with stabilising properties found in lecithin rich in both soluble and insoluble fibre; flaxseed hydrocolloid supports digestive health and can aid in weight management by promoting a feeling of fullness. These oilseed hydrocolloid alternatives contain soluble fibre; psyllium is known for its potential to decrease cholesterol and enhance glycaemic control, making it beneficial for heart health and diabetes management (Hedayati et al., 2022;2).

While seed-based hydrocolloids are often low in protein, some seeds, such as flaxseed and chia, contain a small amount of plant protein. These proteins contribute to the overall nutritional profile and contain essential amino acids required for various biological processes. Seed hydrocolloid contains more protein than most other seeds, including all nine necessary amino acids, making it a complete protein source (Sahraeian et al., 2023;5). The micros nutrient embedded in these oil seeds contains hydrophobic and hydrophilic amino acids, constituting its functional properties, such as solubility, gel formation, and emulsification. Hydrophilic amino acids

have side chains that interact well with water, making them soluble in aqueous environments. These amino acids contribute to the ability of hydrocolloids to dissolve or swell in water, which is essential for their use as thickeners, stabilisers, and gelling agents. An example of glutamine is an amide group in its side chain, making it highly soluble in water. It plays a role in maintaining the structure and stability of proteins in aqueous solutions. Serine is another example of a hydrophilic acid with a hydroxyl group in its side chain, making it polar and able to form hydrogen bonds with water molecules, enhancing the water-binding capacity of the hydrocolloid (Pachimalla et al., 2020;15).

Hydrophobic amino acids have side chains that do not interact well with water; hence, they avoid watery environments. These amino acids typically cluster inside the protein structure, reducing their exposure to water (Raj & Bajpai, 2020;2). This activity is essential for generating hydrophobic contacts, which can influence hydrocolloid emulsification and gelation qualities. Leucine and isoleucine are examples of a hydrophobic protein with similar structures, as they possess an aliphatic side chain that is both non-polar and hydrophobic. It promotes hydrophobic interactions, which help to stabilise protein structures. Phenylalanine has a hydrophobic aromatic chain, affecting its protein structure's stability (Aderinola et al., 2020;5).

The balance between a hydrocolloid's hydrophobicity and hydrophilic tendencies depends solely on the ability to form gels, stabilise emulsions, and bind water, depending on the balance between hydrophilic hydrophobic amino acids. These interactions affect the overall stability of an emulsion.

2.4.2 Functionality of oilseeds as a hydrocolloid

Soybean is a major protein source in the human diet. Snack bars, gluten-free baked goods, and meat analogues contain traditional ingredients like tofu, soy milk, natto, tempeh, and recently developed foods. All of this has made soybean protein a key component in food systems. One of the primary benefits of soybeans is that they contain more protein than any other crop and have well-balanced necessary and non-essential amino acids. Soybean is a major protein source in the human diet. Snack bars, gluten-free baked goods, and meat analogues contain traditional ingredients like tofu, soy milk, natto, tempeh, and recently developed foods. All of this has made soybean protein a key component in food systems. One of the primary benefits of soybeans is that they contain more protein than any other crop and have well-balanced necessary and non-essential amino acids. (Florowski et al., 2019;105). Soy protein has been utilised to make beverages, ice cream, extruded items, dairy alternatives, and meat substitutes. Soy protein has been utilised to make beverages, ice cream, extruded items, dairy alternatives, and meat substitutes. This appeal stems from the protein's varied functional qualities, which may be quantified as solubility, water/oil absorption, foaming, emulsification, and gelation (Raimets et al.,

2020;124). These same functionalities can be reported for moringa, egusi and makataan hydrocolloids, which could be proffered as emerging hydrocolloids in the food and non-food industry. They are easily cultivated, exhibit more user-friendly potential and offer affordable nutritional benefits.

According to past research, *Citrullus lanatus M* (egusi) hydrocolloid is a stabiliser/emulsifier yet to be explored in the food industry. (Olubi, 2018;10). As seen in Figure 2.2, most hydrocolloids exhibit a creamy-white colour; they have a small particle size. They completely dissolve in solution at room temperature or above 70^{o}C, providing a stable emulsion (Olubi, 2018;75). Olubi (2018;71) reported that nine sugars were present in defatted egusi flour, with sucrose being the highest in defatted egusi flour (106 4-109.4 mg/l).

Figure 2.9 (A) Egusi gum: (B) Xanthan gum: (C) Guar gum (Olubi, 2018:192)

Sucrose is a disaccharide composed of two monosaccharides, glucose and fructose, having the chemical formula $C_{12}H_{22}O_{11}$. In humans, sucrase or isomaltase glycoside hydrolases convert sucrose to monosaccharides, glucose, and fructose. Food high in sucrose exhibits good emulsifying properties due to its ability to bond surfaces (Ciurzyńska et al., 2020;7). The systematic investigation into the long-term stability characteristics of novel hydrocolloid sources emerging in the food industry will help improve understanding of their functional properties. Still, it will also help to increase their utilisation, thereby increasing recognition of their vast potential as indispensable constituents in food formulations.

2.5 The Stability and Rheological Properties of Emulsion-based Food Products

The stability of food emulsions is strongly influenced by the droplets' concentration characteristics and other food ingredients' interactions (Zhao et al., 2019;3). Emulsifiers and thickeners contribute to foods' structural and textural properties through aggregation and gelation behaviour. Proteins are generally known for their emulsifying capacity (EC) and foaming ability. Proteins reduce the interfacial tension between immiscible liquids due to their adsorption at the interface. Indeed, they can form films at the droplet surface, providing electrostatic repulsion between the droplets.

On the other hand, polysaccharides are utilised as stabilisers, thickeners, and gelling agents due to their ability to retain water and thicken. Protein-polysaccharide biopolymer complexes are renowned for their hydration, gelation, and excellent interfacial characteristics. These qualities can be used to create new cuisines in composites or as full meals. These charged colloidal particles interact, forming particulate dispersions, foams, gels, and emulsions based on their nutritional components.

Sucrose, a complex sugar, is a readily absorbed macronutrient that provides an immediate energy source. Sucrose, a pure carbohydrate, contains 3.87 kilocalories per gramme (Gomes et al., 2020;5;6). Sucrose has significant emulsifying properties in meals, providing a thickening effect. A good gel's qualities are defined by its ability to react thoroughly with water, resulting in a coagulated gel of a clear gel. Proteins with non-polar residue form a coagulated gel, whereas amino acids that melt in water form a translucent gel (Paudel et al., 2019;7).

The water and oil-holding capacities of defatted egusi flour are 0.7 and 2.6 mL/g, respectively (Olubi, 2018:72). As a result, egusi provides thickening properties through its capacity to create a gel. A polysaccharide's hydrophobicity increases as its contact with water decreases. The hydroxyl group in carbohydrates interacts preferentially with two water molecules, resulting in less interference or interaction with other hydroxyl groups. The rheological and stability features of egusi hydrocolloid in an oil-in-water emulsion will lead to more food use of defatted egusi flour. A new food solution will solve the food security problem associated with today's world. Keisandokht *et al.* (2018) have recently studied the extraction of hydrocolloids with a low pH solvent (pH 4), resulting in higher yield in both microwave and conventional extractions compared with high pH extraction (pH 11) (Horstmann et al., 2018;2).

2.3.1 Application of hydrocolloids in the food industry

In 1983, the United Nations' World Commission on Environment and Development used the term "sustainable development" to address social, economic, and agricultural challenges (Kowalska et al., 2015;5). The food industry's sustainable development principles include providing people with safe, affordable, nutritional food. Food that has a beneficial environmental impact on

agricultural production by conserving natural resources and fostering biodiversity, as well as a healthy climate, safe water, and land. Furthermore, by striving to reduce energy consumption,.0 utilising renewable energy sources to eliminate waste and losses of food components, optimise the supply chain, and reuse byproducts.

The carbon footprint (CF), also known as the "Ecological Footprint" in the field of food production and distribution, is defined as the "total amount of greenhouse gas emissions expressed in carbon dioxide equivalents for a product." CF monitors the raw material's life cycle from storage to disposal; it is measured per kilogramme of a product or unit of area per year (Ciurzyńska et al., 2020;5). The carbon footprint is critical to the producers' image and competitive strategy. However, the ecological assessment of corresponding phases and operations in food production indicators is difficult due to various technical processes and the complexity of environmental impact. The principal carbon footprint of this economic sector comes from energy use in production, raw material transportation, semi-finished and finished products, and packaging. The *product's CF indicator* results from all possible interactions related to all the links that make up the food chain; this gives the extraction of hydrocolloids a vital extension to the production cycle (Ciurzyńska et al., 2020;7).

Food is regarded as a pillar industry inextricably linked to people's lives. Food is vital for economic and social development (Marx et al., 2021). Along with enhancing quality of life and a faster pace, food preferences are shifting from quantity and nutrition to pleasure and health advantages. Customised food products targeting specific groups and providing desired functionality are becoming increasingly significant. For example, the world is seeing an increasing rate of population ageing (Lu et al., 2020). According to epidemiological research, 11% of the global population is over 60, which is expected to climb to 22% by 2050 (Kanasi, Ayilavarapu, & Jones, 2016). As a result, producing specially developed diets for the elderly is urgently needed (Fehlings et al., 2015).

Furthermore, foreign body aspiration (FBA), a serious problem worldwide, is a significant cause of death by asphyxia in newborns and children (Aihole, 2020;2). When a foreign body, such as a small toy, food particle, or other object, enters the airway, it can block airflow to the lungs. Infants and young children's airways are thinner and more easily clogged, rendering them particularly vulnerable to FBA. Furthermore, infants of this age typically investigate their surroundings by placing objects in their mouths, increasing the risk of inadvertent aspiration (Aihole, 2020;2). Food hydrocolloids (polysaccharides, proteins, or lipids) can be thought of as the skeleton of food structures, and their rheological implications and impacts are being explored (Kelly et al., 2020; 7). These functional characteristics pervade all food processing, flavour, nutrition, and health advantages. As a result, investigating the theory and methodology of modern food structure design from the perspective of food hydrocolloids while taking into account the

interconnection of sensory, nutrition, and health benefits provides significant scientific significance and application value (Ajanth Praveen et al., 2019;4).

2.3.2 Functional uses of hydrocolloids

Due to the complexity of hydrocolloid structure and potential interactions with starch and protein molecules, these colloid systems remain an unexplored research topic. Because of the complexity of hydrocolloid structure and potential interactions with starch and protein molecules, these colloid systems remain an underexplored study area. There is a significant research gap, especially concerning their structure-function correlations under specific mechanical situations such as shear, resulting in new food products with distinct sensory and nutritional qualities (Semenova et al., 2021;4 Lupo et al., 2015;2). Besides inducing electrostatic interactions of hydrocolloids by the difference in their molecular flexibility, which affects starch paste/gel properties because of the stiffness and surface properties.

Few research has investigated how shear forces affect the paste/gel properties of starch-hydrocolloid systems (López-ramírez & Duarte-sierra, 2020;1; McClements, 2021;3), although shear occurs during food processing, ingestion, and digestion. A hydrocolloid's properties are not restricted to shear stress and shear rate (Gibouin et al., 2022;6). The nutritional makeup has a considerable impact on how they behave throughout processing. These nutritional qualities behave differently when shear force is not applied (Leverrier et al., 2021;2). These nutritional qualities will influence how droplets form if hydrocolloids are used to make oil-in-water emulsion goods like mayonnaise, salad dressing, and spreads. An emulsion is a thermodynamically unstable system comprising two immiscible liquids: oil and water. These immiscible chemicals can destabilise a stable system over time via physicochemical mechanisms such as creaming, flocculation, coalescence, and phase inversion (Sabri et al., 2019;3).

The internal composition of the stationary phase during emulsion formation can cause mixture instability (Nejadmansouri et al., 2020;4). As a result, the physical stability of valuable emulsions has the greatest influence on their shelf life. Emulsifiers and thickeners are typically used to improve emulsion stability (ES) or make it kinetically stable (Lei et al., 2019;8). The concentration and characteristics of the droplets used in emulsion-based food products have a strong influence on their stability, physicochemical properties, and sensory properties, as can be seen from effects on other food ingredients and their interactions (Angkuratipakorn et al., 2020;4; Zhu et al., 2020;3). Emulsifiers and thickeners improve meals' structural and textural qualities by aggregating and gelling them (Yousefi & Jafari, 2019;468). Complexation of proteins with macromolecules is an efficient technique for increasing protein functional characteristics. The features of protein-polysaccharide biopolymer complexes, such as hydration (solubility and

viscosity), structuration (aggregation and gelation), and interfacial phenomena (foaming and emulsifying), can be used to make new foods.

2.4 Emulsions and Uses

The word "emulsion" comes from the Latin *emulgere,* which means to "milk out " The emulsion from oil-seed species like egusi and makataan can be compared with other known hydrocolloids, which could be from microorganisms, animals and some plant species (REF). The hydrocolloids from a high protein source have higher stability, solubility, and emulsifying tendencies, but they remain known with some selected sources (Zhao et al., 2018;544). These physicochemical properties indicated that the egusi hydrocolloid has advantages in forming a stable droplet. Hydrocolloids of interest are often found in the components of microbial, animal, and some prime plant seeds due to their constructive physicochemical, functional, rheological and biological properties. These properties of the known hydrocolloids are but are not limited to bio-flocculants, bio-emulsifiers, gelling agents, bio-stabilisers, de-pollution agents, anticoagulants, antioxidants, anti-inflammatory agents, antithrombotic, immunomodulation and anti-cancer agent (Kavitake et al., 2019;445). Lactic acid bacteria (LAB) hydrocolloids have attracted more attention as they are generally considered safe. However, the major limitation to the most preferred hydrocolloid is the unaffordable price at which it is sold; also, availability can sometimes depend on importation. Therefore, there is a need to produce hydrocolloids from plant sources that could be more cost-effective and readily available.

Storage stability is an essential indicator in controlling the quality of the oil-in-water emulsion. Storage stability is a vital emulsion property according to the type and method of emulsion preparation. Therefore, storage stability is an age-old issue in the field of asphalt emulsion. Past work showcases the storage stability of different emulsions (Jiang & Charcosset, 2022;5). These works mainly focused on the effect of production parameters on the storage stability as an emulsifier type and consumption dosage. These past studies clarify obtaining an oil-in-water emulsion with good storage stability by considering production parameters, compositional tendencies and overall functionalities.

2.5.1 Rheological properties of an emulsion

Rheological characteristics are mechanical properties that produce deformation and material flow in the presence of stress, and they encompass two critical features of the food system: flow behaviour (viscosity) and solid mechanical properties (texture). Viscosity, often known as dynamic viscosity, refers to the internal friction or resistance to flow. Viscosity increases in colloidal suspensions by thickening the liquid phase due to liquid absorption, which causes expansion of the dispersed colloid. Furthermore, the viscosity of the hydrocolloid system is

determined by several factors, including concentration, temperature, solvation, electrical charge, degree of dispersion, previous thermal or mechanical treatment, the presence or absence of other lyophilic colloids, the age of the lyophilic sol, and the presence of both electrolytes and nonelectrolytes (Dendrobium et al., 2020;4 Liu et al., 2021;2). Many scholarly articles have been published on the rheological characterisation of emulsifiers, which includes all types of hydrocolloids, but only a few research have concentrated on hydrocolloids with nutraceutical effects. As a result, there is an urgent need to investigate hydrocolloid alternatives that provide nutraceutical advantages.

Texture is an organoleptic characteristic that determines the palatability of foods. Food texture profiles include hardness, chewiness, gumminess, adhesiveness, cohesiveness, and springiness (Sahin & Sumnu, 2006, 3). tactile has a significant impact on consumer acceptability of food products since individuals enjoy eating and experiencing tactile changes. Furthermore, texture is important to elderly people and individuals with mastication and swallowing issues who must consume texture-controlled foods such as thickened liquids, pastes, and soft gels. Food hydrocolloids are the primary components (Singh et al., 2019;4; Dendrobium et al., 2020;2). Besides the foods above, most processed products can be modified by adding hydrocolloids to modify their texture. Surface properties are connected with colloidal systems in foods and categorised into gel, emulsion, and foam based on the states of matter in the continuous and dispersed phases. Viscosity and surface activity constitute numerous functions of hydrocolloids in foods. The following are the main functional properties of hydrocolloids.

2.5.2 Thickening property of an emulsion

Hydrocolloids' tendency to thicken typically limits their wide range of applications. When utilising hydrocolloids as emulsifying, stabilising, and bodying agents in foods, the fundamental feature is their thickening property known as viscosity enhancement. Thickeners are classified as functional food additives for labelling purposes, together with thickening agents, texturisers, and bodying agents for technological functions, according to class names and the international numbering system for food additives adopted from the Codex Alimentarius Commission. Thickening occurs above a known concentration known as overlap concentration (C*). The hydrocolloid dispersion acts like a Newtonian fluid below this concentration but not above it (Zhu et al., 2020;6).

Starch is the most widely used hydrocolloid thickener since it is inexpensive and may not contribute to a noticeable taste when used at a low concentration of 1-2.5% (Zheng et al., 2019;550; Dangi et al., 2019;388). In general, natural starch has low water solubility and is therefore limited in industrial uses. Because of the relationship between structure and functionality, modified starch has been investigated to create structures with specialised functionalities. Gelatin melts are substantially lower in temperature because weak hydrogen

bonds, surface activity, and emulsification qualities hold together the junction zones. The infinite combinations of various food components are organised and arranged in complex internal microstructures with diverse assemblies such as dispersions, gels and emulsions. The emulsifier can be a single or a combination of chemical species that facilitate emulsion formation and two-phase stability. The traditional view is that excellent emulsifiers, such as protein emulsifiers, have flexible molecular architectures that allow for rapid adsorption and rearrangement at the interface, resulting in a coherent macromolecular protective layer (Collado-González et al., 2019;6). As a result of their hydrophilicity, large molecular weight, and gelation tendency, stiff hydrocolloids are classified as thickeners rather than emulsifiers.

2.5.3 Properties of a diluted food emulsion

Dilute emulsions are systems with a dispersing phase with volume fractions below 0.02 (i.e., 2%) (Kitunen et al., 2019;156; Sabri et al., 2019;5). Because the emulsion droplets are so far apart, they interact rather weakly under these conditions (Figure 2.3). As a result, one droplet's ability to disrupt the continuous phase's flow pattern does not affect another droplet's flow pattern. As a result, the continuous phase's rheological properties dominate the apparent viscosity of diluted emulsions. Emulsion rheology studies the flow or deformation of emulsion-based fluids or solids in response to applied forces. Understanding the principles and techniques of rheology is critical since it enables the creation of useful analytical tools to investigate emulsion characteristics. These methodologies also assess the impact of physicochemical qualities, sensory features, and nutritional value of emulsion-based meals such as dressings, mayonnaise, creams, milk, sauces, and soups (McClements, 2015;3). For example, a product's low-calorie version could have the same rheological qualities as its original high-calorie counterpart.

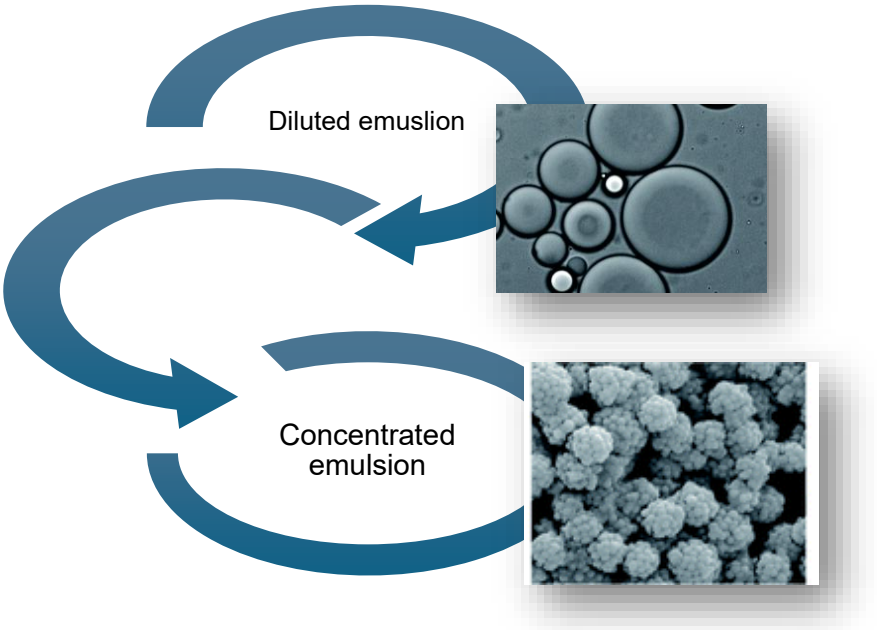

Figure 2.10 Changes in rheological behaviour of emulsion with change in volume/concentration fractions

Albert Einstein developed the famous equation for expressing the apparent viscosity of dilute colloidal suspensions as a function of particle concentration (Manzoor et al., 2020;4; Sharma et al., 2019). Einstein analytically calculated the frictional losses when an ideal fluid flows past an isolated rigid sphere, resulting in the following simple statement. Equation 1 describes dilute emulsions' complex shear modulus (G*[ω]) during an oscillatory sweep test.

$$G^{*}(\omega) = Gc^{*}\,\omega\left[1+5\Phi H^{*}\right]\omega \qquad 1$$

In Equation 2, GC * (ω) represents the continuous phase's complex shear modulus, while H* (ω) is a frequency-dependent quantity that can be derived as follows:

$$H_{D}^{*} = \left[\frac{\left[G_{D}^{*}(\omega) - G_{C}^{*}(\omega)\right]\left[19G_{C}^{*}(\omega) + 16G_{C}^{*}(\omega)\right] + (4Y/R)\left[5G_{D}^{*}(\omega) + 2G_{C}^{*}(\omega)\right]}{\left[2G_{D}^{*} + 3G_{C}^{*}(\omega)\right]\left[19G_{D}^{*}(\omega) + 16G_{C}^{*}(\omega)\right] + (40Y/R)\left[G_{D}^{*}(\omega) + G_{C}^{*}(\omega)\right]}\right] \qquad 2$$

In this expression, γ represents the interfacial tension of the oil-water contact, R is the droplet radius, GD * (ω) is the complex shear modulus of the dispersed phase, and ω is the oscillation frequency. Equation 3 describes the viscosity of the colloidal suspension.

$$\eta = \eta_c \left(\frac{1 + 2+5\lambda}{2\ (1+\ \lambda)}\right)\ \phi \qquad 3$$

In this expression, γ represents the interfacial tension of the oil-water contact, R is the droplet radius, GD * (ω) is the complex shear modulus of the dispersed phase, and ω is the oscillation frequency. Equation 3 describes the viscosity of the colloidal suspension.

2.4.4 Rheology of concentrated emulsions

Rheological studies help understand the molecular structure or distribution of food components and forecast and describe structural changes in foods during production (Kumar et al., 2018;3). As a result, food rheology can provide useful information for product development, quality control, sensory evaluation, and process design. Oscillatory rheology measurements are frequently employed to study the viscoelastic behaviour of a food system (Wei et al., 2020;3). Small amplitude oscillatory shear (SAOS) studies are one of the most significant forms of dynamic rheological tests because they vary stress and strain harmonically with time in the linear viscoelastic region (LVE) (Wang et al., 2022;7). Gels are viscous materials (Kornet et al., 2021;4). As a result, dynamic rheological measurements can be used to assess gel systems' properties and investigate gel characteristics such as gelation and melting. Rheological properties can be retrieved, including the storage modulus (G'), loss modulus (G''), and loss factor (tan d ¼ G''/G'). Small amplitude oscillatory shear (SAOS) studies are one of the most significant forms of dynamic rheological tests because they vary stress and strain harmonically with time in the linear viscoelastic region (LVE) (Wang et al., 2022;7). Gels are viscous materials (Kornet et al., 2021;4). As a result, dynamic rheological measurements can be used to assess gel systems' properties and investigate gel characteristics such as gelation and melting. Rheological properties can be retrieved, including the storage modulus (G'), loss modulus (G''), and loss factor (tan d ¼ G''/G'). Many researchers have explored the dynamic rheological properties of various starch gels in the LVE based solely on the aforementioned parameters (by frequency sweep measurements), ignoring the other relevant dynamic rheological factors (Theocharidou et al., 2022;8). These dynamic rheological factors, such as strain limiting value and gL, result in stress at the LVE range's limit (ty). Stress/strain sweep measurements can determine flow point stress (tf) and modulus (Gf: G0 ¼ G'') (Gürgen, 2019; Lei et al., 2019;2). The specified values were determined for polysaccharides, such as Lepidium perfoliatum seed gum (Hamdani et al., 2019; 48).

The majority of natural food emulsions are semi-dilute or robust systems with high droplet-droplet interaction. In other words, the disruption of fluid flow induced by one droplet affects fluid flow around another droplet. In general, the apparent viscosity of these more concentrated emulsions is more than predicted by Einstein's equation because energy dissipation is better than expected (Zhu et al., 2020;5). In the semi-dilute zone, viscosity typically increases somewhat with

increasing dispersion phase volume percentage but then increases steeply when the emulsion becomes so concentrated that the droplets are packed closely together and cannot easily move past each other (Zhu et al., 2020;4). The rheological properties of colloidal dispersions are intimately related to their dispersed phase volume percentage.

2.4.4.1 Herschel–Bulkley fluid

The Herschel Bulkley model is a generalised model of a non-Newtonian fluid in which the strain experienced by the fluid is connected to stress in a complex, non-linear manner. This connection is defined by three parameters: consistency (k), flow index (n), and yield shear stress (Lin et al., 2024;667). The consistency is a basic constant of proportionality, and the flow index measures the degree to which the fluid is shear-thinning or shear-thickening. Ordinary paint is one example of a shear-thinning fluid, while oobleck provides one realisation of a shear-thickening fluid. Finally, the yield stress quantifies the amount of stress the fluid may experience before it yields and begins to flow. The Herschel Bulkley model is represented by equation 4.

$$\tau=\tau_o+[k(y)]^n \qquad 4$$

Rheological properties of *CLM, lanatus citroides,* and *Moringa Oleifera* seeds, as emergent functional oil seed hydrocolloids, can be investigated using the Herschel-Bulkley model.

This model generalises the behaviour of non-Newtonian fluids, which contain a wide variety of substances, including hydrocolloids. The Herschel-Bulkley model describes the complex, nonlinear relationship between the strain experienced by the fluid and the stress applied to it (Fernandes et al., 2024). This relationship is defined by three fundamental parameters: Consistent k (Wei et al., 2022)): The Herschel-Bulkley model uses this parameter to represent a proportionality constant. The consistency factor for new functional oil seed hydrocolloids such as CLM, *Lanatus citroides*, and *Moringa Oleifera* seeds may indicate their innate capacity to create stable colloidal dispersions when mixed with water or other solvents (Gibouin et al., 2022).

The flow index (n) describes the degree of shear-thinning or shear-thickening behaviour exhibited by the fluid. Shear-thinning fluids, such as conventional paint, lose viscosity as shear rates increase, whereas shear-thickening fluids, such as oobleck, gain viscosity (Lin et al., 2024). The flow index could provide light on the behaviour of hydrocolloid solutions formed from these seeds, providing information about their rheological properties and prospective applications in various food and commercial formulations. The flow index (n) describes how much the fluid shear-thins or thickens. Shear-thinning fluids, like traditional paint, lose viscosity as shear rates rise, while shear-thickening fluids, like oobleck, gain viscosity (Wei et al., 2019). The flow index could

provide light on the behaviour of hydrocolloid solutions derived from these seeds, providing information on their rheological properties and potential applications in a variety of culinary and commercial formulations. Finally, yield shear stress refers to the minimal tension required for the fluid to begin flowing. The yield shear stress of developing functional oil seed hydrocolloids demonstrates how these materials transition from static to flowing states (Wei et al., 2022). Understanding this characteristic can assist you in optimising processing parameters and forecasting the stability and performance of hydrocolloid-based products. The Herschel-Bulkley model can provide researchers with significant insights into the rheological behaviour of CLM seed, *Lanatus citroides*, and *Moringa Oleifera* seeds, paving the path for their use in a wide range of applications from food formulation to industrial processes.

2.4.4.2 Power Law

Power law (Equation 4) describes scalar relationships between two quantities.

$$y=axk \qquad 5$$

Where a is a constant, k (also a constant) is the exponent of the power law and x is the independent variable

Power law relationships appear as straight lines on log-log plots because the preceding equations are transformed into log(y) = log(x) + log(a), which is the same form as the equation for a line (Liu et al., 2022;7). In contrast to fractals, which deal with self-similar geometrical objects, power laws characterise scale-invariance of multivariate relationships or frequency distribution for descriptive aspects of the geographic phenomenon (Kino et al., 2021;4). The rank-size rule of city-size distributions is a well-known empirical example of a power law defined as Pk = P1k-b, where Pk is the size of the kth largest city, P1 is the size of the largest city, and b is the power law's exponent (negative). There is no distinctive scale (size) for the investigated events that follow a power law distribution. This lack of specific characterisation differs from the typical, bell-shaped distribution, in which the mean can be taken as the characteristic scale. Research identifying scale-free social and geographic networks has grown interest in power laws.

The possible development of CLM seed, *Lanatus citroides*, and *Moringa Oleifera* seeds as functional oil seed hydrocolloids can be explained using power laws, which are useful for comprehending multivariate relationships and frequency distributions within geographic phenomena. Because of the logarithmic transformation of equations, power laws show as straight lines on log-log graphs, giving them a linear equation-like shape. This transformation makes it easier to recognise scale-invariant interactions, which occur when the scale changes but the

underlying pattern remains constant (Fernandes et al., 2024;3). Notably, occurrences with a power law distribution lack a characteristic scale or magnitude, as opposed to the conventional bell-shaped distribution, which uses the mean as the identifying scale. Power laws have grown in prominence because of their relevance in delineating scale-free social and spatial networks, in which the structure of links between entities remains consistent across scales. Researchers employed power law principles to examine CLM, CLC, and *Moringa Oleifera* seeds as potential useful oil seed hydrocolloids. This transformation makes it easier to identify scale-invariant interactions, which occur when the scale varies but the underlying pattern remains constant (Jebalia et al., 2022;3). Notably, occurrences with a power law distribution lack a distinguishing scale or magnitude, as opposed to the traditional bell-shaped distribution, which employs the mean as the defining scale. Power laws have gained popularity due to their utility in defining scale-free social and spatial networks in which the structure of links between entities remains consistent across scales. Gain insight into the scale-invariant properties and underlying patterns that govern their behaviour and distribution. This knowledge can help define ways for utilising these seeds' functional properties in a variety of applications, including food formulation and industrial operations (Gravelle & Marangoni, 2021;4).

2.5 Conclusion

Finally, Egusi, Moringa, and Makataan seeds have substantial yet underutilised potential as high-protein hydrocolloids for the food industry's long-term sustainability. Their nutritional content shows that these seeds have the potential to significantly improve the nutritional profile of a variety of food products. The main oilseed hydrocolloid explored over the years remains soybean; despite the promising benefits identified in existing studies, their use in the food business, including areas such as drinks, is restricted. Further research is required to fully realise the promise of these seeds, particularly as functional ingredients capable of improving global food production and public health.

A thorough examination of *Citrullus lanatus* var. *citroides*, Egusi, and *Moringa oleifera* seeds revealed essential insights into their roles in developing functional oilseed hydrocolloids. However, future research must prioritise detailed rheological assessments to realise their potential fully. This includes determining their stability, compatibility with various food matrices, and interactions with other components. Ultimately, this endeavour will aid in developing novel food products and commercial formulations enhanced with these promising oilseed hydrocolloids.

References

Aihole, J.S. 2020. Stridor in a child: It’s diagnostic challenges: stridor in child. *Respiratory*

Medicine Case Reports, 29: 101011. https://doi.org/10.1016/j.rmcr.2020.101011.

Ajanth Praveen, M., Karthika Parvathy, K.R., Jayabalan, R. & Balasubramanian, P. 2019. Dietary fibre from Indian edible seaweeds and its in-vitro prebiotic effect on the gut microbiota. *Food Hydrocolloids*, 96: 343–353.

Angkuratipakorn, T., Chung, C., Koo, C.K.W., Mundo, J.L.M., McClements, D.J., Decker, E.A. & Singkhonrat, J. 2020. Development of food-grade Pickering oil-in-water emulsions: Tailoring functionality using cellulose nanocrystals and lauric arginate mixtures. *Food Chemistry*, 327(May): 127039. https://doi.org/10.1016/j.foodchem.2020.127039.

Bolaji, O. T., Adeyeye, S. A. O., & Ogunmuyiwa, D. (2022). Quality evaluation of bread produced from whole wheat flour blended with watermelon seed flour. Journal of Culinary Science & Technology, 1-24.

Belorio, M., Marcondes, G. & Gómez, M. 2020. Influence of psyllium versus xanthan gum in starch properties. *Food Hydrocolloids*, 105(December 2019).

Cardines, Pedro HF, et al. "*Moringa oleifera* seed extracts as promising natural thickening agents for food industry: Study of the thickening action in yogurt production." *Lwt* 97 (2018): 39-44.

Ciurzyńska, A., Marczak, W., Lenart, A. & Janowicz, M. 2020. Production of innovative freeze-dried vegetable snacks with hydrocolloids in terms of technological process and carbon footprint calculation. *Food Hydrocolloids*, 108(October 2019).

Collado-González, M., Espinosa, Y.G. & Goycoolea, F.M. 2019. Interaction between Chitosan and Mucin: Fundamentals and applications. *Biomimetics*, 4(2).

Chinma, Chiemela Enyinnaya, et al. "Chemical, antioxidant, functional and thermal properties of rice bran proteins after yeast and natural fermentations." *International Journal of Food Science & Technology* 49.10 (2014): 2204-2213.

Dangi, N., Yadav, B.S. & Yadav, R.B. 2019. Pasting, rheological, thermal and gel textural properties of pearl millet starch as modified by guar gum and its acid hydrolysate. *International Journal of Biological Macromolecules*, 139: 387–396. https://doi.org/10.1016/j.ijbiomac.2019.08.012.

Dendrobium, O., Arabic, G. & Alginate, G. 2020. Stabilising the Oil-in-Water Emulsions Using the. *Molecules*: 8–10.

Dollah, Sarafhana, et al. "Physicochemical properties and potential food applications of *Moringa oleifera* seed oil blended with other vegetable oils." *Journal of Oleo Science* 63.8 (2014): 811-822.

El-hoshoudy, A.N., Zaki, E.G. & Elsaeed, S.M. 2020. Experimental and Monte Carlo simulation of palmitate-guar gum derivative as a novel flooding agent in the underground reservoir. *Journal of Molecular Liquids*, 302: 112502. https://doi.org/10.1016/j.molliq.2020.112502.

Fernández-Martínez, J.M. and Velasco, L., 2012. Castor. *Technological Innovations in Major*

World Oil Crops, Volume 1: Breeding, pp.237-265.

Florowski, T., Florowska, A., Chmiel, M., Dasiewicz, K., Adamczak, L. & Pietrzak, D. 2019. The effect of nuts and oilseeds enriching on the quality of restructured beef steaks. *Lwt*, 104(January): 128–133. https://doi.org/10.1016/j.lwt.2019.01.027.

Gervase, A. I., & Oyiza, S. R. (2021). Effects of Different Tuber Crop Flours and Melon Seed Meal on the Physicochemical and Sensory Properties of Biscuits. Asian Journal of Applied Science and Technology (AJAST), 5(3), 196-212.

Gharibzahedi, S.M.T., Roohinejad, S., George, S., Barba, F.J., Greiner, R., Barbosa-Cánovas, G. V. & Mallikarjunan, K. 2018. Innovative food processing technologies on the transglutaminase functionality in protein-based food products: Trends, opportunities and drawbacks. *Trends in Food Science and Technology*, 75(March): 194–205. https://doi.org/10.1016/j.tifs.2018.03.014.

Gibouin, F., van der Sman, R., Benedito, J. & Della Valle, G. 2022. Rheological properties of artificial boluses of cereal foods enriched with legume proteins. *Food Hydrocolloids*, 122: 107096.

Gomes, L.R., Simões, C.D. & Silva, C. 2020. Demystifying thickener classes food additives through molecular gastronomy. *International Journal of Gastronomy and Food Science*, 22(October).

Grasso, N., Alonso-Miravalles, L. & O'Mahony, J.A. 2020. Composition, physicochemical and sensory properties of commercial plant-based yoghurts. *Foods*, 9(3).

Gravelle, A.J. & Marangoni, A.G. 2021. Effect of matrix architecture on the elastic behaviour of an emulsion-filled polymer gel. *Food Hydrocolloids*, 119(April): 106875. https://doi.org/10.1016/j.foodhyd.2021.106875.

Gürgen, S. 2019. Tuning the rheology of nano-sized silica suspensions with silicon nitride particles. *Journal of Nano Research*, 56: 63–70.

Hamdani, A.M., Wani, I.A. & Bhat, N.A. 2019. Sources, structure, properties and health benefits of plant gums: A review. *International Journal of Biological Macromolecules*, 135: 46–61. https://doi.org/10.1016/j.ijbiomac.2019.05.103.

He, X. hong, Xia, W., Chen, R. yun, Dai, T. tao, Luo, S. jing, Chen, J. & Liu, C. mei. 2020. A new pre-gelatinized starch is prepared by gelatinisation and spray-drying rice starch with hydrocolloids. *Carbohydrate Polymers*, 229(October 2019): 115485. https://doi.org/10.1016/j.carbpol.2019.115485.

Horstmann, S.W., Axel, C. & Arendt, E.K. 2018. Water absorption as a prediction tool for the application of hydrocolloids in potato starch-based bread. *Food Hydrocolloids*, 81: 129–138. https://doi.org/10.1016/j.foodhyd.2018.02.045.

Jiang, T. & Charcosset, C. 2022. Encapsulation of curcumin within oil-in-water emulsions

prepared by premix membrane emulsification: Impact of droplet size and carrier oil on the chemical stability of curcumin. *Food Research International*, 157(April): 111475. https://doi.org/10.1016/j.foodres.2022.111475.

Kasprzak, M.M., Macnaughtan, W., Harding, S., Wilde, P. & Wolf, B. 2018. Food Hydrocolloids Stabilisation of oil-in-water emulsions with non-chemical modified gelatinised starch. *Food hydrocolloids*, 81: 409–418. https://doi.org/10.1016/j.foodhyd.2018.03.002.

Katoch, A. & Roy Choudhury, A. 2020. Understanding the rheology of novel guar-gellan gum composite hydrogels. *Materials Letters*, 263: 127234. https://doi.org/10.1016/j.matlet.2019.127234.

Kausar, T., Hassan, M. T., & ud Din, G. M. (2020). 21. Utilisation of watermelon seed flour as a protein supplement in cookies. Pure and Applied Biology (PAB), 9(1), 202-206.

Kavitake, D., Balyan, S., Devi, P.B. & Shetty, P.H. 2019. Interface between food-grade flavour and water-soluble galactan biopolymer to form a stable water-in-oil-in-water emulsion. *International Journal of Biological Macromolecules*, 135: 445–452. https://doi.org/10.1016/j.ijbiomac.2019.05.199.

Keisandokht, S., Haddad, N. & Gariepy, Y. 2018. Food Hydrocolloids Screening the microwave-assisted extraction of hydrocolloids from Ocimum basilicum L . seeds as a novel extraction technique compared with conventional heating-stirring extraction. , 74.

Kelly, C.E., Thompson, D.K., Genc, S., Chen, J., Yang, J.Y., Adamson, C., Beare, R., Seal, M.L., Doyle, L.W., Cheong, J.L. & Anderson, P.J. 2020. Long-term development of white matter fibre density and morphology up to 13 years after preterm birth: A fixel-based analysis. *NeuroImage*, 220(February): 117068. https://doi.org/10.1016/j.neuroimage.2020.117068.

Kitunen, V., Korpinen, R., Bhattarai, M., Pitk, L., Lehtonen, M., Mikkonen, K.S., Ilvesniemi, H. & Kilpel, P.O. 2019. Food Hydrocolloids Functionality of spruce galactoglucomannans in oil-in-water emulsions. , 86: 154–161.

Kornet, R., Penris, S., Venema, P., van der Goot, A.J., Meinders, M.B.J. & van der Linden, E. 2021. How pea fractions with different protein composition and purity can substitute WPI in heat-set gels: food *Hydrocolloids*, 120.

Kumar, S., Haq, R. ul & Prasad, K. 2018. Studies on physicochemical, functional, pasting and morphological characteristics of developed extra thin flaked rice. *Journal of the Saudi Society of Agricultural Sciences*, 17(3): 259–267.

Lei, J., Gao, Y., Ma, Y., Zhao, K. & Du, F. 2019. Improving the emulsion stability by regulation of dilational rheology properties. *Colloids and Surfaces A: Physicochemical and Engineering Aspects*, 583(September): 123906. https://doi.org/10.1016/j.colsurfa.2019.123906.

Leverrier, C., Almeida, G., Cuvelier, G. & Menut, P. 2021. Modelling shear viscosity of soft plant cell suspensions. *Food Hydrocolloids*, 118.

Liu, N., Li, N., Faiza, M., Li, D., Yao, X. and Zhao, M., 2021. Stability and in vitro digestion of high purity diacylglycerol oil-in-water emulsions. *LWT*, *148*, p.111744.

López-ramírez, A.M. & Duarte-sierra, A. 2020. Avocado jelly: formulation and optimisation of an avocado gel using hydrocolloids. *International Journal of Gastronomy and Food Science*: 100234. https://doi.org/10.1016/j.ijgfs.2020.100234.

Lu, W., Nishinari, K., Matsukawa, S. & Fang, Y. 2020. The future trends of food hydrocolloids. *Food Hydrocolloids*, 103.

Lupo, B., Maestro, A., Gutiérrez, J.M. & González, C. 2015. Characterisation of alginate beads with encapsulated cocoa extract to prepare functional food: Comparison of two gelation mechanisms. *Food Hydrocolloids*, 49: 25–34.

Ma, J., Fang, S., Shi, P. & Duan, M. 2019. Hydrazine-functionalized guar-gum material capable of capturing heavy metal ions. *Carbohydrate Polymers*, 223(July): 115137. https://doi.org/10.1016/j.carbpol.2019.115137.

Manzoor, M., Singh, J., Bandral, J.D., Gani, A. & Shams, R. 2020. Food hydrocolloids: Functional, nutraceutical and novel applications for delivery of bioactive compounds. *International Journal of Biological Macromolecules*, 165: 554–567.

Marx, Í.M., Casal, S., Rodrigues, N., Veloso, A.C., Pereira, J.A. and Peres, A.M., 2021. Estimating hydroxytyrosol-tyrosol derivatives amounts in cv. Cobrançosa olive oils based on the electronic tongue analysis of olive paste extracts. *LWT*, *147*, p.111542.

Masalova, I., Tshilumbu, N.N., Fester, V. & Kharatyan, E. 2020. Is the combination of two particles with different degrees of hydrophobicity an alternative method for tuning the average particle hydrophobicity? *Journal of Molecular Liquids*, 313: 113444. https://doi.org/10.1016/j.molliq.2020.113444.

McClements, D.J. 2021. Food hydrocolloids: Application as functional ingredients to control lipid digestion and bioavailability. *Food Hydrocolloids*, 111.

Nadeem, M., Ullah, R., & Ullah, A. (2016). Improvement of ice cream's physical and oxidative stability characteristics through interesterified *Moringa oleifera* oil. Pak J Scienti Ind Res Ser B: Biol Sci, 59(1), 38-43.

Nejadmansouri, M., Shad, E., Razmjooei, M., Safdarianghomsheh, R., Delvigne, F. & Khalesi, M. 2020. Production of xanthan gum using immobilised Xanthomonas campestris cells: Effects of support type. *Biochemical Engineering Journal*, 157(March).

Olubi, O. 2018. Functional characteristics of egusi seed (Citrullus lanatus) hydrocolloid and oil in instant egusi soup. *(Master Thesis) Cape peninsula university of technology*, (April). https://www.semanticscholar.org/paper/Functional-characteristics-of-egusi-seed-(Citrullus-Olubi).

Ouyang, J. & Meng, Y. 2022. Quantitative effect of droplet size and emulsion viscosity on the

storage stability of asphalt emulsion. *Construction and Building Materials*, 342(PB): 127994. https://doi.org/10.1016/j.conbuildmat.2022.127994.

Pachimalla, P.R., Mishra, S.K. & Chowdhary, R. 2020. Evaluation of hydrophilic gel made from Acemannan and *Moringa oleifera* in enhancing osseointegration of dental implants. A preliminary study in rabbits. *Journal of Oral Biology and Craniofacial Research*, 10(2): 13–19. https://doi.org/10.1016/j.jobcr.2020.01.005.

Pang, Z., Luo, Y., Li, B., Zhang, M. & Liu, X. 2020. Effect of different hydrocolloids on tribological and rheological behaviours of soymilk gels. *Food Hydrocolloids*, 101(July 2019): 105558. https://doi.org/10.1016/j.foodhyd.2019.105558.

Paudel, L., Clevenger, J. & McGregor, C. 2019. Refining of the egusi locus in watermelon using KASP assays. *Scientia Horticulturae*, 257(January): 108665. https://doi.org/10.1016/j.scienta.2019.108665.

Pegg, A. 2012. *The application of natural hydrocolloids to foods and beverages*. Woodhead Publishing Limited. http://dx.doi.org/10.1533/9780857095725.1.175.

Rabie, M. M., et al. "Effect of *Moringa oleifera* leaves and seeds powder supplementation on quality characteristics of cookies." *Journal of Food and Dairy Sciences* 11.2 (2020): 65-73.

Raimets, R., Bontšutšnaja, A., Bartkevics, V., Pugajeva, I., Kaart, T., Puusepp, L., Pihlik, P., Keres, I., Viinalass, H., Mänd, M. & Karise, R. 2020. Pesticide residues in beehive matrices are dependent on collection time and matrix type but independent of the proportion of foraged oilseed rape and agricultural land in foraging territory. *Chemosphere*, 238(August 2019): 124555.

Sabri, F., Raphael, W., Berthomier, K., Fradette, L., Tavares, J.R. & Virgilio, N. 2019. One-step processing of highly viscous multiple Pickering emulsions. *Journal of Colloid And Interface Science*, (xxxx). https://doi.org/10.1016/j.jcis.2019.10.098.

Salem, M., Abdel-fattah, A., & Rizk, A. (2022). Nutritional Evaluation of Watermelon and Gurmamelon Seeds Powder and Quality Characteristics of Fortified Biscuits. International Journal of Environment, 11(1), 10-22.

Seifu, E. & Teketay, D. 2020. Introduction and expansion of *Moringa oleifera* Lam. in Botswana: Current status and potential for commercialisation. *South African Journal of Botany*, 129: 471–479. https://doi.org/10.1016/j.sajb.2020.01.020.

Semenova, M., Antipova, A., Martirosova, E., Zelikina, D., Palmina, N. & Chebotarev, S. 2021. Essential contributions of food hydrocolloids and phospholipid liposomes to the formation of carriers for controlled delivery of biologically active substances via the gastrointestinal tract. *Food Hydrocolloids*, 120: 106890.

Sharma, S., Afgan, S., Deepak, Kumar, A. & Kumar, R. 2019. L-Alanine induced thermally stable self-healing guar gum hydrogel as a potential drug vehicle for sustained release of a

hydrophilic drug. *Materials Science and Engineering C*, 99(June 2018): 1384–1391. https://doi.org/10.1016/j.msec.2019.02.074.

Singh, K., Dasaroju, G. & Kumar, V. 2019. Formation, stability and comparison of water/oil emulsion using gum arabic and guar gum and effect of ageing of polymers on drag reduction percentage in water/oil flow. *Vacuum*, 159(October 2018): 247–253. https://doi.org/10.1016/j.vacuum.2018.10.044.

Theocharidou, A., Lousinian, S., Tsagaris, A. & Ritzoulis, C. 2022. Food Hydrocolloids Interactions and rheology of guar gum – mucin mixtures. , 133(January).

Tsai, F.H., Kitamura, Y. & Kokawa, M. 2017. Liquid-core alginate hydrogel beads loaded with functional compounds of radish by-products by reverse spherification: Optimization by response surface methodology. *International Journal of Biological Macromolecules*, 96: 600–610. http://dx.doi.org/10.1016/j.ijbiomac.2016.12.056.

Wang, P., Gao, Y., Wang, D., Huang, Z. & Fei, P. 2022. Amidated pectin with amino acids: Preparation, characterisation and potential application in Hydrocolloids. *Food Hydrocolloids*, 129(February): 107662. https://doi.org/10.1016/j.foodhyd.2022.107662.

Wei, M., Lv, Y., Sun, L. & Sun, H. 2020. Rheological properties of multi-walled carbon nanotubes/silica shear thickening fluid suspensions. *Colloid and Polymer Science*, 298(3): 243–250.

Yildirim-Mavis, C., Yilmaz, M.T., Dertli, E., Arici, M. & Ozmen, D. 2019. Non-linear rheological (LAOS) behaviour of sourdough-based dough. *Food Hydrocolloids*, 96: 481–492.

Yousefi, M. & Jafari, S.M. 2019. Recent advances in the application of different hydrocolloids in dairy products to improve their techno-functional properties. *Trends in Food Science and Technology*, 88(October 2018): 468–483.

Yuasa, M., Tagawa, Y. & Tominaga, M. 2019. The texture and preference of “mentsuyu (Japanese noodle soup base) caviar” prepared from sodium alginate and calcium lactate. *International Journal of Gastronomy and Food Science*, 18(April): 100178. https://doi.org/10.1016/j.ijgfs.2019.100178.

Zhao, Q., Jiang, L., Lian, Z., Khoshdel, E., Schumm, S., Huang, J. & Zhang, Q. 2019. Journal of Colloid and Interface Science High internal phase water-in-oil emulsions stabilised by food-grade starch. *Journal of Colloid And Interface Science*, 534: 542–548. https://doi.org/10.1016/j.jcis.2018.09.058.

Zhao, S., Tian, G., Zhao, C., Li, Chengxiu, Bao, Y., Dimarco-crook, C., Tang, Z., Li, Chunhong & Julian, D. 2018. The stability of three different citrus oil-in-water emulsions fabricated by spontaneous emulsification. , 269(December 2017): 577–587.

Zheng, M., Su, H., You, Q., Zeng, S., Zheng, B., Zhang, Y. & Zeng, H. 2019. An insight into the retrogradation behaviours and molecular structures of lotus seed starch-hydrocolloid blends.

Food Chemistry, 295(May): 548–555. https://doi.org/10.1016/j.foodchem.2019.05.166.

Zhu, Y., Gao, H., Liu, W., Zou, L. & McClements, D.J. 2020. A review of the rheological properties of dilute and concentrated food emulsions. *Journal of Texture Studies*, 51(1): 45–55.

CHAPTER THREE

PHYSICOCHEMICAL AND FUNCTIONAL PROPERTIES OF *CITRULLUS MUCOSOSPERMUS, CITROIDES,* AND *MORINGA* SEEDS HYDROCOLLOID

Abstract

Hydrocolloids form gel-like structures when dispersed in water and have garnered significant attention for their diverse applications in food, pharmaceuticals, and allied industries. The extraction of hydrocolloids from natural sources, such as seeds, presents an intriguing avenue due to the potential diversity in composition and functionality. Utilising seeds from *Citrullus mucosospermus*, *Citrullus citroides*, and Moringa aligns with the growing demand for natural and sustainable ingredients in various industries. This research investigated hydrocolloids extracted from *Citrullus mucosospermus* (CMS), *lanatus citroides*, and *Moringa oleifera* seeds, highlighting their versatile physicochemical and functional attributes. Hydrocolloids were extracted from the seeds using the hot water extraction method and subsequently analysed for proximate composition, particle size distribution, and interfacial tension properties. Protein content variation was observed among the raw oilseed (CMS, *Citroides*, and *Moringa oleifera*) flours. The protein content of the hydrocolloids surpassed that of raw oilseeds, significantly enhancing the amino acid profile. Furthermore, the hydrocolloid ash contents ranged from 4.09% to 6.52% *w*/*w* dry weight, coupled with low-fat levels. The particle size distribution revealed predominantly fine particles with a narrow size distribution. All three hydrocolloids demonstrated remarkable oil- and water-holding capacities, highlighting their suitability for efficient stabilisation and emulsification in food formulations. These findings suggest the potential utilisation of these hydrocolloids as valuable ingredients across a spectrum of applications, encompassing food, pharmaceuticals, and industry, thus contributing to the development of sustainable and functional products. The unique attributes presented herein mark a noteworthy advancement in the understanding and application of novel hydrocolloids from CMS, *Citroides*, and *Moringa oleifera*.

3.1 Introduction

Hydrocolloids from plant sources offer immense nutritional and functional properties, as found in some cucurbit species, namely the *Citrullus mucosospermus* and *caffer* varieties of melon plants. *Citrullus* belongs to the family *Benincaseae* of the subfamily *Cucurbitoideae*. It comprises four species, two of which (*rehmii* and *ecrihosus)* originated in Namibia (Mashilo et al., 2022;29). At the same time, the other two (*colocynthis* and *mucosospermus)* are prone to West Africa, locally

called egusi seed. The Kalahari region species is known locally as makataan and in southern Africa (Nkoana et al., 2022;66). *Citrullus mucosospermus* seed, locally known as egusi seed, a wild member of the gourd family [2], has limitless potential for worldwide use in the food industry (Efavi et al., 2018;99; Paudel et al., 2019;109). Egusi grows between 120-150 days at a pleasant temperature of 26 - 37^{o}C, obtained in any country with autumn/fall and summer (Olubi et al., 2019;5).

The *C. lanatus,* previously known as *Citrullus vulgarisor* or *colocynthis,* comprises three subspecies: subsp. *Vulgaris* are the most common edible pulp cultivars of watermelon. The subsp. *mucosospermus*, growing in West Africa as a wild melon, semi-cultivated and in cultivated forms. The fatty acids of egusi melon are high in conjugated linoleic acid (CLA). CLA is an omega-6 fatty acid, often used as a supplement for weight loss, bodybuilding, and diabetes (Özcan et al., 2019;334). Lastly is the *C lanatus caffer*, comprising two varieties differentiated by the bitterness of its pulp. *Caffer* is predominant in South Africa, with the bitter pulp variety locally known as tsamma, karkoer, and bitterboela (Mashilo et al., 2022;30). The array with a tasteless pulp is the var. *citroides*, locally called (citron melon or makataan) (Nkoana et al., 2022;67). Makataan melons are under cultivation in South Africa (Olubi, 2018). Makataan seed can be dehulled, roasted, or eaten as it is, or its seeds can be subjected to cold press extraction to obtain a nutritious oil high in omega-6 fatty acids of 68% w/w dry weight (Nkoana et al., 2022;66).

The potential of makataan melon seeds is yet to be explored. This seed's sole industrial application, called 'Kalahari seed,' involves cold-pressing to extract oil (Olubi, 2018:7; Yu et al., 2023;100). Limited information exists regarding the nutritional and functional attributes, as well as potential hydrocolloid properties, of its flour. Similar unexplored properties are observed in *Moringa oleifera* Lam seeds sp (MOLS) (Yu et al., 2023;102), specifically as a thickening agent. The coagulation properties of *MOLS* warrant increased scientific attention, with studies indicating the involvement of a soluble protein serving as a natural cationic polyelectrolyte responsible for their coagulant characteristics. This coagulant potential may be harnessed to enhance the technological features of food products requiring improved rheological properties (Iacovino et al., 2024;2).

Addressing food safety concerns is paramount when incorporating natural ingredients into food formulations. Despite limited research on the use of *M*OLS in food applications, existing evidence suggests their safety and potential health benefits (Aiking & de Boer, 2020;8). Given its substantial protein content (42-45% w/w dry weight), exploring diverse applications for makataan melon seeds becomes imperative, making this nutrient-dense seed comparable to MOLS and egusi seeds. This revelation hints at the emergence of a novel and nutritious hydrocolloid with promising implications for consumers.

The nutrient density of egusi seed is 50% w/w dry-weight edible oil and 30% w/w dry-weight pure protein, making it a functional food (Olubi et al., 2021;2) and a potential food hydrocolloid in the food industry. Hydrocolloids are materials that form a gel with water, comprising different polysaccharides and proteins widely used in the food industry (Cui et al., 2023;6). Uruakpa, (2004;353) reported that the rheological data of egusi gels, prepared at varying protein concentrations (3%, 6%, 10%, and 20%, w/v) in 0.15 M NaCl, indicated that 6% (w/v) egusi flour was sufficient to produce properly cross-linked networks (G^0 8724 Pa), confirming the use of egusi as a hydrocolloid which remain limited in usage. The critical observation is that there was evidence of properly cross-linked networks at a 6% (w/v) of egusi flour in the gel. Cross-linking refers to forming bonds between polymer chains, contributing to the gel's structure and strength. The specific rheological property mentioned is the storage modulus (G^o), which has a value of 8724 Pascal (Pa). The storage modulus measures the material's ability to store elastic energy during deformation.

The significance of this finding lies in the confirmation that a 6% concentration of egusi flour is sufficient to produce well-structured gels with cross-linked solid networks. This suggests that egusi has hydrocolloid properties, indicating its potential application as a thickening or gelling agent. However, egusi has yet to be widely adopted or utilised in industrial processes, possibly due to limited commercialisation or technological development.

Using a food hydrocolloid has seen a significant breakthrough in the food industries regarding thickening, gelling, emulsifying, and water-binding (Yu et al., 2023;100). The hydrocolloid properties of egusi seeds have yet to be well explored despite their use chiefly as an emulsifier and thickener in a local soup called egusi soup and research findings on its potential (Olubi et al., 2021;8). Efforts must be geared towards extracting the colloid substance present in egusi seed and the similar variety of this species found in the Kalahari region. Our objective was, therefore, to extract hydrocolloids from the three oil seeds while considering the preservation of the hydrocolloid properties using the hot water extraction method and profile their physicochemical and functional properties.

3.2 Materials and Methods

3.2.1 Sources of materials and equipment

Dehulled egusi was purchased from a local seed store in Cape Town, and moringa seeds were purchased from SupaNutri Pty Ltd., Graaf-Reinet, in South Africa. Makataan fruits were purchased from the Cape Town fruit and vegetable market. All chemical reagents were purchased from Merck, South Africa. All equipment was from the Flow Process & Rheology Centre at the Cape Peninsula University of Technology, Cape Town, South Africa. Figure 3.1 displays an overview of the process.

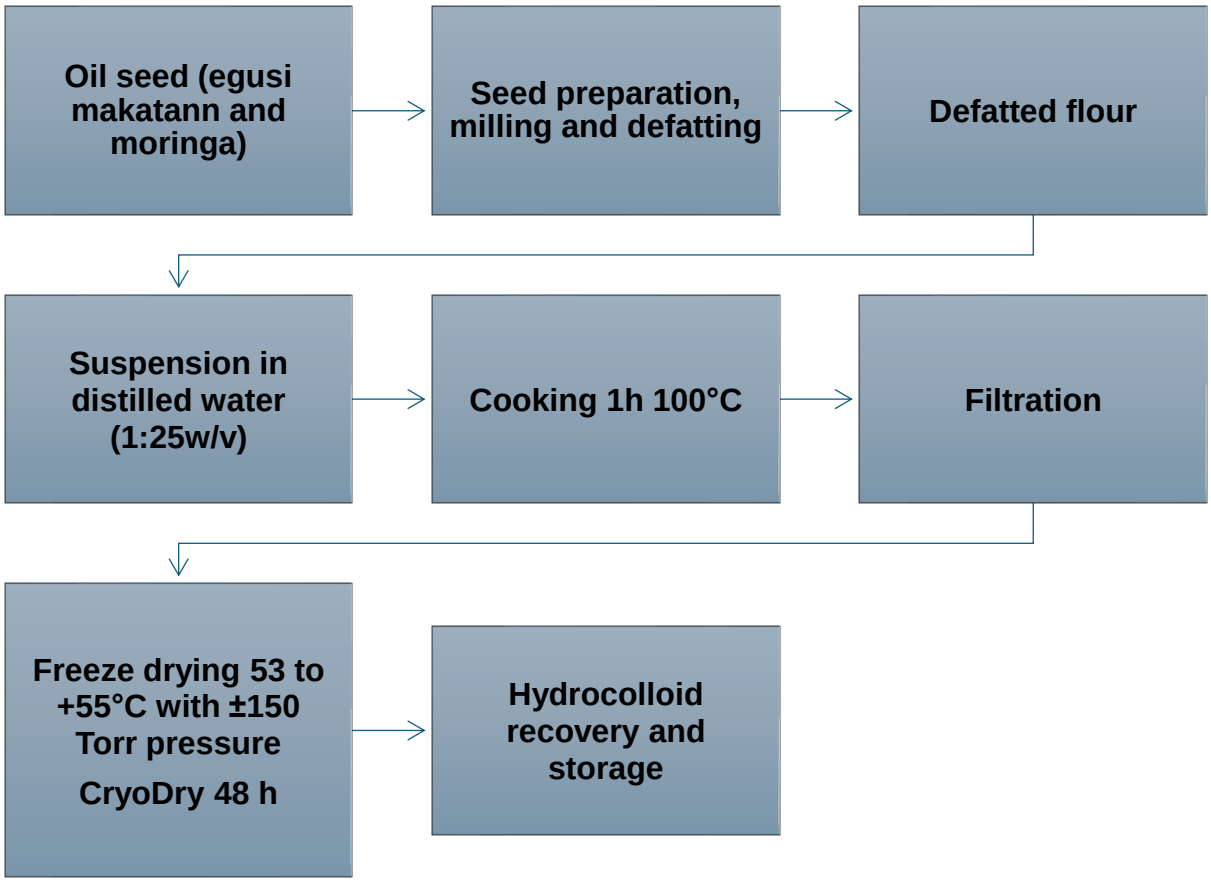

Figure 3.1 Overview of the process

3.2.2 Makataan, moringa and egusi seed preparation and defatting

Makataan seeds were obtained by separating the hard red seeds from the pulp. This was achieved by cutting through the makataan fruit and scooping out the embedded seeds. To every 800 g of the seeds, 500 mL of boiled water was added with 30 g of salt and allowed to soak for 6 hours (Shim et al., 2015). After washing, the saltwater was decanted, and soaked seeds were allowed to air dry for 2 h before dehulling using the roller mill dehuller. Dehulled egusi and moringa seeds were purchased from a seed store in Capetown, South Africa.

Dehulled egusi seeds were first sorted for chaff and other extraneous materials. and then defatted using cold-press methods. In contrast, the seeds of makataan and moringa were defatted using ethanol at 90% w/w concentrations, as seen in Figure 3.2. On the other hand, Moringa seeds were sorted for chaff, dehulled, and milled using a hammer mill; their flours were

then defatted with ethanol (90%), using a flour-to-ethanol ratio of 1:10 and continuously stirred for 12 h. The flour and ethanol mixture was passed through cheesecloth and air-dried in the fume hood for 8 hours. The defatted dried flours were packed in ziplock bags and stored in the refrigerator before use.

3.3 Hot Water Hydrocolloid Extraction of Moringa, Makataan and Egusi Hydrocolloids

Using the modified method of Olubi and Jayasinghe (2018:2016), defatted moringa, egusi, and makataan seed flours were suspended in purified water (1:25 *w/v* flour: water), and the suspension was cooked for an hour at 100°C (Olubi 2018;66 Zhou et al.2020;4). The hot mixture was then filtered through several layers of cheesecloths. The cooking procedure was performed twice while the defatted flour was suspended in boiling water for a second time. Following its combination, the filtrate was placed in a freezer (−50 °C) (Eppendorf F740020016 Freezers CryoCube) (740 L, −86 to −50 °C, Hanoi, Vietnam)) to maintain the sample's frozen state for later freeze-drying (United Scientific CryoDry Level 12, 37 York Street, Sydney NSW 2000 Australia). The moringa seed hydrocolloid (MOSH), egusi seed hydrocolloid (EGSH), and makataan seed hydrocolloid (MASH) were recovered after a 48-h freeze-drying process at −53 to +55°C and ±150 Torr of pressure. The freeze-dried samples were refrigerated till further nutritional analysis. The functional analysis entails colour, scanning electron microscopy, and light microscopy to observe the morphology of the hydrocolloids.

Egusi seed
Sample preparation
- Cold press defatting method
- Hot water extraction at 100°C/1h
- Filteration using cheese cloths
- Freeze drying the filterate at -53°C for 2 days
- Egusi hydrocolloid.

Makataan seed
Sample preparation
- 90% ethanol defatting method
- Filteration and drying out the floor
- Hot water extraction at 100°C/1h
- Filteration using cheese cloths
- Freeze drying the filterate at -53°C for 2 days
- Makataan hydrocolloid.

Moringa seed
Sample preparation
- 90% ethanol defatting method
- Filteration and drying out the floor
- Hot water extraction of defatted flour at 100°c/1h
- Filteration using cheese cloths
- Freeze drying the filterate at -53°C for 2 days
- Moringa hydrocolloid.

Figure 3.2 Seed preparation and extraction of moringa, makataan and egusi hydrocolloids

3.4 Nutritional and Functional Characterisation

The proximate amino acids and sugar content of egusi, moringa and makataan hydrocolloids were analysed. At the same time, the functional analysis, including the colour and morphology of the hydrocolloids, was assessed.

3.4.1 Proximate analysis of moringa, makataan and egusi hydrocolloids

The hydrocolloid samples' moisture content and dry matter were determined using the AOAC Method 934.01 (AOAC, 2005;30). After burning in a muffle furnace (Laboratory 1200C 64L Heating Electric Muffle Furnace with K Type Thermocouple Fujian, China), the amount of ash

was measured gravimetrically (according to AOAC Method 942.05, for two hours at 900 °C (AOAC, 2005). The amount of protein was calculated as a percentage of nitrogen determined using the nitrogen analyser (Leco Truspe N-630-100-200-230 V Amps 12 A, Saint Joseph, MI, USA). Total carbohydrate was calculated by difference (AOAC, 2005;24).

3.4.2 Microstructural analysis of moringa, makataan and egusi hydrocolloids using scanning electron microscopy (SEM)

The MOSH, EGSH, and MASH samples were dried in a 50 °C oven and then placed in a glass desiccator containing anhydrous silica gel overnight before being subjected to SEM examinations. Before applying a gold coating using a Bal-tec SCD 005 sputter coater (Bal-tec AG, Balzers, Liechtenstein), the triplicate hydrocolloid samples were mounted onto an SEM specimen stub using double-sided carbon tape. A Phillips ×L 30 SEM (SEMTech Solutions, Inc., Billerica, MA, USA) was then used to take pictures of the specimens at a magnification of 250 (Singh & Dhaliwal, 2018;55).

3.4.3 Colour parameters of moringa, makataan and egusi hydrocolloids

According to the procedure described by Jakopic et al. (2021;2), the spectrophotometer (Vis Spectrophotometer vinma× 721 LDC Digital Lab Visible Spectrophotometer 350–1020 nm Lamp Lab Constantia, Kloof) was used to measure the colour of EGSH, MASH, and MOSH.(Olubi et al., 2024;4). Following system calibration, the following parameters were found: a* (red-green component: -a* = greenness and + a* = redness), b* (yellow-blue component: -b* = blueness and + b* = yellowness), and L* (luminosity or brightness: L* = 0 black and L* = 100 white). Every analysis was carried out three times. Potato starch was utilised as a benchmark for comparative analysis. Equation (6) was used to compute the hue angle, and Equation (7) for the chroma (*C**).

$$\text{Hue angle} = \text{Tan}^{-1}\left(\frac{b}{a}\right) \quad (6)$$

$$C^{*} = \sqrt{(a^{*})^{2} + (b^{*})^{2}} \quad (7)$$

Where a* = green-red component and b* = yellow-blue component.

3.4.4 Light and polarised light microscopy of moringa, makataan and egusi hydrocolloids structure

The MOSH, EGSH, and MASH were each tested in triplicate on a microscope slide, combined with a drop of distilled water, and secured with a coverslip. Using an optical microscope (Leica Microsystems Wetzlar, Germany) with a digital camera at a magnification of ×40, the hydrocolloid granules were observed in both polarised and unpolarised modes (Lexica) (Zhang et al., 2020;6).

3.4.5 Particle size of moringa, makataan and egusi hydrocolloids

To assess the size distribution of dispersed particles, the Mastersizer 2000 instrument (Malvern/microcell/Claisse/PANanalytical Products. Enigma Business Park, Grovewood Road, WR14 1×Z Malvern, United Kingdom) uses laser diffractography. The measurement procedure was based on sample dispersion controlled by software and the angle dependence of the scattering intensity of a collimated He-Ne laser beam. The hydrocolloid powders were mixed with deionised water at 2000 rpm for two minutes, with a refractive index of 1.36 for both the water and the hydrocolloid. The median diameter of the granules, which is the diameter of 50% of the particles by volume, was used to express the particle size (Tornberg, 2022;4).

3.4.6 Interfacial tension of moringa, makataan and egusi hydrocolloids

Using the Kruss K100 tensiometer (Hamburg, 85 Borsteler Chaussee, Germany), interfacial tension measurements were carried out using the Wilhelmy plate method as the basis for the measurements. Approximately 15 mL of each hydrocolloid slurry was prepared after mixing 10 g of hydrocolloid with 10 g of water at room temperature. The mixture was poured into a spotless glass dish with a 70 mm diameter. Next, a hydrophilic platinum plate was suspended vertically from a force transducer sensitive enough to penetrate the surface by the plate's lower edge. Before completely submerging the plate, around 50 mL of the sunflower oil-based oil phase was introduced, as seen in Figure 3.3. Every measurement was calibrated at 7200 s to enable the system to measure (Yang et al., 2020; 369) accurately.

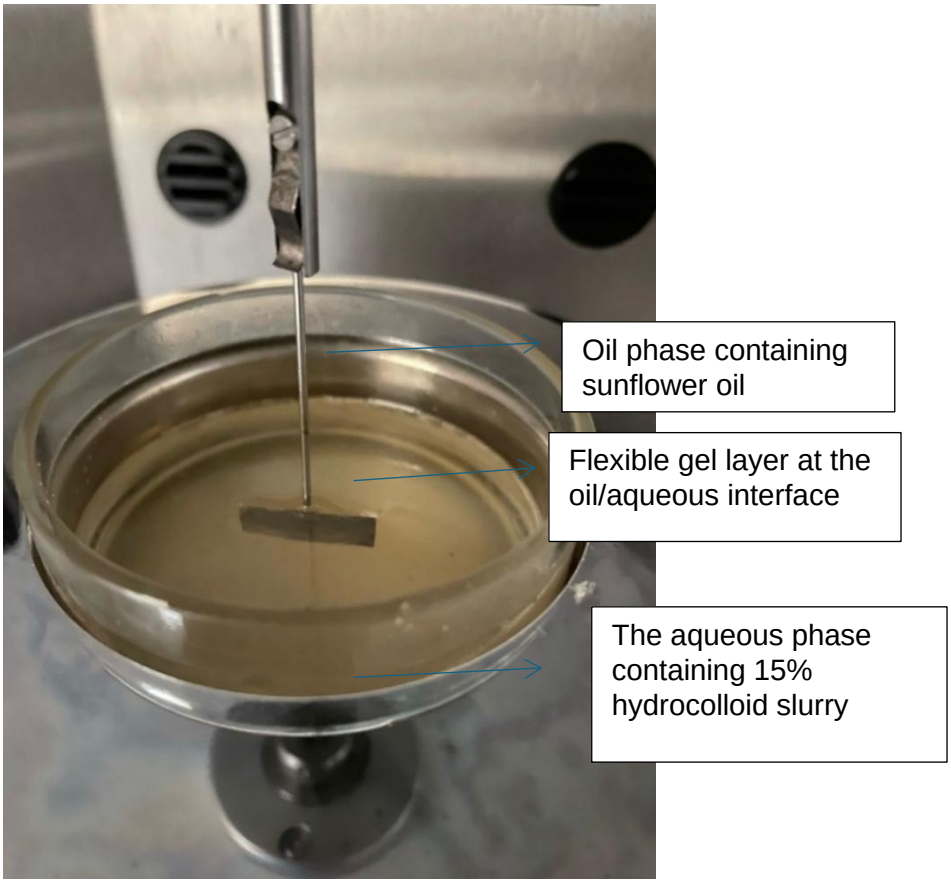

Figure 3.3 Hydrocolloid layer formation across the sunflower interface.

3.4.7 Visual appearance

To observe the visual appearance of extracted hydrocolloids for possible discolouration and particle size visuals. Egusi, makataan and moringa hydrocolloids were taken at time 0 and after 10 days of storage at 40°C in the presence of light. At the same time, the temperature is kept constant at 25^{o}C in an incubator oven. Visual evaluation of stability and colour changes were observed and reported according to the 24 h interval (de Almeida Paula et al., 2018;666) with slight modification.

3.5 Amino Acid Composition of Moringa, Makataan and Egusi Hydrocolloids

The modified ninhydrin method was used as described by (Li et al., 2020;14). Ninhydrin (2 g) was dissolved in distilled water (100 mL) under a stream of nitrogen gas to prepare a ninhydrin solution. Ninhydrin solution (1 mL) was added to 0.1% (wt) aqueous sample solution, heated in a boiling water bath for 5 min, and immediately cooled in an ice bath. Cooling is essential to stop the reaction and stabilise colour development. After 5 minutes of heating, the reaction vail was immediately transferred to an ice bath to cool the solution rapidly. The absorbance measurement

measures the absorbance of each hydrocolloid sample at 580 nm using an Agilent 8453 spectrophotometer. Distilled water is used as a blank for baseline correction with an Agilent 8453 spectrophotometer (USA). The absorbance values for each sample were detected with a calibration curve or standard amino acid solutions to relate absorbance to amino acid concentration. A constant calibration check was done to verify the spectrophotometer's performance. The absorbance measurement measures the absorbance of each hydrocolloid sample at 580 nm using an Agilent 8453 spectrophotometer. Distilled water was used as a blank for baseline correction with an Agilent 8453 spectrophotometer in Santa Clara, California (USA). The absorbance for each sample was detected with a calibration curve or standard amino acid solutions to relate absorbance to amino acid concentration. A constant calibration check was done to verify the spectrophotometer's performance.

3.6 Sugar Profiling of Moringa, Makataan and Egusi Hydrocolloids

According to Wang et al. (2022), the analytical solution was made using a combination of monosaccharide standards. At a 3 mg/mL concentration, hydrocolloids showed enhanced solubility in deionised water. Ten millilitres of the hydrocolloid solution were treated with an equivalent amount of 4 M trifluoroacetic acid and heated to 100°C for two hours to hydrolyse the hydrocolloids into their monomeric forms. For additional analysis, hydrolysis was emphasised as a critical step before derivatisation with 1-phenyl-3-methyl-5-pyrazolone (PMP). An Agilent Technologies ZORBAX Eclipse Plus-C18 HPLC column (250 mm length, 4.6 mm internal diameter, 5 µm particle size) was used to separate monosaccharides. A 2489 UV/V detector fitted to a Waters e2695 HPLC system was used for detection and quantification.

3.7 Statistical Analysis

The results were presented as the mean ± standard deviation of triplicate measurements. Multivariate analysis of variance was conducted to determine the mean differences between treatments where significant ($p \leq 0.05$) differences existed. Duncan's multiple range test was employed to separate the means. All data analysis was conducted using the IBM SPSS version 29 software (2022).

3.8 Results and Discussion

3.8.1 Hydrocolloid extraction yield from hot water extraction

The yield, physical and textural properties of makataan, egusi, and moringa seed hydrocolloids (MASH, EGSH, and MOSH, respectively) differed significantly among the samples. The images of each hydrocolloid show a creamy white powdery flour, as seen in Figure 3.4. Hydrocolloids (EGSH and MASH) gave a 52% yield, while the yield of MOSH was only 42%. It is worth

mentioning that some proteins and carbohydrates, which have the highest composition, were dissolved, as seen from the brown slurry images in Figure 3.5. This finding is similar to those of Hedayati et al. (2021;3), who found that the mucilage seeds were not damaged and that the ultrasonically extracted mucilage powder was purer.

Figure 3.4 Hydrocolloids are from (a) Moringa seed, (b) Egusi seed, and (**c**) Makataan seed.

Moringa seed

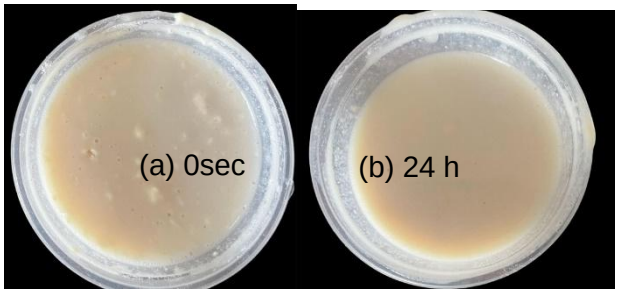

Makataan seed

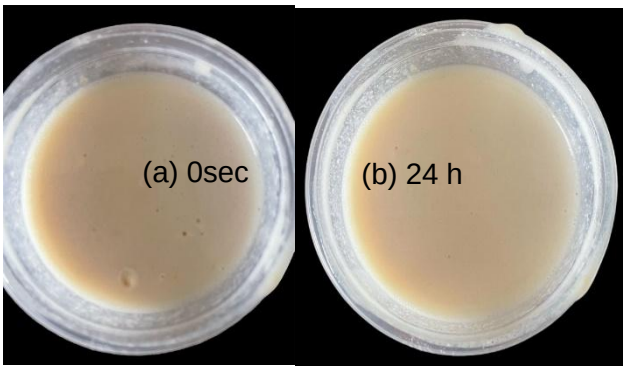

Egusi seed

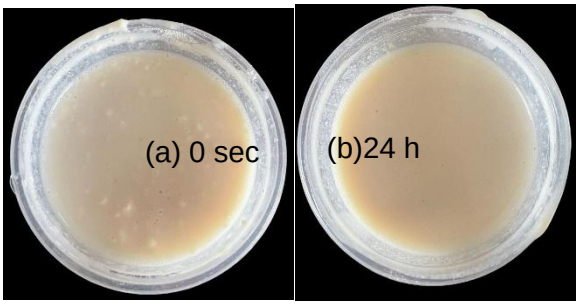

Figure 3.5 Visuals of room temperature water to hydrocolloid (10:10) mi× of Moringa seed (**a**) 0 sec (**b**) 24 h; Makataan seed (**a**) 0 sec (**b**) 24 h and (**a**) 0 sec (**b**) 24 h Egusi seed hydrocolloid.

3.9. Proximate Composition of Moringa, Makataan and Egusi Hydrocolloids

The proximate composition of egusi seed hydrocolloid, makataan seed hydrocolloid and moringa seed hydrocolloid, respectively, EGSH, MASH and MOSH, alongside their raw and defatted flour are presented in Table 3.1. The moisture content of the hydrocolloids varied from 7.01 to 7.80% (*w*/*w* dry weight). The moisture of the raw undefatted flour from the three oilseeds was higher than the defatted flour and was significantly ($p \leq 0.05$) different. The moisture content of the undefatted flours from egusi, makataan, and moringa seeds ranged from 11.34 to 12.96% (*w*/*w* dry weight). These values were higher than the moisture content reported in previous studies on five other species of cucurbit seed (6.45% to 7.56%) by Dimitry et al. (2022;461). However, they were lower than the moisture content found in raw Ukpo (*Mucuna flagellopes*) seeds (approximately 15.50%), as reported by Wilberforce et al. (2017;3).

Table 3.1 Proximate composition of raw, defatted hydrocolloid of the makataan, moringa and egusi oilseeds [1,2].

	Raw Flour			Hydrocolloid		Defatted Flour			
Proximate % *w/w* Dry Weight	RMAS	RMOS	REFS	MOSH	EGSH	DMASF	DMOSF	MASH	DESF
Protein	27.73 ± 1.37^{a}	30.08 ± 0.88^{b}	32.00 ± 3.00^{c}	34.00 ± 2.65^{d}	35.00 ± 1.00^{d}	39.07 ± 0.31^{e}	40.88 ±1.09^{e}	48.12 ±1.00^{f}	58.12 ± 1.06^{g}
Moisture	12.44 ± 0.85^{a}	11.34 ± 0.55^{b}	12.96 ± 0.69^{a}	7.80 ± 0.92^{c}	7.01 ± 0.28^{c}	8.01 ± 0.01^{c}	7.54 ± 0.16^{c}	7.11 ± 1.04^{a}	10.73 ± 0.55^{b}
Ash	3.63 ± 0.56^{a}	5.09 ± 0.48^{a}	3.39 ± 0.72^{a}	4.09 ± 3.26^{a}	5.98 ± 0.05^{b}	12.67 ± 0.58^{d}	10.76 ± 1.26^{d}	6.52 ± 1.48^{c}	15.23 ± 0.48^{e}
Fat	36.12 ± 1.11^{a}	38.26 ± 0.65^{b}	37.73 ± 4.44^{b}	4.53 ± 0.42^{c}	5.88 ± 0.42^{d}	4.68 ± 0.56^{c}	5.52 ± 0.23^{d}	0.53 ± 0.06^{a}	1.54 ± 0.40^{e}
Carbohydrates	10.56 ± 0.63^{a}	7.88 ± 0.20^{b}	9.63 ± 0.55^{b}	29.51 ± 0.49^{c}	26.03 ± 0.26^{d}	27.97 ± 0.08^{e}	20.42 ± 0.03^{d}	23.37 ± 0.72^{e}	18.50 ± 1.32^{e}

1 Values are mean ± standard deviation of 5 replicates. Means with different superscripts in each row differ significantly ($p \leq 0.05$). [2] RMAS = Raw Makaaan seed flour; RMOS = Raw Moringa seed flour; RESF = Raw Egusi seed flour; MOSH = Moringa seed Hydrocolloids; EGSH = Egusi seed Hydrocolloid; DMASF = Defatted Makataan seed flour;

2 DMOSF = Defatted Moringa seed flour; MASH = Makataan, hydrocolloid; DESF = Defatted egusi seed flour

The moisture content of the defatted oilseed flours ranged from 7.54 to 10.73%. These values were higher than the moisture content obtained from defatted Guna flour (5.50%) (Barak & Mudgil, 2014;73). The raw egusi exhibited the highest moisture content among all the samples.

The protein content of the oilseed hydrocolloids was higher than that of the raw oilseeds, with a percentage of 48.12, 34.00, and 35.00% for MASH, MOSH, and EGSH, respectively. Interestingly, the protein content of the defatted oilseeds significantly increased to 39.07%, 40.88%, and 58.18% for defatted makataan seed flour, defatted moringa seed flour and defatted seed egusi flour (DMASF, DMOSF and DESF) respectively, compared to the raw oilseeds and hydrocolloids. Notwithstanding, there was an exception to MASH (39.07%), which had a higher protein content than the raw oilseed (27.73%). The increased protein content of the defatted flour from the three oilseeds had reduced carbohydrate content, as observed with the raw oilseeds, although the carbohydrate in raw flour was higher. The low carbohydrate content (Table 3.1) might be the reason for the comparatively high amount of protein in the three raw oilseeds and the defatted oilseed flours. Food gums with high protein are known to be natural stabilisers. Emulsions form the basis of a vast range of food products, where those stabilised by proteins are of great interest (Bonilla & Clausen, 2022;7). It is worth mentioning that the protein content obtained in this study was similar and within the range of some other previously reported studies (olubi.2018;13; Sahu et al., 2021;2; Haung et al., 2021;4; Adeoye et al., 2020;4; Chao et al., 2023;5).

The interfacial properties of proteins have been studied extensively in food colloid research. Emulsifying properties of proteins depend on two effects: (1) a substantial decrease in the interfacial tension due to the adsorption of the protein at the oil-water interface and (2) the electrostatic, structural, and mechanical energy barrier caused by the interfacial layer that opposes the destabilisation processes (Yue et al., 2022;5; Rostami et al., 2022;4)The increase in macronutrients shows that the defatting methods used for the sample preparation effectively produced nutritious flour, similar to the report by (Famakinwa et al., 2023;8), who reported increased antioxidant activity and nutrients of wheat flour after defatting. Thus, the protein in hydrocolloids isolated from all three sources (Table 3.2) might be precipitated at pH 4.0–4.5 due to the isoelectric point falling in that range. The protein content of EGSH significantly ($p \leq 0.05$) differed from MOSH and MASH, which could be attributed to the different defating method. It is well documented that protein plays an essential role in the emulsifying activities of naturally occurring emulsifiers, such as gum Arabic. Proteins emulsify a polysaccharide covalently attached with a glycosidic linkage (Saleh et al., 2013;282). In the case of gum Arabic, the covalently attached proteins provide additional functionality to the polysaccharide. The presence of proteins enhances the

emulsifying properties of the gum Arabic by improving its ability to form and stabilise oil-in-water emulsions. The proteins act as emulsifiers, promoting a stable interfacial film between the oil and water phases. This film prevents the coalescence and separation of the dispersed oil droplets, thus increasing the emulsion stability.

Table 3.2 Proximate composition of makataan, egusi and moringa seeds hydrocolloids[1.2].

	Hydrocolloid		
Proximate % *w/w* Dry Weight	Makataan	Egusi	Moringa
Protein	34.00 ± 2.65[a]	48.02 ± 1.00[b]	35.00 ± 1.00[a]
Moisture	7.80 ± 0.92[a]	7.19 ± 1.04[a]	7.71 ± 0.28[a]
Ash	4.09 ± 3.28[a]	6.57 ± 0.48[a]	5.98 ± 0.05[a]
Fat	4.53 ± 0.42[a]	0.53 ± 0.06[c]	5.88 ± 0.42[b]
Carbohydrate	29.51 ± 0.49[a]	23.37 ± 0.72[a]	29.57 ± 0.26[b]

[1] Values are mean ± standard deviation of 5 replicates. [2]Means with a different superscript in each row differ significantly ($p \leq 0.05$).

3.9.1. Sugar composition of egusi, makataan and moringa seed hydrocolloid

The sugar composition of MASH, EGSH and MOSH are presented in Table 3.3. The table shows hydrocolloids (MOSH, EGSH) have higher carbohydrate content (29.51 ± 0.49% and 26.03 ± 0.26%) than raw and defatted seed flours in Table 3.2. The hydrocolloids from all three sources have predominant monomeric sugar units which become available after defatting: glucose, a trace amount of fructose (0.35 to 0.57 g/100 g), a dimeric unit: sucrose, a trimeric unit: raffinose and a tetrasaccharide unit: stachyose. Sucrose combines two monosaccharides (glucose and fructose) joined together as disaccharides. Sucrose is found mainly in plants and can be crystallised into refined sugar. The three hydrocolloids showed a high sucrose and raffinose content, ranging from 4.95 to 7.68 g/100 g and 0.48 to 5.99 g/100 g, respectively. During storage, amorphous sucrose tends to crystallise to a more thermodynamically stable crystalline form (Huang et al., 2021;4). Raffinose is a trisaccharide composed of galactose, glucose, and fructose. It is found in beans, cabbage, Brussels sprouts, broccoli, asparagus, other vegetables, and whole grains. MASH and EGSH are high in raffinose 5.85 and 5.99 g/100 g, respectively, compared to MOSH (0.48 g/100 g), while MOSH is higher in sucrose (7.68 g/100 g) than MASH and EGSH (4.95 and 5.90 g/100 g respectively). The raffinose family of oligosaccharides are α-1, 6-galactosyl extensions of sucrose (Li et al., 2020);3, found in plants, is known to serve as a seed

desiccation protectant. They transport sugar in phloem sap and can sometimes act as non-digestible human storage sugar (Shokryazdan et al., 2017;3). These oligosaccharides pass undigested through the stomach and small intestine. In the large intestine, they are fermented by bacteria that possess the α-GAL enzyme and make short-chain fatty acids (SCFA) (acetic, propionic, butyric acids) and the flatulence commonly associated with eating beans and other vegetables (Wang et al., 2022;2).

Table 3.3 Sugars in egusi, makataan and moringa seed hydrocolloids [1,2].

	Hydrocolloids		
Sugar (g/g100)	MASH	MOSH	EGSH
Fructose	0.35 ± 0.02^{a}	0.47 ± 0.01^{b}	0.57 ± 0.78^{c}
Glucose	0.49 ± 0.02^{a}	3.05 ± 0.10^{c}	0.78 ± 0.12^{b}
Sucrose	4.95 ± 0.10^{a}	7.68 ± 0.24^{c}	5.90 ± 0.35^{b}
Maltose	0.18 ± 0.00^{a}	0.00 ± 0.00^{a}	0.22 ± 0.02^{c}
Raffinose	5.99 ± 0.01^{a}	0.48 ± 0.02^{a}	5.85 ± 0.21^{b}
Stachyose	1.48 ± 0.02^{a}	1.24 ± 0.02^{b}	0.38 ± 0.03^{a}

[/1] Values are mean ± standard deviation in 6 replicates. Means with a different superscript in each row differ significantly ($p \leq 0.05$). [2] MOSH = Moringa Seed Hydrocolloids; EGSH = Egusi Seed Hydrocolloid; MASH = Makataan Seed hydrocolloid.

Before freezing procedures (cryopreservation), raffinose provides hypertonicity for cell desiccation. Raffinose or sucrose is used as a base substance for sucralose. Raffinose is also employed in skin moisturisers, smoothers, and prebiotics. It allegedly promotes the growth of lactobacilli and bifidobacterial in food or drinks. The low level of glucose in MASH and EGSH (0.49 and 0.78 g/100 g, respectively) could be due to high sucrose from all three oilseed sources (4.95 and 5.90 g/100 g). The three hydrocolloids also contain stachyose ranging from (0.38 to 1.48 g/100 g). Stachyose is one of the most abundant tetrasaccharides in plants, and it is a higher homolog of raffinose (Table 3.3).

First isolated from the rhizomes of *Stachys tuberifera*, starchose coexists with raffinose and other related oligosaccharides in various organs of many plant species (Khan et al., 2020;6). Reports have it that stachyose inhibits cancer cell proliferation and conversely promotes probiotics' proliferation, which induces their apoptosis in a dose-dependent manner, thereby preventing colon cancer indirectly (Liu et al., 2023). Additionally, sucrose and fructose can help preserve food by inhibiting microbial growth and extending shelf life. These sugars promote browning reactions and flavour development in

specific processes, such as baking or caramelisation. Furthermore, fructose may provide antioxidant properties, contributing to potential health benefits (Kornet et al., 2021;6).

In conclusion, these hydrocolloids with high sucrose and fructose content offer several benefits in various food applications. These benefits include their role as natural sweeteners, providing a pleasant taste and flavour enhancement. The high sugar content can serve as a readily available energy source and contribute to the texture of food products, improving mouthfeel and overall eating experience. However, consuming hydrocolloids with high sucrose and fructose content in moderation is essential, as excessive consumption of these sugars, particularly in processed and high-calorie foods, can have adverse health effects. Balancing their intake as part of a well-rounded diet is crucial to ensure optimal health and well-being.

3.9.2 Amino acids in makataan, moringa and egusi seed hydrocolloids

The amino acid compositions of the three oilseed hydrocolloids are shown in Table 3.4. Each hydrocolloid contained all essential amino acids: threonine, phenylalanine, valine, methionine, lysine, histidine and leucine, although with significant ($p \leq 0.05$) variation in content. MASH was characterised by high glutamine, arginine, aspartine and glycine (Wang et al., 2023;4), reported that after grafting with the amino acids, the viscosity of the amidated pectin was significantly improved. Each hydrocolloid contained appreciable quantities of valine (0.75 to 1.30 g/100 g) and histidine (0.42 to 0.92) mg/100 g) (MOSH). The methionine ranged from 0.75 to 1.58 g/100 g, with the highest EGSH.

The ability of a protein to possess suitable emulsifying and foaming properties depends mainly on the protein conformation and its ability to interact with water and oil at a molecular level. Amino acids are grouped according to their side chains. The nine amino acids with hydrophobic side chains are glycine (Gly), alanine (Ala), valine (Val), leucine (Leu), isoleucine (Ile), proline (Pro), phenylalanine (Phe), methionine (Met), and tryptophan (Trp). The three hydrocolloids contain all the hydrophobic amino acids except tryptophan. The side chains are composed chiefly of carbon and hydrogen, have tiny dipole moments, and tend to repel water. There are six polar amino acids with no charged side chains. These are serine (Ser), threonine (Thr), cysteine (Cys), asparagine (Asn), glutamine (Gln), and tyrosine (Tyr). Four polar amino acids are present in the three hydrocolloid samples. These amino acids are usually found at the surface of proteins (Li et al., 2020;6). Among the various classes of amino acids, depending on the propensity of the side chain to interact with a water molecule, the three hydrocolloids possessed the highest content of hydrophobic amino acids compared to soy lecithin, followed by neutral, basic and acidic amino acids and this was a similar trend recorded in another study (Wang et al., 2022;8). It

is worth noting that the hydrophobic protein content of the three hydrocolloids follows the trend: MOSH > EGSH = MASH. It is worth mentioning that the specific amino acid profile and content varies among different hydrocolloid sources.

Additionally, hydrocolloids' overall nutritional impact and health benefits depend on various factors, including processing methods, product formulation, and individual dietary needs. Hydrocolloids with high amino acid content can serve as a valuable protein source for individuals following vegan or vegetarian diets, where obtaining sufficient protein can be challenging. These hydrocolloids can provide essential amino acids to meet protein requirements (Zhao et al., 2023;2).

Table 3.4 Amino acids of makataan, moringa and egusi seed hydrocolloids[1, 2].

	Hydrocolloids		
Amino Acid	EGSH	MOSH	MASH
Non-essential g/100g			
Arginine	5.99 ± 0.29[a]	4.69 ± 0.53[a]	7.25 ± 0.33[c]
Serine	1.08 ± 0.03[a]	0.78 ± 0.06[a]	1.59 ± 0.03[c]
Glycine	2.26 ± 0.09[a]	1.92 ± 0.12[a]	2.51 ± 0.17[b]
Asparagine	1.63 ± 0.13[a]	1.19 ± 0.03[a]	2.67 ± 0.26[c]
Glutamine	7.80 ± 0.39[a]	6.35 ± 0.08[a]	9.15 ± 0.61[c]
Alanine	1.17 ± 0.08[a]	0.99 ± 0.03[a]	1.58 ± 0.01[c]
Proline	1.15 ± 0.06[a]	1.48 ± 0.07[b]	1.40 ± 0.03[b]
Tyrosine	1.04 ± 0.09[a]	0.61 ± 0.12[a]	1.69 ± 0.25[c]
Essential			
Valine	0.79 ± 0.06[a]	0.75 ± 0.06[a]	1.30 ± 0.02 [b]
Histidine	0.42 ± 0.02[a]	0.62 ± 0.14[b]	0.92 ± 0.01 [c]
Leucine	1.39 ± 0.02[a]	1.25 ± 0.04[a]	1.13 ± 0.02 [c]
Lysine	0.69 ± 0.17[a]	0.45 ± 0.14[a]	0.85 ± 0.38 [a]
Methionine	1.13 ± 0.01[a]	0.75 ± 0.02[a]	1.58 ± 0.05 [c]
Phenylalanine	1.07 ± 0.10[a]	0.92 ± 0.19[a]	2.09 ± 0.30 [b]
Threonine	0.83 ± 0.05[a]	0.86 ± 0.04 [a]	1.10 ± 0.02 [b]

[1] Values are mean ± standard deviation in 15 replicates. Means with a different superscript in each row differ significantly ($p \leq 0.05$). [2] MOSH = Moringa Seed Hydrocolloids; EGSH = Egusi Seed Hydrocolloid; MASH = Makataan Seed hydrocolloid.

3.10 Physical Properties of Moringa, Egusi and Makataan Seed Hydrocolloid

3.10.1 Visual appearance and particle size distribution of egusi, makataan and moringa seed hydrocolloids

The hydrocolloids experienced mechanical and thermal energy when milled into different fractions, resulting in multiple particle sizes and distributions, as shown in Figure 3.6 and Table 3.5.

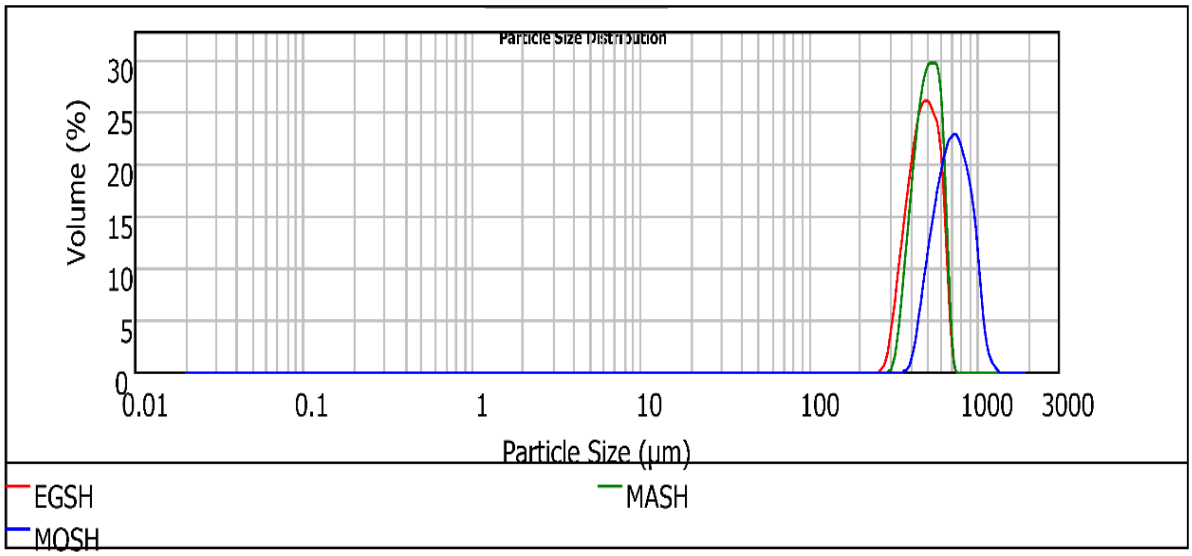

Figure 3.6 Histogram of the particle size distribution of the milled hydrocolloids egusi (EGSH), makataan (MASH), and moringa (MOSH).

Table 3.5. Particle size and particle size distribution of moringa, makataan and egusi hydrocolloids [1,2].

Hydrocolloid	D (0.5)	D [32]	Span	Uniformity
EGSH	437.00 ± 46.81[a]	461.48 ± 55.09[a]	0.64 ± 0.16[a]	0.18 ± 0.04[a]
MOSH	756.44 ± 33.45[b]	730.54 ± 31.99[b]	0.68 ± 0.01[a]	0.20 ± 0.01[b]
MASH	511.59 ± 0.46[a]	497.17 ± 35.45[a]	0.45 ± 0.01[a]	0.15 ± 0.00[a]

[1] The values are mean ± standard deviation with 4 replicas. Different letter in the same column indicates significant differences ($p < 0.05$). [2] Egusi seed hydrocolloid (EGSH), Makataan seed hydrocolloid (MASH), and Moringa seed hydrocolloid (MOSH). D(0.5) (Median Particle Size); D (32) (The surface area-weighted mean diameter)

Regardless of the hydrocolloid type, particles from the milling process consisted of relatively large aggregates. The high particle size of the three hydrocolloids indicates that they will offer a more robust particle in solution, enhancing the absorption dissolution rate in solution.

The particle size (D (0.5)) follows the trend MOSH > MASH > EGSH, whereas the span shows a different trend: MOSH > EGSH > MASH. Even though visual observation revealed that the physical appearance of EGSH and MASH were quite close (larger aggregates of particles had rough surfaces than the fine fraction), EGSH hydrocolloids gave rise to the smallest size. MASH demonstrated a more uniform distribution of particles. Moreover, visual observation of egusi and makataan hydrocolloids revealed a high adhesion tendency of their particles, which could be due to the aggregation of the protein-based particles leading to increased water absorption and homogeneity within the film structure. Conversely to EGSH and MASH, MOSH comprised large numbers of smoothly disintegrated larger particle sizes (756.44 µm) and were less evenly distributed (0.20). This particle size distribution is directly related to the higher mechanical performance of the hydrocolloid from moringa seeds compared to EGSH and MASH. A similar morphology was observed by Lin et al. (2017;5) in soya lecithin substitute for eggs, which presented a significant concentration of stable aggregates. Bearing in mind that hydrocolloids (proteins and polysaccharides) are soluble in water, resulting in a reduction of their size (Lin et al., 2017;4), the droplet size measurement was then taken every two seconds until the process showed no significant changes in the sizes of particles. This observation interval is relevant for the rheological characterisation of these systems. The required time to reach the equilibrium particle size was 10 s in our experimental conditions. The main results of particle size and particle size distributions after 10 s are presented in Table 3.6 and Figure 3.7, respectively. Outcomes associated with the initial time (t = 0 sec) are compared.

Table 3.6 Change in particle size and size distribution of moringa, makataan and egusi hydrocolloids after 10 s[1, 2].

Hydrocolloids	D (0.5)	D [32]	D (0.5) 10 sec	D [32] 10 sec	Span
EGSH	437 ± 46.81[a]	461.48 ± 55.09 [a]	12.31 ± 0.44 [b]	10.60 ± 0.01 [b]	2.33 ± 0.45 [c]
MOSH	756.44 ± 33.45[a]	730.54 ± 31.99 [a]	15.81 ± 0.45 [b]	15.14 ± 0.05 [b]	2.24 ± 0.55 [c]
MASH	511.59 ± 0.46[a]	497.76 ± 0.50 [a]	22.82 ± 1.45 [b]	22.59 ± 0.45 [b]	2,78 ± 0.56 [c]

[1]Values are mean ± standard deviation of 5 replicas in different letters in the same column indicates significant differences ($p < 0.05$) [2] EGSH (Egusi seed hydrocolloid), MASH (Moringa seed hydrocolloid), and MOSH (Moringa seed hydrocolloid)

(a)

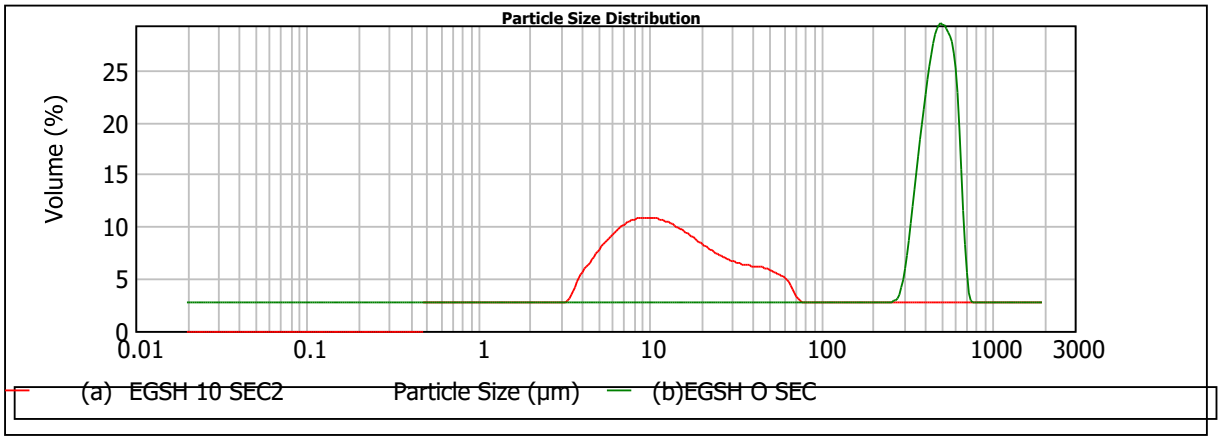

(b)

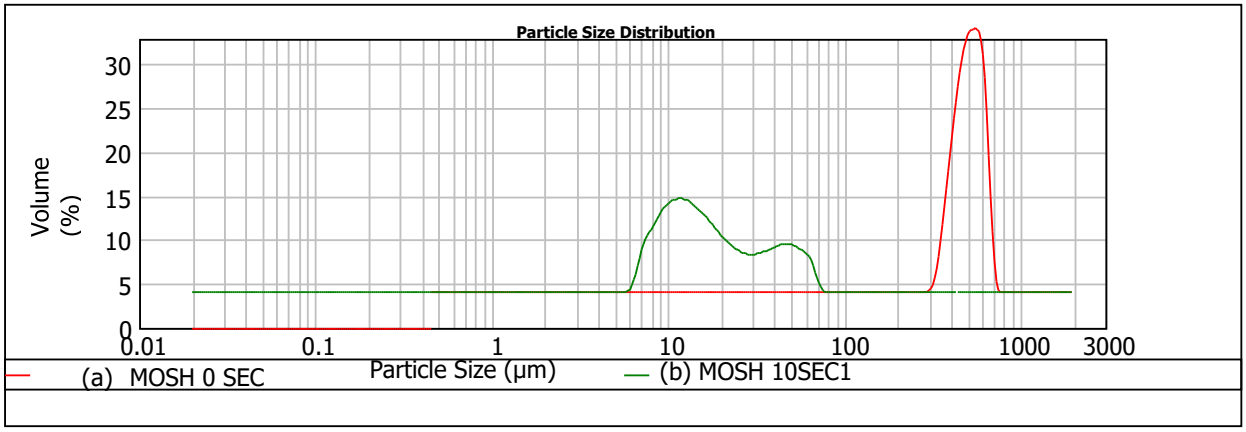

(c)

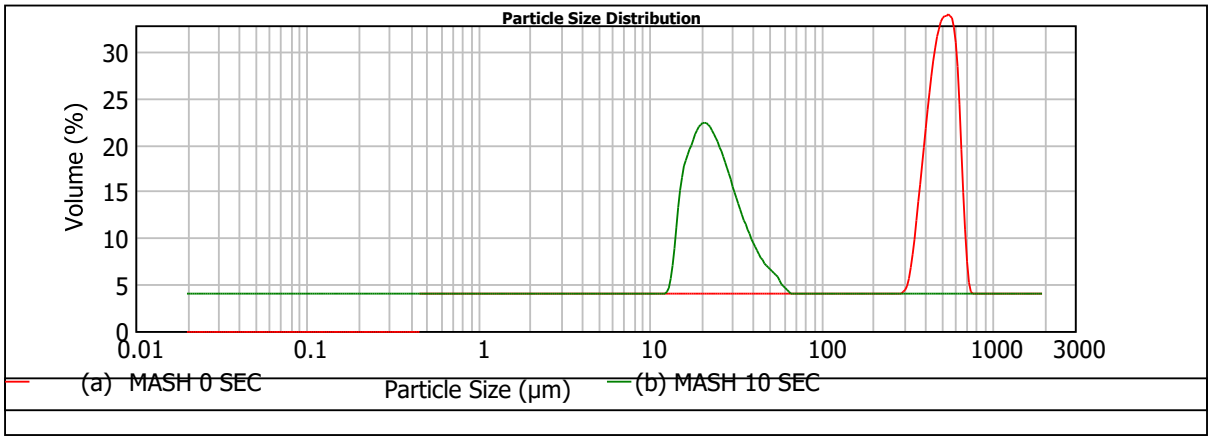

Figure 3.7 Histogram of changes in the particle size distribution of hydrocolloids after 10s (a) Egusi seed hydrocolloid; (b) Moringa seed hydrocolloid; (c) Makataan seed hydrocolloids.

Based on the histograms and Table 3.6, regardless of the hydrocolloid type, the equilibrium particle size after 10 s reached a significantly low value, suggesting a high dissolution rate. This enhancement in the rate is partly related to the agitation of the system (2000 rpm) during droplet size measurement (Zhu et al., 2020;47). The trend EGSH < MOSH < MASH suggests that despite the higher specific areas of MASH particles (small particle size with higher to MOSH), these particles are more difficult to dissolve than MOSH. In conclusion, the trend observed with EGSH < MOSH < MASH, regarding solubility, indicated that despite the smaller particle size and higher roughness of MASH particles compared to MOSH, it was more challenging to dissolve. This finding has implications for the interfacial behaviour of the hydrocolloids and highlights an additional distinction between MASH and EGSH despite belonging to the same botanical family.

3.10.2 Microstructure of moringa, makataan and egusi seed hydrocolloids

The microstructure of the hydrocolloids differed considerably with each hydrocolloid. The MOSH showed a fibrous microstructure composed of loose, interconnected fibres with small cavities (Dick et al., 2020;3). Fewer fibres were evident than in MASH and EGSH. The very interconnected networks are formed in the MASH (Figure 3.8), creating a highly dense and compact structure. The lower the concentration/volume of the hydrocolloid in the solution, the thinner and the more dispersed the molecular bundles, decreasing the gelled system's springiness and hardness.

The compact microstructure observed in MASH and EGSH exhibited lower springiness than MOSH. This finding aligns with reports by Tiwari et al. (2015) and Yuris et al. (2018), which describe gels made with mango pulp, gellan gum, and agar as having more uniform cellular structures. In their studies, the air cells in the gels were homogeneous and smaller, contributing to improved gel uniformity and texture. The MOSH showed a more homogeneous network with smaller polymer-free cavities than the others (Figure 3.8); larger pores indicate the presence of water in large quantities inside the gel network, probably due to the absence of a homogeneous network with large cavities. Aeration during freezing and freeze-drying produced highly uniform samples, indicating that mass and heat transfer were enough to avoid trapped vapour. Different microstructures were identified in MOSH, MASH and EGSH. The MASH and EGSH presented a denser, more compact, and more robust network, leading to high retention, while the MOSH showed a weaker network. Additionally, the elemental composition of each hydrocolloid was observed with the EDX analyses, indicating that carbon and oxygen peaked highest among all the elements in the three hydrocolloids, as seen in Table 3.7. The micrographs and the EDX spectrum revealed that the homogeneous distribution of the hydrocolloid particles over the surface (Figure 3 8) might serve as an artificial bone-like network for cells in vitro. Carbon, oxygen,

sulphur, phosphorus, potassium, and calcium were visibly peaked and varied amongst the hydrocolloids. MOSH had the highest sulphur and potassium compared to EGSH and MOSH.

Table 3.7 Energy Dispersive X-Ray of Moringa, Makataan and Egusi seed Hydrocolloid [1,2].

	EGSH	MOSH	MASH
Carbon	59.3 ± 85.23[a]	57.29 ± 2.24[a]	51.55 ± 9.21[a]
Oxygen	34.01 ± 5.41[a]	37.20 ± 3.07[a]	35.90 ± 2.49[a]
Magnesium	0.58 ± 0.52[a]	0.540 ± 0.17 [a]	0.43 ± 0.25[a]
Phosphorus	1.53 ± 0.35[a]	0.920 ± 0.31[a]	0.930 ± 84[a]
Sulphur	1.16 ± 0.59[a]	1.22 ± 1.04[a]	4.55 ± 0.98[b]
Potassium	1.11 ± 1.01[a]	2.68 ± 1.08[b]	4.28 ± 1.95[c]
Calcium	1.06 ± 1.43[a]	0.07 ± 1.12[a]	0.33 ± 0.52[a]

[1] Mean ± standard deviation of 7 replicas. Different letters in the same row indicate significant differences ($p < 0.05$). [2] Egusi seed hydrocolloid (EGSH); Moringa seed hydrocolloid (MASH); Moringa seed hydrocolloid (MOSH).

EGH at 100µm **10µm**

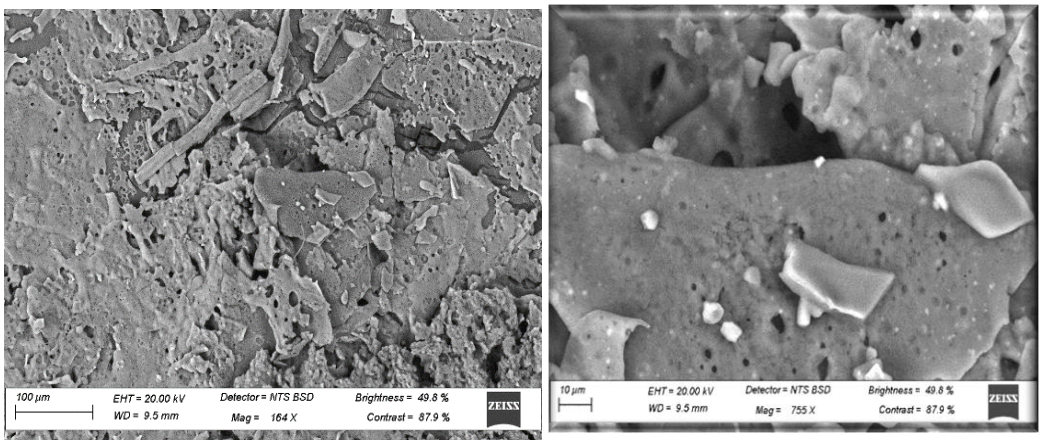

MAH at 100µm **10µm**

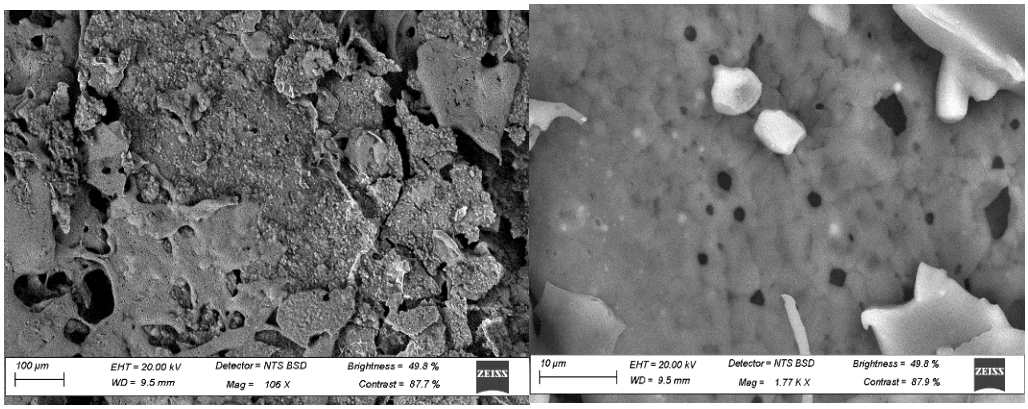

MOH at 100µm **10µm**

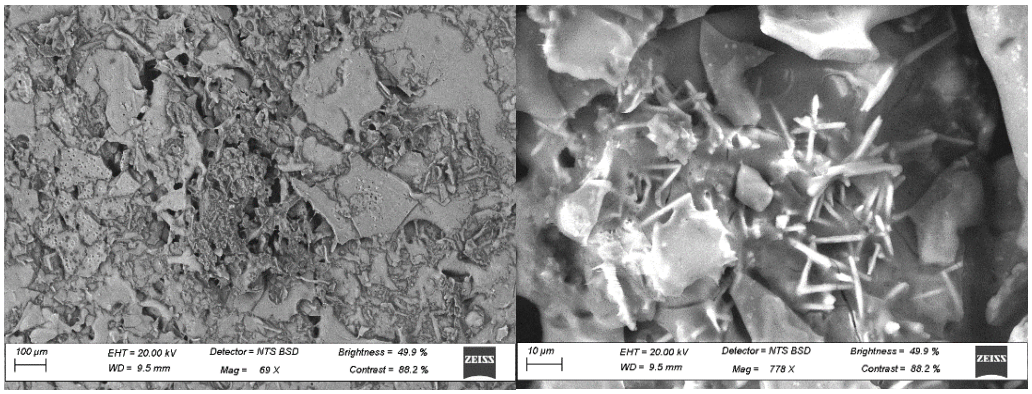

Figure 3.8. Scanning electron microscopy (SEM) images of freeze-dried Moringa seed hydrocolloid (MOSH), Moringa seed hydrocolloid (MASH) and Egusi seed hydrocolloid (EGSH). The 100 µm ima**ge will show a broader area of the sample, allowing you to observe large features or structures. The 10 µm image** focuses on a smaller area, offering a more detailed, zoomed-in view.

The table on the Energy Dispersive X-Ray (EDX) analysis of moringa (MOSH), makataan (MASH), and egusi seed hydrocolloids (EGSH) provides crucial insights into their elemental composition, which is highly relevant to the food industry for the following reasons. The high carbon and oxygen content in all three hydrocolloids reflects their carbohydrate and organic material composition, which is crucial for their functional properties, such as thickening or emulsifying.

3.10.3 Light and partially polarised light of egusi, moringa and makataan seed hydrocolloid

Particle size reduction observed at a magnification of ×40 also confirmed that grinding and sieving effectively reduced the particle size of each hydrocolloid. Morphological results of each hydrocolloid using polarised and non-polarised light are shown in Figure 3.9. Each hydrocolloid was a semi-crystalline polymer alternately stacked with semi-crystalline and vague growth rings.

The primary components were microproteins, linear amylose polymers, and highly branching, partially crystalline amylopectin (Abedi et al., 2024;6). Under a polarising microscope, the starch particles displayed birefringence and cross-polarized crosses.

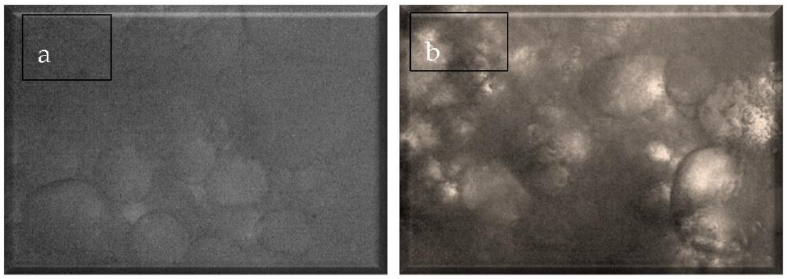

Egusi hydrocolloid

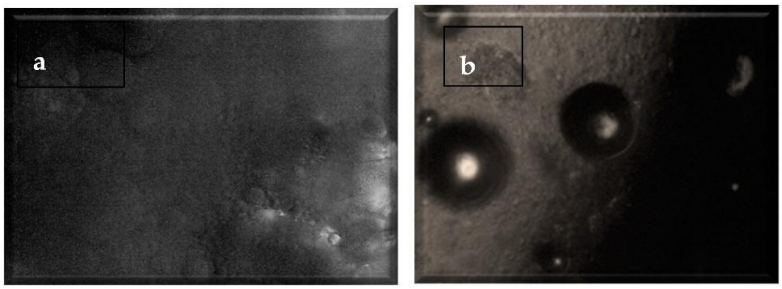

Makataan hydrocolloid

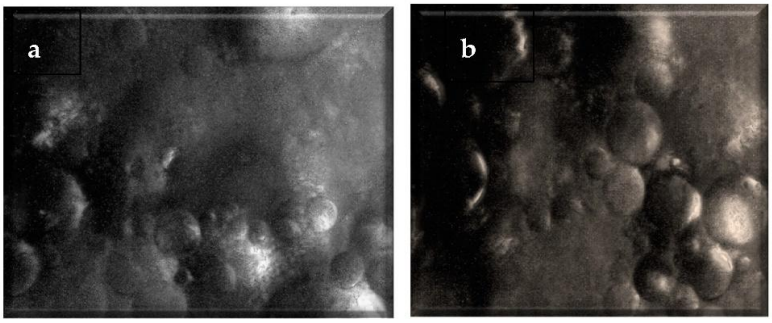

Moringa hydrocolloid

Figure 3.9 Morphology of extracted hydrocolloid using light and polarise microscopy (a) lights (b) partially polarised.

3.11 Colour of Moringa, Egusi and Makataan Hydrocolloids

For each hydrocolloid, the hue was 87.99, 87.03 and 86.87 for EGSH, MOSH and MASH, with no significant differences. Chroma is the attribute that expresses the purity of a colour. The chroma for each hydrocolloid, 16.12, 17.65, and 16.50, for EGSH, MOSH and MASH, respectively, indicated less colour saturation. The lightness (L*), greenness (a*), and redness (b*)

of each hydrocolloid significantly varied 83.03, 0.54, 16.12 and 81.39, 0.61 and 17.65); 78.63, 0.90, 16.50, respectively for Egusi seed hydrocolloid (EGSH), Moringa seed hydrocolloid (MOSH) and Moringa seed hydrocolloid (MASH). MASH showed the lowest lightness, 78.63, with redness (a*) close to zero for all hydrocolloids (0.54 to 0.90), implying a neutral colour.

Furthermore, the yellowness (b*) differed significantly from 16.12 to 17.65, being more yellowish than blue, as shown in Table 3.8. The oilseed sources played a significant role in the colour of each hydrocolloid. The lightness defining colour in terms of how close it is to white or black is a property of the seed coat's type and the number of pigments (tannins and anthocyanins). It depends primarily on plant genetics. The exposure of cotyledon after grinding seeds may be the possible reason for differences in colour parameters amongst the hydrocolloids. The light colour of all the hydrocolloids may find specific applications in foods that require little or no colour change during processing.

Table 3.8 Colours in Moringa, Makataan and Egusi seed hydrocolloids[1, 2].

Hydrocolloid	L*	a*	b*	C	H
Egusi	83.03 ± 0.23^{a}	0.54 ± 0.08^{b}	16.12 ± 0.14^{c}	16.13 ± 0.16^{c}	87.99 ± 0.20^{a}
Moringa	81.39 ± 0.04^{a}	0.61 ± 0.01^{b}	17.65 ± 0.00^{c}	17.66 ± 0.00^{c}	87.03 ± 0.02^{a}
Makataan	78.63 ± 0.10^{a}	0.90 ± 0.02^{b}	16.56 ± 0.13^{c}	16.50 ± 0.09^{c}	86.87 ± 0.06^{d}

[1] Mean ± standard deviation in five replicates. Means with different superscripts in the same column indicate significant differences ($p < 0.05$). [2] EGSH (Egusi seed hydrocolloid); MASH (Moringa seed hydrocolloid): MOSH (Moringa seed hydrocolloid).

3.12 Principal Component Analysis of Nutritional and Functional Properties of Egusi, Makataan, and Moringa Seed Hydrocolloids

The contributions of two principal components (PCs) to the variation in the nutritional and functional properties of moringa, makataan, and egusi seeds hydrocolloids are shown in Figure 3.10. The Principal Component 1 (PC1), accounted for 52.8% of the variability, whereas Principal Component 2 (PC2) explained 47.2%. These elements thoroughly examined the characteristics of the hydrocolloids, accounting for 100% of the overall diversity. The makataan hydrocolloid (MASH) properties were mainly in line with PC1. It revealed positive associations with fat, potassium, carbohydrate and amino acids (such as alanine, phenylalanine, aspartic acid, valine, isoleucine, threonine, histidine, and proline). Sugars (glucose and sucrose) showed negative connections with moringa seed hydrocolloid (MOSH), more closely linked to MOSH. The multipurpose profile that MASH displayed was defined by enhanced hydrophobicity, which probably improved stabilising and emulsifying qualities. The ability to bind water aids in gelation

and thickening in food compositions and the interplay of amino acids, lipids, and carbohydrates produces a variety of actions. The thickening qualities of MOSH are facilitated by the presence of glucose and sucrose. These sugars may interact with other ingredients during processing to improve consistency and viscosity.

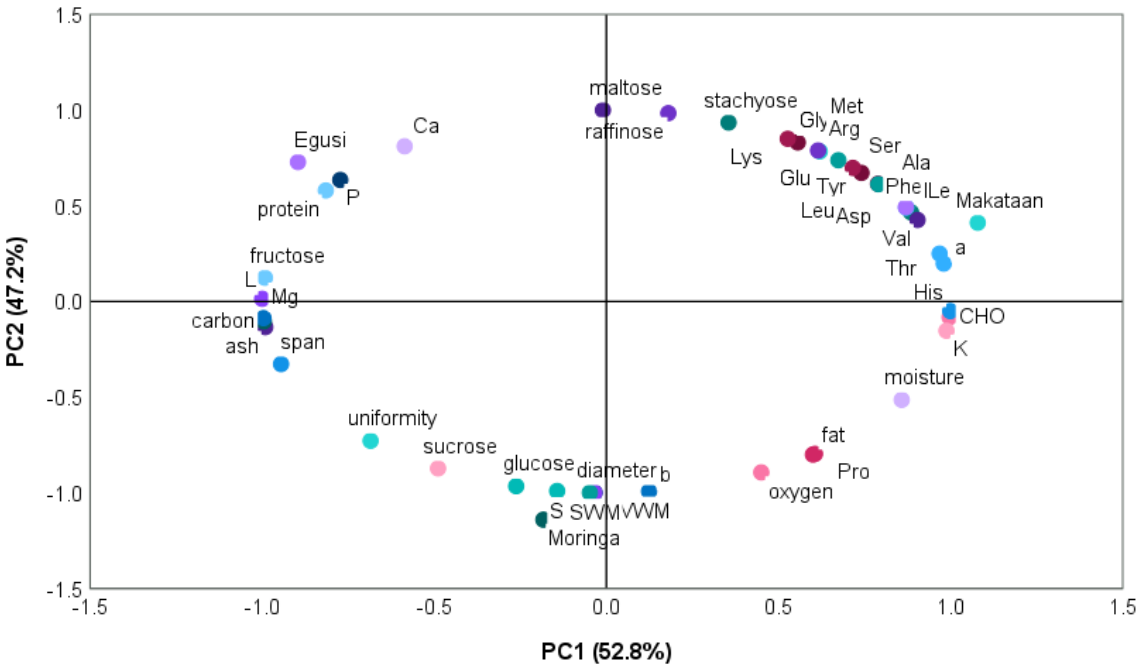

Figure 3.10 Principal component scores and loading plots for the nutritional and functional relationship among the hydrocolloids**.**

The three hydrocolloids also behaved differently, with MOSH having lesser nutritional and functional qualities than makataan and egusi hydrocolloids.

3.13 Interfacial Tension of Egusi, Moringa and Makataan Hydrocolloid

The previous sections (3.9 to 3.10) made it clear that dispersion of the three hydrocolloids (EGSH, MASH, MOSH) in water gave rise to a system containing solid particles in mixtures with an aqueous solution of proteins and polysaccharides, which is the result of hydrocolloid dissolution. The primary purpose of this part of the present investigation was to determine the extent to which

the mixed emulsifier system formed by solid particles (hydrocolloids) and mainly their proteins can modify oil-water interfacial properties. The dynamic interfacial tensions of the three systems were first measured to probe the reduction rate of the interfacial tension and shed light on the mechanism of the emulsion preparation. Then, the equilibrium interfacial tensions were extracted from the graphs to estimate the emulsion stabilisation mechanisms against coalescence and creaming. The results of the dynamic interfacial tension are shown in Figure 3.10.

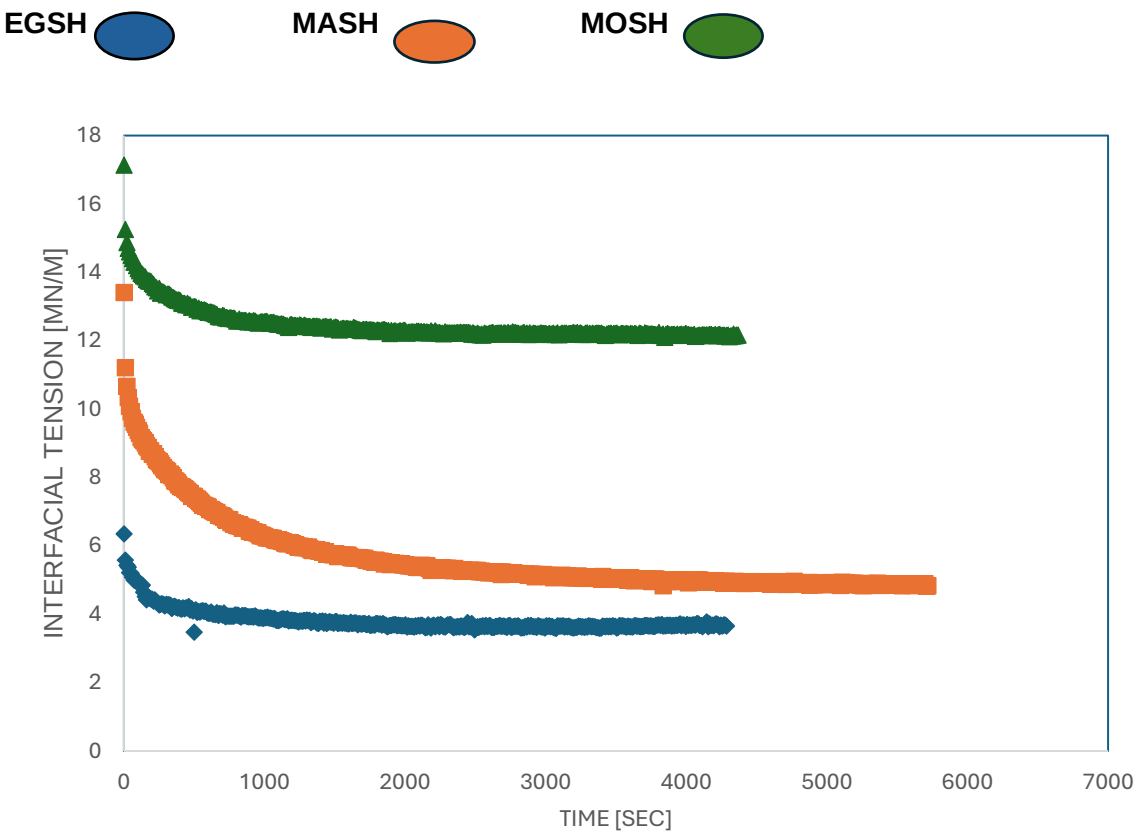

Figure 3.11 Dynamic interfacial tensions of the three hydrocolloids.

Figure 3.11 clearly shows the reduction rate of the interfacial tension, as measured by the slopes of the curves shown for each hydrocolloid. This is in line with the particle dissolution rate in water to release the surface active species (proteins) (see Section 3.9.1) (Okuro et al., 2020;7). Additionally, all hydrocolloids reached the equilibrium interfacial tension; the values are summarised in Table 9. Data related to some conventional surfactants, lecithin and guar, are also compared (Okuro et al., 2020;7).

Table 3.9 Equilibrium interfacial tensions[1, 2].

Emulsifier Type	Emulsifier (%)	γ, (mN/m)
Lecithin	10	9.30[a]
EGSH	10	3.67[b]
MASH	10	4.84[b]
MOSH	10	12.16[c]
Guar	10	4.04[b]

[1]Mean ± standard deviation of different superscripts in the same column indicate significant ($p < 0.05$) differences. [2] EGSH (Egusi seed hydrocolloid); MASH (Moringa seed hydrocolloid): MOSH (Moringa seed hydrocolloid).

Conversely to MOSH, which has an equilibrium interfacial tension higher than the ones associated with conventional surfactants (guar, lecithin), EGSH and MASH demonstrated excellent interfacial activities. The equilibrium interfacial tension of EGSH and MASH is lower than the one associated with lecithin and comparable to the one related to guar (Das et al., 2020;5). This is deemed a critical finding for both scientific interest and technological applications of these systems. Protein is essential in the emulsifying activities of naturally occurring emulsifiers, such as gum Arabic (Bennacef et al., 2021;99). Attaining this perfect extraction state is only possible by using an environmentally friendly process that uses heat instead of the denaturing effect of using a solvent extraction method to obtain hydrocolloids (Dendrobium et al., 2020;7). Additionally, the ability of a protein to possess suitable emulsifying and foaming properties depends mainly on the protein conformation and its ability to interact with water and oil at a molecular level. The rate of interfacial tension reduction in the presence of MASH compared to those associated with EGSH and MOSH. This could be due, first, to the slow rate of proteins released from the hydrocolloids. Second, to slow interfacial rearrangements of its proteins over time to adopt the equilibrium conformation where polar segments move from the oil phase; only non-polar segments adsorb at the interface (Kundu et al., 2018;77). This agrees with the high content of amino acids with polar and non-polar side chains in MASH compared to MOSH or EGSH (Table 3.4). Third, MASH particles could take longer before reaching a size small enough to be adsorbed at the interface.

On the other hand, it seems reasonable to assume that MOSH's high equilibrium interfacial tension, compared to MASH or EGSH, is caused by its high hydrophobic protein (hydrophobic proteins MASH = hydrophobic proteins EGSH > hydrophobic proteins MOSH). Proteins in MOSH likely have more attachment points than the ones in MASH or EGSH, reducing the number of MOSH adsorbed as, in this case, each protein could occupy more sites than MASH or EGSH.

3.14 Conclusion and Recommendation

The study explored the potential of EGSH, MASH, and MOSH as natural emulsifiers that enhance emulsion stability. The hydrocolloids, extracted from egusi, moringa, and makataan seeds through a hot water extraction process at 100°C with a 1:8 ratio, were characterised by their physicochemical and functional properties. The hydrocolloids possessed a higher protein-to-carbohydrate ratio, contributing to improved properties of food. The promising role of these hydrocolloids is key to improving food texture, nutrition, and stability of food quality. The hydrocolloid/dissolved protein system could anchor onto the interface, resulting in equilibrium interfacial tensions comparable to those achieved with standard surfactants. The superior performance exhibited by EGSH and MASH in this context is noteworthy. Additionally, EGSH and MASH hydrocolloids showcased robust particle adhesion, likely attributed to the substantial size of protein-based particles and their consequent high-water absorption, leading to enhanced structural homogeneity. These findings suggest that emulsifier systems comprising hydrocolloids with high protein content hold promise for applications in the food industry. Such systems offer manufacturers greater flexibility in selecting hydrocolloid/dissolved protein mixtures to control rheology—an imperative property for the technological applications of these systems. However, further research is necessary to comprehensively understand and optimise these hydrocolloids' performance, considering the limitations and advantages uncovered in this study in the broader context of food industry applications.

References

Abedi, E., Roohi, R., Mohammad, S., Hashemi, B. & Kaveh, S. 2024. Ultrasonics Sonochemistry Investigation of ultrasound-assisted starch acetylation by single- and dual-frequency ultrasound based on rheology modelling, non-isothermal reaction kinetics, and flow / acoustic simulation. *Ultrasonics Sonochemistry*, 102(December 2023): 106737. https://doi.org/10.1016/j.ultsonch.2023.106737.

Adeloye, J.B., Osho, H. & Idris, L.O. 2020. Defatted coconut flour improved the bioactive components, dietary fibre, antioxidant and sensory properties of nixtamalised maize flour. *Journal of Agriculture and Food Research*, 2(February): 100042. https://doi.org/10.1016/j.jafr.2020.100042.

Afzal, I., Jaffar, I., Zahid, S., Rehman, H.U. & Basra, S.M.A. 2020. Physiological and biochemical changes during hermetic storage of *Moringa oleifera* seeds. *South African Journal of Botany*, 129: 435–441.

Ai, J., Witt, T., Cowin, G., Dhital, S., Turner, M.S., Stokes, J.R. & Gidley, M.J. 2018. Anti-staling of high-moisture starchy food: Effect of hydrocolloids, emulsifiers and enzymes on mechanics of steamed-rice cakes. *Food Hydrocolloids*, 83(May): 454–464.

de Almeida Paula, D., Mota Ramos, A., Basílio de Oliveira, E., Maurício Furtado Martins, E., Augusto Ribeiro de Barros, F., Cristina Teixeira Ribeiro Vidigal, M., de Almeida Costa, N. & Tatagiba da Rocha, C. 2018. Increased thermal stability of anthocyanins at pH 4.0 by guar gum in aqueous dispersions and double emulsions W/O/W. *International Journal of Biological Macromolecules*, 117: 665–672.

AOAC. 2005. Official Methods of Analysis of AOAC INTERNATIONAL. *Official Methods of Analysis of AOAC International, 18th edit* (February): 20877–2417.

Ashton, L., Pudney, P.D.A., Blanch, E.W. & Yakubov, G.E. 2013. Understanding glycoprotein behaviours using Raman and Raman optical activity spectroscopies: Characterising the entanglement induced conformational changes in oligosaccharide chains of mucin. *Advances in Colloid and Interface Science*, 199–200: 66–77. http://dx.doi.org/10.1016/j.cis.2013.06.005.

Ayerza(h), R. 2019. Seed characteristics, oil content and fatty acid composition of moringa (*Moringa oleifera* Lam) seeds from three arid land locations in Ecuador. *Industrial Crops and Products*, 140(March): 111575. https://doi.org/10.1016/j.indcrop.2019.111575.

Balachandramohan, J., Sivasankar, T. & Sivakumar, M. 2020. Facile sonochemical synthesis of Ag2O-guar gum nanocomposite as a visible light photocatalyst for the organic transformation reactions. *Journal of Hazardous Materials*, 385(October 2019): 121621. https://doi.org/10.1016/j.jhazmat.2019.121621.

Bennacef, C., Desobry-Banon, S., Probst, L. & Desobry, S. 2021. Advances on alginate use for spherification to encapsulate biomolecules. *Food Hydrocolloids*, 118(November 2020).

Bulbul, V.J., Bhushette, P.R., Zambare, R.S., Deshmukh, R.R. & Annapure, U.S. 2019. Effect of cold plasma treatment on Xanthan gum properties. *Polymer Testing*, 79(July): 106056. https://doi.org/10.1016/j.polymertesting.2019.106056.

Das, A., Kundu, S., Ghosh, S.K., Basu, A., Gupta, M. & Mukherjee, A. 2020. Guar gum cinnamate ouzo nanoparticles for bacterial contact killing in a water environment. *Carbohydrate Research*, 491(December 2019): 107983. https://doi.org/10.1016/j.carres.2020.107983.

Dendrobium, O., Arabic, G. & Alginate, G. 2020. Stabilising the Oil-in-Water Emulsions Using the. *Molecules*: 8–10.

Department of Agriculture, F. and F. 2013. • PRODUCTION GUIDELINES • *Citrullus lanatus* (Thunberg).https://old.dalrrd.gov.za/Portals/0/Brochures%20and%20Production%20guidelines/Production%20Guidelines%20Bitter%20Watermelon.pdf

Dick, A., Bhandari, B., Dong, X. & Prakash, S. 2020. Feasibility study of hydrocolloid incorporated 3D printed pork as dysphagia food. *Food Hydrocolloids*, 107(April): 105940. https://doi.org/10.1016/j.foodhyd.2020.105940.

Dranca, F., Talón, E., Vargas, M. & Oroian, M. 2021. Microwave vs. conventional extraction of pectin from Malus domestica ‘Fălticeni’ pomace and its potential use in hydrocolloid-based

films. *Food Hydrocolloids*, 121(February).

Drosou, C., Krokida, M. & Biliaderis, C.G. 2022. Encapsulation of β-carotene into food-grade nanofibers via coaxial electrospinning of hydrocolloids: Enhancement of oxidative stability and photoprotection. *Food Hydrocolloids*, 133(March).

Fadele, O.K. & Aremu, A.K. 2018. Optimisation of shelling efficiency of a *Moringa oleifera* seed shelling machine based on seed sizes. *Industrial Crops and Products*, 112 (January): 775–782. https://doi.org/10.1016/j.indcrop.2018.01.011.

Famakinwa, A., Ilo, J., Olubi, O., Oguntibeju, O., Wyk, J.V.A.N. & Obilana, A. 2023. Current Research in Nutrition and Food Science; Extraction and industrial applications of macro Molecules : A Review. *Current Research in Nutrition and Food Science*, 11(3).

Ge, H., Wu, Y., Woshnak, L.L. & Mitmesser, S.H. 2021. Effects of hydrocolloids, acids and nutrients on gelatine network in gummies. *Food Hydrocolloids*, 113(November 2020): 106549. https://doi.org/10.1016/j.foodhyd.2020.106549.

Guzmán-Albores, J.M., Bojórquez-Velázquez, E., De León-Rodríguez, A., Calva-Cruz, O. de J., Barba de la Rosa, A.P. & Ruíz-Valdiviezo, V.M. 2021. Comparison of *Moringa oleifera* oils extracted with supercritical fluids and hexane and characterisation of seed storage proteins in defatted flour: Moringa seed characterisation. *Food Bioscience*, 40(November 2020).

He, X. hong, Xia, W., Chen, R. yun, Dai, T. tao, Luo, S. jing, Chen, J. & Liu, C. mei. 2020. A new pre-gelatinized starch is prepared by gelatinisation and spray-drying rice starch with hydrocolloids. *Carbohydrate Polymers*, 229(October 2019): 115485. https://doi.org/10.1016/j.carbpol.2019.115485.

Hedayati, S., Niakousari, M., Babajafari, S. & Mazloomi, S.M. 2021. Ultrasound-assisted extraction of mucilaginous seed hydrocolloids: Physicochemical properties and food applications. *Trends in Food Science and Technology*, 118(PA): 356–361. https://doi.org/10.1016/j.tifs.2021.10.022.

Huang, R., Huang, K., Guan, X., Li, S., Cao, H., Zhang, Y., Lao, X., Bao, Y. & Wang, J. 2021. Effect of defatting and extruding treatment on the physicochemical and storage properties of quinoa (Chenopodium quinoa Wild) flour. *Lwt*, 147(January): 111612. https://doi.org/10.1016/j.lwt.2021.111612.

Igwenyi, I.O. & Akubugwo, E.I. 2010. Analysis of four seeds used as soup thickeners in northern Nigeria. In *ICE 2010 - 2010 International Conference on Chemistry and Chemical Engineering, Proceedings*. 426–430.

Ijoyah, M.O., Bwala, R.I. & Iheadindueme, C.A. 2012. Response of cassava, maize and egusi melon in a three-crop intercropping system at Makurdi, Nigeria. , 1(2): 135–144.

Jakopic, J., Veberic, R. & Slatnar, A. 2021. Changes in quality parameters in rutabaga (Brassica napus var. napobrassica) roots during long-term storage. *Lwt*, 147(April): 111587. https://doi.org/10.1016/j.lwt.2021.111587.

Kanikireddy, V., Varaprasad, K., Rani, M.S., Venkataswamy, P., Mohan Reddy, B.J. & Vithal, M. 2020. Biosynthesis of CMC-Guar gum-Ag0 nanocomposites for inactivation of food pathogenic microbes and its effect on the shelf life of strawberries. *Carbohydrate Polymers*, 236(December 2019): 116053. https://doi.org/10.1016/j.carbpol.2020.116053.

Karefyllakis, D., Octaviana, H., van der Goot, A.J. & Nikiforidis, C. V. 2019. The emulsifying performance of mildly derived mixtures from sunflower seeds. *Food Hydrocolloids*, 88: 75–85.

Khan, N., Kumar, D. & Kumar, P. 2020. Silver nanoparticles embedded guar gum/ gelatin nanocomposite: Green synthesis, characterisation and antibacterial activity. *Colloids and Interface Science Communications*, 35(January): 100242. https://doi.org/10.1016/j.colcom.2020.100242.

Kundu, S., Das, A., Basu, A., Ghosh, D., Datta, P. & Mukherjee, A. 2018. Carboxymethyl guar gum synthesis in homogeneous phase and macroporous 3D scaffolds design for tissue engineering. *Carbohydrate Polymers*, 191(October 2017): 71–78. https://doi.org/10.1016/j.carbpol.2018.03.007.

Li, C., He, M., Yun, Y. & Peng, Y. 2020. Co-infection with Wolbachia and Cardinium may promote the synthesis of fat and free amino acids in a small spider, Hylyphantes graminicola. *Journal of Invertebrate Pathology*, 169(December 2019): 107307. https://doi.org/10.1016/j.jip.2019.107307.

Lijina, P. & Ganesh Kumar, B.S. 2023. Differentiating planteose and raffinose using negative ion mode mass spectrometry. *International Journal of Mass Spectrometry*, 487: 117027. https://doi.org/10.1016/j.ijms.2023.117027.

Lin, M., Tay, S.H., Yang, H., Yang, B. & Li, H. 2017. Replacement of eggs with soybean protein isolates and polysaccharides to prepare yellow cakes suitable for vegetarians. *Food Chemistry*, 229: 663–673. http://dx.doi.org/10.1016/j.foodchem.2017.02.132.

Liu, H., Ye, C., Zhao, Y., Li, G., Xu, Y. & Tang, Y. 2022. Chemical Engineering and Processing - Process Intensification Performance analysis of biomass gasification coupled with ultra-supercritical power generation system. *Chemical Engineering and Processing - Process Intensification*, 179(August): 109093. https://doi.org/10.1016/j.cep.2022.109093.

Mashilo, J., Shimelis, H. & Ngwepe, R.M. 2022. Genetic resources of bottle gourd (Lagenaria siceraria (Molina) Standl.] and citron watermelon (Citrullus lanatus var. *citroides* (L.H. Bailey) Mansf. ex Greb.)- implications for genetic improvement, product development and commercialisation: A review. *South African Journal of Botany*, 145: 28–47. https://doi.org/10.1016/j.sajb.2021.10.013.

Mohamadzadeh, M., Fazeli, A. & Shojaosadati, S.A. 2024. Polysaccharides and proteins-based bionanocomposites for microencapsulation of probiotics to improve stability and viability in the gastrointestinal tract: A review. *International Journal of Biological Macromolecules*,

259(P2): 129287. https://doi.org/10.1016/j.ijbiomac.2024.129287.

Mohammed Nour, A.A., Mohamed, A.R., Adiamo, O.Q. & Babiker, E.E. 2018. Changes in protein nutritional quality are affected by the processing of millet supplemented with Moringa seed flour. *Journal of the Saudi Society of Agricultural Sciences*, 17(3): 275–281.

Ntui, V.O., Thirukkumaran, G., Iioka, S. & Mii, M. 2009. Efficient plant regeneration via organogenesis in 'Egusi' melon (Colocynthis citrullus L.). *Scientia Horticulturae*, 119(4): 397–402.

Okuro, P.K., Gomes, A. & Cunha, R.L. 2020. Hybrid oil-in-water emulsions applying wax(lecithin)-based structured oils: Tailoring interface properties. *Food Research International*, 138(PB): 109798. https://doi.org/10.1016/j.foodres.2020.109798.

Olubi, O. 2018. Functional characteristics of egusi seed (Citrullus lanatus) hydrocolloid and oil in instant egusi soup. *(Master Thesis) Cape peninsula university of technology*, (April). https://www.semanticscholar.org/paper/Functional-characteristics-of-egusi-seed-(Citrullus-Olubi).

Olubi, O., Felix-minnaar, J. & Jideani, V.A. Nutritional Profiling of Underutilised *Citrullus lanatus mucosospermus* Seed Flour Nutritional Profiling of Underutilised *Citrullus lanatus mucosospermus* Seed Flour.

Olubi, O., Felix-minnaar, J.V. & Jideani, V.A. 2021. Instant *Citrullus lanatus mucosospermus* (Egusi) Soup.

Olubi, O., Obilana, A., Tshilumbu, N., Fester, V. & Jideani, V. 2024. Physicochemical and Functional Properties of Citrullus mucosospermus, *Citroides*, and *Moringa oleifera* Seeds' Hydrocolloids. *Foods*, 13(7).

Opoku-Boahen, Y., Novick, B.D. & Wubah, D. 2013. Physicochemical characterisation of traditional Ghanaian cooking oils, derived from Egusi (Citrullus colocynthis) and Werewere (Cucumeropsis manni) seeds. *Int. J. Biol. Chem. Sci.*, 7(1): 387–395.

Paudel, L., Clevenger, J. & McGregor, C. 2019. Refining of the egusi locus in watermelon using KASP assays. *Scientia Horticulturae*, 257(January): 108665. https://doi.org/10.1016/j.scienta.2019.108665.

Prothro, J., Sandlin, K., Gill, R., Bachlava, E., White, V., Knapp, S.J. & McGregor, C. 2012. Mapping of the Egusi Seed Trait Locus (e.g.) and Quantitative Trait Loci Associated with Seed Oil Percentage in Watermelon. *Journal of the American Society for Horticultural Science*, 137(5): 311–315.

Renzetti, S. & van der Sman, R.G.M. 2022. Food texture design in sugar reduced cakes: Predicting batters rheology and physical properties of cakes from physicochemical principles. *Food Hydrocolloids*, 131(February): 107795. https://doi.org/10.1016/j.foodhyd.2022.107795.

Rostamabadi, H., Chaudhary, V., Chhikara, N., Sharma, N., Nowacka, M., Demirkesen, I.,

Rathnakumar, K. & Falsafi, S.R. 2023. Ovalbumin, an outstanding food hydrocolloid: Applications, technofunctional attributes, and nutritional facts, A systematic review. *Food Hydrocolloids*, 139(November 2022).

Seifu, E. & Teketay, D. 2020. Introduction and expansion of *Moringa oleifera* Lam. in Botswana: Current status and potential for commercialisation. *South African Journal of Botany*, 129: 471–479. https://doi.org/10.1016/j.sajb.2020.01.020.

Shim, Y.Y., Gui, B., Wang, Y. and Reaney, M.J., 2015. Flaxseed (Linum usitatissimum L.) oil processing and selected products. *Trends in Food Science & Technology*, *43*(2), pp.162-177.

Tan, H.L., Tan, T.C. & Easa, A.M. 2020. The use of selected hydrocolloids and salt substitutes on structural integrity, texture, sensory properties, and shelf life of fresh, no-salt wheat noodles. *Food Hydrocolloids*, 108(July 2019): 105996. https://doi.org/10.1016/j.foodhyd.2020.105996.

Tiwari, S., Chakkaravarthi, A. & Bhattacharya, S. 2015. Imaging and image analysis of freeze-dried cellular solids of gellan and agar gels. *Journal of Food Engineering*, 165: 60–65. http://dx.doi.org/10.1016/j.jfoodeng.2015.04.017.

Tornberg, E. 2022. *Influence of dietary fibres and particle size distribution on food rheology*. Elsevier Ltd. http://dx.doi.org/10.1016/B978-0-08-100431-9/00008-5.

Uruakpa, F. 2004. Heat-induced gelation of whole egusi (Colocynthis citrullus L.) seeds. *Food Chemistry*, 87(3): 349–354. http://linkinghub.elsevier.com/retrieve/pii/S0308814603006319.

Wang, M., Yin, Z., Sun, W., Zhong, Q., Zhang, Y. & Zeng, M. 2023. Microalgae play a structuring role in food: Effect of spirulina platensis on the rheological, gelling characteristics, and mechanical properties of soy protein isolate hydrogel. *Food Hydrocolloids*, 136(PA): 108244. https://doi.org/10.1016/j.foodhyd.2022.108244.

Wang, P., Gao, Y., Wang, D., Huang, Z. & Fei, P. 2022. Amidated pectin with amino acids: Preparation, characterisation and potential application in Hydrocolloids. *Food Hydrocolloids*, 129(February): 107662. https://doi.org/10.1016/j.foodhyd.2022.107662.

Yue, J., Yao, X., Gou, Q., Li, D., Liu, N., Yang, D., Gao, Z., Midgley, A., Katsuyoshi, N. & Zhao, M. 2022. Recent advances of interfacial and rheological property-based techno-functionality of food protein amyloid fibrils. *Food Hydrocolloids*, 132(February): 107827. https://doi.org/10.1016/j.foodhyd.2022.107827.

Yuris, A., Matia-Merino, L., Hardacre, A.K., Hindmarsh, J. & Goh, K.K.T. 2018. Molecular interactions in composite wheat starch-Mesona chinensis polysaccharide gels: Rheological, textural, microstructural and retrogradation properties. *Food Hydrocolloids*, 79: 1–12. https://doi.org/10.1016/j.foodhyd.2017.12.007.

Zhao, J., Wang, D., Zhang, L. & Lian, X. 2023. Corrigendum to: “Study on the mechanism of structure modification of amylopectin co-crystalized by sodium chloride to promote disulfide

bond formation of alkali-soluble glutenin" [Food Hydrocolloids 146 (PA) (2023) 109229] (Food Hydrocolloids (2024) 146(P. *Food Hydrocolloids*, 148(PA): 109501. https://doi.org/10.1016/j.foodhyd.2023.109501.

Zhou, P., Eid, M., Xiong, W., Ren, C., Ai, T., Deng, Z., Li, J. & Li, B. 2020. Comparative study between cold and hot water extracted polysaccharides from Plantago ovata seed husk using rheological methods. *Food Hydrocolloids*, 101(August 2019): 105465. https://doi.org/10.1016/j.foodhyd.2019.105465.

Zhu, Y., Gao, H., Liu, W., Zou, L. & McClements, D.J. 2020. A review of the rheological properties of dilute and concentrated food emulsions. *Journal of Texture Studies*, 51(1):

Zhao, J., Wang, D., Zhang, L. & Lian, X. 2023. Corrigendum to: "Study on the mechanism of structure modification of amylopectin co-crystalized by sodium chloride to promote disulfide bond formation of alkali-soluble glutenin" [Food Hydrocolloids 146 (PA) (2023) 109229] (Food Hydrocolloids (2024) 146(P. *Food Hydrocolloids*, 148(PA): 109501. https://doi.org/10.1016/j.foodhyd.2023.109501.

Zhou, P., Eid, M., Xiong, W., Ren, C., Ai, T., Deng, Z., Li, J. & Li, B. 2020. Comparative study between cold and hot water extracted polysaccharides from Plantago ovata seed husk by using rheological methods. *Food Hydrocolloids*, 101(August 2019): 105465. https://doi.org/10.1016/j.foodhyd.2019.105465.

Zhu, Y., Gao, H., Liu, W., Zou, L. & McClements, D.J. 2020. A review of the rheological properties of dilute and concentrated food emulsions. *Journal of Texture Studies*, 51(1): 45–55.

CHAPTER FOUR

RHEOLOGICAL BEHAVIOUR OF *CITRULLUS LANATUS MUCOSOSPERMUS, CITRULLUS CITROIDES AND MORINGA OLEIFERA* SEEDS *HYDROCOLLOID*

Abstract

This study investigated the rheological behaviour of three novel hydrocolloids: Egusi hydrocolloid (EGH), makataan hydrocolloid (MAH), and moringa hydrocolloid (MOH). The high protein content of these hydrocolloids, 48.12%, 34.00%, and 35.00% for MOH, MAH, and EGH, reduced the interfacial tension. This chapter reported the mechanical response of this hydrocolloid in semi-concentrated (20-50 wt%) as well as concentrated (50-75 wt%) slurries when subjected to a steady shear flow to reversible minor strains in amplitude as well as frequency-sweep modes of deformation. Regardless of the hydrocolloid type and process parameters (pH = 4–9; temperatures =30-75 ^{o}C; mixing time = 1-10 minutes; concentration = 20–50 wt%), semi-concentrated slurries are pseudoplastic materials that behave like viscous liquids with no yield stress; $G^{"} > G^{'}$ in the entire range of strain (0.1-200%). The correlation between storage modulus, yield stress, and slurry concentration showed two deflection points/transitional points, 50 and 67 wt%, respectively. The first transition point (onset id structure formation) was present in all three hydrocolloids, whereas the second was only related to EGH and MAH slurries; MOH-based slurries do not display such a point. The bottle test further confirmed this: slurries containing more than 50% by mass hydrocolloids do not flow when inverting the vessels. The second transitional point marks the boundary between the region of the slow or rapid response of the strength or rigidity of the structure of the slurry of EGH and MAH with changes in hydrocolloid concentration. Conversely, the rigidity of the structure of the slurries displays an opposite effect. The contradiction between the yield stress and the shear elastic modulus on either side of this transition point highlights a difference in microstructural phenomena induced by the breaking (yield stress) and small reversible deformations (elastic modulus) of the slurry's network. Interestingly, because of its high content of hydrophobic proteins, the dominating mechanism of structure formation within MOH slurries is the entanglement network of polymers (proteins and polysaccharides) whose yield stress originated from the presence of high concentrations of dispersed particulate material within the structure. This gave rise to a weak, predominantly elastic rather than viscous gel with cohesive energy in the 0,2-0,7 kJ range. On the other hand, due to their high hydrophilic protein content, the dominant mechanism of structure formation within EGH and MAH slurries could be cross-liking rather than entanglement. This cross-linking generated a predominantly elastic gel with a relatively high cohesive energy of 2-7 kJ. The protein composition

of these hydrocolloids varied, influencing their structural and mechanical properties, especially in semi-concentrated and concentrated forms. While all three hydrocolloids demonstrated pseudoplastic behaviour in semi-concentrated slurries, their responses in concentrated slurries exhibited significant variances. EGH and MAH showed transitional points linked to structural rigidity, primarily due to cross-linking mechanisms, resulting in solid and elastic gels. In contrast, MOH structure development was driven by polymer entanglement, resulting in a weaker, more elastic gel. These findings shed light on the significance of protein content and microstructural phenomena in the rheological properties of hydrocolloids, which have potential uses in food formulation and processing.

4.1 Introduction

Rheological behaviour studies how materials deform and flow under various stresses. This notion is crucial for understanding how hydrocolloids, which form gels or thick solutions in water, react during food processing and cooking. Hydrocolloids are commonly utilised in medications and as essential ingredients in food items. They serve an important role in improving the functional aspects of food, such as texture, viscosity, and stability. Still, their nutritional benefits are sometimes neglected due to their primary purpose as additives (Trujillo, 2016; Verkempinck et al., 2018).

Cooking and handling operations, especially heat use, influence hydrocolloids' functionality. Hence, it is necessary to research their stability and rheological behaviour in these settings (Jeirani et al., 2013; 3; Gannasin et al., 2015;4). The physicochemical and functional features of the polysaccharides and proteins in hydrocolloids, such as water absorption and solubility, are crucial to food science and processing (McClements, 2021;3). These qualities are important in identifying meals with several components, such as cereals, wheat, beans, eggs, and various meats and vegetables, particularly during thermal processing (Kitunen et al., 2019;5). In multi-component food systems like cereals, wheat, beans, eggs, meats, and vegetables, the rheological behaviour of hydrocolloids plays a significant role in maintaining the desired texture and consistency during cooking. How hydrocolloids respond to heat and other processing conditions can affect the final quality of these foods, making it essential to study their rheological properties under such conditions (Kitunen et al., 2019;4). Understanding these aspects is critical to optimising food formulations and ensuring that the functional benefits of hydrocolloids are fully realised in the final product.

The cooking process involves multiple operations—cutting, crushing, mixing, and kneading—related to the deformation, fluidity, and rupture of food ingredients (Mahmood et al., 2017; 3; Rosa-sibakov et al., 2016;7). Understanding the phase behaviour of hydrocolloids is vital for optimising their calorific properties, including their reaction to temperature fluctuations, congelation, liquefaction, and thermal insulation (Marić et al., 2018;2 Kavitake et al., 2019;3).

Hydrocolloids also influence cooking attributes like colour, glazing, transparency, emulsifying, fat-holding, and suspending, which can be measured using rheological characterisation (Vignola et al., 2018;3 Gomes et al., 2020;2).

While much research has been done on the rheological characteristics of various dietary hydrocolloids from unique underutilised sources, such as egusi flour, remain unknown. Egusi, like moringa and makataan hydrocolloids, is high in protein and has emulsifying qualities, making it an essential addition to the expanding worldwide hydrocolloid market. This chapter characterises the stability and phase behaviour of slurries containing these hydrocolloids, using nutritional profiling to evaluate their rheological properties in aqueous states, with the overview displayed in Figure 4.1. Furthermore, by profiling the amino acids and sugars in hydrocolloids and connecting them with rheological tests (such as shear rate measurements), you may determine how compositional components influence v.

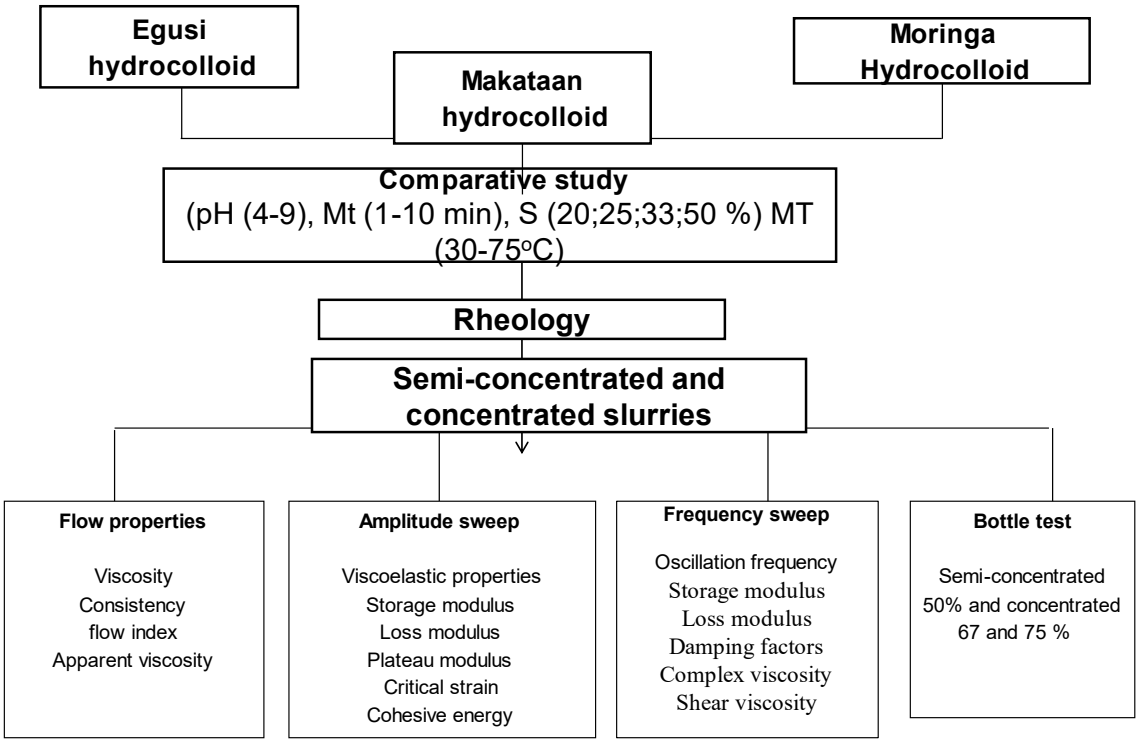

Figure 4.1 Overview of Chapter Four

4.2 Materials and Methods

4.2.1 Sources of materials and equipment

Moringa, egusi and makataan hydrocolloids used in this study were obtained using hot water extraction, described in Chapter 3. MCR 301 Paar Physical Rheometer by Anton Paar GmbH, headquartered in Graz, Austria. Situated at the rheology laboratory of the Flow Process & Rheology Centre at the Cape Peninsula University of Technology District 6 campus.

4.2.2 Moringa, egusi and makataan hydrocolloid slurry preparation

The cooking parameters under varied conditions provide insights into food products' texture, flow, stability, and overall structure. A comparative study ensures that food products are optimised for consistency, consumer appeal, and functional performance. To achieve this, the method of Kitunen *et al*. (2019;155), with some modification, 10 g each of egusi hydrocolloid slurry (EGHS), makataan hydrocolloid slurry (MAHS) and moringa seed hydrocolloid slurry (MOHS) was prepared at four levels using a wide range of process conditions and analysed using comparative

study. For a 50% slurry mixture, 10 g of hydrocolloid sample was weighed into a 50 mL beaker. Water of 10 mL was added and mixed at 30^{o}C with a magnetic stirrer at pH 4 for 1500 rpm for 1 min, as seen in Table 4.1. The mixing time (Mt), mixing temperature (MT), pH of the mixture (PM), and added water (AW) were varied at four levels each, as shown in Table 4.1. The Mt was 1,4,6 and 10 minutes. Similarly, the PM at 4, 6,7 and 9: AW was observed at 10, 20, 30 and 40 g. Lastly, temperature (MT) was evaluated between 30,40,60 and 75°C. Mixing was done with a Magimix mixer (Cuisine system 5200L automatic), Bourg-les-Valence, France, starting at the highest speed of 1500 rpm for all levels. The pH of each slurry was adjusted to the different pH levels using either 0.5 M HCl or 0.5 M NaOH solution. All operations were conducted at an atmospheric ambient temperature of about 25°C. Each slurry was subjected to functional and rheological profiling. The best-performing slurry was identified based on the displayed functional and rheological behaviours. The above comparative study was repeated for all the hydrocolloids. All hydrocolloid slurry was mixed 2 min before each analysis.

Table 4. 1 Comparative study for egusi, makataan and moringa slurry at four-levels

Factors	Mixing condition	Level			
		1	2	3	4
F1	pH of mixture	4	6	7	9
F2	Mixing time [min]	1	4	6	10
F3	Added water [g]	10	20	30	40
F4	Temperature [°C]	30	40	60	75

4.3 Rheological Measurements and Bottle Test of Egusi, Makataan and Moringa Slurry

A Physica MCR301 controlled stress/strain rheometer (Anton Paar GmbH, Ostfildern, Germany) with a bob-in-cup geometry system was utilised to perform flow characteristics and oscillatory measurements using the Yousefi and Razavi technique (2015;567). Physica Rheometer Data Analysis software was used to calculate dynamic rheological properties, such as storage modulus (G') and loss modulus (G"), loss tangent (tan ø), and complex viscosity (ü*). Each oscillatory

measurement was performed in triplicate. Each hydrocolloid underwent a bottle test to ensure the flow at each concentration.

4.3.1 Flow properties

All rheological studies were done with a Paar Physica MCR 301 Graz, Austria. rotational stress rheometer and bob-in-cup measuring units. The bob surfaces were sandblasted to reduce sliding potential (Masalova et al., 2006;4). The wide range of shear rates (from about 10^{-6} to 103 s−1) and shear stress available for inquiry allows one to get parameters of rheological properties throughout a vast range. The shear rate was gradually increased from 10^{-5} to 10^{3} s−1. Chapter 2 described the flow behaviour (equation 1) using the power law model.

$$\tau = k\dot{\gamma}^{n} \quad \textbf{(1)}$$

Where τ is the shear stress (Pa), $\dot{\gamma}$ Is the shear rate (s^{-1}), k is the consistency coefficient ($Pa.s^{-n}$), and n is the flow index.

4.3.2 Amplitude sweep measurements

To guarantee that all dynamic measurements were conducted in the linear viscoelastic area (LVE), amplitude sweep tests (0.01-100%) were performed at 25°C and 1 Hz. Based on the results, a 0.5% strain was perfectly inside the LVE range for all samples. Hence, it was employed in all dynamic experiments. The storage modulus (G' LVE), loss modulus (G'' LVE), strain limiting value (γ_c), and amplitude sweep measurements were used to calculate the loss tangent (tan (ø) and cohesion energy for all hydrocolloid samples at the LVE region (Zhao et al., 2019;3). An amplitude sweep is performed on the hydrocolloid slurry to estimate its linear viscoelastic region (LVR). This is the zone in which the material responds consistently and elastically without structural failure. By gradually raising the strain in an amplitude sweep, researchers can determine the maximum strain or stress that the slurry can sustain before its internal structure deforms irreversibly.

In hydrocolloids, this aids in evaluating gel strength, stability, and viscoelastic behaviour under various stress circumstances, which is critical for applications where texture and consistency are important, such as food formulations.

4.3.3 Frequency sweep measurements

The frequency sweep test involved submitting the slurry samples to oscillatory measurements at frequencies ranging from 0.01 to 100 Hz while maintaining a constant strain at the LVE area (0.5%). As a result, the mechanical spectra were described as G' and G'' (Pa) as a function of

frequency at 25°C (Masalova et al., 2020;6). A frequency sweep is performed on the hydrocolloid slurry to determine its viscoelastic behaviour across a variety of oscillation frequencies. It aids in determining the material's response to various deformation rates, providing information about its elastic (storage modulus, G') and viscous (loss modulus, G'') properties.

4.3.4 Bottle test

The bottle test method, which measures the amount of flow five minutes after the bottle is fully inverted, provided an early indication of the hydrocolloid aggregation capabilities of fresh slurries (Tshilumbu & Masalova, 2015;6).

4.4 Statistical Analysis

Statistical analyses were carried out using SPSS 25 (2018). The experimental data were examined using analysis of variance (ANOVA) with a 95% confidence level. Data were collected in duplicate and provided as mean ± standard deviation.

4.5 Results and Discussion

4.5.1 Rheological properties of moringa, makataan and egusi hydrocolloid in semi-concentrated slurries

The primary purpose of this section is to explore the effect of process factors (hydrocolloid content, pH, temperature, and mixing time) described in Table 4.1 on slurry flow properties using visual and rheological approaches. Typical flow curves for the three hydrocolloids (MAH, EGH, and MOH) (Figure 4.2) show shear thinning with little yield stress. In other words, no solid-like behaviour was found at low stresses regardless of the hydrocolloid type or processing conditions used in this study. Figure 4.3 visibly demonstrates the absence of a solid-like characteristic. The test tubes were filled with various types of hydrocolloids with differing formulation contents before being inverted. All slurries flowed without evident yield stress five minutes after switching the tube, as the images were obtained at a five-minute standing time. The typical best fitting of the power law model on the flow curves of MAH hydrocolloid slurry is shown in Figure 4.4. The shear rate of 50 s^{-1} was selected because it is an effective oral shear rate (Benitez et al., 2020;5). Regardless of the hydrocolloid type and processing parameters, the flow index n was less than 1, thus confirming the shear-thinning behaviour of the slurries. This shear thinning is characteristic of the `semi-concentrated region' of polymers in solution where the polymer molecules, proteins and polysaccharides, which are, are not accessible to move independently in solution without interpenetration (Lastra-Ripoll et al., 2022;2; Gürgen, 2019;3).

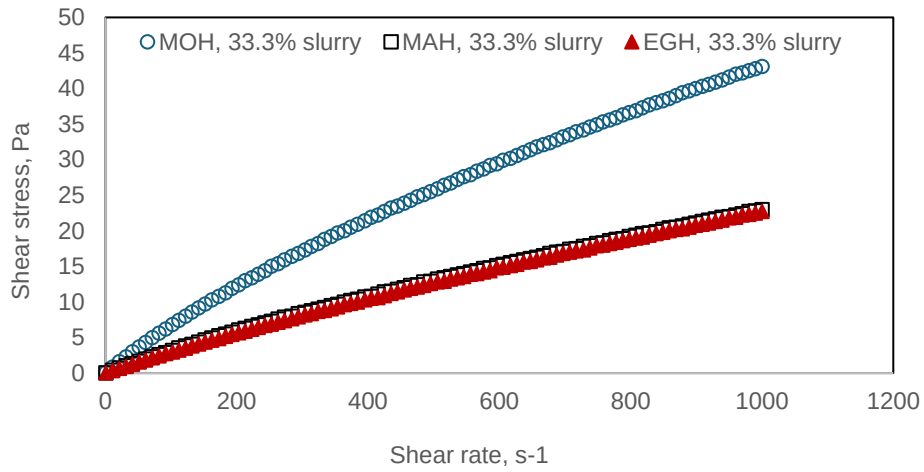

Figure 4.2 Typical shear stress dependence on the shear rate for EGH (egusi), MAH (makataan) and MOH (moringa hydrocolloid)

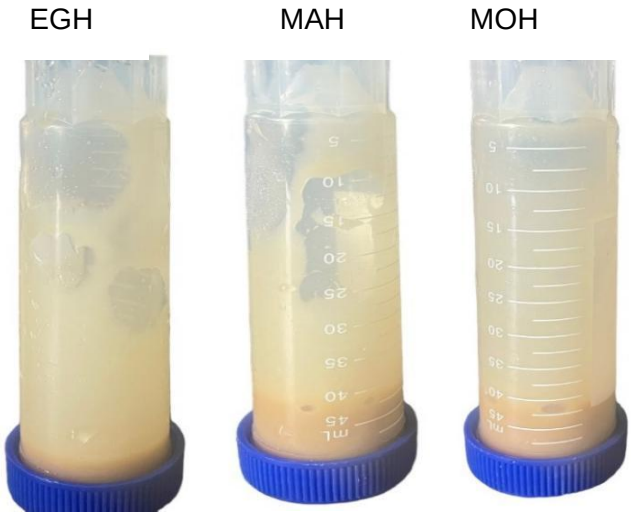

Figure 4.3 Hydrocolloids slurries (pH = 7, Mt = 6min, S = 25 %, MT = 60˚C) five minutes after inverting the vessels

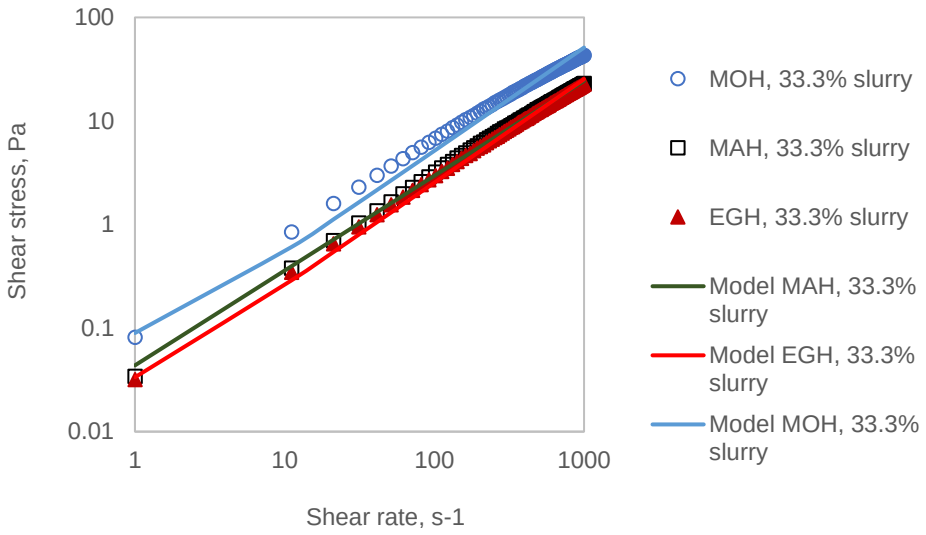

Figure 4.4 Typical best fittings of power law (continuous line) model on flow curves of the hydrocolloid at moringa, makataan and egusi, 30% concentration in water

Molecular crowding causes the overlap of polymer coils, resulting in the interpenetration of polymer chains (Ponzini et al., 2019;513). It seems reasonable to assume that, in this case, the thickening of hydrocolloid slurries arises predominantly from physical entanglement. As evident from Figure 4.4, the power law model fits the experimental data quite satisfactorily. Thus, this model was used to describe the flow curves of semi-concentrated slurries. The values obtained for the consistency (k) and flow index (n) for all three types of hydrocolloids are summarised in Table 4.2. For non-Newtonian fluids, apparent viscosity, η_{app}, is reported as a function of a specific shear rate (El-hoshoudy et al., 2020). This study computed it at a shear rate of 50 s^{-1} using power law parameters (k, n) as shown in equation 9.

$$\eta_{app=K\dot{\gamma}^{n-1}} \quad \textbf{(9)}$$

Table 4.2 Consistency, flow Index and apparent viscosity of a semi-concentrated slurry of egusi, moringa and makataan slurry[1, 2]

Hydrocolloid slurries	Consistency index (k)	Power law index (n)	η_{app} (50 s^{-1})	R^2
EGHS %				
20	0.68 ± 0.01[a]	0.41 ± 0.01[b]	3.38 ± 0.01[a]	0.99
25	0.07 ± 0.00[a]	0.40 ± 0.01[a]	0.33 ± 0.01[a]	0.98
33	0.98 ± 0.01[a]	0.42 ± 0.00[a]	4.87 ± 0.01[b]	0.98
50	0.26 ± 0.00[a]	0.30 ± 0.01[a]	0.84 ± 0.01[a]	0.99
MAHS %				
20	0.07 ± 0.01[a]	0.42 ± 0.01[b]	0.36 ± 0.01[a]	0.97
25	0.31 ± 0.01[a]	0.38 ± 0.01[a]	1.37 ± 0.00[a]	0.98
33	0.90 ± 0.01[a]	0.37 ± 0.00[a]	3.83 ± 0.00[a]	0.98
50	0.08 ± 0.01[a]	0.29 ± 0.01[a]	0.25 ± 0.01[a]	0.96
MOHS %				
20	0.18 ± 0.01[a]	0.27 ± 0.01	0.52 ± 0.00[a]	0.98
25	0.73 ± 0.01[a]	0.33 ± 0.01[a]	2.65 ± 0.01[a]	0.96
33	0.07 ± 0.01[a]	0.35 ± 0.01[a]	0.28 ± 0.00[a]	0.98
50	0.07 ± 0.01[a]	0.43 ± 0.01[a]	0.38 ± 0.01[a]	0.99

[1]Values are mean, ± standard deviation of 4 replicates. Means with a different superscript in each row differ significantly ($p \leq 0.05$).

[2]MOHS = Moringa Hydrocolloids slurry; EGHS = Egusi Hydrocolloid slurry; MAHS = makataan hydrocolloid slurry. Consistency and power law index of the diluted slurry of moringa, makataan and egusi hydrocolloid slurry at four factorial levels of preparation (1) pH of mixture 4: mixing time 1 min: added water 10g; Temperature 30ºC (2) pH of mixture 6: mixing time 4 min: added water 20g; Temperature 40ºC (3) pH of mixture 7: mixing time 6 min: added water 30g; Temperature 55ºC (4) pH of mixture 9: mixing time 10 min: added water 40 g; Temperature 75ºC

4.5.2 Shear viscosity at 50 s^{-1}

Figure 4.5 details the effect of varying the processing parameters (pH =4-9%; S = 20-50 wt%; Mt = 1-10trs/min; T=10-75ºC) on the shear viscosity at 50 s^{-1} of semi-concentrated hydrocolloids of EGH, MAH and MO

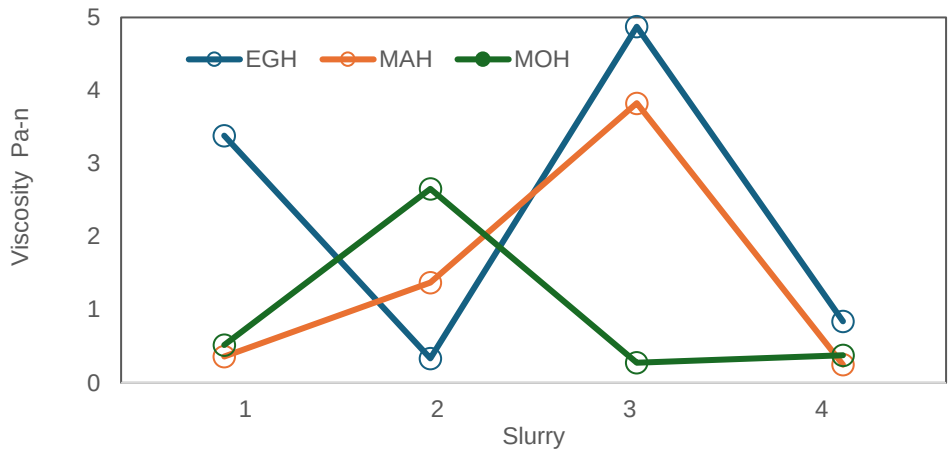

Figure 4.5 Shear viscosity of hydrocolloid slurries at 50 s^{-1}

EGH (egusi hydrocolloid) MAH (makataan hydrocolloid) MOH (moringa hydrocolloid). (1); pH 4; Mt 1 mins; S 50% and T 30ºC; (2) pH 6; Mt 4 mins; S 33% and T 40ºC; (3) pH = 7; Mt = 6 mins; S = 25% and T = 60ºC; (4) pH = 9; Mt = 10 mins; S = 20% and T = 75ºC.

Unlike MOH, which demonstrates a maximum viscosity at pH = 6; Mt = 4 mins; S = 33.3% and T = 40 º C, EGH and MAH show a maximum at pH = 7; Mt = 6 mins; S = 25% and T = 60 º C. The maxima associated with EGH and MAH are higher than those corresponding to MOH. Furthermore, the maximum apparent viscosity follows the trend: EGH > MAH > MOH. This trend corresponds to the opposite of the line of the hydrophobic protein content of the three hydrocolloids (MOH > EGH ≈ MAH; see section 3.9) and opposite to the trend of particle size (D_{50} MOH > D_{50} MAH > D_{50} EGH; see section 3.10.1). It is well known that particle size significantly affects the rheological response, especially increasing viscosity as the particle size decreases (Aghababaei et al., 2024;3). On the other hand, the equilibrium interfacial tension trend suggested that hydrophilic proteins associate better than their hydrophobic counterpart (section 3.9), in line with the observations of You et al. (2023;14). So, it is fair to conclude that the relatively high maximum viscosity associated with EGH or MAH hydrocolloids as compared to MOH is a combination of the increased ability of hydrophilic proteins to associate in solution (entanglements or micelles) and the relatively small particles associated with EGH or MAH. The maximum viscosity of EGH and MAH occurs at a neutral pH because, at acidic or basic pH, the degree of hydration of hydrophilic proteins could increase due to a greater net positive charge on protein molecules, leading to a greater affinity for water molecules (Li et al., 2023;4).

It is worth mentioning that the relatively higher shear viscosity for MAH and EGH in semi-concentrated slurries, combined with their high ability to reduce the interfacial tension, show the higher potential of these hydrocolloids as suitable thickeners (in increasing the consistency of food systems) and emulsifiers (Tan et al., 2020;3).

4.5.3 Amplitude sweep to determine structure formation

The lack of structure formation in semi-diluted hydrocolloid slurries with varying processing conditions is confirmed by the results of the elastic and loss moduli measurements as a function of applied strain. Figure 4.6 demonstrates the amplitude dependencies of the elastic and loss modulus at a constant frequency (1Hz) for all four levels of the processing parameters for MAH semi-concentrated slurries. Regardless of the processing conditions, the storage and viscous moduli are very low, with G" being relatively higher than G' in the entire strain range (0.1-200%). This low G' is characteristic of a liquid-like viscoelastic material where viscous properties dominate over the elastic behaviour.

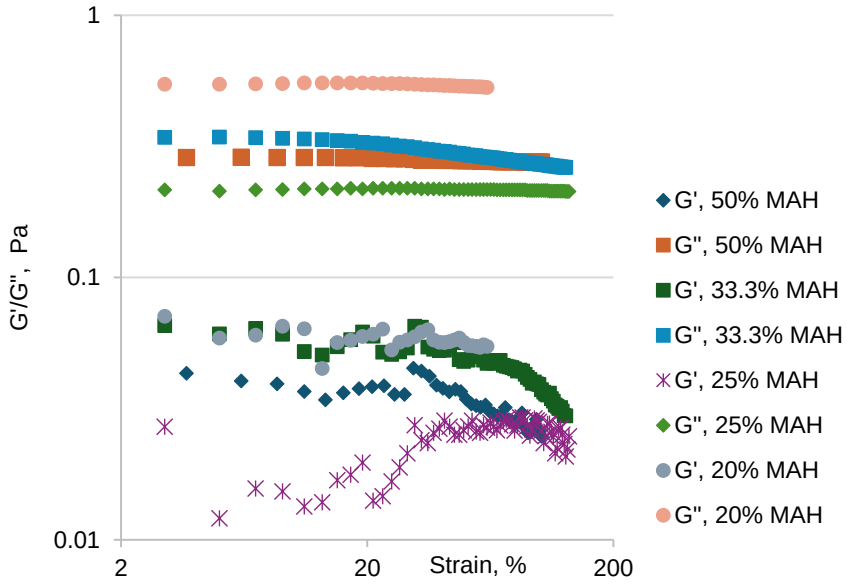

Figure 4.6 Typical amplitude sweep for makataan hydrocolloid (MAH) hydrocolloid slurries (20, 25, 33.3, 50 wt%)

Despite the lack of structure formation with varying processing conditions, some helpful information is evident from the results on semi-concentrated hydrocolloid slurries. The apparent viscosity results highlight the difference in rheological behaviour between the proteins released

by MOH dissolution and those released by EGH or MAH, as evidenced by amino acid composition (section 3.9.2). This behaviour follows the interfacial tension where EGH and MAH demonstrated higher interfacial than MOH. Hydrophilic proteins associate better in water or at the oil-water interface than their hydrophobic counterparts (Náthia-Neves et al., 2023;2; Meder et al., 2012;1222). Suppose this difference in the type of proteins translates into differences in the onset of structure formation (as defined by the existence of the yield stress) and structure parameters (as defined by the modulus of rigidity) of the hydrocolloid slurries in water. In that case, it is necessary to look at the effect of nutrients on rheology. This difference in structure formation is critical for both scientific interest and technological applications of these systems. It will first complete the understanding of the functional properties of the hydrocolloids under investigation. Second, it will guide the user on when to use them in food and non-food, such as for thickening, stabilising, emulsifying and sometimes for dual functions. To discover this potential hydrocolloid food usage, a series of hydrocolloid slurries were prepared using MAH, MOH and EGH at a constant pH = 7; the constant temperature of 30^{o}C, constant mixing time of 1 minute, with varying solids concentrations: 50, 67 and 75 wt%, to evaluate their flow and viscoelastic properties (amplitude and frequency sweeps).

4.6 Rheology of concentrated hydrocolloid slurries of moringa, makataan and egusi

One of rheology's central goals is to measure the viscoelastic properties of a flowing material using sophisticated laboratory techniques to probe the material structure. Then, these data can be applied to predict the behaviour of this material in industrial settings, particularly for designing transport characteristics of pipelines (Hundschell & Wagemans, 2019;2; Moelants et al., 2014;383; Boehm et al., 2019;385). This section’s objectives were to clarify the influence of hydrocolloid concentration in concentrated slurries and determine the hydrocolloids' stabilisation mechanism.

4.6.1 Flow properties of concentrated hydrocolloid slurries

The shear rate was controlled in the increasing deformation regime over a range of 10^{-6} to 1000 s^{-1}. Typical flow curves obtained for EGH (75% by mass) and EGH (67% by mass) hydrocolloids are shown in Figure 4.7. Conversely, to the semi-concentrated slurries, characteristic flow curves demonstrate apparent yield stress, suggesting a solid-like behaviour at low stresses.

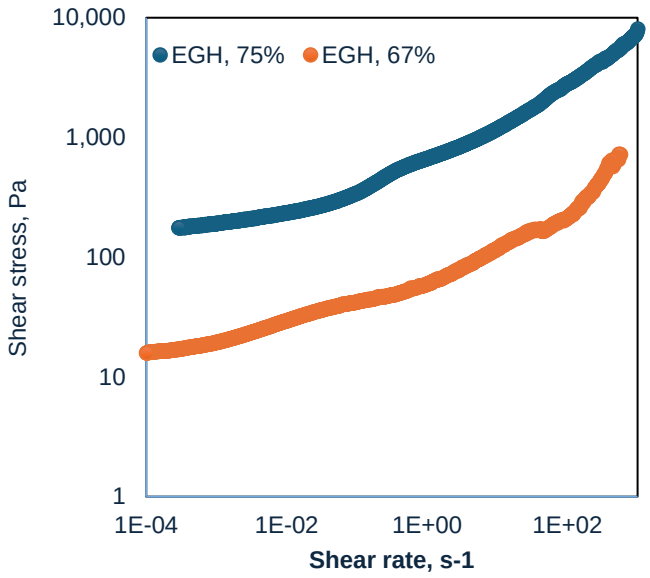

Figure 4.7 Typical flow curves obtained for egusi hydrocolloids EGH (67 and 75 wt%)

The experimental data was fitted using the Herschel-Bulkley model to describe the flow behaviour of concentrated hydrocolloid slurries as shown in Equation 4 (Section 2.4.4.1) for Where τ_y (pa) is the yield stress, n and K (Pa·s) are empirical constants named flow index and consistency. Figure 4.8 shows the Herschel-Bulkley model's typical best fittings on the MOH hydrocolloid slurry's flow curve (67%).

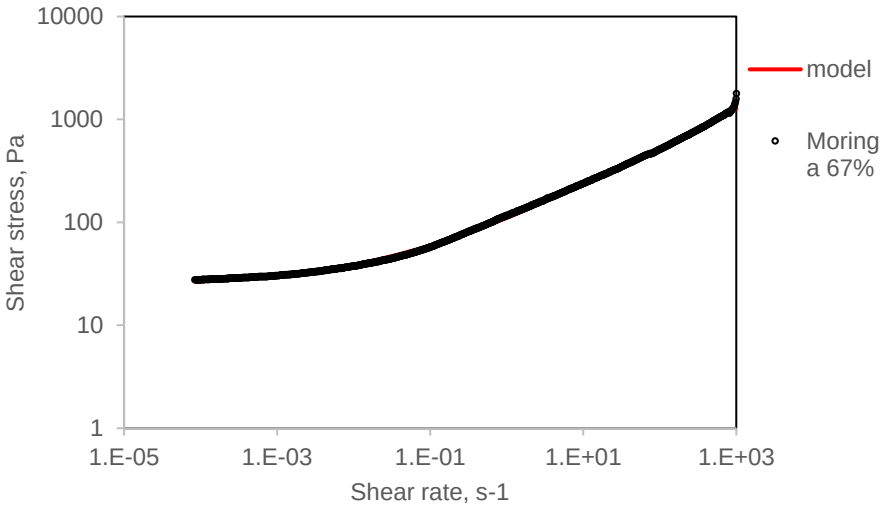

Figure 4.8 Typical best fit of the Herschel-Bulkley model on the flow curve of (67%) moringa hydrocolloid slurry

Table 4.3 summarises the values obtained for the yield stress, consistency, and flow index. Figure 4.9 demonstrates the dependence of the yield stress of EGH, MAH, and MOH hydrocolloids on the slurry concentration.

Table 4.3 Herschel Buckley flow behaviour parameter for moringa, makataan and egusi hydrocolloid slurry[1, 2]

Hydrocolloid	Consistency index	Yield stress	Flow index	R^2
50% w/w				
EGH	6.00 ± 0.00[a]	0.41 ± 0.00[b]	0.4 ± 0.00[a]	0.98[a]
MOH	3.00 ± 0.01[a]	0.30 ± 0.01[a]	0.5 ± 0.01[a]	0.97[a]
MAH	5.00±0.03[a]	0.42 ± 0.02[b]	0.4 ± 0.01[a]	0.98 [a]
67% w/w				
EGH	25.00 ± 0.03[a]	55.00 ± 0.08[a]	0.40 ± 0.00[a]	0.99[a]
MOH	86.50 ± 0.00[a]	24.00 ± 0.38[b]	0.38 ± 0.00[a]	0.99[a]
MAH	10.50 ± 0.02[a]	50.00 ± 0.42[b]	0.63 ± 0.00[a]	0.98[a]
75% w/w				
EGH	57.20 ± 0.01[a]	58.50 ± 0.03[a]	0.41 ± 0.02[a]	0.99[a]
MOH	48.00 ± 0.00[a]	54.00 ± 0.05[a]	0.39 ± 0.01[a]	0.98[a]
MAH	1.80 ± 0.00[a]	58.00 ± 0.04[a]	0.90 ± 0.04[b]	0.98[a]

[1]Values are mean and standard deviation in 3 replicas. Means with a different superscript in each row differ significantly ($p \leq 0.05$).
[2]MOH = Moringa Hydrocolloids; EGH = Egusi Hydrocolloid; MAH = makataan hydrocolloid. Consistency and power law index of the semi-concentrated moringa, makataan and egusi hydrocolloid slurry at 50, 67 and 75% w/w hydrocolloid concentration in water.

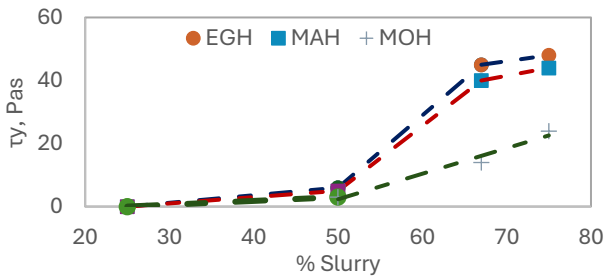

Figure 4.9 Dependence of the yield stress of egusi, makataan and moringa hydrocolloids on the slurry concentration.

The correlation between the yield stress and the slurry concentration shows two transition points.at 50 wt% and 67 wt%. The first transition point (50 wt%), present in all three hydrocolloids, is associated with the onset of structure formation ($\tau_y \leq 5$ Pa). Above this critical point, it is evident that the hydrocolloid slurries created spatial structures with quite discernible strength. This structure was observed by the bottle test (figure 4.10), where it was seen that slurries containing more than 50% by mass hydrocolloids do not flow on inverting the vessels.

On the other hand, the second transition point is only related to EGH and MAH slurries; MOH-based slurry does not display such a point.

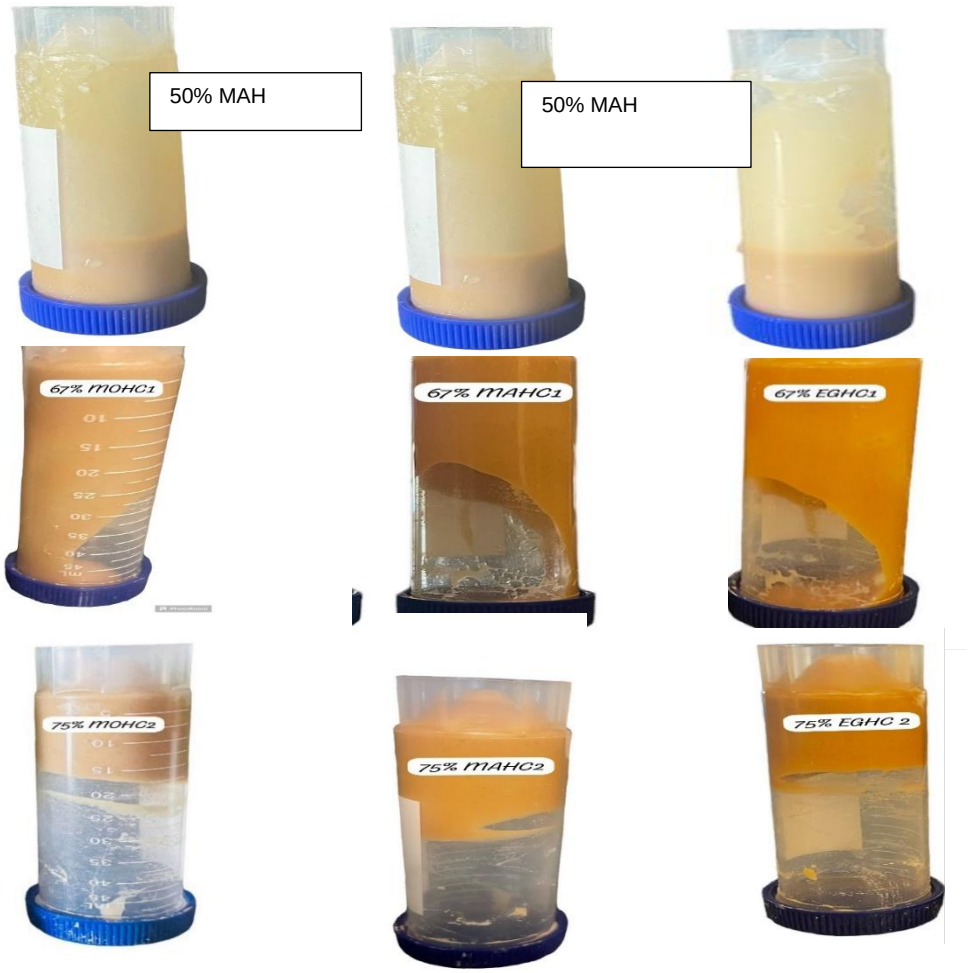

Figure 4.10 Hydrocolloids dispersion in water at five minutes after inverting the vessels MAH, MOH and EGH (50%); EGHC, MAHC and MOHC 1 (67%); EGHC, MAHC and MOHC 2 (75%)

The latter demonstrates a monotonic yield stress increase beyond the onset of structure formation. Below the second transitional point, the yield stress values for EGH and MAH increase

enormously with the rise in hydrocolloid concentration (50-67 wt%) compared to MOH-based slurry. Treating the yield stress as the measure of the strength of a structure formed in the slurry, the strength of the structure increased rapidly with an increase in the hydrocolloid concentration for EGH and MAH compared to MOH-based slurry. Above this critical point (in the range of 67-75 wt% hydrocolloid concentration), the yield stresses of EGH and MAH demonstrate a prolonged increase (from 45 and 40 Pa to 48 and 44 Pa for EGH and MAH, respectively), which represents only a 6% and 10% improvement on the strength of the structure associated with 67% hydrocolloids.

4.6.2 Viscoelastic properties of concentrated hydrocolloid slurry of moringa, makataan and egusi

Dynamic rheology aims to improve understanding of the microstructure of different hydrocolloids used in this study. The use of steady shear rheology in the previous section does not offer a suitable basis for comparing other systems because, first, it does not separate the elastic from the viscous effects (Lin et al., 2024;6). For hydrocolloidal slurries, the elastic modulus (G′) and loss modulus (G”) are the most meaningful rheological parameters to use in characterising a system. Second, the use of steady shear requires the disruption of structures at rest, and characteristics such as viscosity necessitate the solution of hydrodynamic equations (Pant et al., 2021;2; Grasso et al., 2020;3). As a result, dynamic rheology was used to investigate the mechanisms behind structure development in hydrocolloid systems (Wei et al., 2022;1347).

The viscoelasticity determination was conducted with amplitude and frequency sweeps. The amplitude sweep test was used to probe the microstructure; hence, the hydrocolloid interactions were estimated. This technique is beneficial because it helps determine the linear viscoelastic region (LVE). In this region, tests were carried out in the stress range, where the material is continuously stressed while the sample structure is undisturbed. Furthermore, from this test, the cohesive energy. The storage and loss modulus of suspensions were then measured in a frequency sweep in the determined LVE range to evaluate each hydrocolloid strength according to concentration.

4.6.3 Elastic behaviour of concentrated hydrocolloids in slurry systems

The oscillation amplitude was selected as a variable, and the frequency was kept constant in the amplitude sweep test. Second, the use of steady shear requires the disruption of structures at rest, and characteristics such as viscosity necessitate the solution of hydrodynamic equations (Pant et al., 2021;2; S. Grasso et al., 2020;3). As a result, dynamic rheology was used to investigate the mechanisms behind structure development in hydrocolloid systems (Wei et al., 2022;1347). Regardless of the hydrocolloid type, the response is primarily elastic, as evident from

the dominance of the elastic modulus G' on the viscous modulus G" and this is expected of concentrated hydrocolloids (Lastra-Ripoll et al., 2022;4). In a focused slurry, the rest of the structure is preserved during low-amplitude shear strain; hence, the energy loss is kept at a minimum. It was related only to the equilibrium microscopic structure, forces, and inherent dissipation of fluctuations (Ptaszek, 2022;110). The dissolved polymers (proteins and polysaccharides) and undissolved particles were crowded (entangled) or linked in this linear region. They could not move freely past one another up to the maximum measured strain called critical strain, which defined the limit of the elastic domain. As indicated by the drop in G' at strains above 0.2 – 0.7%, much of the elasticity is lost, and hence, many of the bonds inside the slurry's structure were broken. The polymers/particles mixture moves more freely in the aqueous phase, but there is still a more elastic response than a viscous one. In other words, entangled or linked polymers/ particles are still present, striving to preserve a network structure in the aqueous phase.

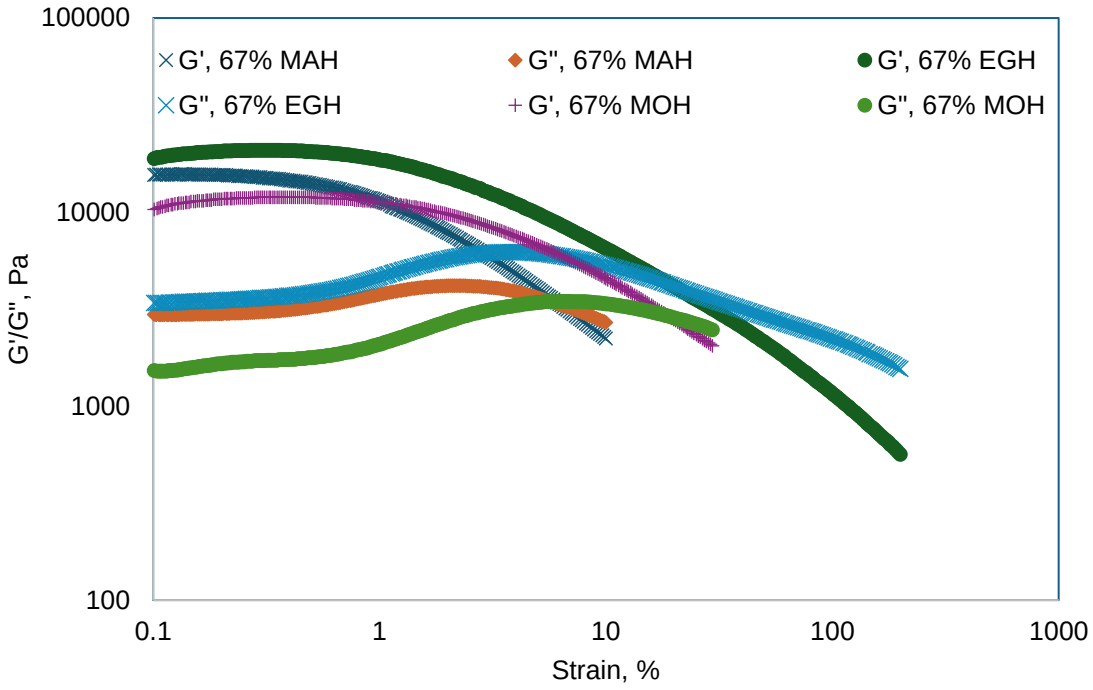

Figure 4.11 Typical amplitude sweep for egusi (EGH), makataan (MAH), and moringa (MOH) hydrocolloid slurries (67 wt%)

At higher deformation, the storage modulus decreased with a deformation increase, the applied strain being sufficient to allow the polymers/particles to move past one another and induce a

transition to the viscous domain (Zheng et al., 2019;550; Ben-Harb et al., 2018;77). Above this critical shear strain corresponding to the crossing point between G' and G", the slurries lose their viscoelasticity and become fluid.

The length of the plateau of the elastic modulus indicated the structure's flexibility to deformation, and the drop of modulus was related to the breakdown of the solid structure (γ_{crit}) (Montoya et al., 2021;7). The storage modulus was obtained from the linear region of the storage modulus by extrapolating the curve to zero deformation (G_p). The cohesive energy (E_{coh}) was calculated using equation 9.

Table 4.4 Plateau modulus, critical strain and cohesive energy of concentrated moringa, makataan and egusi hydrocolloid slurry

Concentrations	G_p [Pa] (GLVR)	γ_{crit} [%]	$E_{cohesion}$ [Joules]
50% w/w			
EGH	6.00a	0.41	0.4
MOH	3.00	0.30	0.5
MAH	5.01	0.42	0.4
67% w/w			
EGH	20500	0.47	2264.2
MOH	13600	0.20	232
MAH	15603	0.46	1650.8
75% w/w			
EGH	59397	0.5	7424.6
MOH	21100	0.3	1489.5
MAH	46900	0.5	5862.5

EGH)(egusi) MAH (makataan) MOH (moringa)

$$E_{coh} = \frac{1}{2} G'_{LVR} \gamma^2_{crit} \qquad \textbf{9}$$

The obtained values for G_p, γc_{rit} and E_{coh} are reported in Table 4.5.

The evolutions of the storage modulus and the cohesive energy as functions of slurry concentration are shown in Figures 4.12 and 4.13, respectively.

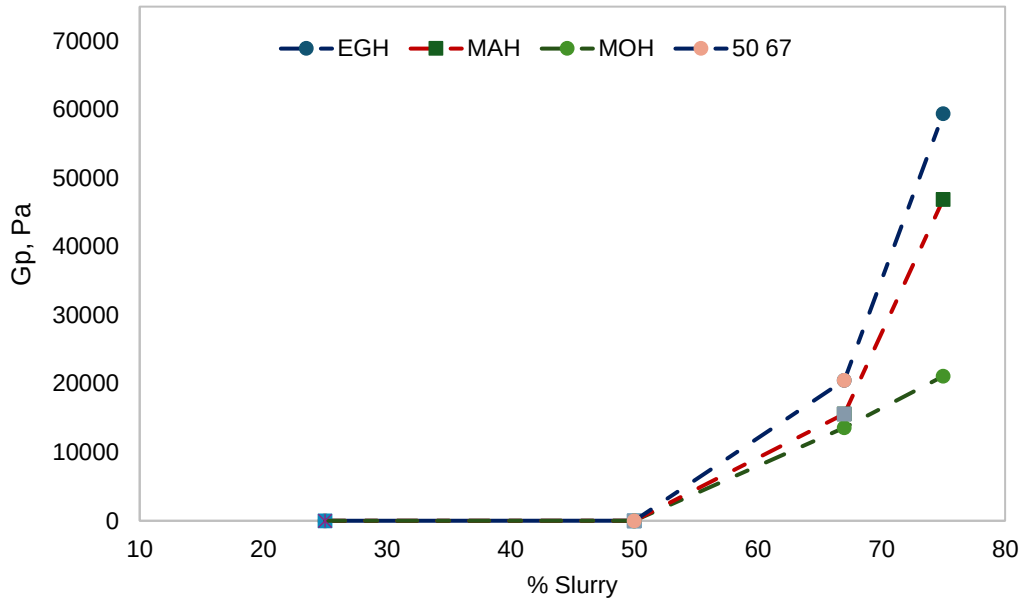

Figure 4.12 Dependence of the storage of EGH (egusi), MAH (makataan) and MOH moringa hydrocolloids on the slurry concentration

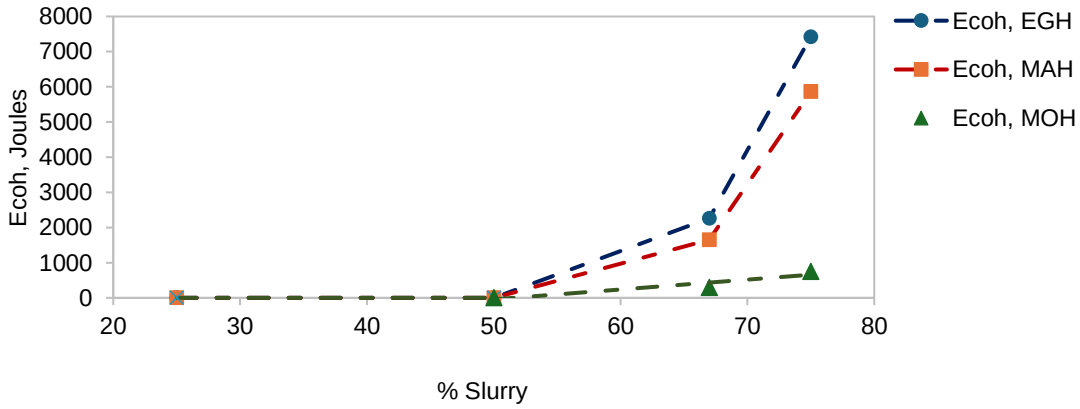

Figure 4.13 Dependence of the cohesive energy of EGH (egusi), MAH (makataan) and MOH (moringa) hydrocolloids on the slurry concentration

The increase in slurry concentration strongly modifies the solid-like structure of hydrocolloid slurries. As with the yield stress, the correlation between the shear modulus and slurry

concentration shows two transitional points for EGH and MAH, at 50 wt% and 67 wt%; only one critical point for MOH. The latter demonstrates a monotonic increase of the storage modulus beyond the first transition point by the yield stress. As it will be recalled, the first critical point (50 wt%) was associated with the onset of structure formation. On the other hand, the second transition point marks, as before, the boundary between the region of slow or rapid increase of the slurry's rigidity with increasing hydrocolloid concentration. However, an opposite trend is observed in contrast to the yield stress. It is worth noting that the elastic shear modulus describes the mechanical response of the system submitted to reversible minor strain (Wang & Selomulya, 2022;222). In contrast, yield stress is related to the breakage of the slurry's network (Balachandramohan et al., 2020;3). So, the difference in the behaviour of the yield stress and elastic modulus in the region beyond the second transitional point is an indication that there is a difference in microstructural phenomena induced by the breaking (yield stress) and small reversible deformations (elastic modulus) of the slurry's network (Vatansever et al., 2021:5). Both elastic modulus and yield stress depend on the slurry's microstructure but provide different information. Hence, we chose G' over yield as the correct expression of our system's interactive forces governing structure formation. This decision is because G′ is a static parameter (the materials are in their equilibrium state, and their response to the applied stress is made without disrupting their underlying structures). Hence, its correlation with the interaction force in the slurry is more direct, unlike parameters such as yield stress, which involves structural rupture (Fernandes et al., 2024;3).

Below this transitional point, the increase of the elastic modulus value for EGH or MAH is relatively slow in agreement with the increase in the cohesive energy. This is expected since, at long separation distances, repulsive forces dominate over attractive ones (Wang & Selomulya, 2022;224); above this point, the slurry's rigidity and the cohesive energy of EGH or MAH increases rapidly. The observed sharp increase in both the storage modulus and the cohesive energy at relatively high slurry concentrations (in the 67-75% range) could indicate an increase in the attractive forces due to the close approach of polymers and particles (van der Waals and possible covalent bonds) (Kongjaroen et al., 2022;7). This apparent higher ability of hydrophilic proteins to form stronger bonds than their hydrophobic counterpart is in line with the ability of MAH or EGH to significantly reduce the interfacial tension to low values characteristic of well-established surfactants.

In contrast, the coherent energy in MOH slurry is deficient, showing once again a monotonic increase with a slight dependency on concentration (Figure 4.13). The monotonic variation of the yield stress, elastic modulus, and cohesive energy in MOH slurry is an indication that the mechanism of structure formation in this slurry does not change even at high concentrations where the close approach of polymers and particles would be expected to introduce other types of potential energy/attractive forces (e.g. van der Waals and possible covalent bonds). As

mentioned earlier, it seems reasonable to assume that the behaviour of MOH slurry is caused by its high hydrophobic protein content (hydrophobic proteins MAH = hydrophobic proteins EGH < hydrophobic proteins MOH). It is likely that the best way for hydrophobic proteins to associate and hide most of the hydrophobic segments from water is through entanglement or micelles rather than cross-linking (Grasso et al., 2020;3). This will be further discussed in the section related to the correlation between shear and complex viscosities in section 4.7.3.2.

4.7.3 Frequency sweep of concentrated slurry

The frequency spectrum for a given system, i.e., the variation of elastic modulus (G′) and viscous modulus (G″) with oscillation frequency, provides a signature of the at-rest microstructure existing in the system. Based on frequency sweep information, our goal is to classify the hydrocolloids in one of the classifications: (i) dilute solution, (ii) entanglement network system (or concentrated solution), (iii) weak gel, and (iv) strong gel (Mistry et al., 2023;4). This will shed more light on the structure formation mechanism in the hydrocolloid slurries under investigation.

4.7.3.1 Storage modulus, Loss modulus and damping factor

Figures 4.14 and 4.15 show typical changes in storage modulus (G'), loss modulus (G") and the damping factor (loss tangent) of the EGH, MAH and MOH samples as a function of frequency at a concentration.

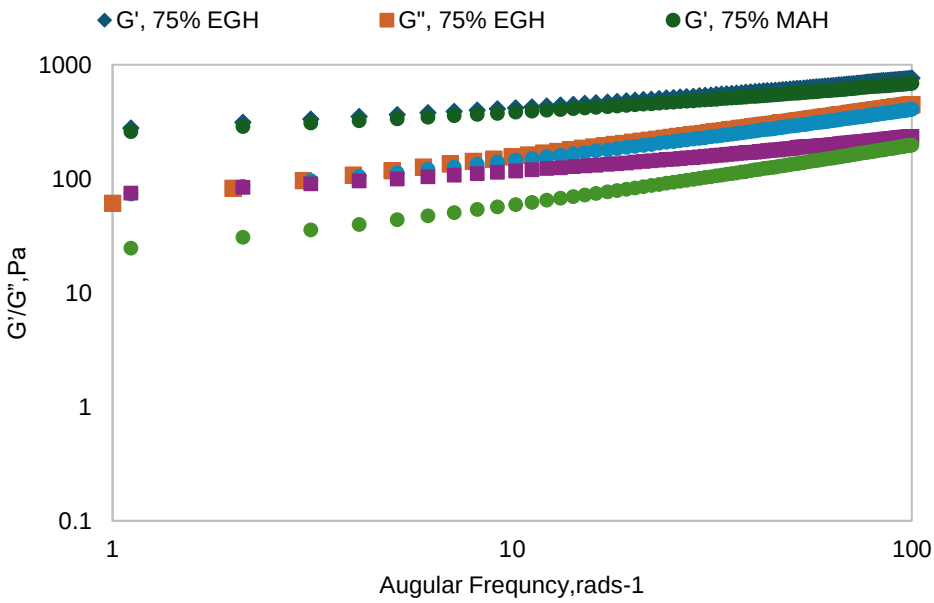

Figure 4.14 Typical Frequency sweep for EGH (egusi), MAH (makataan), and MOH (moringa) hydrocolloid slurries (75 wt%) showing the storage modulus, loss modulus and damping factor

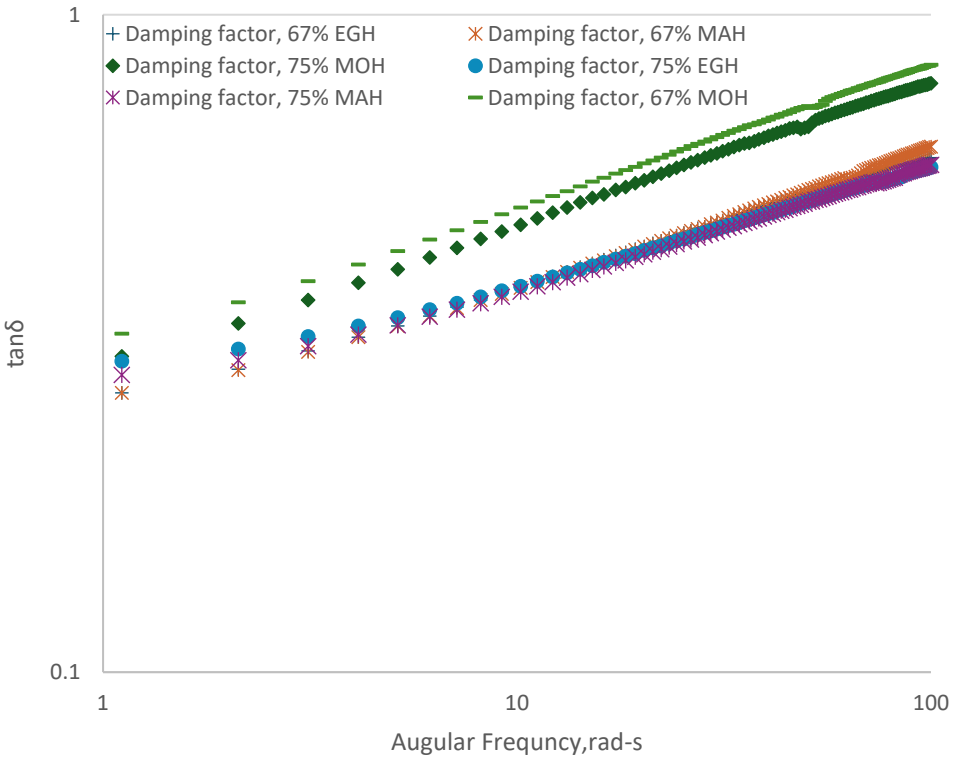

Figure 4.15 Plot for the effect of hydrocolloid concentration on the damping factor

EGH (egusi), MAH (makataan), and MOH (moringa) hydrocolloid slurries (67 and 75 wt%) showing the storage modulus, loss modulus and damping factor

Regardless of hydrocolloid type and concentration, the mechanical spectra showed that within the experimental frequency range (0.1–100 rad/s), G' > G" and no crossover point occurred, indicating a predominantly elastic behaviour of the hydrocolloid slurries. This solid-like behaviour is confirmed by the values of the damping factor, which are less than one for all concentrated slurries. The magnitude of G', G" as well as loss tangent increase with an increase in frequency with a small dependency, showing typical weak gel-like behaviour of the samples. A gel is “a

continuous network of macroscopic dimensions immersed in a liquid medium and exhibiting no steady-state flow" (Zheng et al., 2019;549; Lastra-Ripoll et al., 2022;4). The extent of solid-like behaviour is independent of the slurry concentration within the range of 67-75%, as shown in Figure 4.15, where the damping factor is independent of concentration for EGH and MAH and varies slightly in the case of MOH.

According to the polymer's dynamic theory, the frequency dependency of G' for a physical gel exhibits a power law relation (Yun et al., 2023;5). So, the degree of frequency dependence can be determined by Power law parameters.

$$G' = K'\omega^{n'} \qquad \textbf{10}$$

where G' (Pa) is the storage modulus, ω (rad/s) is the oscillation frequency, and K' (Pa.s^n) is a constant. The constant n' (dimensionless) is the slope in a log–log plot of G' versus ω.

From the structural point of view, it is known that n' = 0 is related to a proper (covalent) gel, while for a physical gel, n' > 0. The n' value can be used to compare the gels to a natural gel. A low n' value is characteristic of an elastic gel, whereas the system behaves as a viscous gel for an n' value close to 1. Typical best fittings of the power law model on frequency sweep data of MAH and MOH hydrocolloid slurries (75% w/w) are shown in Figure 4.16). As evident from Figure 4.16, the power law model fits our experimental data well. Thus, this model was used to describe the frequency sweep data and power law parameters determined for all samples are given in Table 4.5. It is clear from Table 4.5 that the n' values of EGH, MAH and MOH samples were within the range of 0.22–0.25, reflecting a predominantly elastic gel behaviour (very close to a true gel; n' = 0), which is not influenced by the concentration in the range of 67-75%. This aligns with the observed small dependency of loss tangent on hydrocolloid concentration. On this basis, we can advance an argument that the increase of the rigidity and the cohesion energy with increasing the concentration, observed in EGH and MAH slurries during amplitude sweep measurements, is related to the increase in the coordination number (number of close neighbours) rather than the change in the overall potential interaction energy.

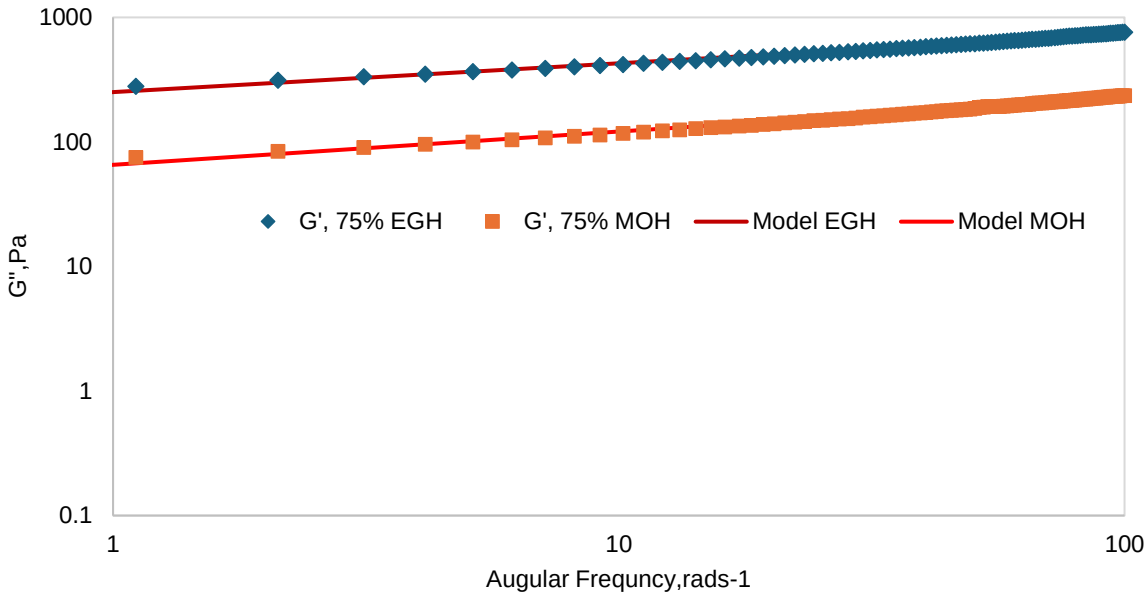

Figure 4.16 Typical best fittings of the power law model on frequency sweep data of MAH (makataan) and MOH (moringa) hydrocolloid slurries.

Table 4.5 Amplitude sweeps of semi-concentrated moringa, makataan and egusi hydrocolloid slurry

Concentrations	K (GLve)	n	R^2
67% w/w			
EGH	147.00±11.00[a]	0.22±0.00[a]	0.99[a]
MOH	54.70±7.50[a]	0.25±0.00[a]	0.99[a]
MAH	147.00±9.90[a]	0.22±0.00[a]	0.98[a]
75% w/w			
EGH	251.00±21.00[a]	0.23±0.00[a]	0.98[a]
MOH	65.50±8.99[a]	0.25±0.00[a]	0.97[a]
MAH	251.50±19.99[a]	0.23±0.00[a]	0.98[a]

[1]Values are mean ± standard deviation. Means with a different superscript in each column differ significantly

The relatively low cohesive energy characteristic of MOH hydrocolloids (E_{coh} = 0.3-0.7 kJ) indicates that although these hydrocolloids form predominantly elastic gels, the latter are fragile. This means that if subjected to a steady shear flow, it will flow rather than fracture (Horstmann et al., 2018;132). Once again, its relatively high hydrophobic proteins could inhibit the construction of strong bonds between the polymers, thus giving rise to a fragile gel (Semenova et al., 2021;3).

On the other hand, MAH and EGH slurries give rise to relatively strong elastic gels (E_{coh} = 2-7 kJ) and can be classified as relatively strong gels. In other words, EGH and MAH-based gels possess a higher structural resilience (the ability of the material to maintain structural integrity without significant modification and destruction as strain increases) than MOH-based gels.

4.7.3.2 Complex viscosity

Figure 4.17 shows the complex viscosities of hydrocolloid slurry at 67 % w/w and 75% w/w for EGH, MAH, and MOH slurries.

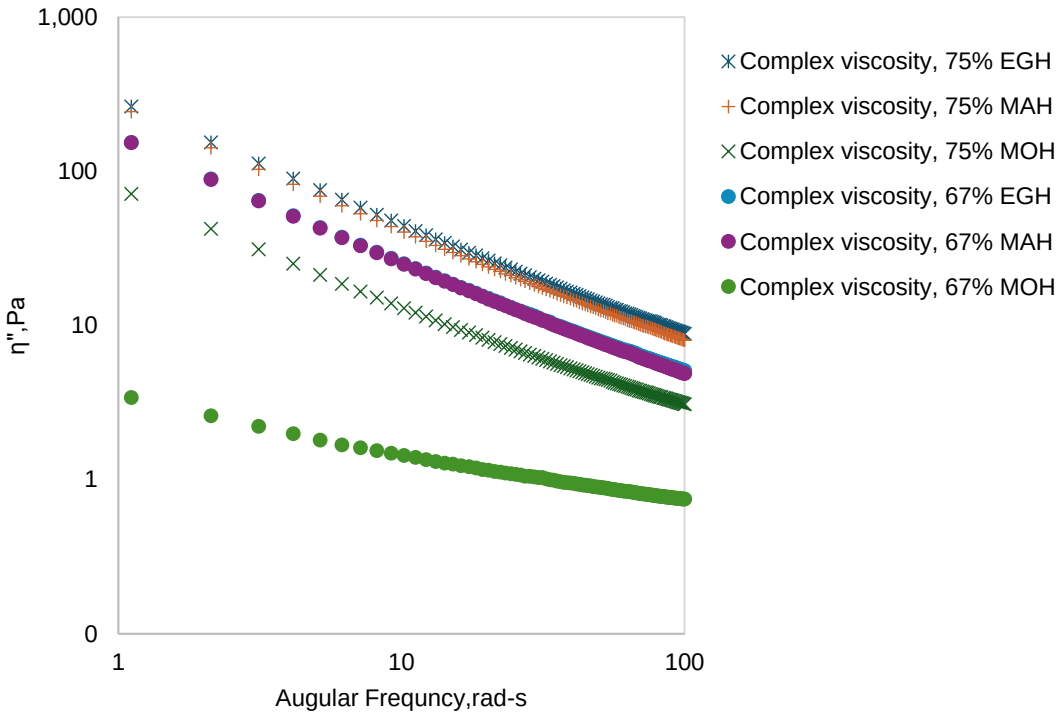

Figure 4.17 Complex viscosity of hydrocolloid slurry at 67 % w/w and 75% w/w for EGH (egusi), MAH (makataan) and MOH (moringa) hydrocolloid slurries.

First, based on a double logarithmic scale, all hydrocolloid gels' complex dynamic viscosity (η*) decreased linearly with increasing frequency, showing a non-Newtonian shear thinning flow behaviour (Figure 4.17). This aligns with the results obtained when the samples were subjected to a steady shear flow. This behaviour has also been observed for corn starch (Kanikireddy et al., 2020;3), sweet potato starch–xanthan gum mixtures (Choi & Yoo, 2009;639; Cheng et al., 2024;5), sweet potato starch (Yue et al., 2022), and Peruvian carrot starch (dos Santos et al., 2018;3). Second, in the 67-75% range, the complex viscosity of EGH and MAH is higher than

that associated with MOH; even the viscosity related to 67% EGH or MAH is higher than that associated with 75% MOH. Third, the complex viscosity of MOH is more sensitive to an increase in concentration than MAH or EGH. Once again, higher values of η^* for MAH and EGH, combined with their high ability to reduce the interfacial tension, show the higher potential of these hydrocolloid gels as suitable thickeners, emulsifiers and stabilisers in increasing the consistency of food systems.

4.7.3.4 Complex viscosity vs. Shear viscosity

For many polymer solutions, the frequency dependence of the complex viscosity and the shear rate dependence of η are closely superposable when the exact numerical values of ω and γ are compared. This empirical correlation, often called the Cox-Merz rule, has already been observed for several biopolymer solutions, but there are also a few exceptions. Even in these cases, helpful information may be extracted from the comparison of (η, γ) and (η, ω) profiles. Figure 4.18 shows the superimposition of the shear and complex viscosities.

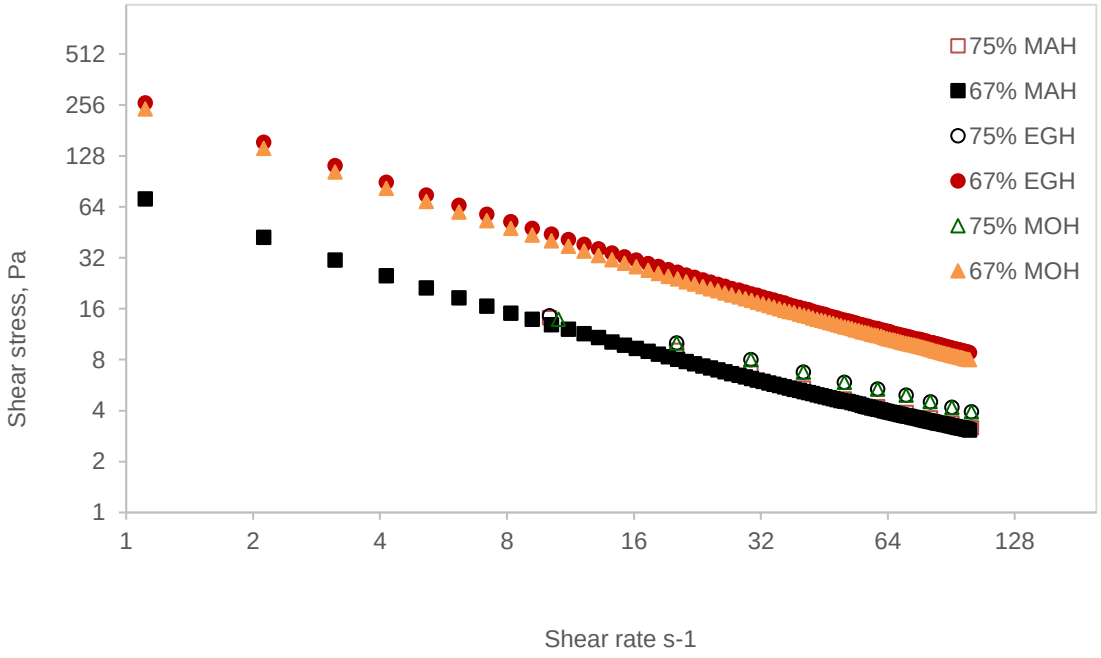

Figure 4.18 Plot for the superimposition of the shear and complex viscosity

The following conclusions can be drawn from Figure 4.18. First, for MOH slurry, the superposition between the shear viscosity and the complex viscosity in the typical range of shear rate and angular frequency (10 – 100 s^{-1}) is perfect. This confirms that the entanglement network of

polymers within the MOH-based slurry is the dominating mode of structure formation. The fact that a Newtonian plateau is absent and instead a yield stress behaviour is observed (and thus a gel is produced) is probably due to high concentrations of dispersed undissolved particulate material characteristic of MOH slurry. Such behaviour is often observed in xanthan, schizophyllan, and scleroglucan solutions (Ahmed, 2017;220; Verheyen et al., 2021;23). The macromolecule is highly stiff in all cases, tending towards rod-like (Santos et al., 2020;750). One explanation for this behaviour is that an element of liquid crystallinity is being developed (isotropic to nematic or cholesteric phase transition), which is inappropriate for every condition. It is likely that in our case, the high presence of undissolved particles (MOH had an appearance of a granulate slurry rather than a milky one) behave like fillers to the entangled polymers (proteins and polysaccharides) and thus generate yield stress. Second, for EGH and MAH, $\eta^* > \eta$, the difference becomes increasingly large with decreasing frequencies and shear rates. This is typical of the weak gel "power law" behaviour described above, not entangled systems (Liu et al., 2021;4). So, it seems reasonable to assume that the structure formation mechanism in this case is cross-liking rather than entanglement. Similar results were obtained for cross-linked waxy maize starch (Huang et al., 2021;3) and native and cross-linked potato starches. Moreover, the smaller sizes of EGH or MAH residual particles, compared to MOH (MAH and EGH had a milky appearance), behave like more robust fillers, thus strongly reinforcing the structure.

4.7 Conclusion

A detailed investigation into the rheological behaviour of EGH, MAH and MOH hydrocolloids in semi-concentrated (20-50 wt%) and concentrated (50-75 wt%) slurries was made. The influence of the process parameters (pH=4-9; temperatures =30-75^{o}C; mixing time =1-10 minutes; concentration = 20-50 wt%) and slurry concentration on the mechanical response when these systems are subjected to a steady shear flow to reversible minor strain in amplitude as well as frequency sweep modes of deformation was evaluated. It has been found that regardless of the hydrocolloid type and process parameters, semi-concentrated slurries are pseudoplastic materials which behave like viscous liquids with no yield stress; G" > G' in the entire strain range (0.1-200%). The correlation between the storage modulus and the slurry concentration, following the correlation between the yield stress and the slurry concentration, shows two deflection points/transitional points, 50 wt% and 67 wt%. The first transition point is present in all three hydrocolloids, whereas the second is only related to EGH and MAH slurries; MOH-based slurry does not display such a point. The first transition point (50 wt%) is associated with the onset of structure formation. The second transitional point marks the boundary between the regions of the slow or rapid response of the strength or rigidity of the structure of the slurry of EGH and MAH with changes in hydrocolloid concentration. Understanding the balance between yield stress and elastic modulus helps create food products with the right texture for spreading, pouring, or

spooning. It ensures that the product remains stable until consumed. This is key in designing products that are easy to use but maintain quality during storage, handling, and consumption. Interestingly, it was found that because of its high content of hydrophobic proteins, the dominating mechanism of structure formation within MOH slurries is the entanglement network of polymers (proteins and polysaccharides) whose yield stress originating from the presence of high concentrations of dispersed particulate material within the structure. This gives rise to a weak, predominately elastic gel rather than viscous with a cohesive energy of 0.2-0.7 kJ. On the other hand, the dominating mechanism of structure formation within EGH and MAH slurries is cross-linking rather than entanglement, due probably to their high content of hydrophilic proteins. This generates a predominantly elastic gel with a relatively high cohesive energy of 2-7 kJ. Higher values of the complex viscosity for MAH and EGH, combined with their high ability to reduce the interfacial tension, show the higher potential of these hydrocolloid gels as suitable thickeners, emulsifiers and stabilisers in increasing the consistency of food systems. These systems should be studied further to probe their ability to stabilise the oil-in-water emulsion. Applying the Cox-Merz rule has proved to be a valuable guide to characterising the nature of structured liquids in the presence of MOH, MAH, and EGH.

References

Aghababaei, F., McClements, D.J., Martinez, M.M. & Hadidi, M. 2024. Electrospun plant protein-based nanofibers in food packaging. *Food Chemistry*, 432(August 2023): 137236. https://doi.org/10.1016/j.foodchem.2023.137236.

Ahmed, J. 2017. *Time-Temperature Superposition Principle and its Application to Biopolymer and Food Rheology*. Elsevier Ltd. http://dx.doi.org/10.1016/B978-0-08-100431-9/00009-7.

de Almeida Paula, D., Mota Ramos, A., Basílio de Oliveira, E., Maurício Furtado Martins, E., Augusto Ribeiro de Barros, F., Cristina Teixeira Ribeiro Vidigal, M., de Almeida Costa, N. & Tatagiba da Rocha, C. 2018. Increased thermal stability of anthocyanins at pH 4.0 by guar gum in aqueous dispersions and double emulsions W/O/W. *International Journal of Biological Macromolecules*, 117: 665–672.

Balachandramohan, J., Sivasankar, T. & Sivakumar, M. 2020. Facile sonochemical synthesis of Ag2O-guar gum nanocomposite as a visible light photocatalyst for the organic transformation reactions. *Journal of Hazardous Materials*, 385(October 2019): 121621. https://doi.org/10.1016/j.jhazmat.2019.121621.

Ben-Harb, S., Panouillé, M., Huc-Mathis, D., Moulin, G., Saint-Eve, A., Irlinger, F., Bonnarme, P., Michon, C. & Souchon, I. 2018. The rheological and microstructural properties of pea, milk, mixed pea/milk gels and gelled emulsions designed by thermal, acid, and enzyme treatments. *Food Hydrocolloids*, 77: 75–84.

Boehm, M.W., Warren, F.J., Baier, S.K., Gidley, M.J. & Stokes, J.R. 2019. A method for developing structure-rheology relationships in comminuted plant-based food and non-ideal soft particle suspensions. *Food Hydrocolloids*, 96: 475–480.

Chavoshpour-Natanzi, Z. & Sahihi, M. 2019. Encapsulation of quercetin-loaded β-lactoglobulin for drug delivery using modified anti-solvent method. *Food Hydrocolloids*, 96: 493–502.

Chen, J., Mu, T., Goffin, D., Blecker, C., Richard, G., Richel, A. & Haubruge, E. 2019. Applying soy protein isolate and hydrocolloid-based mixtures as promising food material in 3D food printing. *Journal of Food Engineering*, 261(December 2018): 76–86. https://doi.org/10.1016/j.jfoodeng.2019.03.016.

Chen, W., Yu, H., Shi, R., Ma, C., Gantumur, M.A., Qayum, A., Bilawal, A., Liang, G., Oh, K.C., Jiang, Z. & Hou, J. 2023. Corrigendum to “Comparison of carrying mechanism between three fat-soluble vitamins and alpha-lactalbumin: Effects on the structure and physicochemical properties of alpha-lactalbumin” [Food Hydrocolloids 116 (2021) 106662] (Food Hydrocolloids (2021) 116, (S0. *Food Hydrocolloids*, 135(October 2022): 108258. https://doi.org/10.1016/j.foodhyd.2022.108258.

Cheng, Y., Wang, B., Lv, W., Zhong, Y. & Li, G. 2024. Effect of xanthan gum on physicochemical properties and 3D printability of emulsion-filled starch gels. *Food Hydrocolloids*, 149(December 2023): 109613. https://doi.org/10.1016/j.foodhyd.2023.109613.

Choi, H.M. & Yoo, B. 2009. Steady and dynamic shear rheology of sweet potato starch-xanthan gum mixtures. *Food Chemistry*, 116(3): 638–643. http://dx.doi.org/10.1016/j.foodchem.2009.02.076.

El-hoshoudy, A.N., Zaki, E.G. & Elsaeed, S.M. 2020. Experimental and Monte Carlo simulation of palmitate-guar gum derivative as a novel flooding agent in the underground reservoir. *Journal of Molecular Liquids*, 302: 112502. https://doi.org/10.1016/j.molliq.2020.112502.

Gannasin, S.P., Adzahan, N.M., Hamzah, M.Y., Mustafa, S. & Muhammad, K. 2015. Physicochemical properties of tamarillo (Solanum betaceum Cav.) hydrocolloid fractions. *Food Chemistry*, 182: 292–301. http://dx.doi.org/10.1016/j.foodchem.2015.03.010.

Gomes, L.R., Simões, C.D., & Silva, C. (2020). Demystifying thickener classes of food additives through molecular gastronomy. *International Journal of Gastronomy and Food Science,* 22(October), 100277. https://doi.org/10.1016/j.ijgfs.2020.100277.

Grasso, N., Alonso-Miravalles, L. & O’Mahony, J.A. 2020. Composition, physicochemical and sensory properties of commercial plant-based yoghurts. *Foods*, 9(3).

Grasso, S., Liu, S. & Methven, L. 2020. LWT - Food Science and Technology Quality of mu fi ns enriched with upcycled defatted sunflower seed flour. , 119(October 2019).

Green, A.J., Littlejohn, K. A., Hooley, P. & Cox, P.W. 2013. Formation and stability of food foams and aerated emulsions: Hydrophobins as novel functional ingredients. *Current Opinion in Colloid and Interface Science*, 18(4): 292–301.

Gürgen, S. 2019. Tuning the rheology of nano-sized silica suspensions with silicon nitride particles. *Journal of Nano Research*, 56: 63–70.

Huang, R., Huang, K., Guan, X., Li, S., Cao, H., Zhang, Y., Lao, X., Bao, Y. & Wang, J. 2021. Effect of defatting and extruding treatment on the physicochemical and storage properties of quinoa (Chenopodium quinoa Wild) flour. *Lwt*, 147(January): 111612. https://doi.org/10.1016/j.lwt.2021.111612.

Hundschell, C.S. & Wagemans, A.M. 2019. Rheology of common uncharged exopolysaccharides for food applications. *Current Opinion in Food Science*, 27: 1–7.

Jeirani, Z., Jan, B.M., Ali, B.S., Noor, I.M., See, C.H. & Saphanuchart, W. 2013. Formulation and phase behaviour study of a nonionic triglyceride microemulsion to increase hydrocarbon production. *Industrial Crops & Products*, 43: 15–24.

Kanikireddy, V., Varaprasad, K., Rani, M.S., Venkataswamy, P., Mohan Reddy, B.J. & Vithal, M. 2020. Biosynthesis of CMC-Guar gum-Ag0 nanocomposites for inactivation of food pathogenic microbes and its effect on the shelf life of strawberries. *Carbohydrate Polymers*, 236(December 2019): 116053. https://doi.org/10.1016/j.carbpol.2020.116053.

Kavitake, D., Balyan, S., Devi, P.B. & Shetty, P.H. 2019. The interface between food-grade flavour and water-soluble galactan biopolymer forms a stable water-in-oil-in-water emulsion. *International Journal of Biological Macromolecules*, 135: 445–452. https://doi.org/10.1016/j.ijbiomac.2019.05.199.

Kitunen, V., Korpinen, R., Bhattarai, M., Pitkänen, L., Lehtonen, M., Mikkonen, K.S., Ilvesniemi, H., & Kilpeläinen, P.O. (2019). Functionality of spruce galactoglucomannans in oil-in-water emulsions. *Food Hydrocolloids,* 86, 154–161. https://doi.org/10.1016/j.foodhyd.2018.03.021

Kongjaroen, A., Methacanon, P., Seetapan, N., Fuongfuchat, A., Gamonpilas, C. & Nishinari, K. 2022. Effects of dispersing media on the shear and extensional rheology of xanthan gum and guar gum-based thickeners used for dysphagia management. *Food Hydrocolloids*, 132(March): 107857. https://doi.org/10.1016/j.foodhyd.2022.107857.

Lastra-Ripoll, S.E., Quintana, S.E. & García-Zapateiro, L.A. 2022. Chemical, technological, and rheological properties of hydrocolloids from sesame (Sesamum indicum) with potential food applications. *Arabian Journal of Chemistry*, 15(10).

Li, C., Ji, Y., Li, E. & Gilbert, R.G. 2023. Interactions between leached amylose and protein affect the stickiness of cooked white rice—food *Hydrocolloids*, 135(October 2022).

Lin, M., Tay, S.H., Yang, H., Yang, B. & Li, H. 2017. Replacement of eggs with soybean protein isolates and polysaccharides to prepare yellow cakes suitable for vegetarians. *Food Chemistry*, 229: 663–673. http://dx.doi.org/10.1016/j.foodchem.2017.02.132.

Lin, Q., Shang, M., Li, X., Sang, S., Chen, L., Long, J., Jiao, A., Ji, H., Qiu, C. & Jin, Z. 2024. Rheology and 3D printing characteristics of heat-inducible pea protein-carrageenan-glycyrrhizic acid emulsions as edible inks. *Food Hydrocolloids*, 147(PB): 109347.

https://doi.org/10.1016/j.foodhyd.2023.109347.

Liu, N., Li, N., Faiza, M., Li, D., Yao, X. & Zhao, M. 2021. Stability and in vitro digestion of high purity diacylglycerol oil-in-water emulsions. *Lwt*, 148(January).

Mahmood, K., Kamilah, H., Shang, P.L., Sulaiman, S., Ariffin, F. & Alias, A.K. 2017. A review: Interaction of starch/non-starch hydrocolloid blending and the recent food applications. *Food Bioscience*, 19(May): 110–120.

Marić, M., Grassino, A.N., Zhu, Z., Barba, F.J., Brnčić, M. & Rimac Brnčić, S. 2018. An overview of traditional and innovative approaches for pectin extraction from plant food wastes and by-products: Ultrasound, microwave, and enzyme-assisted extraction. *Trends in Food Science and Technology*, 76(January): 28–37.

Masalova, I., Tshilumbu, N.N., Fester, V. & Kharatyan, E. 2020. Is combining two particles with different degrees of hydrophobicity an alternative method for tuning the average particle hydrophobicity? *Journal of Molecular Liquids*, 313: 113444. https://doi.org/10.1016/j.molliq.2020.113444.

McClements, D.J. 2021. Food hydrocolloids: Application as functional ingredients to control lipid digestion and bioavailability. *Food Hydrocolloids*, 111.

Meder, F., Daberkow, T., Treccani, L., Wilhelm, M., Schowalter, M., Rosenauer, A., Mädler, L. & Rezwan, K. 2012. Protein adsorption on colloidal alumina particles functionalised with amino, carboxyl, sulfonate and phosphate groups. *Acta Biomaterialia*, 8(3): 1221–1229. http://dx.doi.org/10.1016/j.actbio.2011.09.014.

Mistry, S., Fuhrmann, P.L., de Vries, A., Karshafian, R. & Rousseau, D. 2023. Structure-rheology relationship in monoolein liquid crystals. *Journal of Colloid and Interface Science*, 630: 878–887. https://doi.org/10.1016/j.jcis.2022.10.115.

Moelants, K.R.N., Cardinaels, R., De Greef, K., Daels, E., Van Buggenhout, S., Van Loey, A.M., Moldenaers, P. & Hendrickx, M.E. 2014. Effect of calcium ions and pH on the structure and rheology of carrot-derived suspensions. *Food Hydrocolloids*, 36: 382–391.

Montoya, J., Medina, J., Molina, A., Gutiérrez, J., Rodríguez, B. & Marín, R. 2021. Impact of viscoelastic and structural properties from starch-mango and starch-arabinoxylans hydrocolloids in 3D food printing. *Additive Manufacturing*, 39(February).

Náthia-Neves, G., Calix-Rivera, C.S., Villanueva, M. & Ronda, F. 2023. Microwave radiation induces modifications in the protein fractions of the flours and modulates their derived techno-functional properties—International *Journal of Biological Macromolecules*, 253(August).

Pant, A., Lee, A.Y., Karyappa, R., Lee, C.P., An, J., Hashimoto, M., Tan, U.X., Wong, G., Chua, C.K. & Zhang, Y. 2021. 3D food printing of fresh vegetables using food hydrocolloids for dysphagic patients. *Food Hydrocolloids*, 114(October 2020): 106546. https://doi.org/10.1016/j.foodhyd.2020.106546.

Ponzini, E., Natalello, A., Usai, F., Bechmann, M., Peri, F., Müller, N. & Grandori, R. 2019. Structural characterisation of aerogels derived from enzymatically oxidised galactomannans of fenugreek, sesbania and guar gums. *Carbohydrate Polymers*, 207(December 2018): 510–520. https://doi.org/10.1016/j.carbpol.2018.11.100.

Ptaszek, P. 2022. *Large amplitude oscillatory shear measurement and Fourier-transform rheology: food application*. Elsevier Ltd. http://dx.doi.org/10.1016/B978-0-08-100431-9/00005-X.

Rosa-sibakov, N., Hakala, T.K., Sözer, N., Nordlund, E., Poutanen, K. & Aura, A. 2016. Birch pulp xylan works as a food hydrocolloid in acid milk gels and is fermented slowly in vitro. *Carbohydrate Polymers*, 154: 305–312. http://dx.doi.org/10.1016/j.carbpol.2016.06.028.

Santos, J., Alcaide-González, M.A., Trujillo-Cayado, L.A., Carrillo, F. & Alfaro-Rodríguez, M.C. 2020. Development of food-grade Pickering emulsions stabilised by a biological macromolecule (xanthan gum) and zein. *International Journal of Biological Macromolecules*, 153: 747–754. https://doi.org/10.1016/j.ijbiomac.2020.03.078.

dos Santos, T.P.R., Franco, C.M.L., Demiate, I.M., Li, X.H., Garcia, E.L., Jane, J. lin & Leonel, M. 2018. Spray-drying and extrusion processes: Effects on morphology and physicochemical characteristics of starches isolated from Peruvian carrot and cassava. *International Journal of Biological Macromolecules*, 118: 1346–1353. https://doi.org/10.1016/j.ijbiomac.2018.06.070.

Semenova, M., Antipova, A., Martirosova, E., Zelikina, D., Palmina, N. & Chebotarev, S. 2021. Essential contributions of food hydrocolloids and phospholipid liposomes to the formation of carriers for controlled delivery of biologically active substances via the gastrointestinal tract. *Food Hydrocolloids*, 120: 106890.

Tan, H.L., Tan, T.C. & Easa, A.M. 2020. Using selected hydrocolloids and salt substitutes affects the structural integrity, texture, sensory properties, and shelf life of fresh, no-salt wheat noodles. *Food Hydrocolloids*, 108(July 2019): 105996. https://doi.org/10.1016/j.foodhyd.2020.105996.

Trujillo, A.J. 2016. Food Hydrocolloids Enhanced stability of emulsions treated by Ultra-High Pressure Homogenization for delivering conjugated linoleic acid in Caco-2 cells. *Food hydrocolloids*: 1–11.

Vatansever, S., Whitney, K., Ohm, J.B., Simsek, S. & Hall, C. 2021. Physicochemical and multi-scale structural alterations of pea starch induced by supercritical carbon dioxide + ethanol extraction. *Food Chemistry*, 344: 128699. https://doi.org/10.1016/j.foodchem.2020.128699.

Verheyen, D., Altin, O., Skipnes, D., Erdogdu, F., Skåra, T. & Van Impe, J.F. 2021. Thermal inactivation of Listeria monocytogenes in the Shaka agitated reciprocal retort: Influence of food matrix rheology and fat content. *Food and Bioproducts Processing*, 125: 22–36. https://doi.org/10.1016/j.fbp.2020.10.007.

Verkempinck, S.H.E., Kyomugasho, C., Salvia-trujillo, L., Denis, S., Bourgeois, M., Loey, A.M. Van, Hendrickx, M.E. & Grauwet, T. 2018. Food Hydrocolloids Emulsion stabilising properties of citrus pectin and its interactions with conventional emulsifiers in oil-in-water emulsions. *Food Hydrocolloids*, 85(March): 144–157. https://doi.org/10.1016/j.foodhyd.2018.07.014.

Vignola, M.B., Bustos, M.C. & Pérez, G.T. 2018. Comparison of quality attributes of refined and whole wheat extruded pasta. *LWT - Food Science and Technology*, 89(October 2017): 329–335. http://dx.doi.org/10.1016/j.lwt.2017.10.062.

Wang, Y. & Selomulya, C. 2022. Food rheology applications of large amplitude oscillation shear (LAOS). *Trends in Food Science and Technology*, 127(June 2021): 221–244. https://doi.org/10.1016/j.tifs.2022.05.018.

Wei, M., Lin, K. & Sun, L. 2022. Shear thickening fluids and their applications. *Materials & Design*, 216: 110570.

You, H., Zheng, S., Li, H. & Lam, K.Y. 2023. A model with contact maps at both polymer chain and network scales for tough hydrogels with chain entanglement, hidden length and unconventional network topology. *International Journal of Mechanical Sciences*, 262(August 2023): 108713. https://doi.org/10.1016/j.ijmecsci.2023.108713.

Yousefi, A.R. & Razavi, S.M.A. 2015. Dynamic rheological properties of wheat starch gels as affected by chemical modification and concentration. : 567–576.

Yue, J., Yao, X., Gou, Q., Li, D., Liu, N., Yang, D., Gao, Z., Midgley, A., Katsuyoshi, N. & Zhao, M. 2022. Recent advances of interfacial and rheological property-based techno-functionality of food protein amyloid fibrils. *Food Hydrocolloids*, 132(February): 107827. https://doi.org/10.1016/j.foodhyd.2022.107827.

Yun, H.J., Jung, W.K., Kim, H.W. & Lee, S. 2023. Embedded 3D printing of abalone protein scaffolds as texture-designed food production for older people. *Journal of Food Engineering*, 342(October 2022): 111361. https://doi.org/10.1016/j.jfoodeng.2022.111361.

Zhao, Q., Jiang, L., Lian, Z., Khoshdel, E., Schumm, S., Huang, J. & Zhang, Q. 2019. Journal of Colloid and Interface Science High internal phase water-in-oil emulsions stabilised by food-grade starch. *Journal of Colloid And Interface Science*, 534: 542–548. https://doi.org/10.1016/j.jcis.2018.09.058.

Zheng, M., Su, H., You, Q., Zeng, S., Zheng, B., Zhang, Y. & Zeng, H. 2019. An insight into the retrogradation behaviours and molecular structures of lotus seed starch-hydrocolloid blends. *Food Chemistry*, 295(May): 548–555. https://doi.org/10.1016/j.foodchem.2019.05.166.

CHAPTER FIVE
RHEOLOGY AND STABILITY OF OIL-IN-WATER EMULSION STABILIZED BY *CITRULLUS LANATUS MUCOSOSPERMUS*, *LANATUS CITROIDES* AND *MORINGA OLEIFERA* HYDROCOLLOID

Abstract

This study investigates the sensitivity of oil-in-water (O/W) emulsions' rheological properties to several hydrocolloids, notably egusi (EGH), makataan (MAH), and moringa (MOH) hydrocolloids. The findings show that the hydrocolloid type substantially influences essential metrics such as elastic modulus, yield stress, and complicated viscosity, with EGH > MAH > MOH decreasing. Despite these variances, the solid-like behaviour of all emulsions showed a modest frequency dependency, indicating reasonably strong gel properties (n'=0.11-0.13), similar to genuine gels. Beyond interfacial tension and droplet size, additional sources of elasticity dominated the system, driven by hydrocolloids' physical and chemical interactions in the continuous phase and at the interface between droplets. The magnitude of these forces, including van der Waals attraction and steric or electrostatic repulsion, was influenced by hydrocolloid composition and molecular weight, further affecting the emulsions' structure and viscosity. The study concludes that the type of hydrocolloid plays a crucial role in modifying interfacial properties and contributing additional elasticity, with these effects most pronounced in EGH, followed by MAH and MOH.

5.1 Introduction

According to Horstmann et al. (2018), natural hydrocolloids are polysaccharides of several sugar units, including glucose, galactose, rhamnose, arabinose, xylose, mannose, and uronic acids. These hydrocolloids are crucial for rheology and stability. They are widely available industrial raw materials that are low toxicity and biodegradable. The strength of hydrocolloids, which are three-dimensional molecular networks known as gels or colloids, is controlled by their concentration and structure. Their characteristics are also influenced by environmental elements such as temperature, pH, and ionic strength (Olubi, 2018; Issara & Rawdkuen, 2017; Zettel & Hitzmann, 2018). Natural hydrocolloids are favoured over synthetic ones because they are readily available and harmless; they are used as food additives and in medication delivery systems (Hamdani et al., 2019).

Underutilised high-nutrient hydrocolloids derived from Moringa oleifera seeds (moringa), *Lanatus* var. *citroides* (makataan) seeds, and *Lanatus mucosospermus* seeds (egusi) have the potential to serve as more nutritious and effective stabilisers in oil-in-water emulsions. Exploring these options may offer enhanced functionality in both food and pharmaceutical applications. Likewise, oil derived from makataan and egusi seeds exhibits functional and nutritional similarities (Nyam et al., 2010; Komane et al., 2017; Highland Essential Oil, 2019), indicating a good nutritious composition. Generally, emulsions are a mixture of two immiscible liquids, which can be more than two. Emulsions are always under investigation as they change with the product's internal and external properties during processing.

Emulsions are composed of two phases, and emulsifiers are essential in the stable emulsifying process. The addition of appropriate surfactants influences the stability of emulsions by decreasing the interfacial tension between oil and water phases (Ouyang & Meng, 2022;2). Moreover, using a mixture of surfactants for stable emulsions has attracted research and commercial attention because of interactions and mechanisms in emulsifying systems. Oil-water combinations are generally divided into immiscible blends and emulsions (Jiang & Charcosset, 2022;2; Gravelle & Marangoni, 2021;2). The immiscible oil-water mixture is the most elementary mix type in which densities of oil and water stratify mixtures. Oil/water emulsion is a more intensive mix type in which microdroplets (typically smaller than 20mm) of oil or water are dispersed in another medium (Verkempinck et al., 2018;146). This study aims to (1) describe the kinetics of flow during the optimisation process; (2) establish the rheological properties of egusi, moringa and makataan hydrocolloid within an oil-in-water emulsion; (3) establish the properties and stability profile of the emulsion formed.

5.2 Source of Materials and Equipment

Moringa, egusi, and makataan hydrocolloids were obtained from the experimental procedures in chapter three, sections 3.2.1 and 3.3.2. Food-grade ethanol with a purity higher than 99% was purchased from Merck Ltd. Distilled water was used to prepare the solutions in all experiments. MCR 301 Paar Physical Rheometer was obtained from the rheology laboratory of the Flow Process & Rheology Centre at the Cape Peninsula University of Technology District 6 campus.

5.2.1 Emulsion preparation and optimisation

A D-optimal point exchange design was used to examine the impacts of hydrocolloid, oil, and water on emulsion stability. The three components contributed 100%, with hydrocolloids ranging from 10% to 35%, sunflower oil from 16% to 45%, and water from 25% to 74%. As shown in Table 5.1, the experimental design contained 11 formulations. Each hydrocolloid sample was combined

with water and sunflower oil in the appropriate proportions. The hydrocolloid, water, and oil were mixed and tested to ensure excellent stability and functional qualities.

Table 5.1 Emulsion formulation with hydrocolloid, oil and water

Formulation	Hydrocolloid	Oil	Water
1	10.00	20.00	70.00
2	9.20	16.70	74.20
3	30.00	25.00	45.00
4	30.30	40.30	20.40
5	20.50	37.50	44.30
6	27.50	40.00	52.50
7	25.00	20.00	52.50
8	35.00	40.00	25.00
9	28.00	35.00	37.00
10	15.00	30.00	45.00
11	10.00	40.00	49.10

For each of the 11 combinations, the hydrocolloid was weighed into a 200 mL beaker before adding the dispersion phase (water). The liquid was agitated for 5 minutes using a magnetic stirrer to hydrate the hydrocolloid particles. The external phase (sunflower oil) was gradually added during the homogenisation. The hydrocolloid slurries were homogenised with sunflower oil in a Silverson L4RT high-speed mixer at 2500 rpm for 25 minutes at 25°C (Révérend et al. 2011). Emulsion development was observed at each time point using a Mastersizer 2000 (Malvern, United Kingdom), which uses laser diffractometry to measure particle size. The generated emulsions were immediately evaluated for particle size and stored at room temperature for 21 days to examine the creaming index and ageing, with measurements conducted every 7-day interval (Ursu et al., 2018).

5.3 Optimal Oil-in-Water Emulsion

Each mix was subjected to different stability and functional tests to determine the optimum oil-in-water formulation. The mix with the best stability profile was analysed further for its rheological properties.

5.3.1 Functional properties of moringa, egusi and makataan oil-in-water emulsion

The droplet size and polydispersity index of the oil-in-water emulsions were obtained using Malvern Mastersizer. The Silverson L4RT high-shear mixer is manufactured by Silverson Machines, a company headquartered in Chesham, Buckinghamshire, United Kingdom The creaming index of emulsions was evaluated according to the method of Zhang et al. (2023;3). The measurements were done immediately after emulsion preparation. Emulsions (0.1 mL) were diluted in the glass cell filled with distilled water (100 mL). The microscopic emulsion morphology was observed using an optical microscope (KB-320, Optinity) at a magnification of 40 um. One emulsion drop was placed on a glass slide and covered with a cover slip. The microscopic morphology and ageing of emulsions were measured at 7-day intervals for 21 days.

5.3.2 Creaming index of moringa, egusi and makataan oil-in-water emulsion

The emulsions were stored in a 30 mL vial and sealed with a cap. All 11 samples were assessed after 7 days of cycles at room temperature. After the cycles, a phase separation of emulsion samples appeared. The creaming index was determined from the percentage of the height of the serum layer at the bottom over the height of the total emulsion as below in Equation 11 (Zhao et al., 2022;4):

$$\text{Creaming index } \% = \frac{H_S}{H_T} \times 100 \qquad 11$$

Where Hs is a serum layer's height, HT is an emulsion's total height.

5.4 Dynamic Rheological Measurements of Moringa, Egusi and Makataan Oil-in-water Emulsion

Dynamic rheological measurements assessed emulsions using MCR 300 Paar Physical Rheometer (Discovery HR-1, hybrid rheometer) New Castle, USA, with cone and plategeometry (35 mm diameter, 0.105 mm cone gap). The temperature was fixed at 25 ^{o}C during the measurements with an accuracy of 0.1^{o}C. Samples were placed on the measuring cone and left for 2 min for structure recovery and temperature equilibrium. Flow experiments were performed for shear stress from 0.1 to 100 Pa. The flow curves of shear rates, shear strains and shear viscosities were measured. The yield stress values were expressed from a plot of shear stress as a function of shear strain by the tangent crossover method. Emulsion viscoelastic parameters such as storage modulus (G') and loss modulus (G") were determined, and frequency was fixed to 1 rad/s. All measurements were an average from three replicates (Lacovino et al., 2024;3).

5.4.1 Stability profile of moringa, egusi and makataan in o/w emulsion

Amplitude and frequency sweep of Moringa, Egusi and makataan oil-in-water Emulsion. Measuring the mechanical properties and flow point of moringa, egusi and makataan seed hydrocolloid o/w emulsion, the samples were tested for amplitude sweep as well as frequency sweep at a temperature of 25 ºC (Dai *et al.*, 2019;134). The amplitude sweep was carried out at an angular frequency of 6.28 rad/s at strains from 0 to 100%. The loss factor was calculated with equation 12 below:

$$\tan \delta = {G''}/{G'} \qquad \textbf{12}$$

For ideally elastic behaviour, δ = 0°. There is no viscous portion. Therefore, G" = 0 and with that tan δ = G"/ G' = 0. For ideally viscous behaviour, δ = 90°.

5.5 Statistical Analysis

All data were collected in triplicate. They were subjected to a multivariate analysis of variance to establish mean differences between treatments. Duncan multiple range tests were used to separate means where differences existed. All data were carried out using IBM SPSS statistics version 29, 2022.

5.6 Results and Discussion

5.6.1 Emulsification process

This part of the research is devoted to screening three hydrocolloids (EGH, MAH, and MOH) during emulsification, according to the sample matrix in Table 5.1.

5.6.1.1 Ability of hydrocolloid dispersions to form emulsions

The ability of each hydrocolloid to form an emulsion in different formulations was set in Table 5.1. The typical results of these experiments for MOH hydrocolloids are shown in Figure 5.1. These visual observations showed that emulsion formed with all formulations used. The average droplet size roughly follows the trend EGH > MAH > MOH. Still, in most emulsions, the hydrocolloid type has little effect on D_{50} after 25 minutes of emulsification. Some system parameters were introduced to better compare the emulsification process in the presence of different hydrocolloids (mixed-emulsifier systems containing dissolved proteins and undissolved hydrocolloid particles). Experimental studies using online light transmittance undertaken by Raj & Bajpai (2020;6) have shown that the droplet size is exponentially reduced for emulsification systems with a dispersed phase volume fraction of 5 and 20%. The exponential decrease in the droplet size during

emulsification was further corroborated by Gao et al. (2022;152) in the case of emulsion explosives stabilised with a surfactant mixture in a system with a mixture of surfactants and nanoparticles. Thus, the kinetics of emulsification in the system was calculated using Equation 13 (Tshilumbu & Masalova, 2015;220).

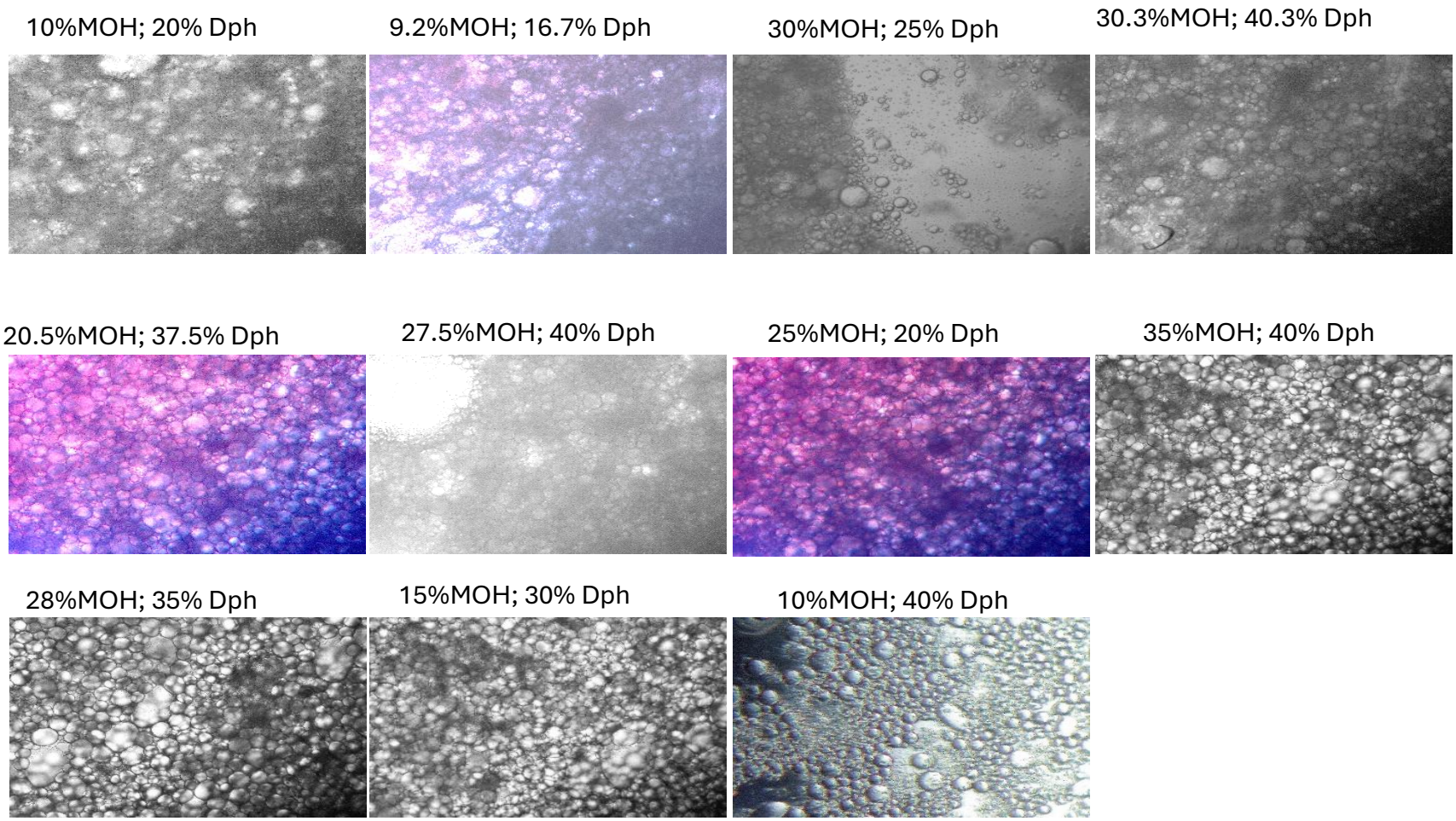

Figure 5.1 Typical microscopic images of fresh emulsion (samples prepared using MOH hydrocolloids)

$$(D_{crit}+e^{-(t/\theta)}(D_o-D_{crit}) \quad 13$$

where D_o is the initial droplet size, that is, the first droplet which appeared while the emulsion just formed, and Θ is the characteristic time of the process. It is the required time to reduce the droplet size by 1/e, almost by half.

5.7 Effect of Hydrocolloid Type on the Droplet Size and Kinetics of Refinement

Figure 5.2 shows the effect of hydrocolloid type on the average droplet size after 25 minutes of emulsification for different emulsion samples.

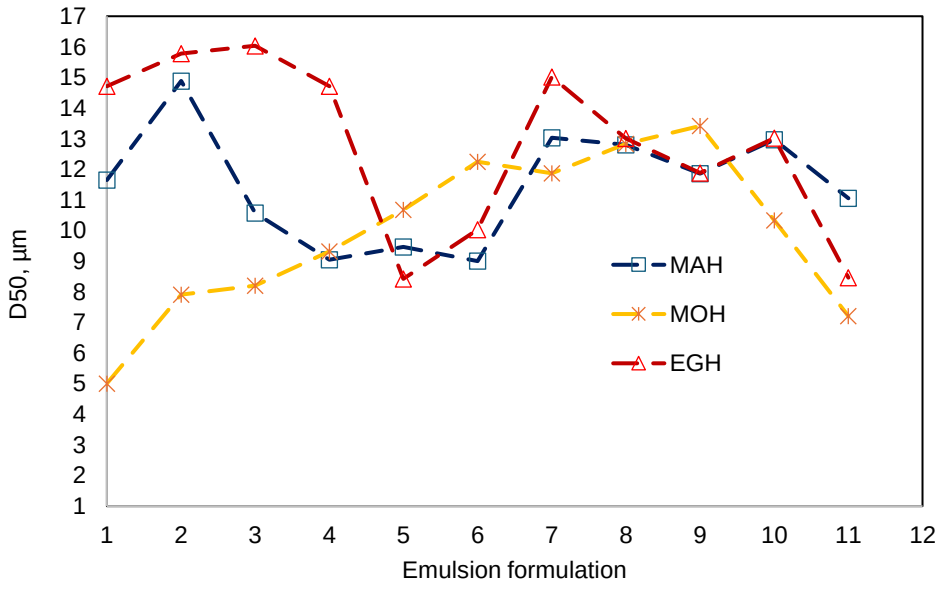

Figure 5.2 Effect of Different Emulsion Formulations on Particle Size Distribution (D50) after 25 mins of emulsification of EGH (egusi hydrocolloid), MAH (makataan hydrocolloid) and MOH (moringa hydrocolloid)

It is thus a reflection of the kinetics of emulsification or a measure of the shear stability of the emulsion under the emulsification process (Masalova et al., 2020;4). High values of Θ correspond to low kinetics of emulsification or high shear stability of the emulsion's droplets. D_{crit} is the critical droplet size which can finally be reached due to emulsification. Figure 5.3 shows the typical best fitting of the model on the emulsification of oil-in-water emulsion in the presence of MAH hydrocolloids.

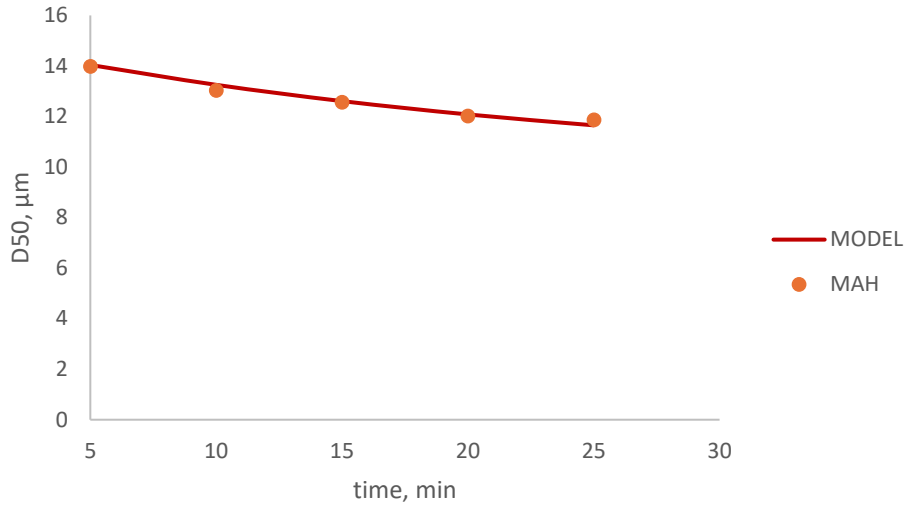

Figure 5.3 Typical best fit of the model on the emulsification of oil-in-water in the presence of MAH hydrocolloids

The obtained values of Do, D_{crit}, and Θ concerning the three hydrocolloids according to the formulation presented in Table 5.1 are summarised in Tables 5.2, 5.3, and 5.4 for EGH, MAH, and MOH, respectively.

Table 5.2 Values of D_o, D_{crit} and Θ for emulsions prepared using EGH

	Hydrocolloid	**Oil**	**Water**	**D_{crit}, µm**	**Θ, min**	**D_0,µm**
1	10	20	70	0.0 ± 0.0^a	123.4 ± 0.7^b	18.8 ± 0.0^c
2	9.2	16.7	74.2	0.2 ± 0.0^a	311.8 ± 0.5^b	17.5 ± 0.0^c
3	30	25	45	0.3 ± 0.0^a	166.03 ± 0.6^b	18.98 ± 0.0^c
4	30.3	40.3	20.4	0.4 ± 0.0^a	143.4 ± 0.5^b	17.8 ± 0.0^c
5	20.5	37.5	44.3	0.0 ± 0.0^a	59.5 ± 0.4^b	12.96 ± 0.0^c
6	27.5	40	52.5	0.03 ± 0.0^a	59.3 ± 0.3^b	15.3 ± 0.0^c
7	25	20	52.5	11.5 ± 0.1^a	27.7 ± 0.3^b	20.4 ± 0.0^c
8	35	40	25	9.2 ± 0.0^a	35.05 ± 0.3^b	16.9 ± 0.0^c
9	28	35	37	10.9 ± 0.0^a	12.3 ± 0.0 ^{b}	17.06 ± 0.0^c
10	15	30	45	7.9 ± 0.0^a	60.6 ± 0.2^b	15.7 ± 0.0^c
11	10	40	49.1	0.0 ± 0.0^a	97.4 ± 0.4^b	11.08 ± 0.0^c

[1]Values are mean ± standard deviation. Means with a different superscript in each column differ significantly.

Table 5.3 Values of D_o, D_{crit} and Θ for emulsions prepared using MAH

	Hydrocolloid	Oil	Water	D_{crit}, μm	Θ, min	D_0,μm
1	10	20	70	8.0 ± 0.0[a]	30.0 ± 0.7[b]	22.0 ± 0.0[c]
2	9.2	16.7	74.2	9.5 ± 0.0[a]	31.0 ± 0.5[b]	19.0 ± 0.0[c]
3	30	25	45	7.0 ± 0.0 [a]	20.0 ± 0.6[b]	16.0 ± 0.0[c]
4	30.3	40.3	20.4	6.5 ± 0.0 [a]	17.0 ± 0.5[b]	15.7 ± 0.0[c]
5	20.5	37.5	44.3	7.2 ± 0.0 [a]	13.0 ± 0.4[b]	18.0 ± 0.0[c]
6	27.5	40	52.5	7.2 ± 0.0[a]	35.0 ± 0.3[b]	15.0 ± 0.0 [c]
7	25	20	52.5	9.7 ± 0.1[a]	27.7 ± 0.3[b]	15.5 ± 0.0[c]
8	35	40	25	9.5 ± 0.0[a]	37.0 ± 0.3[b]	12.8 ± 0.0[c]
9	28	35	37	9.7 ± 0.0[a]	25.0 ± 0.0 [b]	17.06 ± 0.0[c]
10	15	30	45	9.5 ± 0.0[a]	52.0 ± 0.2[b]	15.7 ± 0.0[c]
11	10	40	49.1	9.5 ± 0.0[a]	35.0 ± 0.4[b]	11.08 ± 0.0[c]

[1]Values are mean ± standard deviation. Means with a different superscript in each column differ significantly.

Table 5 4 Values of Do, Dcrit and Θ for emulsions prepared using MOH

	Hydrocolloid	Oil	Water	D_{crit}, μm	Θ, min	D_0,μm
1	10	20	70	0.0 ± 0.0[a]	50.9 ± 0.7[a]	8.9 ± 0.0[a]
2	9.2	16.7	74.2	0.0 ± 0.0[a]	74.3 ± 0.5[b]	11.3 ± 0.0[a]
3	30	25	45	0.0 ± 0.0 [a]	44.8 ± 0.6[b]	14.7 ± 0.0[a]
4	30.3	40.3	20.4	0.4 ± 0.0 [a]	204.0 ± 0.5[c]	10.6 ± 0.0[a]
5	20.5	37.5	44.3	1.5 ± 0.0 [a]	100.0 ± 0.4[b]	12.9 ± 0.0[a]
6	27.5	40	52.5	0.0 ± 0.0[a]	160.0 ± 0.3[b]	14.0 ± 0.0[a]
7	25	20	52.5	0.0 ± 0.1[a]	182.3 ± 0.3[c]	14.1 ± 0.0[a]
8	35	40	25	0.5 ± 0.0[a]	251.04 ± 0.3[c]	14.4 ± 0.0[a]
9	28	35	37	0.1 ± 0.0[a]	134.06 ± 0.0 [b]	16.4 ± 0.0[a]
10	15	30	45	10.2 ± 0.0[b]	51.0 ± 0.2[b]	10.3 ± 0.0[a]
11	10	40	49.1	0.1 ± 0.0[a]	79.2 ± 0.4[b]	9.9 ± 0.0[a]

[1]Values are mean ± standard deviation. Means with a different superscript in each column differ significantly.

5.7.1. Effect of hydrocolloid type on D_{crit} and Θ

This section is devoted to oil-in-water emulsification in the presence of the three hydrocolloids (EGH, MAH and MOH) to estimate the emulsion's shear stability in the emulsification process. The effect of hydrocolloid type on Θ for different emulsion formulation contents is presented in Figure 5.4. The same experiments with lecithin, a well-established food emulsion emulsifier,

for formulations associated with processing conditions, 5, 8 and 11 are added for comparison. High emulsion stability in samples 5 and 11 have Dcrit = 0.0 µm, suggesting they form extremely fine and stable emulsions. In comparison**,** Sample 8 was chosen as an intermediate case compared with the extremely stable samples.

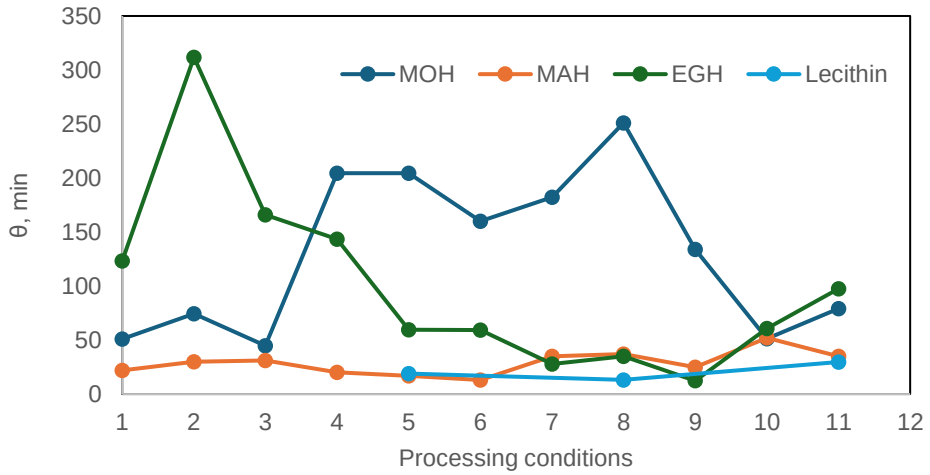

Figure 5.4 Characteristic refinement time for different processing conditions, emulsions stabilised by EGH (egusi hydrocolloid), MAH makataan hydrocolloid) and MOH (moringa hydrocolloid)

It can be seen from Figure 5.4 that in most of the emulsion formulations, the characteristic refinement time follows the trend: Lecithin ≈ MAH < EGH < MOH. In other words, in most formulations, the kinetics of droplet refinement increases in the sequence Lecithin ≈ MAH - EGH - MOH. This shows that in terms of measurement MOH (moringa hydrocolloid) and EGH (egusi hydrocolloid) have more significant peaks at formulation 2, 3 and 4 (9.2H,16.7O,74.2W; 30.0 Hydrocolloid,25.0 oil, 45 water and 30.3 hydrocolloid, 40.3 oil and 20.40 water), reaching over 300 minutes in some conditions (formulation 2), indicating that they take longer to achieve stability. MAH (makataan hydrocolloid) maintains relatively lower refinement times but is still higher than lecithin. Some arguments can be advanced to explain these observations.

It is well known that various processes occur during emulsification, including – droplet break-up, adsorption of the emulsifier and droplet collision – which may or may not lead to droplet re-coalescence (Angkuratipakorn et al., 2020;5). These processes all have their characteristic timescale. In this sense, the relatively high values of the rate of droplet refinement observed in most samples prepared with MOH as compared to MAH or EGH are

due both to the inability of MOH hydrocolloids to reduce the interfacial tension significantly (see section 3.12) and their low ability to resist coalescence of droplets (see section 5.6.1.1). The relatively low rate of droplet refinement observed in most samples prepared with EGH as compared to MAH, which is in contradiction with the ability to reduce the interfacial tension, is mainly due to the ease with which coalescence is induced in samples prepared with EGH see (section 5.6.1.1).

It is worth mentioning that while Θ represents a true characteristic of the system (a given dispersed volume fraction, surfactant type and concentration and the ratio between the dispersed and continuous phases), D_{crit} does not; it depends on D_o. To get a true characteristic of the system, D_{crit} was divided by D_o to remove the latter's influence; this allowed a comparison of the three hydrocolloids to stabilise the emulsion under shearing during the emulsification system. This suggests that MAH and lecithin would be preferable for applications requiring faster stabilisation or minimal variability in processing. This application can be recommended in salad dressing and instant emulsified products (instant coffee creamer or instant soup mix). However, MOH and EGH may offer more flexibility for products needing greater emulsion refinement (mayonnaise, ice cream and chocolate). The main results on the effect of hydrocolloid type on D_{crit}/D_o are presented in Figure 5.5.

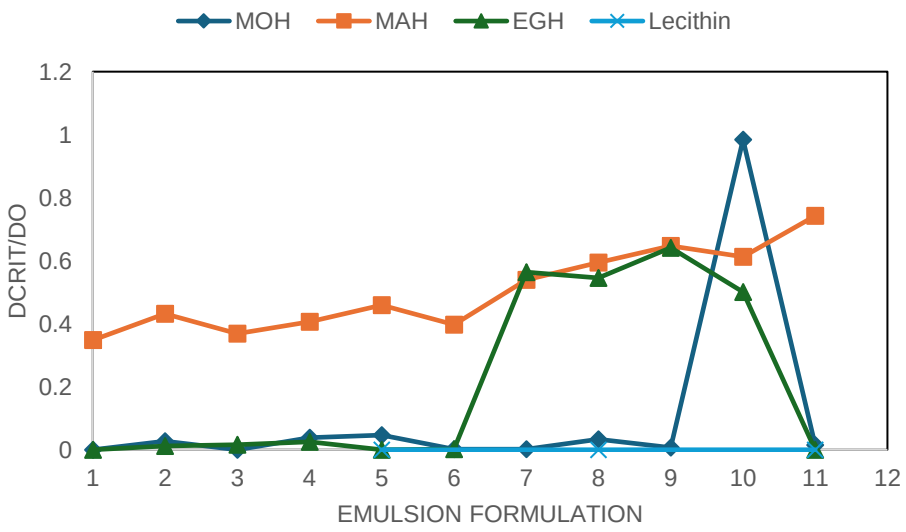

Figure 5.5 Dimensionless Critical diameters (µm) for different processing conditions emulsions stabilised by EGH (egusi hydrocolloid), MAH (makataan hydrocolloid)and MOH (moringa hydrocolloid)

It is clear from Figure 5.5 that in most of the emulsion formulations, D_{crit}/D_o increases in the sequence: Lecithin - MOH - EGH - MAH. In other words, in most formulations, the ability to break up droplets into smaller ones to reach a smaller final equilibrium size (steady state droplet size) follows the trend: Lecithin > MOH > EGH > MAH. This is due to the ability of MOH and EGH to reduce the interfacial tension.

5.7.2 Effect of dispersed phase concentration on Θ

The focus of this section was the investigation into the effect of the hydrocolloid type on the emulsion stability during the emulsification process, it is impossible not to consider also the influence of dispersed phase concentration on the kinetics of refinement as this can be extracted from the results in Tables 5.2, 5.3 and 5.4. The evolutions of the characteristic refinement time (Θ) as a function of the mass fraction for emulsions stabilised by EGH, MAH and MOH are shown in Table 5.5. MAH (Makataan Hydrocolloid) concentration: 1.4%; Dph concentration: 1.98%; Θ = 20 min. With a short refinement time (20 minutes), this formulation could be perfect for quickly stabilising emulsions such as salad dressings or sauces that require rapid emulsification.

Table 5.5 Effect of dispersed phase mass fraction on Θ for emulsions stabilised by EGH, MAH and MOH

Hydrocolloid concentration, %.	**Dph concentration, %**	**Θ, min**
MAH		
1.4	1.98	20.00
	1.60	37.00
0.47	0.85	17.00
	0.38	35.00
MOH		
1.4	1.98	215.70
	1.60	251.00
0.47	0.85	105.00
	0.38	149.20
EGH		
1.4	1.98	215.7
	1.60	251.00

0.47	0.85	59.50
	0.38	27.70

EGH (egusi hydrocolloid), MAH (makataan hydrocolloid)and MOH (moringa hydrocolloid)

The hydrocolloid concentration is 1.4%, and the Dph concentration is 1.60% (Θ = 37 min). This increased refinement time indicates that the emulsion takes longer to stabilise as the dispersed phase mass fraction reduces significantly. This may be appropriate for thicker, semi-solid items such as dips, spreads, or mayonnaise.

With a low concentration of both hydrocolloid and dispersion phase, the fast refining time (17 minutes) suggests that it is suitable for light emulsions that require rapid stabilisation, such as beverages or low-fat sauces. The stability under shear in the emulsification process is sensitive to the dispersed phase concentration. It decreases with the increase in the dispersed phase mass fraction for the emulsions prepared using MAH or MOH, while it increases for emulsions prepared with EGH. This is true for both hydrocolloid concentrations under consideration, that is, 0.46% and 1.4%. It is well known that increasing the dispersed phase concentration increases the system's viscosity and, thus, the viscous stress responsible for droplet breakup. On the other hand, at high dispersed phase concentrations, the collision timescales are significantly smaller than the emulsifier adsorption time (Okuro et al., 2020;4). Thus, the propensity to recoalescence is high. On this basis, it seems reasonable to assume that in the case of MAH or MOH, because of their relatively high resistance to the initiation of coalescence (see section 5.8.2), the increase of the coalescence rate is dominated and masked by the increase in the viscous stress. On the contrary, in the case of EGH, as discussed in section (5.8.2), the observed trend agrees with the emulsions' relatively low ability to resist coalescence initiation.

5.8 Emulsion Stability with Time

The stability of emulsions stabilised by EGH, MAH, or MOH hydrocolloid dispersions was assessed regarding coalescence and creaming with time or ageing. The former was visual observation with a Leica optical microscope equipped with a digital camera and droplet size measurements using the Malvern master size. The operation was repeated daily until significant changes in the sizes of droplets were observed.

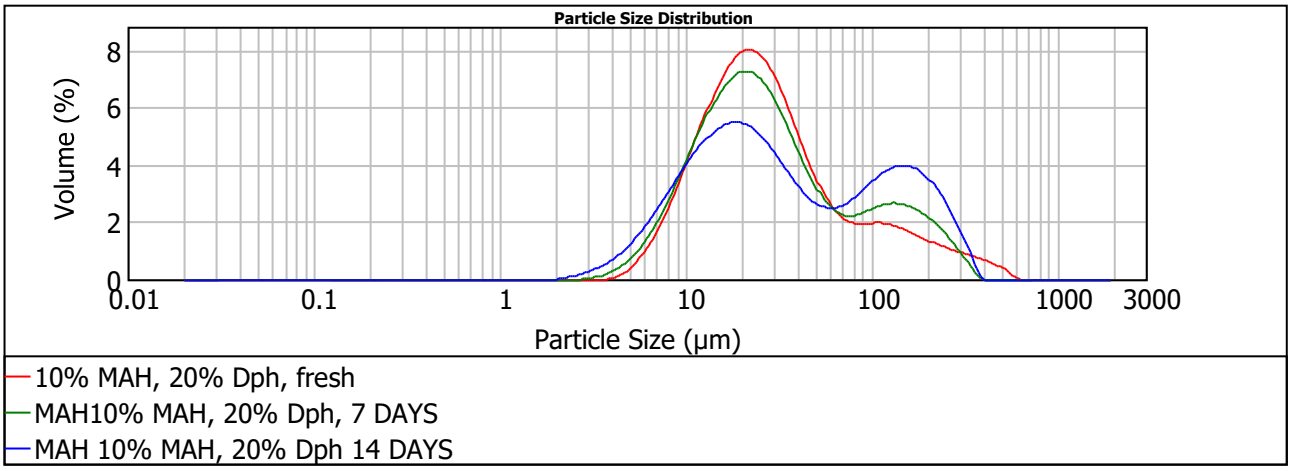
Particle Size Distribution
Volume (%)
8
6
4
2
0
0.01
0.1
1
10
100
1000
3000
Particle Size (µm)
10% MAH, 20% Dph, fresh
MAH10% MAH, 20% Dph, 7 DAYS
MAH 10% MAH, 20% Dph 14 DAYS

(a)

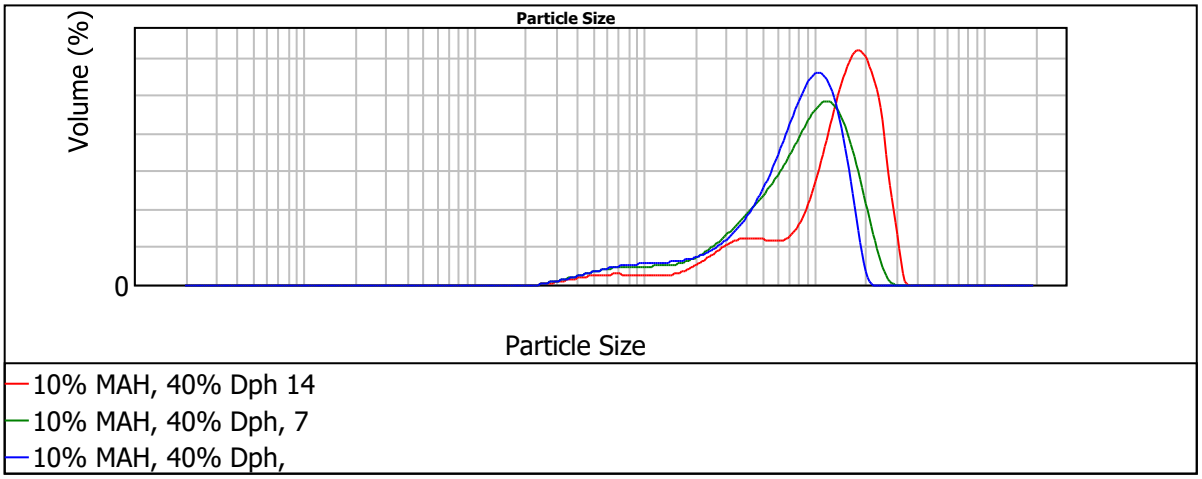
Particle Size
Volume (%)
0
Particle Size
10% MAH, 40% Dph 14
10% MAH, 40% Dph, 7
10% MAH, 40% Dph,

(b)

(c)

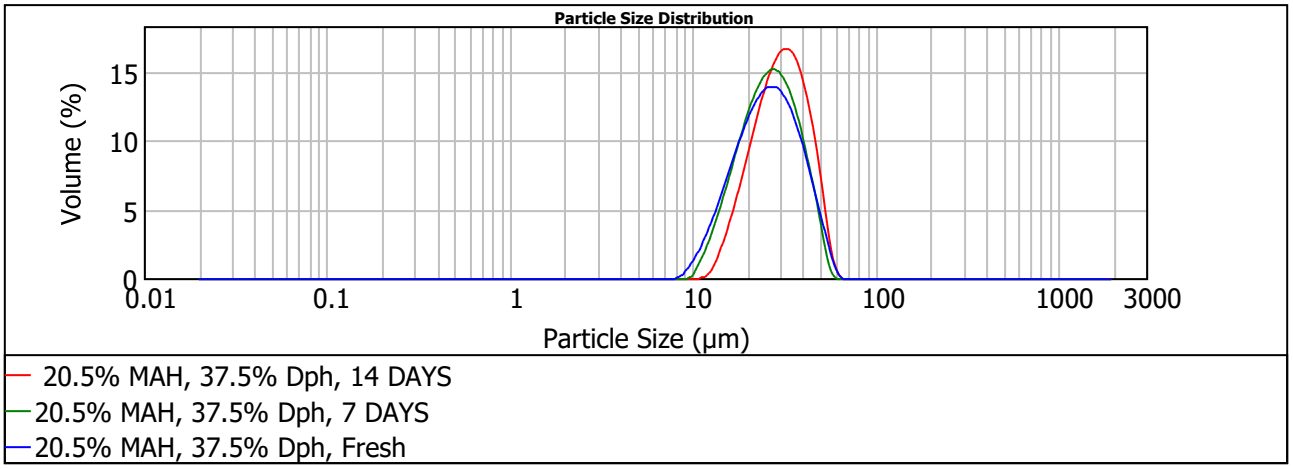

(d)

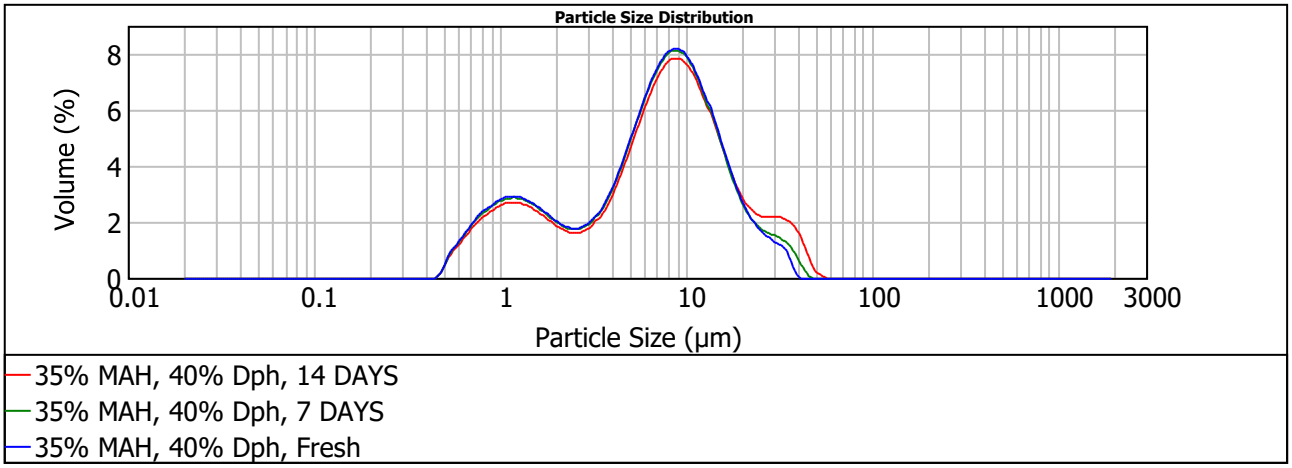

Figure 5.6 Typical droplet size distribution curves associated with different processing conditions at various stages of ageing for the sample prepared using MAH (makataan) hydrocolloids

Based on the above histogram, it is clear that for regular and bimodal distributions, ageing is associated with an increase in the average and droplet size distribution. It may be concluded that our emulsions' first instability mechanism is related to coalescence. On the other hand, Figure 5.6 shows that creaming of the dispersed droplets is another instability mechanism.

The observed onset of coalescence and the creaming index were used as quantitative measures of emulsion stability with time. For each formulation, observations for droplet size increase were made for five samples of 20 mg each, taken randomly from different parts of the stored emulsions (1.4 kg), a process repeated daily until an average droplet size increase of 5% was observed. This droplet size increase was acknowledged as the start of

coalescence. Additional information was obtained by following the kinetics of coalescence. In contrast, creaming was evaluated by keeping the 33 emulsion samples at room temperature every day until phase separation took place and storing them in 30 mL vials that were sealed with caps The creaming index was determined from the percentage of the height of the serum layer at the bottom over the height of the total emulsion sample using Equation 5.1.

5.8.1 Effect of the hydrocolloid type on the onset of coalescence

The effect of changing the hydrocolloid type on the onset of coalescence for different emulsions is shown in Figure 5.7.

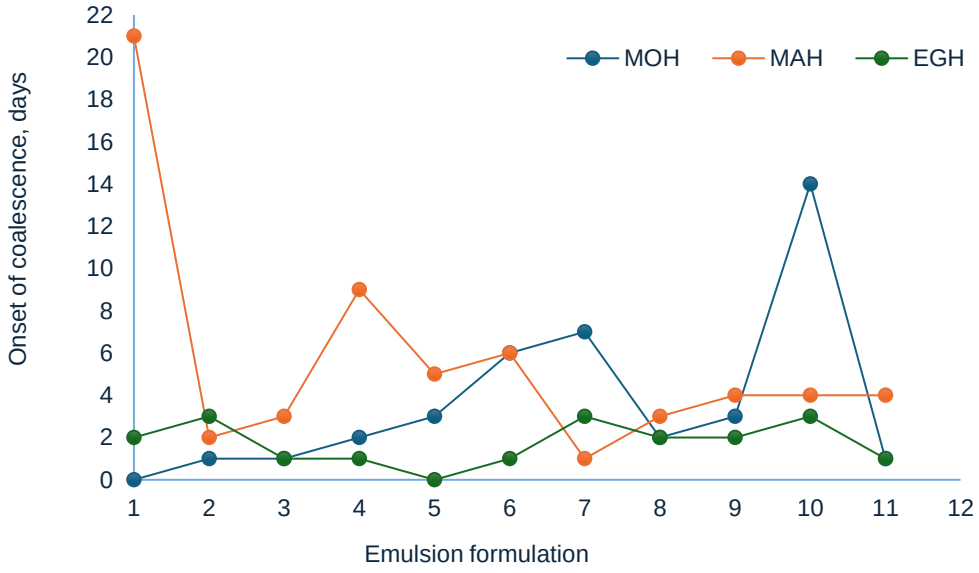

Figure 5.7 Effect of varying the hydrocolloid type on the start time of coalescence for different emulsion formulation contents EGH (egusi hydrocolloid), MAH (makataan hydrocolloid) and MOH (moringa hydrocolloid)

Two significant conclusions can be drawn from Figure 5.7. First, coalescence is initiated within one week of storage in most emulsion formulations. Second, the emulsion prepared with MAH shows relatively higher times before coalescence in most formulations. In contrast, coalescence is initiated earlier in samples prepared with EGH than MOH. In other words, the emulsions prepared with EGH are more likely to initiate coalescence than MAH or MOH. Some arguments can be advanced to explain these observations.

Bearing in mind that the complex viscosities (at low values of frequency) of the hydrocolloid slurries decrease in the sequence EGH - MAH - MOH (see section 4.6.3.2), it is clear that in the case of EGH and MAH, the high viscosity of the continuous phase significantly reduces the droplets diffusion coefficient, the rate of water drainage from the thin film between droplets on close approach and thus the droplets collision frequency and their coalescence rate are reduced (Ouyang & Meng, 2022;4). However, this stabilisation mechanism cannot explain that in most formulations, the stability of MOH emulsions is relatively high compared to the ones associated with EGH. What needed to be determined at this research stage is if the degree of deformation of the droplets (deformability) following their collisions before an eventual coalescence plays a significant role in emulsions stabilised with EGH, MAH or MOH. This will help elucidate if this mechanism is the main factor controlling the stability against the initiation of coalescence in MOH-based emulsions. To discover this, we first calculated the Laplace pressure of each emulsion formulation using the equation for a spherical droplet (Equation 14). The Laplace pressure was plotted as a function of the emulsion formulation content for different types of hydrocolloids (EGH, MAH, MOH).

$$\Delta p = \frac{2\sigma}{r} \qquad 14$$

Where σ is the interfacial tension between water and oil and r is the droplet radius.
Figure 5.8 shows results on the effect of hydrocolloid type on the Laplace pressure for different emulsion formulation contents.

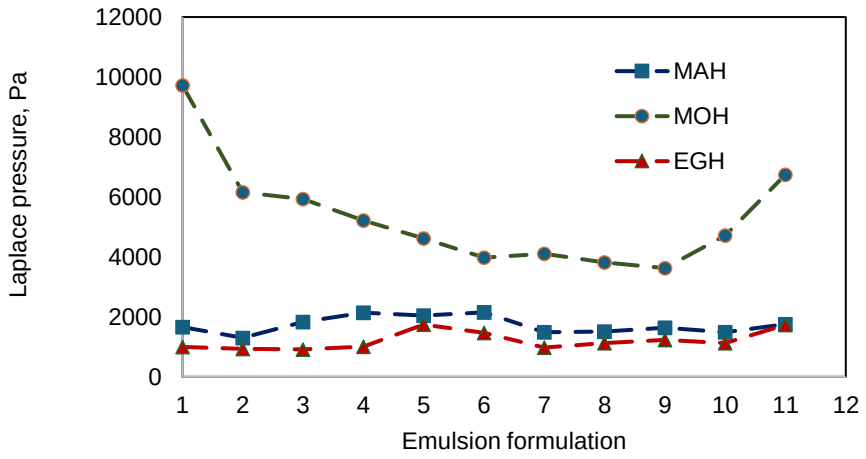

Figure 5.8 Effect of hydrocolloid type on the Laplace pressure

Figure 5.8 makes it clear that in all emulsion formulations, the Laplace pressure is significantly higher in the case of MOH than in MAH or EGH. It decreases according to the MOH–MAH–EGH sequence, which is the line for decreasing interfacial tension. On this basis, it seems reasonable to assume that in the case of MOH, the dominating mechanism of emulsion stability against the initiation of coalescence is the relatively high resistance to droplet deformation, and this could explain the fact that in most formulations, the stability of MOH emulsions is relatively high compared to the ones associated with EGH. It is worth mentioning that coalescence is initiated earlier in EGH-based emulsions than in MAH-based ones, which will be discussed in section 5.8.2.

5.8.2 Effect of dispersed phase concentration on the onset of coalescence for emulsions stabilised by EGH, MAH and MOH

Table 5.6 shows the evolution of the onset of coalescence as a function of the mass fraction (at constant hydrocolloid concentration, 0.47% or 1.4% in water) for emulsions stabilised by EGH, MAH, and MOH.

Table 5.6 Effect of dispersed phase mass fraction on Dcrit and Θ for emulsions stabilised by EGH, MAH and MOH.

Emulsifier Conc. %	Mass fraction, %	Onset of coalescence, %
MAH		
1.4	1.98	9
	1.6	3
0.47	0.85	5
	0.38	1
MOH		
1.4	1.98	2
	1.6	2
0.47	0.85	3
	0.38	7
EGH		
1.4	1.98	1
	1.6	2
0.47	0.85	0
	0.38	3

EGH (egusi hydrocolloid) MAH (makataan hydrocolloid) MOH (moringa hydrocolloid)

Similarly to the stability under shear in the emulsification process, the stability against initiation of coalescence of the emulsions is sensitive to the dispersed phase concentration. It decreases with the increase in the dispersed phase mass fraction for the emulsions prepared using MAH or MOH, while it increases for emulsions prepared with EGH. This is once again true for both hydrocolloid concentrations under consideration, that is, 0.46% and 1.4%. As mentioned for the characteristic refinement time (section 5.8.1), these observations will be discussed in detail in the next section.

5.8.3 Effect of ageing on the kinetics of coalescence

In this section, the effect of ageing on the kinetics of coalescence for different emulsion formulation contents was investigated to glean more profound insight into the stabilisation mechanism. The main results of these experiments for emulsions prepared using EGH, MAH or MOH hydrocolloids are shown in Figure 5.9, 5.10 and 5.11, respectively.

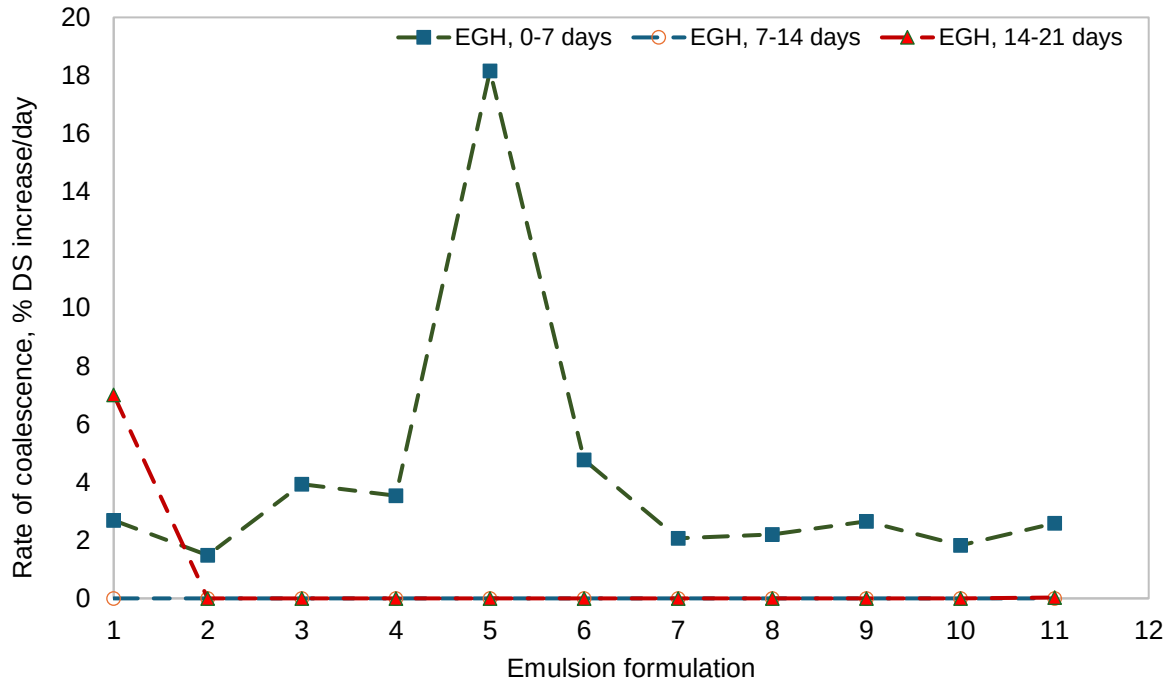

Figure 5.9 Effect of ageing on the kinetics of coalescence for different emulsion formulation contents for emulsions prepared using EGH

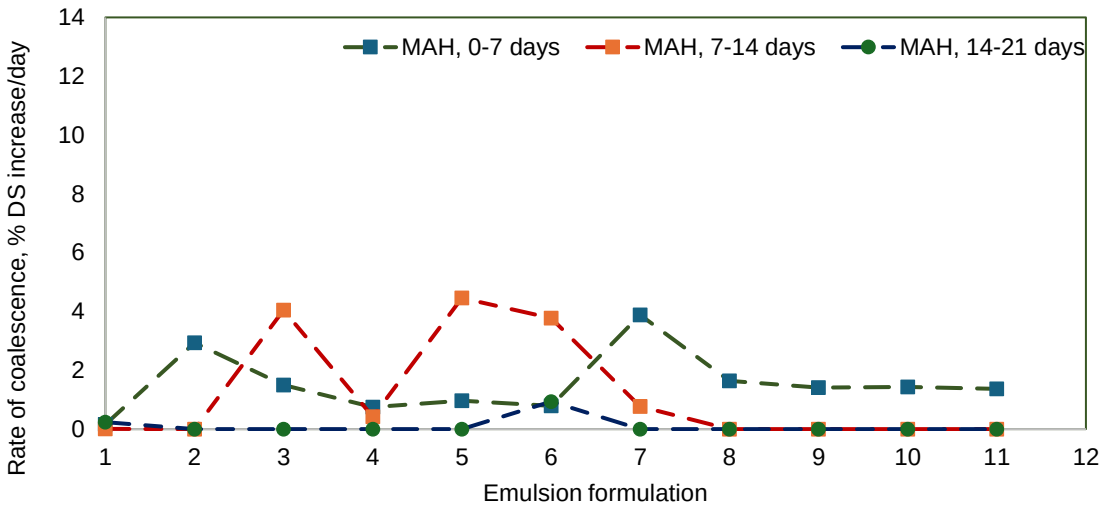

Figure 5.10 Effect of ageing on the kinetics of coalescence for different emulsion formulation contents for emulsions prepared using MAH (makataan hydrocolloid)

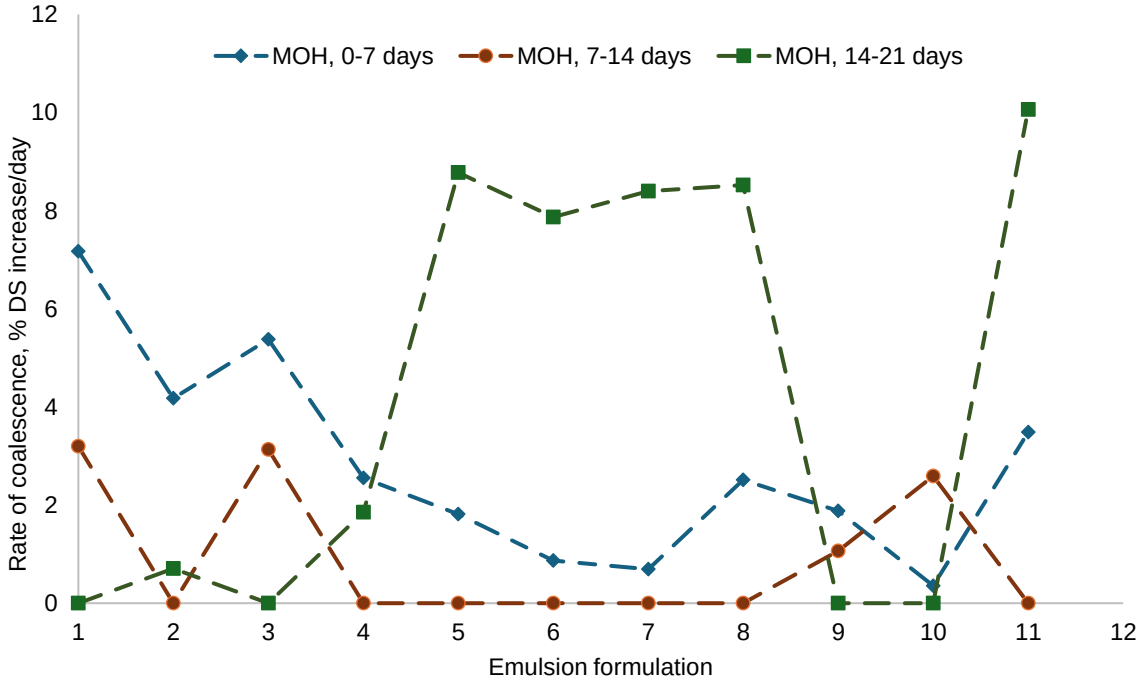

Figure 5.11 Effect of ageing on the kinetics of coalescence for different emulsion formulation contents for emulsions prepared using moringa hydrocolloid (MOH)

Generally, these results show a reduction in the coalescence rate with ageing. To such an extent for EGH and MAH-based emulsions, coalescence was suppressed entirely in most emulsion formulations within the range of 14-21 days. These unexpected observations are essential findings for both scientific interest and technological applications of these systems.

As coalescence proceeds, the concomitant increase in the size of droplets renders the emulsion more vulnerable to coalescence because of the reduction of the Laplace pressure. Indeed, bigger droplets are more prone to deformation, which is expected to increase the water drainage rate from the thin film between droplets on close approach; thus, the droplet's collision frequency and coalescence rate are increased (Liu et al., 2021;4). On the other hand, when protein blends, proteins/particle mixtures or emulsifier mixtures are used to stabilise many traditional and emerging emulsion products, this results in complex, non-equilibrated interfacial structures. The interface composition after emulsification depends on the competitive adsorption between proteins and particles (Lei et al., 2019;5). Over time, non-adsorbed proteins or particles can displace the initially adsorbed ones. Such rearrangements are essential to consider since the integrity of the interfacial film could be compromised after partial displacement, which may result in the physical destabilisation of emulsions (Santos et al., 2020;750; Masalova et al., 2019;355; Benitez et al., 2020;5) improved stability (Lei et al., 2019;6). For EGH-based emulsions, even though coalescence was initiated earlier than in samples prepared using MAH or MOH (section 5.8.3), it was utterly suppressed after 7 days (Figure 5.9). The relatively high rate of interfacial rearrangement in the presence of EGH is in line with the observed shorter time required to reach the equilibrium interfacial tension in the presence of EGH as compared to MAH or MOH (see section 3.10).

Figure 5.10 makes it clear that in the case of MAH, the process requires more time as active coalescence with a noticeable rate occurred up to 14 days and completely disappeared after that. Again, the slowness of interfacial rearrangements in the presence of MAH agrees with the longer time required to reach the equilibrium interfacial tension in the presence of this hydrocolloid (see section 3.12). Protein concentrations and amino acid composition control the kinetics of droplet stabilisation and coalescence suppression. EGH proteins operate faster and generate a more stable emulsion, whereas MAH takes longer to alter the interfacial layers. Furthermore, these variances are most likely caused by differences in protein hydrophobicity, molecular weight, and charge distribution between EGH and MAH.

However, the coalescence rate exhibits an entirely different behaviour in the case of MOH-based emulsions than EGH or MAH (Figure 5.11). In most formulations, a minimum coalescence rate is observed within the 7 - 14 days range. Above this transitional range, a complete suppression of coalescence (suggesting the formation of a viscoelastic solid interfacial film) is observed in almost 50% of the emulsion formulations used in this study. On the contrary, the other formulations demonstrate coalescence rates more significant than the

ones encountered within the initial period (0-7 days) (expression of physical destabilisation of emulsions). In other words, in the presence of MOH, there is an almost equal chance for physical destabilisation and an increase in emulsion stability during ageing. Considering that MOH-based emulsions rely primarily on the Laplace pressure for their stabilisation, it can be concluded that these observations result from a competition between coalescence and interfacial rearrangement (Nonfodji et al., 2020;7). As coalescence is initiated, the Laplace pressure is reduced, and the emulsion becomes more prone to coalescence, thus leading to physical destabilisation. In contrast, the interfacial rearrangement improves emulsion stability (Chen et al., 2023;6).

What becomes evident from the preceding investigation is that coalescence, which was initiated earlier in most formulations, tends to disappear completely or partially during ageing, especially for emulsion formulations containing EGH or MAH. These results indicate that the interface's composition (the metastable structure) obtained after emulsification progressively changes toward the thermodynamically one during ageing. This could happen over time by replacing the initially adsorbed surface-active species with a more protective film (Tshilumbu & Masalova, 2015;226). or through the ageing of the adsorbed layer (Dimitry et al., 2022;462). In this sense, it transpires from the results that the kinetics, such as interfacial rearrangements and the resulting structure (a viscoelastic interface that can suppress coalescence completely), could strongly depend on the hydrocolloid type. At this point, some arguments needed to be advanced to support this hypothesis.

It was shown in Chapter 3 that the three hydrocolloids generate three types of surface active species, that is, low molecular weight sugar molecules, proteins and undissolved particles. Each hydrocolloid contains some low molecular weight surfactants, such as sucrose (Mm = 342.3 $gmol^{-1}$) and fructose (Mm = 180.16 $gmol^{-1}$), following the trend: MOH > EGH > MAH. These simple sugars result from the enzymatic breakdown of higher molecular weight polysaccharide structures during extraction and processing. On the other hand, the molecular weight of proteins contained could follow the trend EGH > MAH > MOH. Indeed, EGH has higher quantities of non-essential amino acids such as arginine, glutamine, and serine than MAH and MOH. These amino acids, arginine and glutamine, may imply a greater molecular weight protein structure, as they are commonly present in bigger proteins.

Furthermore, proline, abundant in collagen and structural proteins, could indicate a larger molecular weight. MAH contains moderate quantities of non-essential and essential amino acids, such as alanine, glycine, and asparagine levels, suggesting a protein structure with an intermediate molecular weight. MOH has a well-balanced amino acid profile, including important amino acids like leucine, phenylalanine, and methionine (Wang et al., 2022;232). These necessary amino acids may point to a protein structure with a lower molecular weight than EGH and MAH. Chapter 3 clarified that the trend of hydrocolloids' molecular weight is

EGH > MAH > MOH. On this basis, the following arguments seem reasonable. First, during the emulsification of EGH-based emulsions, because of their high mobility, the low molecular weight sugar molecules adsorb quickly onto the droplet surface, thus improving stability under shearing conditions. This could explain the earlier initiation of coalescence in EGH emulsion (stabilisation by low molecular weight surfactants) and the fact that regardless of the hydrocolloid type, during the first 7 days, coalescence was active in all samples with comparable rates. During storage, the high molecular weight surfactants, proteins and undissolved particles progressively replace the low molecular weight surfactants from the interface and thus significantly improve the emulsion stability against coalescence.

Coalescence is suppressed earlier in EGH emulsions than MAH and earlier in MAH than MOH, which is in line with the expected trend of the molecular weights of proteins/hydrocolloids. This is per the observations in explosive emulsions where a mixed emulsifier system which comprised a derivatised Polyisobutylene Succinic Anhydride surfactant (PIBSA) in combination with a low molecular weight co-surfactant such as Sorbitan MonoOleate (SMO) (Masalova et al., 2020;5) or animal oil fatty acids (Muñoz et al., 2019;21) or a low molecular weight surfactant (SMO) with fumed silica nanoparticles (Tshilumbu & Masalova, 2015; 220). After emulsification, the authors demonstrated that adsorbed film was dominated by SMO or animal oil fatty acid after emulsification. During ageing, PIBSA molecules or fumed nanoparticles progressively replaced SMO; thus, the emulsion stability was greatly improved. The adsorption of proteins and particles to fluid/fluid interfaces leads to the formation of viscoelastic layers, which play a crucial role in the prevention of drainage, coalescence, or coarsening/ripening, which results in the formation of very stable particle-stabilized foams and emulsion (Sudhakaran & Doseff, 2020;7). Furthermore, it is known that in mixed emulsifier systems containing surfactants and particles, maximum stability is obtained through synergetic interaction between particles and surfactant; surfactant-induced particle flocculation is the key to maximum strength. Emulsifier may help promote partial particle flocculation and network rearrangements at the interface, which is perhaps observable through changes in interfacial rheology (Chignola et al., 2022;4), or this flocculation can occur before adsorption (Dwari & Mishra, 2019;750; Cheng et al., 2020;17) and may be detectable through bulk rheology (Tshilumbu & Masalova, 2015;218).

Our bulk rheology results on the particle emulsifier mixtures demonstrated a high ability of structure formation in systems containing EGH or MAH hydrocolloids (as expressed by both high values of yield stress and elastic modulus) (see section 4.6.3). This aligns with the high ability of the mixed particle-proteins systems associated with EGH or MAH hydrocolloids to significantly reduce the oil-water interfacial tension. It seems reasonable to assume that forming a mixed interfacial film through synergetic interaction between proteins and particles could lead to the complete suppression of coalescence observed in emulsion systems

containing EGH or MAH. It was thought that protein bridging mechanisms would lead to small oligomeric particle flocs, which, when adsorbed onto the oil-water interface, would cause more robust networks, increasing hindrance to lateral movement (the main form of instability) (Okuro et al., 2020;5).

5.8.4 Effect of hydrocolloid type on the creaming of the emulsion

In this section, the effect of the hydrocolloid type on the creaming index for different emulsion formulations, as set in Table 5.1, was investigated to glean more profound insight into the stabilisation mechanism in the mixed emulsifier system (proteins and undissolved particles).

Table 5.7 Values of the creaming index for emulsions prepared using MAH

	Hydrocolloid	**Oil**	**Water**	7 days	14 days
1	10	20	70	11.68	18.69
2	9.2	16.7	74.2	11.65	18.66
3	30	25	45	11.76	18.74
4	30.3	40.3	20.4	5.30	24.53
5	20.5	37.5	44.3	0.00	0.00
6	27.5	40	52.5	8.54	22.46
7	25	20	52.5	5.22	24.88
8	35	40	25	0.00	0.00
9	28	35	37	8.67	21.04
10	15	30	45	6.32	24.67
11	10	40	49.1	0.00	0.00

Table 5.8 Values of the creaming index for emulsions prepared using MOH

	Hydrocolloid	**Oil**	**Water**	7 days	14 days
1	10	20	70	3.96	34.55
2	9.2	16.7	74.2	17.24	25.01
3	30	25	45	0.00	0.00
4	30.3	40.3	20.4	15.38	26.01
5	20.5	37.5	44.3	0.00	0.00
6	27.5	40	52.5	35.96	52.81

7	25	20	52.5	37.89	42.01
8	35	40	25	0.00	0.00
9	28	35	37	15.30	26.74
10	15	30	45	15.38	0.00
11	10	40	49.1	0.00	34.55

Table 5.9 Values of the creaming index for emulsions prepared using EGH

	Hydrocolloid	**Oil**	**Water**	7 days	14 days
1	10	20	70	0.00	0.00
2	9.2	16.7	74.2	3.07	10.94
3	30	25	45	7.31	23.61
4	30.3	40.3	20.4	1.29	9.73
5	20.5	37.5	44.3	0.00	0.00
6	27.5	40	52.5	6.17	10.84
7	25	20	52.5	2.12	7.35
8	35	40	25	0.00	0.00
9	28	35	37	10.26	19.75
10	15	30	45	0.00	0.00
11	10	40	49.1	0.00	0.00

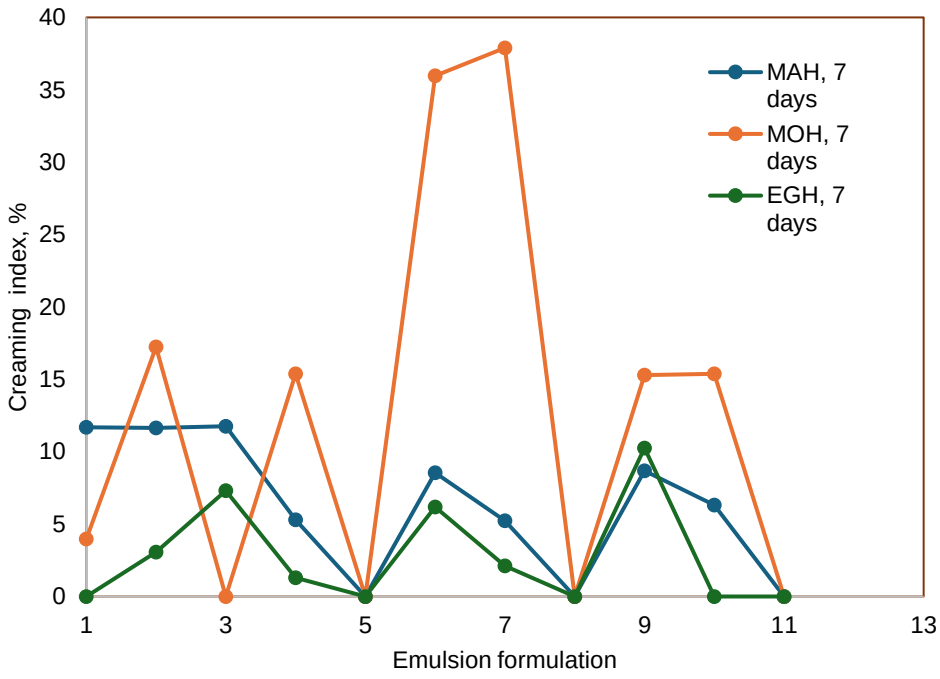

Figure 5.12 Effect of hydrocolloid type on the creaming index for different emulsion formulation contents (7 days of ageing**)** MOH (moringa hydrocolloid), MAH (makataan hydrocolloid) and EGH (egusi hydrocolloid)

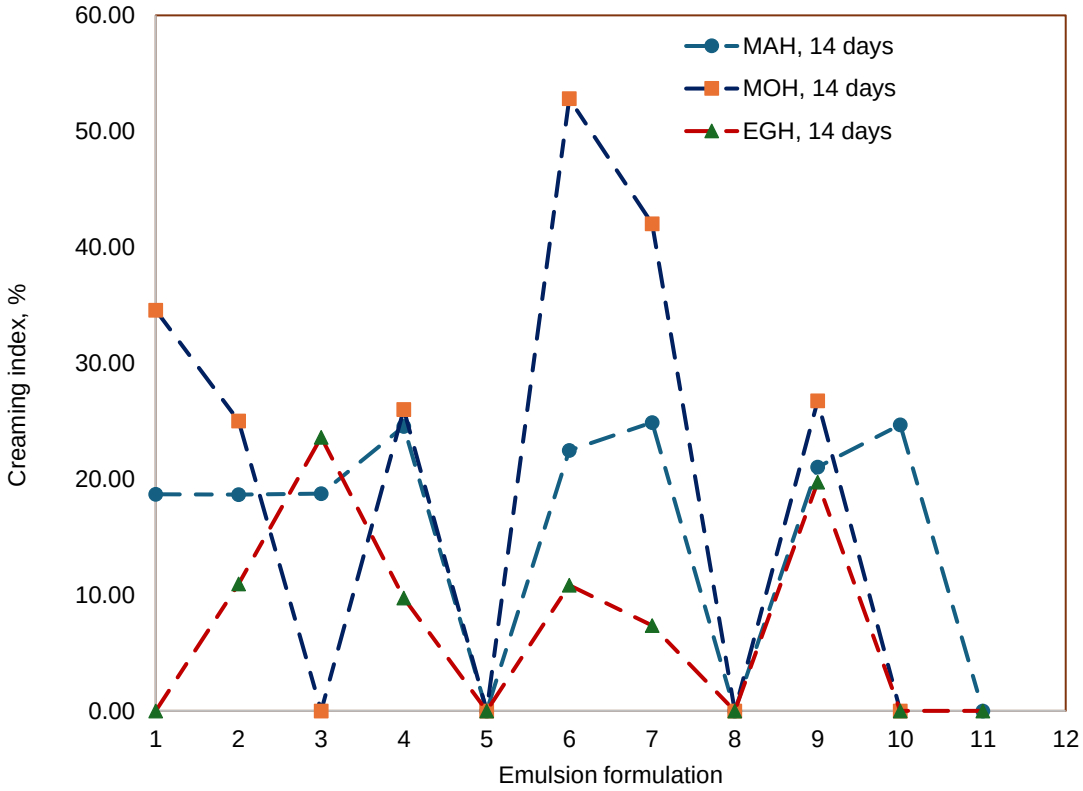

Figure 5.13 Effect of hydrocolloid type on the creaming index for different emulsion formulation contents (14 days of ageing). MOH (moringa hydrocolloid), MAH (makataan hydrocolloid) and EGH (egusi hydrocolloid)

The main results of these experiments for different emulsion formulation contents are shown in Table 5.7, Table 5.8, Table 5.9, Figure 5.12, and 5.13, respectively. Figures 5.12 and 5.13 make it clear that first, regardless of the ageing, in most emulsion formulations, the emulsion stability against creaming follows the trend: EGH > MAH > MOH. This is in agreement with the trend of the strength or rigidity of the hydrocolloid structure in the continued phase, which strongly affects its viscosity and density. Second, the creaming index increases with ageing regardless of the hydrocolloid type. This is due to the reduction of both the bulk viscosity and the bulk density with ageing. Indeed, as the droplets ascend on top with time.

The concentration of the internal phase in the bulk is reduced, reducing both the medium's density and viscosity. Additionally, the coalescence of droplets in bulk could further promote the creaming process during ageing. Third, the number of emulsion formulations that showed no creaming after 14 days follows the trend EGH > MOH > MAH. The latter emulsions contain three formulations in which no creaming was observed regardless of the hydrocolloid used: run 5, run 8, and run 11. These formulations appear to be the best in emulsion stabilisation with the hydrocolloids under scrutiny. What transpires from the previous investigation is that the three hydrocolloids under investigation are suitable emulsifiers and stabilisers for oil-in-water emulsions:

- As emulsifiers, first, the three hydrocolloids can significantly reduce the interfacial tension at the oil/water interface. This is especially true for EGH and MAH, where the equilibrium interfacial tension is comparable to well-established surfactants like Lecithin. Second, the three hydrocolloids have a high ability to improve stability under shearing conditions used during emulsification. The kinetics droplet refinement is comparable to well-established surfactants like lecithin; it follows the trend: Lecithin ≈ MAH < EGH < MOH.
- As stabilisers, EGH and MAH-based emulsions first demonstrated an outstanding resistance to coalescence for over 21 days. Even though coalescence was initiated during the first days of storage, it was quickly suppressed. This phenomenon was not observed in MOH-based emulsions, where coalescence continued throughout the storage period once coalescence was initiated. Stability followed the trend EGH > MAH > MOH. Second, EGH and MAH-based emulsions demonstrated a higher stability

against creaming than MOH-based emulsions. Similar to coalescence, stability followed the trend EGH > MAH > MOH.

In terms of food applications, Formulations 5 (20.50 hydrocolloid; 37.50 oil; 44.30 water), 8 (35.00 hydrocolloid; 44.00 oil; 25.00 water) and 11(10.00 hydrocolloid; 40,00 oil; 49.10) exhibit distinct behaviours that make them suitable for different types of emulsified food products based on their refinement time (Θ), critical droplet size (Dcrit), and initial droplet size (D_0). Formula 5 with Dcrit (Critical Diameter): 1.5 µm, Refinement Time (Θ): 100 minutes Initial Droplet Size (D_0): 12.9 µm. In food application, will proffer semi-stable emulsions: The critical diameter of 1.5 µm and moderate refinement time of 100 minutes make Formulation 5 well-suited for semi-stable emulsions. It can withstand moderate coalescence before breaking down, allowing it to maintain its emulsion properties over a reasonable period. The possible products applicable to this emulsion type are salad dressing and cream-based sauces. For formulation 8 with Dcrit (Critical Diameter): 0.5 µm, refinement time (Θ): 251 minutes (longest) with an initial Droplet Size (D_0): 14.4 µm, has a long-term stability in high-fat emulsions. The small critical diameter (0.5 µm) and very long refinement time (251 minutes) make formulation 8 ideal for emulsions that require extended stability over time, such as high-fat or high-viscosity products. The larger initial droplet size (14.4 µm) contributes to a thicker, more viscous texture, which is often desired in rich, fat-heavy emulsions with an example of butter spread and fat-based frosting.

Formulation 11 with Dcrit (Critical Diameter): 0.1 µm (smallest), refinement time (Θ): 79.2 minutes, and initial Droplet Size (D_0): 9.9 µm (smallest). The food application for formulation 11, offering high-Stability for light emulsions: The minimal critical diameter (0.1 µm) and moderate refinement time (79.2 minutes) make Formulation 11 ideal for light, highly stable emulsions that need to maintain small droplet sizes for smooth textures. This formulation would be excellent in products that require smooth consistency and fast refinement, ensuring a stable emulsion over a shorter processing time and applicable in beverages. What needs to be determined is the rheological characterisation of the emulsion. This will help further elucidate the mechanism of emulsion stabilisation against coalescence and creaming and the emulsions' flowability with EGH, MAH or MOH. Samples corresponding to runs 5, 8, and 11 were used to do this. These formulations appear to be the best in emulsion stabilisation with the hydrocolloids under scrutiny. Each run represents a unique combination of hydrocolloid, oil, and water proportions, providing a platform to explore the intricate interplay of the viscoelasticity of the interfacial film around the droplet and the hydrocolloid structure in the continuous phase of oil-in-water emulsion.

5.8.5 Rheological characterisation of egusi makataan and moringa o/w emulsion

Previously (chapter 4), the three hydrocolloids used in this study, EGH, MAH and MOH, create spatial structure in the aqueous phase with discernible strength and rigidity. This strength/rigidity was demonstrated to decrease in the following order: EGH, MAH and MOH. The results showed that because of its high content of hydrophobic proteins, the dominating mechanism of structure formation within MOH slurries is the entanglement network of polymers (proteins and polysaccharides) whose yield stress originating from the presence of high concentrations of dispersed particulate material within the structure. On the other hand, it was observed that the plastic solid-like behaviour of EGH and MAH slurries originated mainly from cross-liking rather than entanglement, due probably to their high content of hydrophilic proteins. This section aims to present the results and findings of the investigation, using rheological techniques, of the effect of adding oil droplets in the form of an o/w emulsion on the strength/rigidity of the hydrocolloid slurry network. The specific objectives are as follows:
To measure flow properties of fresh emulsion in bulk as functions of hydrocolloid types for different emulsion formulations associated with runs 5, 8 and 11. To measure viscoelastic properties of fresh emulsions in bulk as functions of hydrocolloid types for different emulsion formulations associated with runs 5, 8 and 11. To determine the strength and rigidity of the emulsion network, as measured by characteristic rheological parameters (yield stress or shear modulus), of different emulsion formulations and compare them to the ones associated with the corresponding hydrocolloid slurries.

5.8.6 Flow properties

The shear rate was controlled in the increasing deformation regime over a range of 10^{-6} to 1000 s^{-1}. Figure 5.14 shows typical flow curves for an emulsion prepared with MOH and MAH (runs 5) hydrocolloids.

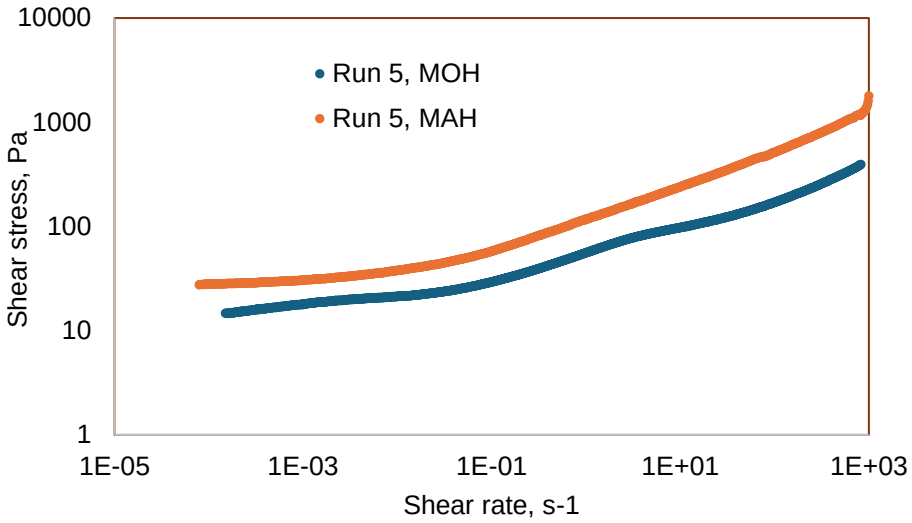

Figure 5.14 Typical flow curves of emulsions prepared with MOH (moringa hydrocolloid MAH hydrocolloids (runs 5)

By hydrocolloid slurries, characteristic flow curves demonstrate a shear thinning behaviour and apparent yield stress, suggesting a solid-like behaviour at low stresses.

The Herschel Bulky model was used to describe this flow behaviour of the emulsion.

Where T_y is the yield stress, n and K are empirical constants named flow index and consistency, respectively.

Typical best fittings of the Herschel-Bulkley model on the flow curve of flow curves of MOH stabilised emulsions (Run 5) are shown in Figure 5.15.

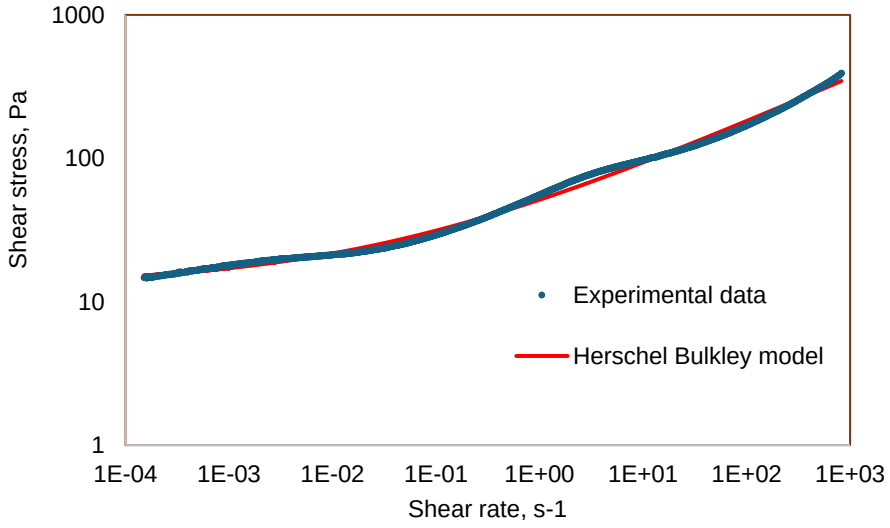

Figure 5.15 Best fittings of Herschel Buckley model on flow curves of MOH (moringa hydrocolloid) stabilised emulsions (Run 5)

Figure 5.15 shows that the Herschel Buckley model fits our experimental data well. The obtained values of the yield stress are summarised in Table 5.10 and presented in Figure 5.16. The corresponding values of the consistency and flow index are also added in Table 5.10.

From the table below, it is clear that the measured values of the yield stress depend on the type of hydrocolloid. Treating the yield stress as the measure of the strength of a structure formed in emulsions, it can be confirmed that, regardless of the emulsion formulation, EGH provides the highest rheological characteristics of o/w emulsion. The influence is especially evident in run 8, where all the samples have the same droplet size (see third column from the left in Table 5.10). Without a doubt, the yield stress decreases according to the sequence EGH-MAH-MOH. This does not align with the Laplace pressure (see third column from the left in Table 5.10). Thus, the ability to resist droplet deformation through the interfacial tension does not play a significant role in the strength of bulk o/w emulsion stabilised with EGH, MAH or MOH hydrocolloids. On the contrary, the above trend is per the yield stress and elastic modulus of the hydrocolloids in the continuous phase (see section 4.7), with the ability to reduce the interfacial tension (see section 3.10) as well as the expected trend of the interfacial skin on the droplet surface (see section 5.5.2.3).

Table 5 10 Herschel Buckley for Optimised egusi, moringa and makataan emulsion

Emulsion	Droplet size [µm]	Laplace pressure σ/R	Yield stress [Pa]	(R^2)
MOHE5	10.68 ± 0.01[a]	4616.65 ± 0.01[a]	17.01 ± 0.01[a]	0.97 ± 0.01[a]
MAHE5	9.47 ± 0.01[a]	2047.59 ± 0.01[b]	27.6 ± 0.01[a]	0.92 ± 0.01[a]
EGHE5	8.42 ± 0.01[a]	1742.79 ± 0.01[b]	47.01 ± 0.01[a]	0.90 ± 0.01[a]
MOHE8	12.83 ± 0.01[a]	3811.14 ± 0.01[b]	49.6 ± 0.01[b]	0.92 ± 0.01[a]
MAHE8	12.81 ± 0.01[a]	1511.71 ± 0.01[b]	65.4 ± 0.0[a]	0.93 ± 0.01[a]
EGHE8	13.01 ± 0.01[a]	1128.08 ± 0.01[b]	218 ± 0.01[b]	0.93 ± 0.01[a]
MOHE11	7.21 ± 0.01[a]	6746.19 ± 0.01[b]	31.5 ± 0.01[a]	0.95 ± 0.01[a]
MAHE11	11.06 ± 0.01[b]	1750.48 ± 0.01[b]	38.5 ± 0.01[a]	0.93 ± 0.01[a]
EGHE 11	8.46 ± 0.01[a]	1734.59 ± 0.01[b]	70.6 ± 0.01[a]	0.93 0 ± 0.01[a]

[1]Values are mean ± and standard deviation. Means with a different superscript in each row differ significantly ($p \leq 0.05$). [2]MAHE= makataan o/w emulsion, EGHE= egusi o/w emulsion, MOHE= moringa o/w emulsion

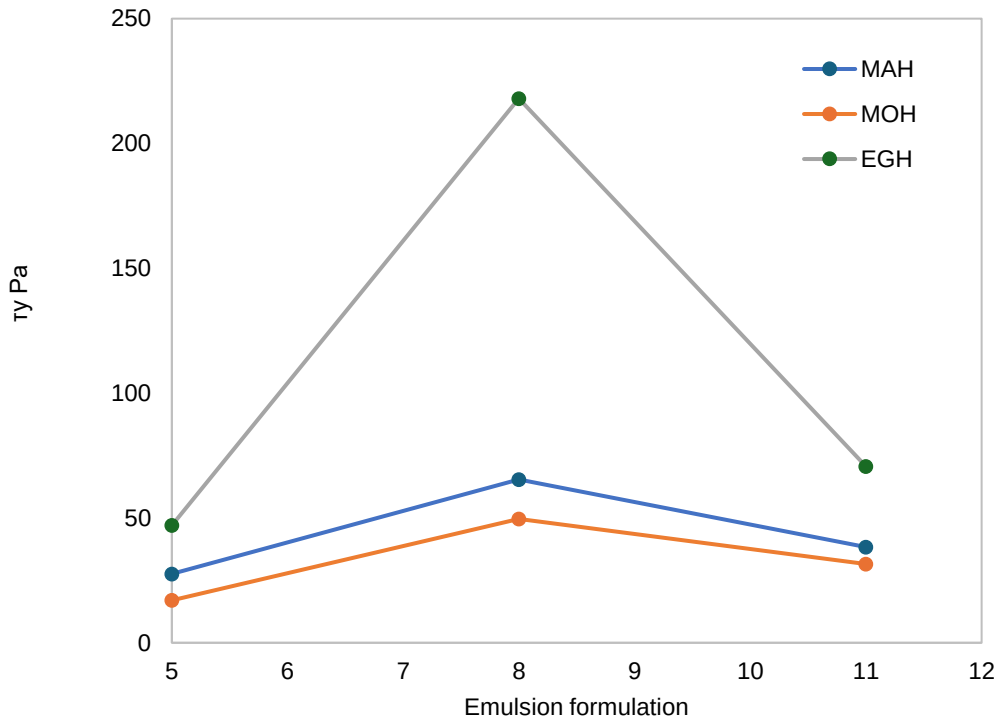

Figure 5.16 Dependence of o/w emulsion yield stress on hydrocolloid type. MOH (moringa hydrocolloid), MAH (makataan hydrocolloid) and EGH (egusi hydrocolloid)

On this basis, it seems reasonable to conclude that the ability of the hydrocolloids to structure in the continuous phase and probably at the interface is the primary source of the observed strength of the emulsion.

5.8.6.1 Elastic properties

The results of elastic modulus measurements confirm structure formation in o/w emulsions stabilised by the hydrocolloids. Typical experimental data for an o/w emulsion stabilised with MOH hydrocolloid (run 5) are presented in Figure 5.17.

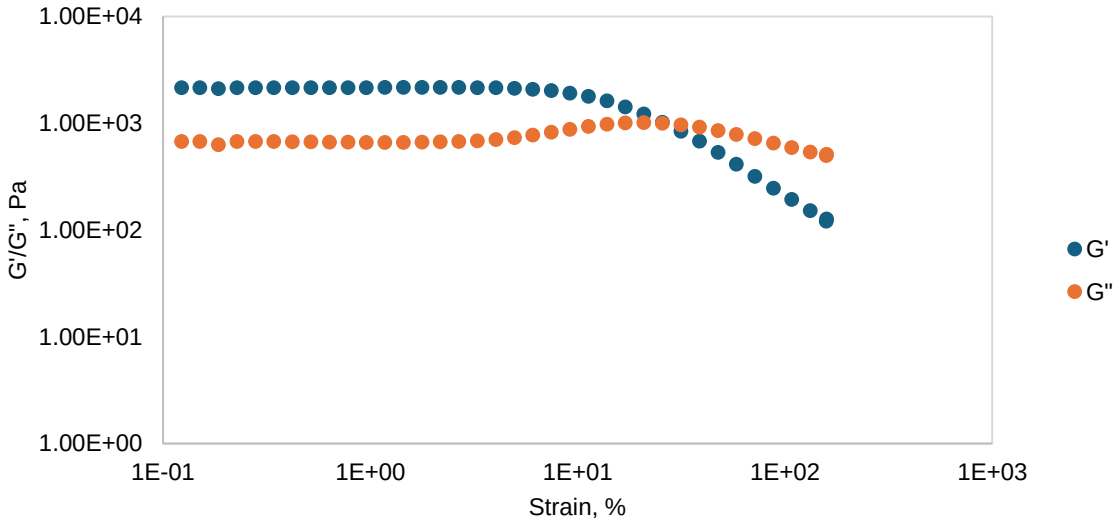

Figure 5.17 Typical amplitude sweep for o/w emulsion stabilise with hydrocolloids (moringa hydrocolloid; run 5)

For the material, the elastic modulus G' was more significant than the viscous modulus G" over a wide range of applied strain, indicating the predominantly elastic behaviour of the material at low test strains. As can be seen, the storage modulus was independent of strain amplitude up to some critical deformation, a zone of constant response (plateau region) indicating an unaltered structure not disturbed by shear. It was related only to the equilibrium microscopic structure, forces, and inherent dissipation of fluctuations (Gamonpilas et al., 2023;5). In this linear region, the particles could not move freely past one another, which defined the elastic domain. At higher deformations, the storage modulus values decreased with a deformation increase, the applied strain being sufficient to allow the particles to move past one another and induce a transition to the viscous

domain. Above the critical shear stress value, emulsions lose their viscoelasticity and become fluid. This stress is known as yield stress. The peak in loss modulus also confirms and elucidates the transition from elastic to viscous region. From an empirical point of view, a loss modulus maximum means a transition phenomenon in most cases, whatever its nature. From a microstructural point of view, this peak probably means that the dissipation of energy is maximal when the droplets are deformed and flattened enough to allow flow despite the crowding (Jiang & Charcosset, 2022;5)

The length of the elastic modulus's plateau indicates the structure's flexibility to deformation, and the drop of modulus is related to the breakdown of the solid structure. The storage modulus was obtained from the linear region of the storage modulus by extrapolation of the curve to zero deformation. The effect of varying the hydrocolloid type on the plateau modulus and damping factor is shown in Figure 5.18 and summarised in Table 5.11.

Table 5.11 The effect of varying the hydrocolloid type on the plateau modulus and damping factor

Emulsion	Droplet size [µm]	Laplace pressure σ/R	G' [Pa]	tan φ
MOHE5	10.68	4616.65	1660	0.158
MAHE5	9.47	2047.59	2470	0.151
EGHE5	8.42	1742.79	2820	0.214
MOHE8	12.83	3811.14	1440	0.218
MAHE8	12.81	1511.71	2270	0.206
EGHE8	13.01	1128.08	4000	0.205
MOHE11	7.21	6746.19	1230	0.216
MAHE11	11.06	1750.48	1720	0.176
EGHE 11	8.46	1734.59	1890	0.19

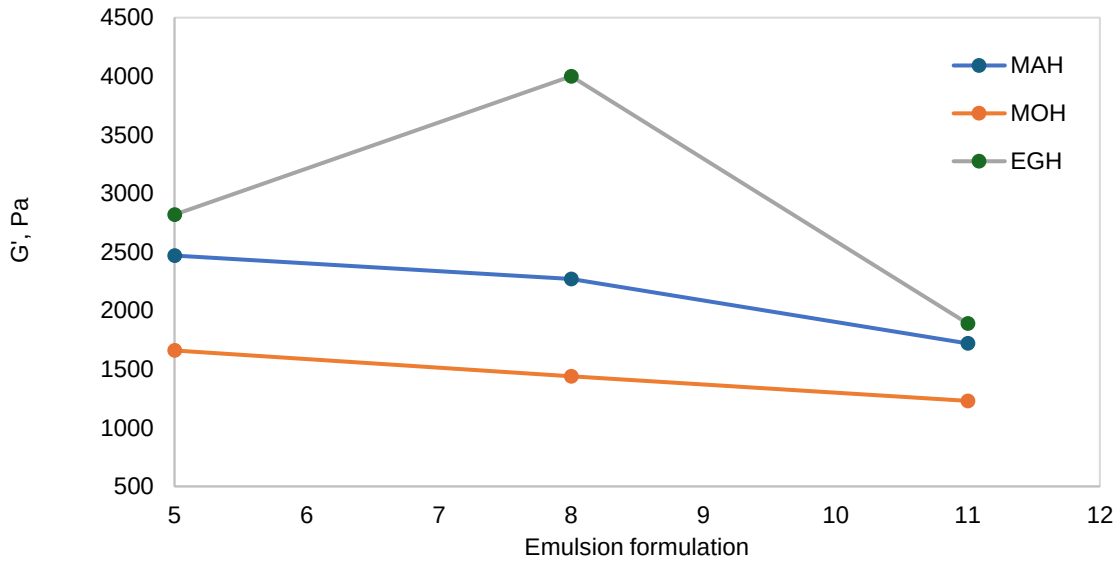

Figure 5.18 Dependence of emulsion elasticity on hydrocolloid type (runs 5,8,11). MOH (moringa hydrocolloid), MAH (makataan hydrocolloid) and EGH (egusi hydrocolloid)

The nature of the hydrocolloid influences the elasticity of o/w emulsions and Gp, pursuing the same trend as yield stress. Without a doubt, the elastic modulus decreases at low amplitude according to the sequence EGH-MAH-MOH; EGH provides the highest rheological characteristics of o/w emulsion. Once again, the influence is especially evident in run 8 where all the samples have the same droplet size (see third column from the left in Table 5.11). This does not align with the Laplace pressure (see third column from the left in Table 5.11). This means that if the data obtained for emulsions stabilised by different hydrocolloid types in the G'/(σ/R) - γ coordinates is plotted with σ being the interfacial tension and R being the mean drop radius, they will not collapse on a single master curve (Maldonado-Rosas et al., 2022;10). Thus, as already observed with the yield stress, the interfacial tension is not the only source of elasticity; additional sources exist in the system. As for the yield stress, the above trend is per the yield stress and elastic modulus of the hydrocolloids in the continuous phase (see section 4.7), with the ability to reduce the interfacial tension (see section 3.10) as well as the expected trend of the interfacial skin on the droplet surface (see section 5.5.2.3). Moreover, the above trend is in line with the trend of emulsion stability against coalescence as well as against creaming. Considering these facts as somewhat necessary, it is reasonable to accept them as proof of the active role of a hydrocolloid not only as a compound responsible for the interfacial tension but also as creating additional sources of elasticity using their physical /chemical interactions in the continuous phase as well as between interface layers of different

droplets; these interactions are more pronounced in EGH than in MAH and more pronounced in MAH than in MOH.

Hydrocolloids reduce interfacial tension in food items while adding flexibility through interactions between droplets and in the continuous phase. This is especially noticeable in emulsions stabilised with EGH, making it ideal for emulsions that require excellent stability and resistance to coalescence and creaming, such as sauces, dressings, and spreads. MAH is somewhat good in providing stability, but MOH has the least elasticity and stability, making it better suited for lighter emulsions or products with lower stability demands.

The ability of hydrocolloids to improve emulsion stability via these interactions is crucial for guaranteeing long shelf life, smooth texture, and resistance to phase separation in various culinary applications.

5.8.6.2 Frequency sweep

The frequency spectrum for a given system, i.e., the variation of elastic modulus (G′) and viscous modulus (G″) with oscillation frequency, provides a signature of the at-rest microstructure existing in the system. Based on frequency sweep information, the goal is to classify the emulsions in one of the mentioned classifications: (i) dilute solution, (ii) concentrated solution, (iii) weak gel, and (iv) strong gel (Mistry et al., 2023;882).

5.8.6.3 Storage modulus, Loss modulus and damping factor

Figure 5.18 and Figure 5.19 show typical changes in storage modulus (G'), loss modulus (G'') and the damping factor (loss tangent) of the EGH, MAH and MOH samples as a function of frequency for an emulsion formulation associated with run 5.

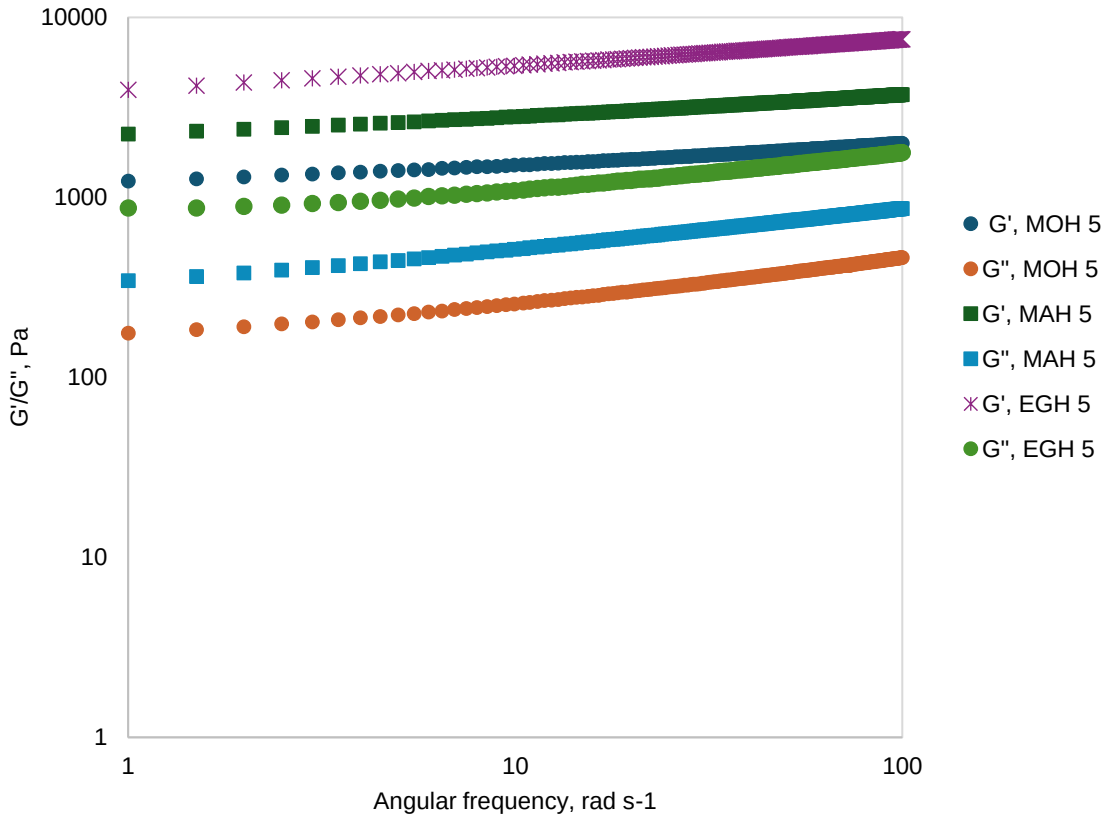

Figure 5.19 Typical Frequency sweep for emulsions prepared with EGH (egusi hydrocolloid), MOH (moringa hydrocolloid), and MAH (makataan hydrocolloid) showing the storage modulus, loss modulus (run 5)

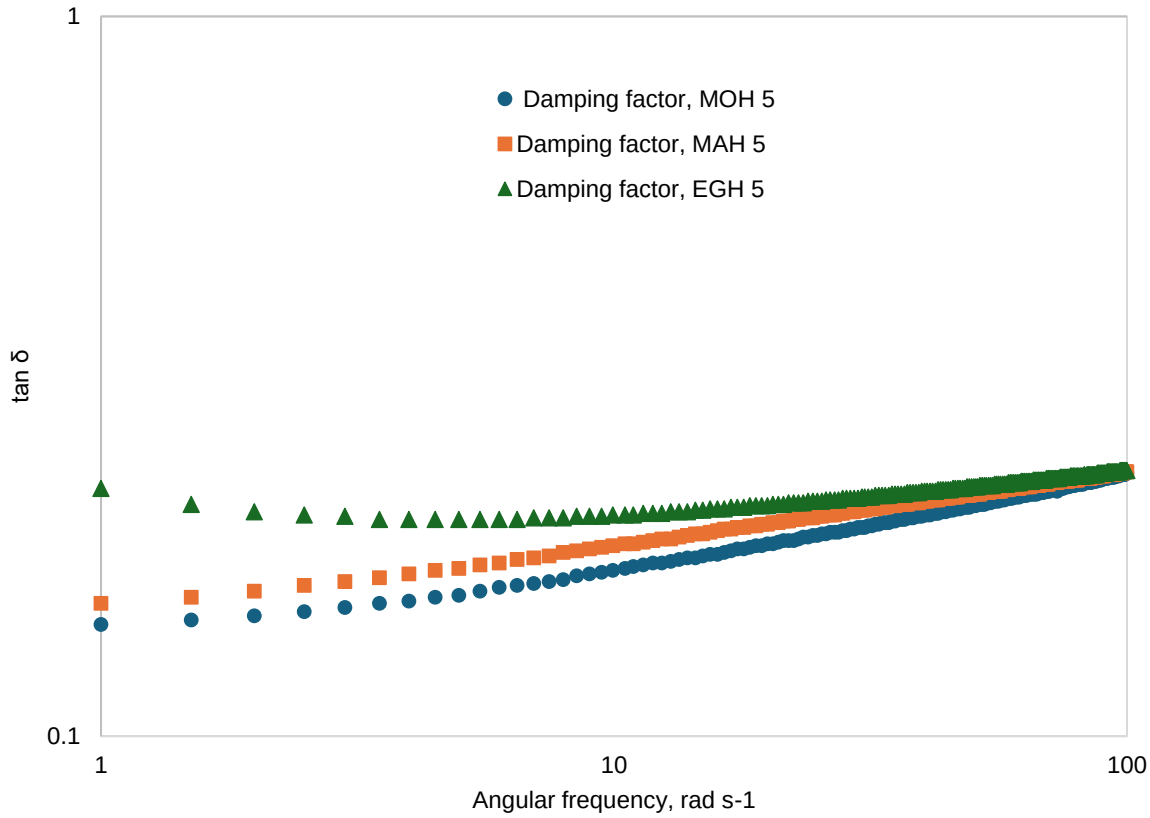

Figure 5.20 Typical Frequency sweep for emulsions prepared with MOH (moringa hydrocolloid), MAH (makataan hydrocolloid) and EGH (egusi hydrocolloid) EGH, MAH, and MOH showing the damping factor (run 5)

The following conclusions can be drawn from Figure 5.20. and Figure 5.21. First, regardless of hydrocolloid type and concentration, the mechanical spectra show that within the experimental frequency range (0.1–100 rad/s), G' > G" and no crossover point occurs, indicating a predominantly elastic behaviour of the emulsion. This solid-like behaviour is confirmed by the values of the damping factor, which are less than one for all emulsion formulations under investigation. Second, the magnitude of G', G" as well as loss tangent increase with an increase in frequency with a small dependency, showing typical weak gel-like behaviour of the samples experimented. A gel is “a continuous network of macroscopic dimensions immersed in a liquid medium and exhibiting no steady-state flow” (Zheng et al., 2019;550; Lastra-Ripoll et al., 2022;). We tried to fit our experimental data using a power law model. So, the degree of frequency dependence can be determined by Power law parameters (Yun et al., 2023;5) where G’ (Pa) is the storage modulus, ω (rad/s) is the oscillation frequency,

and K' (Pa.s^n) is a constant. The constant n' (dimensionless) is the slope in a log-log plot of G' versus ω.

From the structural point of view, it is known that n' = 0 is related to a proper (covalent) gel, while for a physical gel, n' > 0. The n' value can be used to compare the gels to a natural gel. A low n' value is characteristic of an elastic gel, whereas the system behaves as a viscous gel for an n' value close. Typical best fittings of the power law model on frequency sweep data of emulsions prepared with EGH, MAH and MOH hydrocolloid are shown in Figure 5.22.

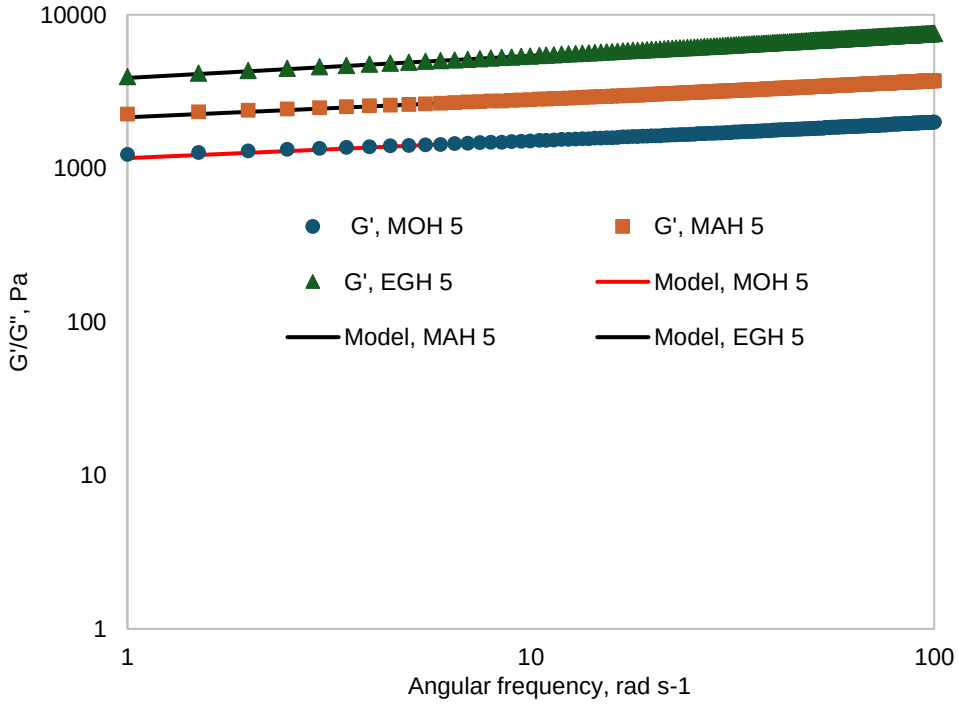

Figure 5.21 Typical best fittings of the power law model on frequency sweep data of o/w emulsions prepared with MOH (moringa hydrocolloid), MAH (makataan hydrocolloid) and EGH (egusi hydrocolloid)

As evident from Figure 5.24, the power law model fits our experimental data well. Thus, this model was used to describe the frequency sweep data and power law parameters determined for all samples, which are given in Table 5.12.

Table 5.12 The effect of varying the hydrocolloid type on the plateau modulus and damping factor

Emulsion	K	n'	R^2
MOHE5	1164,95	0,11	0.99
MAHE5	2148,97	0,12	0.99
EGHE5	3878	0,14	0.99
MOHE8	1164,95	0,11	0.99
MAHE8	1164,95	0,11	0.99
EGHE8	1164,95	0,11	0.99
MOHE11	1156,66	0,11	0.99
MAHE11	1867,01	0,14	0.99
EGHE 11	2148,97	0,12	0.99

It is clear from Table 5.12 that the n' values of EGH, MAH and MOH samples were within the range of 0.11–0.14, reflecting a predominantly elastic gel behaviour (very close to a true gel; n' = 0).

In terms of food applications, Table 5.12 shows how different hydrocolloid types (EGH, MAH, and MOH) affect the plateau modulus (K) and damping factor (n') of emulsions, providing information about their elasticity and stability. These characteristics are critical in determining how effectively emulsions can maintain their structure and resist flow under stress, directly affecting their performance in various food products. The n' values (0.11-0.14) show that all emulsions have essentially elastic gel behaviour, which is advantageous for food applications requiring texture and structure stability. This gel-like activity allows emulsions to retain shape, resist separation, and withstand physical stressors such as stirring or spreading. An n' value near 0 denotes a genuine gel, which implies that these emulsions are approaching a firm, stable.

EGH (Egusi Hydrocolloid) typically has the most significant plateau modulus (K), particularly in EGHE5 (3878) and EGHE11 (2148.97). This high modulus shows that EGH imparts the most elasticity and rigidity to the emulsion, making it excellent for products that require a firm, stable texture over a lengthy shelf life. EGH-based emulsions would be ideal for thick sauces (such as mayonnaise and aioli). MAH (Makataan Hydrocolloid) has intermediate modulus values, including 2148.97 in MAHE5 and 1867.01 in MAHE11. This means that MAH delivers intermediate elasticity and stability, making it appropriate for medium-thick emulsions or goods that require stability but can accept additional flexibility in low-fat spread. MOH (Moringa Hydrocolloid) consistently has the lowest K values (about 1156

in varied formulations), suggesting the lowest elasticity and stiffness. This makes it ideal for lighter emulsions or goods that require a softer, more flowable texture. Beverages are one possible application. Food manufacturers can modify the texture, stability, and shelf life of emulsified products to match the needs of their application, whether it's thick spreads, stable sauces, or light beverages.

5.8.6.4 Complex viscosity

The typical complex viscosities of emulsions prepared with EGH, MAH and MOH hydrocolloids (run 5) are shown in Figure 5.22. First, based on a double logarithmic scale, all emulsions' complex dynamic viscosity (η*) decreased linearly with increasing frequency, showing a non-Newtonian shear thinning flow behaviour (Figure 5.22). This is in line with the results obtained when the samples were subjected to a steady shear flow and the results associated with hydrocolloid slurries. This behaviour has also been observed for corn starch (Kanikireddy et al., 2020), sweet potato starch–xanthan gum mixtures (Choi & Yoo, 2009; Cheng et al., 2024), sweet potato starch (Yue et al., 2022), and Peruvian carrot starch (dos Santos et al., 2018). Second, the hydrocolloid's nature influences the emulsion's complex viscosity. Without a doubt, the complex viscosity decreases according to the sequence EGH, MAH, and MOH.

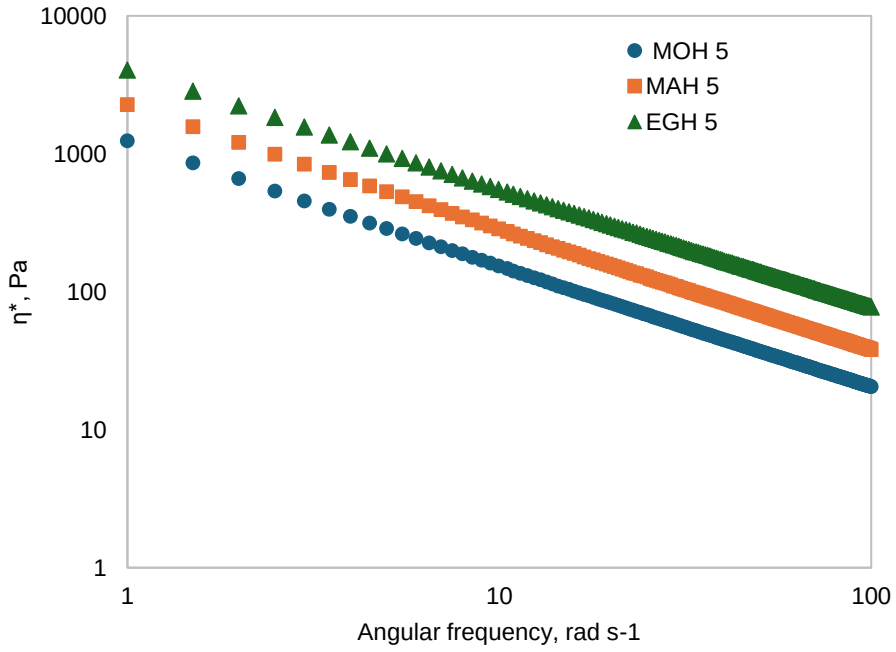

Figure 5.22 The typical complex viscosities of emulsions prepared with MOH (moringa hydrocolloid), MAH (makataan hydrocolloid) and EGH (egusi hydrocolloid) (run 5)

Once again, higher values of η* for MAH and EGH, combined with their high ability to reduce the interfacial tension to form and stabilise o/w emulsions, show the higher potential of this hydrocolloid as suitable thickeners, emulsifiers and stabilisers in increasing the consistency of food systems.

5.9 Conclusion

The sensitivity of the rheological properties of oil-in-water emulsions to the type of hydrocolloid has been investigated for different emulsion formulations. It was found that the kind of hydrocolloid affects the rheological properties of oil-in-water emulsions. The elastic modulus, the yield stress and the complex viscosity decrease in the following order: EGH-MAH-MOH. However, the sensitivity of the solid-like behaviour to the type of hydrocolloid is less pronounced; in all cases, a weak dependence of G' on the frequency ($G' = K'\omega^{n'}$; n'=0.11-0.13), characteristics of relatively strong gels were observed (very close to a true gel; n' = 0). In the linear regime, the elastic modulus was found not to be dependent only on the Laplace pressure. This indicates that the deformability of the droplet, which depends on the interfacial tension and droplet size, is not the only source of elasticity; additional sources exist in the system. Moreover, the additional elasticity dominates over the intrinsic one. It was also found that changing the hydrocolloid type affects the inherent elasticity of the droplets (by changing the interfacial tension) and the magnitude of the additional elasticity. The structure of the emulsion is directly related to its rheology, and the rheological properties of the emulsions are governed by the different forces that occur in the system, which, in turn, depend on the thickness of the inner droplet layer and the type of hydrocolloid. All changes observed could be understood by considering that changes in hydrocolloid type give rise to modification of both the interfacial properties (interfacial tension and interfacial elasticity) and the hydrocolloid structure in the water phase. In the particular case of the hydrocolloid-based emulsion used in this study, on the one hand, because of the non-ionic character of surfactants, the dominant interaction energy between droplets could be ascribed to van der Waals attraction on close approach. On the other hand, because of the polymeric nature of most surfactants released by particle dissolution (proteins and polysaccharides), their structure in the inner droplet layers increases the complex viscosity. It might induce both steric and electrostatic repulsive forces. The hydrocolloids play an active role not only as a compound responsible for the interfacial tension but also as creating additional sources of elasticity employing their physical /chemical interactions in the continuous phase and between interface layers of different droplets. Because of the dependence of the molecular weight as well as the hydrophile -lipophile balance of the proteins and polysaccharides on the hydrocolloid type, these interactions are also dependent on the hydrocolloid type and decrease in the sequence in EGH - MAH - MOH.

References

Angkuratipakorn, T., Chung, C., Koo, C.K.W., Mundo, J.L.M., McClements, D.J., Decker, E.A. & Singkhonrat, J. 2020. Development of food-grade Pickering oil-in-water emulsions: Tailoring functionality using cellulose nanocrystals and lauric arginate mixtures. *Food Chemistry*, 327(May): 127039. https://doi.org/10.1016/j.foodchem.2020.127039.

Benitez, L.O., Castagnini, J.M., Añón, M.C. & Salgado, P.R. 2020. Development of oil-in-water emulsions based on rice bran oil and soybean meal as the basis of food products can be included in ketogenic diets. *Lwt*, 118(July 2019): 108809. https://doi.org/10.1016/j.lwt.2019.108809.

Chen, X., Chu, X., Li, X., Cao, F., Guo, Q. & Wang, J. 2023. Non-thermal plasma modulation of the interaction between whey protein isolate and ginsenoside Rg1 to improve emulsion's rheological and oxidative properties. *Food Research International*, 165(November 2022): 112548. https://doi.org/10.1016/j.foodres.2023.112548.

Cheng, S.Y., Show, P.L., Juan, J.C., Ling, T.C., Lau, B.F., Lai, S.H. & Ng, E.P. 2020. Sustainable landfill leachate treatment: Optimize use of guar gum as natural coagulant and floc characterisation. *Environmental Research*, 188(February).

Cheng, Y., Wang, B., Lv, W., Zhong, Y. & Li, G. 2024. Effect of xanthan gum on physicochemical properties and 3D printability of emulsion-filled starch gels. *Food Hydrocolloids*, 149 (December 2023): 109613. https://doi.org/10.1016/j.foodhyd.2023.109613.

Chignola, R., Mainente, F. & Zoccatelli, G. 2022. Rheology of individual chitosan and polyphenol/chitosan microparticles for food engineering. *Food Hydrocolloids*, 132(December 2021): 107869. https://doi.org/10.1016/j.foodhyd.2022.107869.

Choi, H.M. & Yoo, B. 2009. Steady and dynamic shear rheology of sweet potato starch-xanthan gum mixtures. *Food Chemistry*, 116(3): 638–643. http://dx.doi.org/10.1016/j.foodchem.2009.02.076.

Dimitry, M.Y., Edith, D.M.J., Therese, B.A.M., Emmanuel, P.A., Armand, A.B., Leopold, T.N. & Nicolas, N.Y. 2022. Comparative evaluation of bioactive compounds, nutritional and physicochemical properties of five Cucurbita species flours of South Cameroon. *South African Journal of Botany*, 145: 458–467. https://doi.org/10.1016/j.sajb.2022.03.006.

Dwari, R.K. & Mishra, B.K. 2019. Evaluation of flocculation characteristics of kaolinite dispersion system using guar gum: A green flocculant. *International Journal of Mining Science and Technology*, 29(5): 745–755. https://doi.org/10.1016/j.ijmst.2019.06.001.

Efavi, J.K., Kanbogtah, D., Apalangya, V., Nyankson, E., Tiburu, E.K., Dodoo-Arhin, D., Onwona-Agyeman, B. & Yaya, A. 2018. The effect of NaOH catalyst concentration and

extraction time on the yield and properties of Citrullus vulgaris seed oil as a potential biodiesel feedstock. *South African Journal of Chemical Engineering*, 25: 98–102. https://doi.org/10.1016/j.sajce.2018.03.002.

Gao, K., Zha, F., Yang, Z., Rao, J. & Chen, B. 2022. Structure characteristics and functionality of water-soluble fraction from high-intensity ultrasound treated pea protein isolate. *Food Hydrocolloids*, 125(September 2021): 107409. https://doi.org/10.1016/j.foodhyd.2021.107409.

Gravelle, A.J. & Marangoni, A.G. 2021. Effect of matrix architecture on the elastic behaviour of an emulsion-filled polymer gel. *Food Hydrocolloids*, 119(April): 106875. https://doi.org/10.1016/j.foodhyd.2021.106875.

Hamdani, A.M., Wani, I.A. & Bhat, N.A. 2019. Sources, structure, properties and health benefits of plant gums: A review. *International Journal of Biological Macromolecules*, 135: 46–61. https://doi.org/10.1016/j.ijbiomac.2019.05.103.

Highland Essential Oil. 2019. KALAHARI MELON SEED OIL. , 27(0): 8253.

Horstmann, S.W., Axel, C. & Arendt, E.K. 2018. Water absorption as a prediction tool for applying hydrocolloids in potato starch-based bread. *Food Hydrocolloids*, 81: 129–138. https://doi.org/10.1016/j.foodhyd.2018.02.045.

Iacovino, S., Trivisonno, M.C., Messia, M.C., Cuomo, F., Lopez, F. & Marconi, E. 2024. A combination of empirical and fundamental rheology characterises dough from wheat flours with different extraction rates. *Food Hydrocolloids*, 148(PA): 109446. https://doi.org/10.1016/j.foodhyd.2023.109446.

Issara, U. & Rawdkuen, S. 2017. Physicochemical and stability of organic rice bran milk added with hydrocolloids. *Food and Applied Bioscience Journal*, 5(1): 1–10.

Jarret, R.L. & Levy, I.J. 2012. Oil and fatty acid contents in the seed of Citrullus lanatus Schrad. *Journal of Agricultural and Food Chemistry*, 60(20): 5199–5204.

Jiang, T. & Charcosset, C. 2022. Encapsulation of curcumin within oil-in-water emulsions prepared by premix membrane emulsification: Impact of droplet size and carrier oil on the chemical stability of curcumin. *Food Research International*, 157(April): 111475. https://doi.org/10.1016/j.foodres.2022.111475.

Kanikireddy, V., Varaprasad, K., Rani, M.S., Venkataswamy, P., Mohan Reddy, B.J. & Vithal, M. 2020. Biosynthesis of CMC-Guar gum-Ag0 nanocomposites for inactivation of food pathogenic microbes and its effect on the shelf life of strawberries. *Carbohydrate Polymers*, 236(December 2019): 116053. https://doi.org/10.1016/j.carbpol.2020.116053.

Kapseu, C., Kamga, R. & Tchatchueng, J.B. 1993. Triacylglycerols and fatty acids composition of egusi seed oil (Cucumeropsis Mannii Naudin). *Grasas y Aceites*, 44(6): 354–356.

Komane, B., Vermaak, I., Kamatou, G., Summers, B. & Viljoen, A. 2017. The topical efficacy and safety of Citrullus lanatus seed oil: A short-term clinical assessment. *South African*

Journal of Botany, 112: 466–473. http://dx.doi.org/10.1016/j.sajb.2017.06.028.

Lastra-Ripoll, S.E., Quintana, S.E. & García-Zapateiro, L.A. 2022. Chemical, technological, and rheological properties of hydrocolloids from sesame (Sesamum indicum) with potential food applications. *Arabian Journal of Chemistry*, 15(10).

Lei, J., Gao, Y., Ma, Y., Zhao, K. & Du, F. 2019. Improving the emulsion stability by regulation of dilational rheology properties. *Colloids and Surfaces A: Physicochemical and Engineering Aspects*, 583(September): 123906. https://doi.org/10.1016/j.colsurfa.2019.123906.

Liu, N., Li, N., Faiza, M., Li, D., Yao, X. & Zhao, M. 2021. Stability and in vitro digestion of high purity diacylglycerol oil-in-water emulsions. *Lwt*, 148(January).

Maldonado-Rosas, R., Tejada-Ortigoza, V., Cuan-Urquizo, E., Mendoza-Cachú, D., Morales-de la Peña, M., Alvarado-Orozco, J.M. & Campanella, O.H. 2022. Evaluation of rheology and printability of 3D printing nutritious food with complex formulations. *Additive Manufacturing*, 58(March).

Masalova, I., Tshilumbu, N.N., Fester, V. & Kharatyan, E. 2020. Is the combination of two particles with different degrees of hydrophobicity an alternative method for tuning the average particle hydrophobicity? *Journal of Molecular Liquids*, 313: 113444. https://doi.org/10.1016/j.molliq.2020.113444.

Masalova, I., Tshilumbu, N.N., Mamedov, E., Kharatyan, E. & Katende, J.K. 2019. Stabilisation of highly concentrated water-in-oil emulsions by polyhedral oligomeric silsesquioxane nanomolecules. *Journal of Molecular Liquids*, 279: 351–360. https://doi.org/10.1016/j.molliq.2019.01.104.

Mistry, S., Fuhrmann, P.L., de Vries, A., Karshafian, R. & Rousseau, D. 2023. Structure-rheology relationship in monoolein liquid crystals. *Journal of Colloid and Interface Science*, 630: 878–887. https://doi.org/10.1016/j.jcis.2022.10.115.

Muñoz, C., Sánchez, R., Peralta, A.M.T., Espíndola, S., Yan, T., Morales, R. & Ungerfeld, E.M. 2019. Effects of feeding unprocessed oilseeds on methane emission, nitrogen utilisation efficiency and milk fatty acid profile of lactating dairy cows. *Animal Feed Science and Technology*, 249(April 2018): 18–30. https://doi.org/10.1016/j.anifeedsci.2019.01.015.

Nonfodji, O.M., Fatombi, J.K., Ahoyo, T.A., Osseni, S.A. & Aminou, T. 2020. Performance of *Moringa oleifera* seeds protein and *Moringa oleifera* seeds protein-poly aluminium chloride composite coagulant in removing organic matter and antibiotic-resistant bacteria from hospital wastewater. *Journal of Water Process Engineering*, 33(September 2019).

Nyam, K.L., Tan, C.P., Karim, R., Lai, O.M., Long, K. & Man, Y.B.C. 2010. Extraction of tocopherol-enriched oils from Kalahari melon and roselle seeds by supercritical fluid extraction (SFE-CO2). *Food Chemistry*, 119(3): 1278–1283.

Okuro, P.K., Gomes, A. & Cunha, R.L. 2020. Hybrid oil-in-water emulsions applying wax(lecithin)-based structured oils: Tailoring interface properties. *Food Research International*, 138(PB): 109798. https://doi.org/10.1016/j.foodres.2020.109798.

Olubi et al. 2019. Physicochemical and fatty acid profile of egusi oil from supercritical carbon dioxide extraction. *Heliyon*, (April 2018): e01083. https://doi.org/10.1016/j.heliyon.2018.e01083.

Olubi, O. 2018. Functional characteristics of egusi seed (Citrullus lanatus) hydrocolloid and oil in instant egusi soup. *(Master Thesis) Cape peninsula university of technology*, (April). https://www.semanticscholar.org/paper/Functional-characteristics-of-egusi-seed-(Citrullus-Olubi).

Ouyang, J. & Meng, Y. 2022. Quantitative effect of droplet size and emulsion viscosity on the storage stability of asphalt emulsion. *Construction and Building Materials*, 342(PB): 127994. https://doi.org/10.1016/j.conbuildmat.2022.127994.

Raj, V. & Bajpai, A. 2020. Synthesis of hydrophobically modified guar gum film for packaging materials. *Materials Today: Proceedings*, (xxxx). https://doi.org/10.1016/j.matpr.2020.05.339.

Révérend, Le, ., Taylor, B.J.D, & Norton M.S, 2011. 'Design and application of water-in-oil emulsions for use in lipstick formulations'. *International Journal of Cosmetic Science*, 33(3):263–268. doi:10.1111/j.1468-2494.2010.00624.x.

Santos, J., Alcaide-González, M.A., Trujillo-Cayado, L.A., Carrillo, F. & Alfaro-Rodríguez, M.C. 2020. Development of food-grade Pickering emulsions stabilised by a biological macromolecule (xanthan gum) and zein. *International Journal of Biological Macromolecules*, 153: 747–754. https://doi.org/10.1016/j.ijbiomac.2020.03.078.

dos Santos, T.P.R., Franco, C.M.L., Demiate, I.M., Li, X.H., Garcia, E.L., Jane, J. lin & Leonel, M. 2018. Spray-drying and extrusion processes: Effects on morphology and physicochemical characteristics of starches isolated from Peruvian carrot and cassava. *International Journal of Biological Macromolecules*, 118: 1346–1353. https://doi.org/10.1016/j.ijbiomac.2018.06.070.

Sudhakaran, M. & Doseff, A.I. 2020. The targeted impact of flavones on obesity-induced inflammation and the potential synergistic role in cancer and the gut microbiota. *Molecules*, 25(11).

Tshilumbu, N.N. & Masalova, I. 2015. Stabilisation of highly concentrated emulsions with oversaturated dispersed phase: Effect of surfactant/particle ratio. *Chemical Engineering Research and Design*, 102: 216–233. http://dx.doi.org/10.1016/j.cherd.2015.06.025.

Ursu, A.-V., Djelveh, G., Pierre, G., Delattre, C., Michaud, P., Nasirpour, A. & Saeidy, S. 2018. Emulsion properties of Asafoetida gum: Effect of oil concentration on stability and rheological properties. *Colloids and Surfaces A: Physicochemical and Engineering*

Aspects.

Verkempinck, S.H.E., Kyomugasho, C., Salvia-trujillo, L., Denis, S., Bourgeois, M., Loey, A.M. Van, Hendrickx, M.E. & Grauwet, T. 2018. Food Hydrocolloids Emulsion stabilising properties of citrus pectin and its interactions with conventional emulsifiers in oil-in-water emulsions. *Food Hydrocolloids*, 85(March): 144–157. https://doi.org/10.1016/j.foodhyd.2018.07.014.

Wang, P., Gao, Y., Wang, D., Huang, Z. & Fei, P. 2022. Amidated pectin with amino acids: Preparation, characterisation and potential application in Hydrocolloids. *Food Hydrocolloids*, 129(February): 107662. https://doi.org/10.1016/j.foodhyd.2022.107662.

Yue, J., Yao, X., Gou, Q., Li, D., Liu, N., Yang, D., Gao, Z., Midgley, A., Katsuyoshi, N. & Zhao, M. 2022. Recent advances of interfacial and rheological property-based techno-functionality of food protein amyloid fibrils. *Food Hydrocolloids*, 132(February): 107827. https://doi.org/10.1016/j.foodhyd.2022.107827.

Yun, H.J., Jung, W.K., Kim, H.W. & Lee, S. 2023. Embedded 3D printing of abalone protein scaffolds as texture-designed food production for the elderly. *Journal of Food Engineering*, 342(October 2022): 111361. https://doi.org/10.1016/j.jfoodeng.2022.111361.

Zettel, V. & Hitzmann, B. 2018. Applications of chia (Salvia hispanica L.) in food products. *Trends in Food Science and Technology*, 80(January): 43–50. https://doi.org/10.1016/j.tifs.2018.07.011.

Zhang, X., Rong, X., Zhang, D., Yang, Y. & Li, B. 2023. Fabrication of natural W1/O/W2 double emulsions stabilised with gliadin colloid particles and soybean lecithin. *Food Hydrocolloids*, 144(February): 108978. https://doi.org/10.1016/j.foodhyd.2023.108978.

Zheng, M., Su, H., You, Q., Zeng, S., Zheng, B., Zhang, Y. & Zeng, H. 2019. An insight into the retrogradation behaviours and molecular structures of lotus seed starch-hydrocolloid blends. *Food Chemistry*, 295(May): 548–555. https://doi.org/10.1016/j.foodchem.2019.05.166.

CHAPTER SIX
OVERVIEW OF CHAPTERS, CONCLUSION AND RECOMMENDATION

6.1 Summary and Conclusions

The thesis reported the extraction and characterisation of hydrocolloids from *Citrullus mucosospermus* (egusi), *Citrullus lanatus citroides* (makataan), and *Moringa oleifera* seeds, with a focus on their potential industrial applications. The study aims to study the nutritional, rheological and stability properties of the hydrocolloids extracted from *Citrullus lanatus mucosospermus*, *lanatus citroides* and *Moringa oleifera* seed in an oil-in-water emulsion. The isolated hydrocolloids—Moringa hydrocolloid (MOH), Makataan hydrocolloid (MAH), and Egusi hydrocolloid (EGH)—had significant protein content, which improved their amino acid profiles and added to their nutritional value. Their small particle sizes and pseudoplastic behaviour in semi-concentrated slurries suit emulsification and other applications. The researchers investigated the extraction and characterisation of hydrocolloids from *Citrullus mucosospermus* (egusi), *Citrullus lanatus citroides* (makataan), and *Moringa oleifera* seeds, with a focus on their potential industrial applications. This study aimed to determine the metabolite profile and rheological and stability properties of the hydrocolloids extracted from *Citrullus lanatus mucosospermus*, *lanatus citroides* and *Moringa oleifera* seed in an oil-in-water emulsion. The study's objectives were to extract hydrocolloids from defatted egusi, makataan and Moringa seed flours using conventional heat and characterise the metabolite and functional profiles of the defatted flours obtained from makataan, egusi melon and moringa seeds. Further objectives were to evaluate the rheological properties of moringa, egusi and makataan seed hydrocolloids in a water-based slurry, and the last objective was to evaluate the rheological and phase behaviour of egusi, makataan and moringa seed hydrocolloids in an oil-in-water emulsion.

A high protein of carbohydrates was extracted from the three oil seeds. The study was divided into three research chapters, chapters three to five. The first three objectives were to extract hydrocolloids using the hot water extraction method and characterise them for nutritional and functional composition. The extraction and characterisation of hydrocolloids from *Citrullus mucosospermus* (CMS), *Citrullus lanatus citroides*, and *Moringa oleifera* seeds have demonstrated their potential as versatile ingredients in various industrial applications. Moringa Hydrocolloid (MOH), Makataan hydrocolloid (MAH) and Egusi hydrocolloid (EGH) exhibited high protein content, enhancing their amino acid profiles compared to raw oilseeds. hydrocolloids derived from oilseeds: EGH, MAH, and MOH. The hydrocolloids demonstrated high protein contents of 48.12%, 34.00%, and 35.00% for MOH, MAH, and EGH, respectively, reducing interfacial tension. The ash content and low-fat levels further contribute to their

nutritional value. Particle size analysis revealed fine particles with narrow distribution, essential for stable emulsification and water- and oil-holding capacities. Their small particle sizes and pseudoplastic behaviour in semi-concentrated slurries suit emulsification and other applications.

The objective of chapter four was to characterise the rheology of moringa, egusi and makataan seed hydrocolloids in a water-based slurry. The result confirmed that the hydrocolloids exhibit pseudoplastic behaviour in semi-concentrated slurries, with significant differences in mechanical response at varying concentrations. The structural formation in MOH slurries is predominantly driven by polymer entanglement, whereas cross-linking mechanisms govern EGH and MAH slurries. These findings underscore the hydrocolloids' functionality and potential to enhance the development of sustainable and functional products in food, pharmaceuticals, and other industries.

This study comprehensively examined the rheological behaviour of three novels. Rheological analysis under steady shear flow and reversible minor strains revealed that semi-concentrated slurries (20-50 wt%) of these hydrocolloids are pseudoplastic materials, characterised by viscous liquid behaviour without yield stress n and a greater loss modulus (G") than storage modulus (G') across all strain levels. Two critical transition points were identified in the correlation between storage modulus or yield stress and slurry concentration: 50 wt% and 67 wt%. The first transition point, observed in all hydrocolloids, marks the onset of structure formation. The second transition point, present only in EGH and MAH slurries, delineates a rapid increase in structure strength below this concentration and a slower increase above it. MOH-based slurries did not exhibit this second transition point due to the predominance of hydrophobic proteins, which lead to the formation of weak, predominantly elastic gels via polymer. These findings highlight the potential of EGH, MAH, and MOH hydrocolloids as functional components in culinary, medical, and industrial applications, opening up possibilities for developing valuable and sustainable solutions.

The broad objective of chapter five was to evaluate the rheological and phase behaviour of egusi, makataan and moringa seed hydrocolloids in an oil-in-water emulsion. The study of the sensitivity of oil-in-water emulsions' rheological properties to various hydrocolloids (EGH, MAH, and MOH) yielded noteworthy results about their impact on emulsion behaviour. The kind of hydrocolloid significantly impacts the emulsions' elastic modulus, yield stress, and complex viscosity, with these parameters decreasing in the order EGH > MAH > MOH. Despite these variances, the emulsions' solid-like behaviour showed a weak frequency dependence, indicating that all hydrocolloids utilised had reasonably robust gel properties. These findings highlight the potential of EGH, MAH, and MOH hydrocolloids as functional components in culinary, medical, and industrial applications, opening up possibilities for developing valuable and sustainable solutions. The study of the sensitivity of oil-in-water emulsions' rheological

properties to various hydrocolloids (EGH, MAH, and MOH) yielded noteworthy results about their impact on emulsion behaviour. Despite these variances, the emulsions' solid-like behaviour showed a weak frequency dependence, indicating that all hydrocolloids utilised had reasonably robust gel properties.

In the linear domain, the elastic modulus was discovered to be impacted not only by Laplace pressure but also by other sources of elasticity. This suggests that the deformability of the droplets, dependent on interfacial tension and droplet size, is supplemented by other elasticity sources within the system. The hydrocolloid type affects the droplets' intrinsic and additional elasticity magnitude. These changes are attributed to the modifications in interfacial properties (interfacial tension and interfacial elasticity) and the hydrocolloid structure in the water phase, driven by the different hydrocolloid types.

The forces inside the system determine the structure and rheology of the emulsions, including van der Waals attraction and steric and electrostatic repulsive forces caused by the surfactants' polymeric nature. Hydrocolloids contribute to these forces by altering interfacial tension and adding elasticity via physical and chemical interactions in the continuous phase and at droplet interfaces. The order of these effects is EGH > MAH > MOH, corresponding to the hydrocolloid proteins and polysaccharides' molecular weight and hydrophile-lipophile balance.

The first hypothesis was confirmed, indicating that hydrocolloids from egusi, makataan, and moringa seeds have significant nutritional and functional significance. The high protein content, small particle size distribution, and functional flexibility all support this theory. For the second theory, hydrocolloids have distinct rheological properties determined by their structural composition and slurry concentration.

The following conclusions can, therefore, be drawn from this study:

1 Hydrocolloid was produced from egusi, makataan and moringa seed flour.

2 Each hydrocolloid's nutritional, physicochemical, and functional properties are superior and, at times, similar to soy lecithin.

2.1 EGH, MAH and MOH can be used as a fortifier, thickener, stabiliser and fat binder in the food industry, amongst other functions.

2.2 EGH can be used in high-temperature food processes.

2.3 The hydrocolloids have a fine particle size with a narrow distribution, crucial for emulsification, water- and oil-holding capacities, and other industrial applications.

3 All hydrocolloids demonstrated pseudoplastic behaviour in semi-concentrated slurries (20–50 wt%) and showed no yield stress. The slurries behaved like viscous liquids with a greater. MOH slurries are primarily governed by polymer entanglement, forming

weak elastic gels. EGH and MAH slurries exhibit cross-linking mechanisms, forming stronger elastic gels with higher cohesive energy, ideal for certain food and industrial applications.

4 All three hydrocolloids were found to enhance oil-in-water emulsion stability, with EGH showing the greatest impact, followed by MAH and MOH, making them suitable as natural emulsifiers.

5. EGH (Egusi hydrocolloid) showed the lowest creaming index, indicating the most stable emulsions due to its strong ability to form a stable network and reduce oil separation. MAH (Makataan hydrocolloid) had a slightly higher creaming index than EGH but maintained stability. MOH (Moringa hydrocolloid) had the highest creaming index among the three, indicating relatively lower stability, though it still helped reduce creaming compared to emulsions without hydrocolloids.

6. Each hydrocolloid is a cost-effective, natural emulsion stabiliser that will be invaluable as an alternative to synthetic stabilisers and other commonly used hydrocolloids

7. EGH, MAH and MOH stabilised emulsions should be stored at a refrigeration temperature (5°C).

6.2 Future Studies and Recommendations

Future studies should evaluate the effect of processing parameters to understand the interaction of the hydrocolloid properties for EGH, MAH, and MOH hydrocolloids. Also, there is a need to assess their emulsifying, stabilising, and gelling properties in the real world. All extraction processes and end products should comply with regulatory standards and guidelines. Conduct thorough safety assessments and obtain necessary certifications to facilitate market entry and consumer trust.

Interdisciplinary Research and Development: Foster interdisciplinary collaborations between food scientists, pharmacologists, and industrial engineers to explore innovative applications of these hydrocolloids. Leverage cross-sector expertise to develop new products that meet consumer demands for natural and functional ingredients. Further research should focus on the interfacial properties of emulsions stabilised by the different hydrocolloids to understand better the mechanisms driving additional elasticity and its relationship with droplet deformability and interfacial tension. Exploration of Synergistic Effects: Investigate potential synergistic effects by combining different hydrocolloids to achieve optimal rheological properties and emulsions' stability. Explore combinations that may enhance the overall performance compared to individual hydrocolloids. Development of New Hydrocolloid-Based Products: Leverage the unique properties of each hydrocolloid type to develop innovative products that meet specific market needs, emphasising natural and sustainable ingredients.